Recent and future climate conditions and their impact on viticulture at the Upper Moselle region

Dissertation
zur
Erlangung des Doktorgrades (Dr. rer. nat.)
der
Mathematisch-Naturwissenschaftlichen Fakultät
der
Rheinischen Friedrich-Wilhelms-Universität Bonn

vorgelegt von
Steffi Urhausen
aus
Waldbredimus (Luxemburg)

Bonn, 2012

Angefertigt mit Genehmigung der Mathematisch-Naturwissenschaftlichen
Fakultät der Rheinischen Friedrich-Wilhelms-Universität Bonn

1. Referent: Prof. Dr. Clemens Simmer

2. Referent: Prof. Dr. Andreas Hense

Tag der Promotion: 04.03.2013

Erscheinungsjahr: 2013

Abstract

Climate plays a decisive role in viticulture. It has a large impact on the duration of the vegetative cycle, on the health of the vines and on the quality of the harvest. Under a changing climate wine characteristics may change and some vine varieties could become unproductive. The goal of this study is to develop statistical models for phenological event dates (budburst and flowering) and must quality (must density and acidity) for the Upper Moselle region, especially for the Luxembourgian viticulture. First, the regional climate and the phenological states of different vine varieties during the time period 1951-2005 are analysed. Significant trends are detected in annual, spring and summer temperatures. Vine phenology is also found to have changed significantly: budburst date and flowering events occur earlier by about two weeks, must density has increased and acidity decreased. The derived models are based on a linear multiple regression method using forward and backward steps. The predictors tested are mainly temperature means for different time periods or temperature derived indices. In addition, precipitation and sunshine duration for different time periods are evaluated. The most important predictors for budburst and flowering dates are temperature based variables. Depending on the vine variety and the phenological event, the model explains 80-89% of the variance. Besides temperature, sunshine duration and precipitation become important for must density and acidity estimations. The models reproduce must density with an explained variance between 59 % and 79 %, and acidity with 62 %-88 % explained variance depending on vine variety. The regional climate model COSMO-CLM (CCLM) is used to estimate future climate conditions under different scenarios and the future evolution of phenology and must quality. The realisations of CCLM during 1960-2000 differ significantly from the observations and thus a calibration of the model output was needed. The results show a large variability of the climate model output and clear estimations for future phenological event dates and must quality are difficult. Assuming the A1B scenario, budburst and flowering dates are likely to become earlier. Must density has significant increasing and acidity decreasing trends. The B1 scenario shows more moderate results: budburst date may move backward but flowering dates seem to not change significantly. Large changes in must density and acidity are not expected.

Ballade of Multiple Regression

If you want to deal best with your questions
Use multiple regression techniques:
A computer can do in a minute
What, otherwise done, would take weeks.
For 'predictor selection' procedures
Will pick just the ones best for you
And provide the best-fitting equation
– For the data you've fitted it to.

But did you collect the right *data?*
Were there 'glaring omissions' in yours?
Have the ones that score highly much meaning*?*
Can you tell the effect from the cause?
Are your 'cause' factors ones you can act on?
If not, you've got more work to do;
Your equation's as good – or as bad – as
The data you've fitted it to.

But it's worse when new factors have entered
The field since your survey was made,
Or even the old ones have varied
Beyond all the bounds you surveyed.
Has your leading competitor faltered?
Have you got, with old brands, one that's new*?*
This won't have come in your regression
Or the data you've fitted it to.

So 'get with' the Efroymson programme.
And list out your factors with zeal,
With their sesquipedalian labels
And wonderful client appeal.
But, brothers, please always remember,
Be you Marplan or Schwerin, or who–
Your optimum only is bonum
For the data you've fitted it to.

Corlett (1963)

Table of Contents

Chapter 1
1 Introduction

Anomalies in nature and in life quality are natural ways to perceive climate change. The exact values for temperature, for instance, are often not of interest, but rather the leisure activities which become possible or impossible at a certain temperature, or the quality of some agricultural products which are related to climate conditions. Crop loss and the resulting effects on the economic market remain easier in the mind of people and are often better documented as the particular weather which caused these events.

1.1 Vine – climate relationship: State of the art

In numerous studies, climate conditions act as predictors for vine properties and the other way round vine properties are used as proxies for climate variability. A "two way" ($\rightleftarrows$) relationship between climate and vine properties exists.

In fact, past climate is frequently reconstructed by analysing literature on plant and animal phenology. The unusual occurrence or actions of animals (e.g. migration of birds) in some regions, flowering dates of plants, crop quality and quantity, or harvest dates are often documented. Harvest dates of wine grapes can be found in parish and municipal archives and may serve as proxies for climate variations. In a study of *Chuine* et al. (2004), grape harvest dates since 1370 are used to reconstruct spring-summer temperature anomalies in Burgundy. A similar study by *Menzel* (2005) compares the exceptionally warm summer in 2003 to the last 500 years by estimating the growing season temperatures from historical grape harvest dates recorded since 1484 in Western Europe. Both studies focus on the year 2003 as an extraordinary warm year and they estimate summer temperature anomalies from grape harvest dates for the last 700 years. They agree that 2003 was the warmest summer since 1370.

In the last decades, interest raised in the question to which extent the changing climate may be responsible for the past, recent and future evolution of agricultural production, including vine cultivation (*Maurer* et al., 2009; *Vučetić*, 2011; *Caffarra and Eccel*, 2011; *Dalla Marta* et al., 2010; *Tomasi* et al., 2011).

The Fourth Assessment Report of the Intergovernmental Panel on Climate Change, IPCC (*Solomon* et al., 2007) summarises the status of understanding climate changes in the past and the expectation for the future on global and regional scales. Accordingly, global mean screen-level temperature has increased by 0.74 ℃ ± 0.18 ℃ between 1906 and 2005 in a non-linear way: 0.07 ℃ ± 0.02 ℃ per decade over the last 100 years, 0.13 ℃ ± 0.03 ℃ per decade over the last 50 years and 0.18 ℃ ± 0.05 ℃ per decade over the last 25 years. The years between 1995 and 2006 (except 1996) are among the 11 warmest years since 1850. The number of cold/warm nights, defined by the IPCC report by the 10th/90th percentile between 1961-1990, has decreased/increased between 1951 and 2003.

Comparable trends are observed on a regional scale. *Tondut* et al. (2007) investigated the evolution of temperatures in Herault County (Southern France). They detected three different temperature periods. Between 1949 and 1976, temperature was relatively low, in contrast to the period 1986 until 2004 where temperature was relatively high. During the latter period all annual mean temperatures were higher than the average of the whole period. The period 1976 to 1985 is marked as a transition state.

Jones et al. (2005a) investigated climate trends during for the growing season (April - October) in nine different wine growing regions in Europe. Mean temperature during the growing season has generally risen significantly, but the magnitude of the trends varies from region to region and from period to period. In Colmar (France), the mean temperature increased by 2.1 ℃ in 33 years, while in Bordeaux (France) a similar temperature increase has been observed for 55 years. At Geisenheim (Germany), mean temperature has increased by about 1.1 ℃ over 53 years. Indices for plant development (e.g. growing degree days) or for wine growing profitability (e.g., Huglin Index) also show significant positive trends because they are solely related to temperature. Precipitation, however, has significantly changed during the growing seasons only in two regions: in Bordeaux (France) an increase of 21 mm/decade has been observed during the period 1943 until 2003, and even 58 mm/decade between 1952 and 2004 in Pontevedra (Spain).

These changes affect phenology in general and the viticultural phenology in particular. Amongst others, the vegetative period lengthens when temperatures, especially spring and autumn temperatures, increase because the frost-free period starts earlier and lasts longer. Clear changes in the dates of phenological vine stages are observed in Europe (*Bois*, 2007; *Jones and Davis*, 2000; *Jones* et al., 2005b; *Menzel*, 2005). In Alsace, budburst and flowering event trends between 1965 and 2003 show a significant move towards earlier dates of about two weeks. The period between flowering and change of colour of the berries (véraison) shortened by 8 days and the véraison occurred almost 23 days earlier (*Duchêne and Schneider*, 2005) compared to 1965. In Murg (Switzerland) the flowering event advanced to earlier dates by 22.1 days in 47 years (*Defila*, 2003).

The observed trends in climate and phenology are expected to change in the future. For the time period 2071-2100, *Schär* et al. (2004) expect a further increase in summer temperature of 3 ℃ compared to the period 1961-1990 in the Luxem-

bourgian region, and even 5 °C in the southern parts of Europe. In Central Europe, the standard deviation of summer temperature means is expected to increase by 60 % to 100 % between 2071 and 2100 compared to the control period 1961-1990.

Climate change will affect both wine quality and viticultural practices (*Schultz*, 2005; *Hoppmann and Schmitt*, 2001). For northern regions, such as the one studied in this work (Upper Moselle region), a longer vegetation period and higher temperatures would allow to select vine varieties which up to now have only been cultivated in southern wine regions. Wine styles could change as acidity decreases, thus sweeter wines are expected. This shift is not necessarily welcomed by wine growers since wines could alter or even loose their typical regional style.

Consequently, models for predicting phenological event dates and must quality are of high interest. Different concepts of plant developing models exist: theoretical, statistical and mechanistic models (*Chuine* et al., 2003). The theoretical models are developed to understand biological/chemical processes of plants and remain constant in a changing environment. The statistical models use statistical fitting methods to combine phenological and climate observations. They can be used for forecasts but normally do not include internal biological plant processes (e.g. assimilation of nutritive substances) therefore no conclusions about cause and effect can be drawn. This type of models can be very elementary. E.g. *Lüers* (2003) calculates simple correlations between the phenological stages and climate parameters (usually temperature or temperature indices). Others can be more complex and their development is computer time consuming when using regression methods (e.g. *Hoppmann*, 1994; *Riou*, 1994; *Jones and Davis*, 2000). The third type of model, the mechanistic model, allows only relationships which have a known or assumed effect on the biological processes. Here, the idea of cause-effect relationships is more important than for the statistical models, but a clear delimitation between statistical and mechanistic models is not always possible.

One of the first phenological studies were conducted by *Réaumur* (1735). He observed relationships between phenological dates and temperatures during a certain period, location, and year. His revolutionary concept was that temperature at the phenological event was less important than sum of temperature beginning at an arbitrary date until the phenological event date. Nowadays several models are based on this idea; they uses as predictors accumulated temperature above a certain threshold during a certain time period. Laboratory experiments have confirmed the influence of temperature on the time length between start and end of budburst, and that the vine needs a temperature sum above a certain threshold to start growing (*Pouget*, 1964, 1968). Summing up the temperature values, a budburst prediction model can be established for different vine varieties (*Pouget*, 1988).

Temperature accumulation methods like the Huglin Index (*Huglin*, 1978) and the Winkler Index (*Amerine and Winkler*, 1944) as well the concept of degree days with different responses to temperature (*Zalom* et al., 1983) can serve as base for measures for wine productivity. Following *Due* et al. (1993), accumulations of temperature are correlated in time and can lead to artificial performance. Therefore

such indices should not be considered as the only predictor for plant developing models. Temperature accumulating models are not able to describe the physiological processes sufficiently, e.g. the effect of CHILLING on DORMANCY release cannot be taken into account. Furthermore these models are usually valid for a specific region and thus limited to certain climate zones (*Caffara and Eccel*, 2010).

Usually, models require several variables to better capture the complex physiological relationships. In the following, examples are given for estimating budburst and flowering event dates, as well as for MUST quality, i.e., MUST DENSITY (sugar content of the grapes) and ACIDITY.

The model developed by *Hoppmann* (1994) estimates the start of flowering time and wine quality of Riesling using a regression method. He used phenological data from Geisenheim (Germany) starting 1947. The input variables for the flowering period, which explain 87 % of the variance, are bud burst date, maximum temperature and precipitation during different time periods. The model for wine quality uses the date of full flower, maximum temperature, precipitation, water balance and insolation during different time periods. His model for must quality has an explained variance of 91 %.

Another model for must density for Riesling proposed by *Hoppmann and Hüster* (1993) is based on monthly means of the following predictors sorted by descending importance: sunshine duration in July, maximum temperature in May, August and October, precipitation in September, must quantity and sunshine duration in June. This model, which was developed using a 100 year record available for Schloss Johannisberg (Germany), explains 75 % of the variability of must density. In spite of the relatively high explained variance, the predictor must quantity, which describes 5 % of the variance, is difficult to estimate in advance.

In *Riou* (1994) a model based on multiple regression is given for the calculation of flowering and ripening periods using latitude and the sums of temperature in April, May and June as predictors. The estimated flowering describes 56 % of the observed variability and has an explained variance of 36 % for the ripening period. In addition, the budburst velocity (i.e. time from "closed" buds until shoots come out) defined by Pouget (1964) is revised. The results show a root mean squared difference with the observations between 6 and 9 days.

Jones and Davis (2000) have introduced models for determining flowering and ripening period as well as must density and acidity for Cabernet Sauvignon (CS) and Merlot (M) for the Bordeaux region. They performed a regression analysis testing many possible climatic variables and their combinations. In their work, the flowering event is calculated using the number of hours of insolation and precipitation amount at budburst time. The computed date correlates as high as 0.53 with observations. *Jones and Davis* (2000) investigated also the variability of must density and acidity of Cabernet Sauvignon and Merlot. The predictors for sugar content estimation are precipitation (CS, M), insolation (CS, M), number of days with maximum temperature above 25 ℃ (M) and 30 ℃ (CS) during flowering period and precipitation (CS, M) and sum of average temperature (M) during véraison period. Acidity can be estimated by using precipitation (CS), number of

days with maximum temperature above 30 ℃ (CS) and potential evapotranspiration (M) during flowering, and number of days with maximum temperature above 25 ℃ (M) during véraison. The acidity model explains 66 % and 77 % of the variability for Cabernet Sauvignon and Merlot, respectively. The must density model has an explained variance of 68 % and 79 %, respectively.

1.2 Objectives of this study

The goal of this study is to develop models for phenological event dates and must quality for the Upper Moselle region, which are suitable for predictions under climate change for this region. In fact, *Ashenfelter and Storchmann* (2010) and *Storchmann* (2005) investigated the effect of global warming on vineyard quality and prices and predict a large potential increase in value of the vineyards at the Moselle river. Wine cultivation has a long tradition in Luxembourg and it still plays an important economic role; wine growing accounts for one third of the national botanic production (*Statec*, 2008) although the wine growing area is with 1299 ha (*Weinjahr*, 2006) compared to other countries very small.

Following the previous section most of the existing vine phenology models include predictors which are related directly (the date of a prior phenological event) or indirectly (a climate variable during a certain phenological event) to phenological event dates, or to observations which are not measured area-wide (e.g. soil moisture) and thus cannot be used to calibrate the model. Some models do not distinguish between vine varieties or are not applicable in different regions. Often, models were developed from very small datasets, thus a reliable validation becomes difficult. Phenological models have to be coupled with climate models in order to estimate the future framework for vine cultivation. In view of the changing climate and already changed phenology, a quantitative assessment of phenological events and wine quality for future periods is of highest interest in the wine growers and salesmen community. This is also valid for Luxembourg, where wine production has a strong impact on economy.

In the Upper Moselle region white wine cultivars are traditionally used, while red wine varieties are relatively new. The set of predictors for the phenological stages should be restricted to meteorological data measured by climate stations. Thus climate model results can be used to predict future phenological development of vine cultivars determined by climate conditions. For statistical reasons, the evaluation of the data requires time series of at least 30 years length. The models should represent a high number of varieties, where the final model is based on the mean of all or on a group of vine varieties in order to exploit existing independencies between vine varieties. Subsequently, the models are also generated for the single varieties.

Before the derivation of the models for vine phenology and must quality, it is important to understand the major physiological and chemical processes during the vegetative cycle. This knowledge helps to select predictors which probably

affect the phenological events or must quality. These aspects are explained in Chapter 2. Chapter 3 reviews the observed changes in phenology and must quality while the climate conditions during the period 1951-2005 in the Upper Moselle region are investigated in Chapter 4. Using information about the vine itself (e.g., vegetative cycle and the corresponding climate requirements), and the observed trends in viticulture and meteorological parameters, statistical models are set up and cross validated in Chapter 5. In order to estimate future phenological trends, a climate model is required. In this study the COSMO-CLM (abbr. CCLM), the climate version of the COSMO model (*Doms and Schättler*, 2002), is used. Its characteristics are described and validated for the past period (1960-2000) for the Upper Moselle region in Chapter 6. Future climate projections for 2001-2050 are presented in Chapter 7. Finally, estimates for budburst and flowering dates, must density and acidity for future periods are given in Chapter 8 using the climate model as input to the phenology and must quality models.

Parts of this thesis have already been published in the refereed literature; a brief description of the climatic and phenological development during 1951-2005 in the Upper Moselle region, the phenological model derivation and the results for budburst and flowering event dates have been published in *Urhausen* et al. (2011a). The time series of must density and acidity during 1966-2005 and the results of the corresponding must quality model are explained in *Urhausen* et al. (2011b).

Chapter 2

2 The grape vine

2.1 The history of vine cultivation and wine production

Fossil records from the Tertiary period document that grape vine plants are older than 60 million years (*Vogt and Schruft*, 2000). The oldest indications of wine making are confirmed by clay jugs found in the village Hajji Firuz Tepe in the Zagros Mountains in Iran, which are dated 5400-5000 BC (*Koblet*, 1997; *McGovern*, 2003). Not every wild vine could, however, be cultivated for wine making or was well tasting. In North America the existence of wine was not documented in the pre-Christian period even though the plant was widely spread. Wines made from American vines have still a strong taste, called foxy odour. In the Old World wine was often flavoured with honey or absinthe. Grapes with a high sugar content occurred in the Middle East, and botanists called this vine type *Vitis vinifera*, i.e., the vine for wine making (*Priewe*, 2008).

The Greeks cultivated the vine in the Mediterranean region starting around 1600 BC, and the knowledge of wine making was highly developed subsequently. The Greek colonists brought the wine and the vines into the Mediterranean area, e.g., to Marseille (600 BC) and to Sicily (500 BC). After the Greeks, the Romans spread wine making very fast, as wine was a status symbol. They also began to distinguish between different vine varieties (*Priewe*, 2008) and to experiment with different training forms. Figure 2.1 from the early 16th century (*Robinson*, 1995) shows the roman training methods using trees, arcades, high espaliers and stakes in Alsace.

In the Middle Ages the vine spread out further, as the monasteries were build in whole Europe. In the 16th century the geographic extent of vine cultivation in Germany and Alsace was largest (Figure 2.2) and covered an area almost four times larger than today; the wine consumption per capita and year was estimated to be 200 litre.

Wars, diseases, introduction of customs duty, sales difficulties due to overproduction, and a changing climate reduced the vine cultivation areas to approximately

those regions which are cultivated nowadays (Figure 2.2). Turning points in viticulture were the occurrence of plant diseases, especially powdery mildew and the grape louse (phylloxera) imported from America and first observed in 1863 in France and spread over Europe. Several vine varieties were already extinct, before a counteragent was found in 1910.

2.2 Morphology and taxonomy of the vine

The grape louse infestation in Europe between 1860 (France and England) and 1913 (region of Baden) is responsible for the initiation of the classification of the vine (*Huglin and Schneider*, 1998). An area of 700.000 ha, especially in Southern France, was destroyed and all wine-growing countries around the World, except Chile and Cyprus, were affected (*Blaich*, 2000b). Because these damages had huge economical and cultural consequences, the morphology and taxonomy were studied in more detail in that time.

The family of Vitaceae belongs to the order of the Rhamnales and is divided into 12 genera (Figure 2.3). The genus in which the cultivated grapevine is classified in, is the Vitis genus with the two subgenera Muscadinia and Vitis (formerly called Euvitis). These subgenera are differing not only genetically by a different amount of chromosomes but also physically. The bark of Vitis is shredded and its inner pith is interrupted at the nodes by wooden tissue. The TENDRILS are branched and the seed is pear-shaped. The Muscadinia, however, has a tight bark, no separations in the pith, unbranched tendrils and boat-shaped seeds.

Nearly all cultivated vines belong to the Vitis subgenus which is separated into three groups: Asiatic, European-Asiatic and American. The Asiatic group contains about ten different species where the most common is Vitis amurensis. These species are very resistant against mildew and winter frost and are therefore often used for CROSSING. The American species contain about 20 subspecies and are not very suitable for wine making. Vitis labrusca, for example, has a foxy taste. However, the American vines are very resistant against diseases and climatic extremes. They are often used as stock on which Vitis vinifera is engrafted. The most suitable ones for wine-making are the European-Asiatic. Vitis vinifera Linné is the only species belonging to theis group.

Vitis vinifera L. is divided into wild (sylvestris) and domesticated (sativa) vine (Figure 2.4). The cultivated vine has bisexual flowers (hermaphrodite) whereas the wild sort is dioecious. Another important indicator of domestication used in archeology is the seed index, the ratio of seed width to seed length, which correlates with a shift from cross- to self-fertilisation (*Jackson*, 2008). The Vitis vinifera sylvestris has round seeds and thus a higher seed ratio.

The domesticated vine has been classified by *Negrul* (1938) into three groups depending on ecology, geography and morphology. The first group, the proles pontica, originates from Georgia, Asia Minor, Greece, Bulgaria, Hungary, and Romania and belongs to the oldest vine species.any varieties are good for winemaking, but

Figure 2.1: Four training systems in the early 16 century in Alsace: on trees (left), along a pergola (centre), training on high espalier (right) and on stakes (background). From *Robinson* (1995)

.

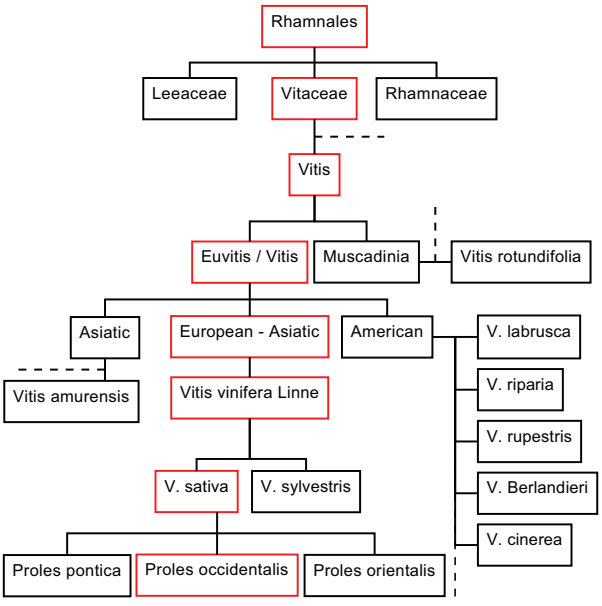

Figure 2.3: Biological classification of the vine. The red boxes show the taxonomy of the vine most suitable for wine making (*Huglin*, 1986; *Villa*, 2005; *Currle* et al., 1983; *Robinson*, 1995).

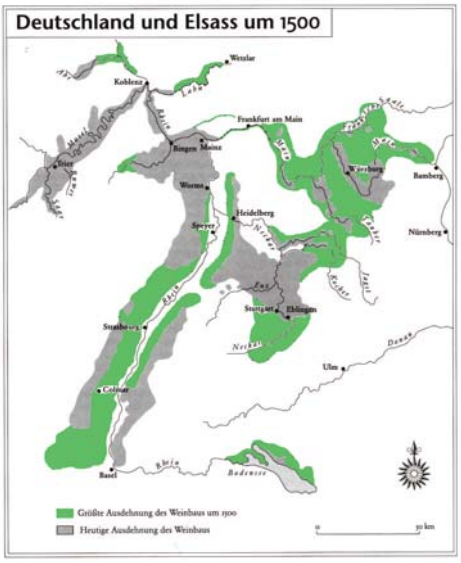

Figure 2.2: Comparison of the extent of viticulture in Germany and the Alsace region around 1500. The grey shadowed areas are the regions cultivated today and the green ones show the additional areas around 1500. Adapted from *Robinson* (1995).

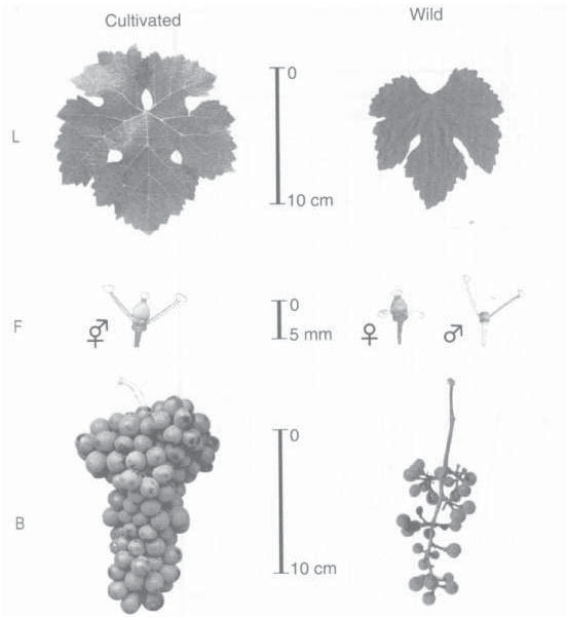

Figure 2.4: Differences in morphology for cultivated (sativa) and wild (sylvestris) grapevines (*Jackson*, 2008).

a few are suitable for table grapes (*Jackson*, 2008). Their leaves and shoot tips are covered with tight white hairs. The second group, proles orientalis, contains vine species mainly used for table grapes because many varieties are partially seedless and some seedless. They are coming from Central Asia, Afghanistan, Iran, Armenia and Azerbaijan. Their berries are big, oval, have less juice and sugar. The seedless varieties are mostly used to produce raisins like the varieties Sultana or Muscat of Alexandria. The last group, proles occidentalis, classifies the main varieties for red and white wine production like Riesling, Chardonnay, Cabernet Sauvignon. The origins are in France, Germany, Spain and Portugal. Their berries are small and juicy.

2.3 Environmental influences on vine cultivation

Essential for the growth and health of the vine plant are the environmental climate conditions; especially temperature, sunlight, precipitation and wind are the most important factors, and they have different effects on different spatial scales. In this work a macro and a micro scale are distinguished. The macro scale includes an entire region or a whole vineyard, whereas the micro scale covers a row in a vineyard or one single plant. Sometimes micro climate can be very different from macro climate. It can be highly influenced by the site and its environment. The site is mainly characterised by orography and land use (e.g., forests, fields, cities), by the geographical location and by soil properties. All these factors are closely linked and interacting, therefore they cannot be investigated separately. They are responsible for an optimal macro and micro climate and are very important in plantation planning like selection of the suitable vine variety and reallocation of vineyards.

2.3.1 Site exposure

Altitude, cardinal orientation, and slope gradient influence the macro climate and thus the vine growth besides soil properties and water availability. These geographical factors affect local temperature, insolation and wind, while insolation and wind feed back to temperature. Surrounding vegetation and human-made structures, like forests, water surfaces or buildings, influence the micro climate and may even have a positive impact on underprivileged sites.

Under normal conditions, i.e., excluding inversion or strong convection, mean temperature decreases with height, 0.6 ℃ - 1 ℃ for every 100 meters in altitude (*Kraus*, 2001) depending on air moisture, additionally large variations are possible due to local wind systems or consistent cloud cover (*Jackson*, 2008). Thus altitude affects the length of the growing season and grape maturation. Therefore vineyards are typically planted at low altitudes at high latitudes in order to profit from a higher temperature. Normally, at lower latitudes there is sufficient or even too

much heat available, and vineyards are planted at higher altitudes. For this reason, in Bolivia, vineyards are planted up to 2500 m, while in Europe (South Tyrol) up to 1000 m (*Robinson*, 1995).

Insolation is highest on sites oriented southwards in the Northern Hemisphere. Besides orientation also inclination determines how much insolation is available during the year. Figure 2.5 depicts how much insolation a southward or northward oriented site with different inclination angles receives compared to a plain site. In summer the differences between plain or southward oriented areas are small. The effects of inclination are higher in spring and highest in autumn. North sites should not have high inclination angles in regions where insolation is a limiting factor. A north site with an inclination of 30° gets in summer 50 % of the insolation compared to a plain area and only 10 % during the harvest period. A southward oriented site gets more insolation when the inclination angle is high, with an optimum of 50° (*Jackson*, 2008). Slopes this steep are, however, very difficult to work, although crawler-mounted machines already manage slopes with green cover up to 70° (*Vogt and Schruft*, 2000). But solar exposure is only slightly less at a slope of 30°. During harvest time a southward oriented site with an angle of 30° gets 70 % more insolation than a plain area, therefore vineyards in cooler climate regions are inclined and mostly southward oriented. Differences in insolation between a plain, eastward or westward oriented site are negligible. In autumn, however, radiation and steam fog occur quite often during the morning hours and attenuate insolation in eastward oriented sites where the insolation maximum is in the morning (Figure 2.6). Therefore a westerly slope gradient is preferred to an easterly slope gradient, as the sunshine maximum is during early afternoon.

Furthermore, the slope gradient and cardinal orientation effects become important for *cold air mass advection* and *frost* damage risks by radiational and advectional frost. Elevated areas are usually colder during the day compared to lower areas, but they do not cool so much during calm nights. As cold air is heavier than warmer air, cold air mass flows during still nights from elevations to depressions (katabatic winds) and form so-called cold air pockets (Figure 2.7). In regions were warmth is a limiting factor, vineyards are set up in sloping areas where the cold air can flow off. Elevated sites are less exposed to temperature fluctuations during night and day, and to less radiational frost during autumn, winter and spring. A careful selection of the area can extend the yearly frost free period by several days.

On the other hand, elevated sites which are unprotected against wind often show a delay of the vegetative cycle in springtime not only due to the temperature gradient with height but rather because the wind dissolves the (usually warmer) micro climate between the vine rows. This retardation can be caught up in autumn because the insolation is more intensive at higher altitudes and fog is not attenuating sun radiation. Nevertheless, late ripening vine varieties should not be planted on elevated sites which are not protected against wind because they need high temperatures and a delay in ripening is an economic risk.

Cold air mass can flow into the vineyard from the hilltop, as described before, or from over hundreds of kilometres (e.g. polar air mass). Frost periods in autumn

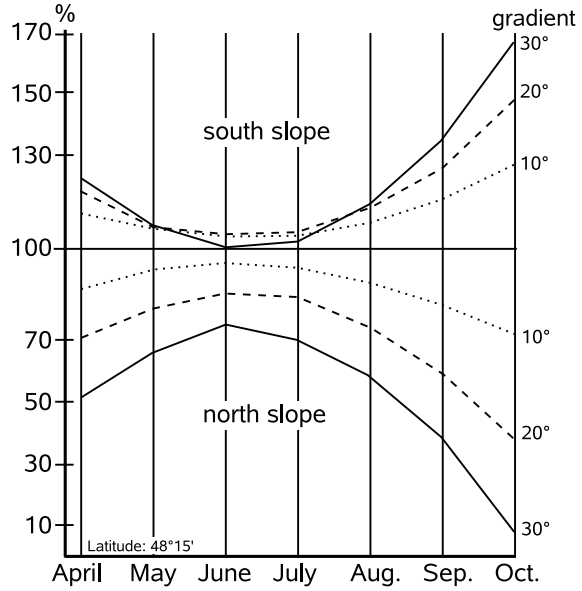

Figure 2.5: Exposition to sunlight relative to orientation and different inclination of slope in the upper Rhine Valley (48°15'N). Redrawn after *Vogt and Schruft* (2000)

inhibit maturation of late ripening vines. Before the LIGNIFICATION is completed, the wood is much more sensitive to cold temperatures. For ice wine production in autumn, however, frost periods below -10 ℃ are desired. Too cold temperatures damage the new shoots and the vine may not have as many buds as usual. During the growing phases temperatures below 10 ℃ can already be risky. In this case the decrease of temperature is often in parallel with an increase of humidity which leads to fog and/or the formation of dew on the leaves which enhances the risk of fungal disease because spores develop faster. Light wind, however, dries the vines after rain or dew and limits the risk of fungal infections.

During sunny days, temperature inside the vineyard canopy can be up to 10 ℃ higher than outside. This micro climate can be destroyed by wind via *turbulence*. At full foliage, this effect becomes significant at wind speeds above 1 m/s parallel to the line of vines and above 2 m/s at right angles to the line of vines (*Vogt and Schruft*, 2000). Vineyards are thus often constructed in such a way that the main wind direction is perpendicular to the row of vines; this also reduces the risk of damage due to storms. At high latitudes, vine rows are usually planted in rows directed up steep slopes to facilitate cultivation. Offsetting row orientation in order to minimise the negative effects of wind channeling is not practical on steep slopes. Terracing vineyards would allow an orientation of the vine rows depending on the prevailing winds, but would also increase soil erosion problems when banks are too high and become unstable.

Not only the geometric shape of the vineyards is important but also the land use of the surroundings. The vicinity of large water areas, like lakes and rivers, creates

Figure 2.6: During the morning in end of August, radiation fog and a small amount of steam fog is inhibiting the insolation, whereas in the afternoon the vineyards are getting sunlight. (View on “Wormeldange Koeppchen”, Luxembourg)

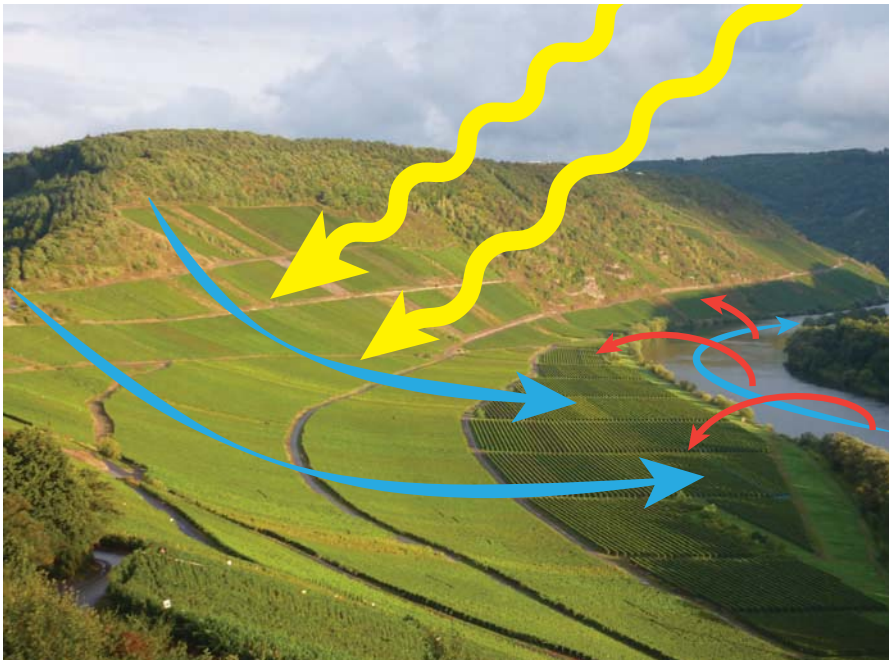

Figure 2.7: Cold air mass flows from elevations to valleys during calm nights and further flows off downstream. During autumn nights the river is warmer than the air and heats the vineyards.

a microclimate which protects the vines against low temperatures. The water stores thermal energy during the day and during summer. The release of this energy to the air during night and early autumn reduces the risk of frost (Figure 2.8). Water surfaces may reflect sunshine to nearby vineyards installed on steep slopes and thus increase the amount of light. Rivers help channeling the heavy cold air masses and due to the low surface roughness, the cold air flows downstream (Figure 2.7).

Other energy storing objects are buildings or cities. They form heat islands and the larger the cities are the higher the magnitude of the urban heat island

Figure 2.8: Cold air mass above the warmer river water is responsible for steam fog, also called sea smoke. The importance of steam fog for viticulture increases with the the water surface area.

(*Oke*, 1973). They may also keep strong wind away. Depending on the cardinal direction, however, the buildings may also shadow off the vineyard and the vines are not getting enough insolation.

Plain land above sloped sites increases the production and off-flow of cold air masses. In order to prevent this danger, forests may be planted at the top of the slope. Forests do not emit as much warmth as fields and grassland do during night and do not produce as much cold air masses. Similar to buildings, woods protect also against wind but may also shadow the vineyard on sunny days.

More expensive techniques to protect the vineyards are wind machines (e.g., Napa Valley) or helicopters, which mix the cold air with warmer air. Also ovens can be installed inside the vineyard in order to initiate circulation in the cold air. This method is not often used, as the consumption of combustible and the disturbance of neighbour residential houses due to smoke are high. Another method is to irrigate the whole plants at frost temperatures. The freed heat of freezing and a coat of ice protects the plants from colder temperatures.

2.3.2 Soil characteristics

The influence of the soil on grape and wine quality seems secondary besides climatic impacts and site exposition. But soil properties influence surface heat absorption and release, water holding capacity and nutrient availability.

Most agricultural soils are classified by their relative contents of sand, silt and clay. Their composition defines soil texture. Clay has a plate-like structure, consists of small particles ($\varnothing < 2$ µm) and is negatively charged (*Jackson*, 2008). As a consequence, soil with a high clay amount becomes slippery when wet and can retain large quantities of positively charged nutritional substances (like Ca^{2+}, Mg^{2+} and H^{+}) and water. Bivalent ions and water help to bind clay plates together, but the strong bond makes water unavailable for the plant. Also the pore diameter decreases with higher water capacity leading to a lower aeration of roots. Together with the more difficult penetration of roots due to the small clay particles, the roots remain near the surface, potentially leading to severe water stress under drought conditions. Light soil with a high amount of sand is nutrient-poor and does not retain water very well as the particles are bigger ($\varnothing$: 0.06-2 mm). Nevertheless, these deficits can be compensated if the roots have access to ground water. The water which is kept in the coarse soil can be readily extracted by plant roots.

Deficits of heavy and light soils can be corrected by viticultural practices. Adding humus modulates pore size, facilitates the movement of water, increases water absorbency, and retains water at tensions that permit roots access to the water. Green cover of the rows is the cheapest and easiest technique to regulate the amount of humus. It prevents compression of soil and regulates soil water in humid and bad aerated soils. On the other side, green cover is not helpful on dry sites or during dry years, as more water is needed. In these cases the soil is ploughed; unfortunately, this technique has several disadvantages like soil erosion, reduction of humus, and provides a high energy input. Soil water can be sustained by covering bare soil with straw, tree bark or other organic substances. In order to compromise between green cover and bare soil rows, one can green every second row. The water availability can then be regulated without relinquishing the advantages of greening.

Normally vines are planted on permeable soil with limited but sufficient water supply and low nutrient supply in order to limit growth. The leaves remain small and leaves and grapes have enough sunlight exposure. The berries remain also small and are less vulnerable to fungal diseases as they are less compact and are not easily crushed when they grow. The proportion of flesh and skin is high and the flavours and pigments are less diluted. The water availability should be low enough to profit from these advantages, but not too low so that the vital functions of the vine (e.g., no drying out, photosynthesis) are preserved.

Most part of the incoming direct and diffuse insolation in the viticultural area is transformed into heat by leaves and soil. The other part is reflected into the atmosphere. How much heat the soil is absorbing depends on soil colour and texture. In fine textured soils the heat of insolation is transferred to the soil water. This energy is almost completely lost when the water evaporates. Stony soils retain most of the heat in their structural components and radiate back into the air. This radiated heat can significantly reduce the risk of frost damage and accelerate fruit ripening during autumn (*Verbrugghe* et al., 1991).

2.3.3 Vegetative cycle of vine and climate conditions

The material presented in this section is a summary drawn from *Currle* et al. (1983); *Gladstones* (1992); *Jackson* (2008); *Villa* (2005); *Vogt and Schruft* (2000); *Blaich* (2000c). For technical terms see also Figure 2.11 and the Glossary.

Plants change their requirements for climate conditions during the vegetative cycle which depends also on the geographic location. In the following, the vegetative cycle of a wine producing vine, growing between 46°N and 52°N, and the correspondent optimal environmental conditions are presented.

The annual vegetative cycle of vines (Figure 2.9) begins in mid March with the mobilisation of reserve substances from the subsurface parts of the plant to the overground parts. This process, called BLEEDING, becomes visible about one month later, when liquid exits the PRUNING cuts. During this time period, the buds begin to swell, and a few weeks later, in mid April, budburst marks the first signs of green in the vineyard. Bud break indicates the peak of the translocation of reserve substances to the upper parts of the plant and the beginning of plant growth. The growth and synthesis phase begins around end of April and lasts until October, when the leaves begin to fall. During this period the grapes are developing from flowering state to maturation. In June the vine is flowering and starts to develop berries. Only parts of the berries will be maturing, the others will fall off (called COULURE, MILLERANDAGE OR BLOSSOM DROP), usually at a size of about 5 mm.

Berry growth can be divided into three phases. Phase I, which lasts from 6 weeks to 2 months, is marked by rapid cell division, thus rapid enlargement of the berry. Phase II is a transition phase in which berry growth slows down and the seed is developing. This process is very variable in time (1-6 weeks) and is a distinguishing mark for early or late maturating cultivars. This stage is, however, not visible until its end in August, when the berries are changing colour, which is called VÉRAISON. During the third phase (August-October), the seed matures and the berry reaches its final size. The tissue is becoming soft, acidity decreases, and sugars are accumulated (Figure 2.10). This phase usually lasts 5-8 weeks. The exact time of ripeness depends on the vine variety but also on the judgement of the winegrower. Usually, the grapes are mature in September or October and are then harvested. At this point the wood of the vine is maturing, which means that the green shots are becoming hard, as lignin is stored in the cell wall (i.e., lignification or aoûtement). The leaves are changing colour and fall down in October or November. The dorming buds, which did not come out because of CORRELATIVE INHIBITION between buds, are now in an inactive phase, called dormancy period. They will become active in spring the following year. The single phases and their relation to seasonal conditions are presented in the following in more detail.

Winter buds and bud dormancy The development process of shoots and grapes begins already in summer of the preceding year. The development of the shoot system is very complex. Buds are named by their position, germination sequence and fertility. Buds of grapevine plants are axillary buds, as they are

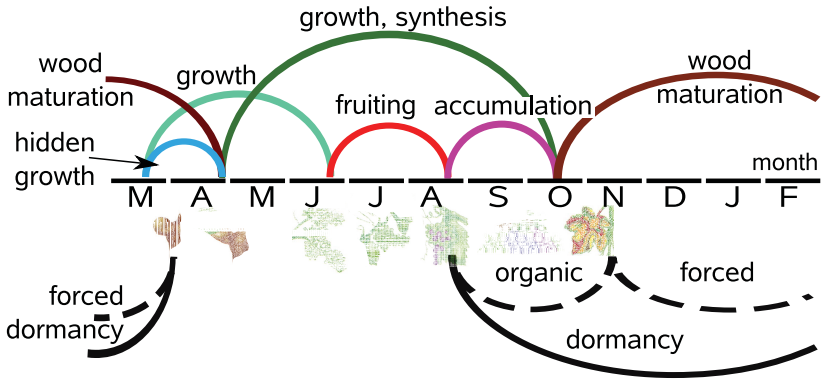

Figure 2.9: Vegetative cycle of the vine, based on *Stoev and Ivantchev* (1977) and *Villa* (2005), adapted for the Upper Moselle region.

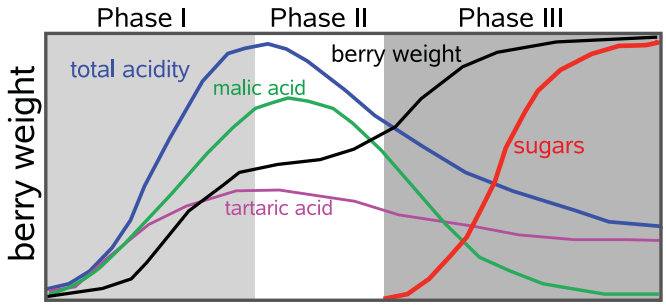

Figure 2.10: Development of berry weight, acids and sugars during the phases of berry growth. (Redrawn after *Blaich* (2000a))

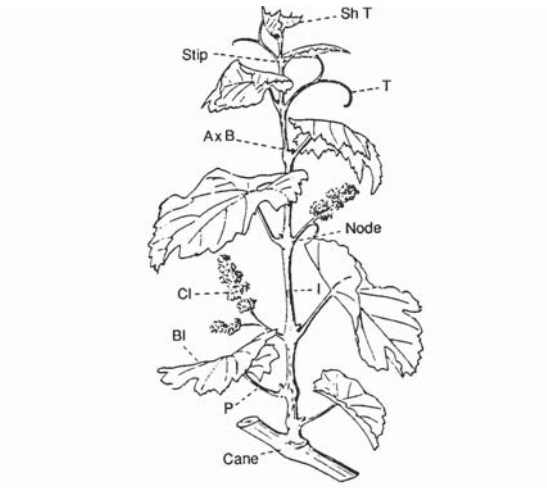

Figure 2.11: Vitis vinifera shoot, showing the arrangement of leaves, clusters (Cl), tendrils (T), axillary buds (Ax B), blade (Bl), internode (I), petiole (P), shoot tip (Sh T), and stipule (Stip); (*Jackson*, 2008).

formed in the axils of foliar leaves (Figure 2.11). Each shoot node potentially can develop an axillary bud complex including lateral and COMPOUND BUDS. Lateral buds degenerate or form lateral summer shoots in the same year, which may be removed or trimmed by grape growers to inhibit growth. The compound buds are latent buds containing three buds of different development states named primary, secondary, and tertiary buds. The compound buds can remain dormant for one or more seasons. These buds normally remain inactive during the growing season in which they are formed. The primary buds are the most developed and are fertile. If they are not destroyed (e.g., by freezing temperatures, insect damage, pathogenic influences or physiological disturbances) they generate the primary shoots in the following year. The primordial (i.e., embryonic) leaves, primordial inflorescences and primordial lateral buds of the primary bud are prepared in the previous year before the compound bud becomes dormant. The secondary buds are also mostly fertile and developed but they become active, only if the primary bud dies. After very cold winters when the primary buds are weakened the yield might not turn out substantially lower given the secondary buds are highly fertile. The tertiary buds are infertile, they do not bear inflorescences.

The compound buds are not coming into leaf in the same year they are created as they are inhibited by the terminal (i.e., the highest) and the summer buds and partly by the leaves. This fact is called correlative inhibition and is probably due to competition for nutritive substances. If the terminal bud, terminal leaf, and lateral shoots above the dormant bud are cut of, the dormant bud shoots. Lateral shoots below the dormant bud seem to not have an influence on the inhibition (*Huglin*, 1958). When the growing process is slowing down, after June, the repression of dormant buds should decrease. However, the dormant bud has lost its ability of shooting and enters into a so called organic dormancy. The start and length of this period depends on the vine sort and begins between August (varieties with late budburst) and September (varieties with early budburst). The duration lasts for a late variety longer than for vines with an earlier budburst and is usually finished between October and November (*Pouget*, 1972). After organic dormancy follows forced dormancy due to lower temperature and less sunlight. In order to terminate this state, a colder period of more than one week with temperatures below 10 ℃ is needed; frost temperatures are not required but favourable. Afterwards temperatures above 13 ℃ for early and 8 ℃ for late vines are required to end the forced dormancy period. The buds are now able to break, given temperatures are high enough.

Vine varieties exist, however, which do not need colder temperatures to terminate the organic rest phase like the Sultana grape (*Antcliff and May*, 1961). Other vines do not have a rest phase like Vitis caribaea, originating from the Caribbean (*Pouget*, 1972).

Hibernation and frost resistance In some regions and/or at certain periods cool temperatures are favourable for the development of the vine or the quality of wine. If the exposure to cool temperatures lasts too long, however, irreversible

physiological damage may occur which can retard ripening or destroy the yield. The vine, as other plants too, has developed strategies in order to self-protect against low temperatures and minimise frost and winter damages.

During the winter period, the water content of the vine is reduced by 50 % compared to summer values. Depending on WOOD MATURATION, season, and site, European vines survive temperatures down to about -15 ℃ without harm. Particularly frost resistant are Kerner and Riesling, while Rivaner and Silvaner are rather frost sensitive. Chardonnay and Riesling can experience severe bud kill (80-90 %) and still produce substantial yield by activating the remaining buds.

During wood maturation, before dormancy starts, starch is stored in the CANE. The maximal amount of starch is observed almost simultaneously with leaf fall (Figure 2.12). During adaption to the cold season, the starch is hydrolysed to oligosaccharides and simple sugars. This process decreases the osmotic potential of the CYTOPLASM, and the freezing point is reduced. Growth regulators or nutrient influences may prolong cellular activity and late season growth in autumn. Thus carbohydrate accumulation is reduced and the vine may not be frost resistant any more.

The highest sugar concentration in the wood is found during December and January. After February, sugar is retransformed into starch; the second starch maximum is between March and April. Thus, strong frost periods after February are very harmful as the vine has almost lost the ability to mobilise sugar. Relatively high temperatures during winter prevent, however, the transformation of starch; i.e., wood maturation is low. In this case sugar is retransformed too early, and subsequent (even light) frost periods may become destructive. Rapid temperature changes are often more destructive as the lowest observed annual temperature might suggest. Thus, a highly frost resistant vine is characterised by the ability of quickly reducing water content and transforming starch into sugar also at very low temperatures (-20 ℃) and during a long period, and by an adequate bud retention on healthy canes.

Period of budburst Parallel to the second starch maximum, the vine starts intensive water absorption before the pruning cuts are bleeding and the dormant buds are swelling. The bleeding occurs as soon as upper soil temperatures exceed a threshold value. Observations showed that bleeding is irregular at soil temperatures below 8 ℃ and continuously at temperatures between 8 ℃ and 12 ℃. Above 12 ℃, bleeding is intensive (*Reuther and Reichardt*, 1963). The vine may loose up to five litres of sap during bleeding (*Robinson*, 1995).

Bud swelling and subsequent bud break depend on temperature. Many studies define a threshold temperature for different vine varieties, but this threshold differs between studies. *Pouget* (1968) explains this discordance with different laboratory conditions and author-specific concepts of growing processes. In order to make the ideas clear, he suggests two states of growth: invisible growth (apparent growth) and visible growth (real growth). For both phases different temperatures are applied. *Pouget* (1964) investigates also velocity of bud development in dependence

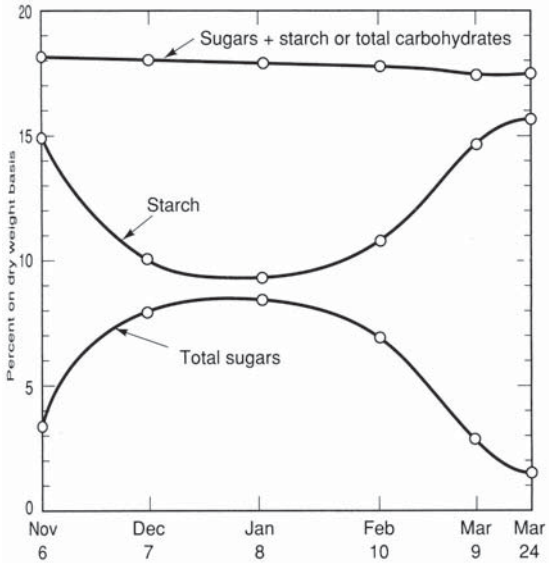

Figure 2.12: Seasonal interconversion of starch and sugars during fall cold acclimatisation and winter deacclimatisation. (From *Winkler* (1934))

of temperature. He concludes that budburst occurs later during low temperatures, and vine varieties with late bud breaks need higher temperature accumulations than varieties with earlier budburst. But high temperatures may be ineffective in the accumulation if previous temperatures were very low. Also at sites where the minimal temperature is very low, the vines require a higher temperature sum (*Vogt and Schruft*, 2000; *Becker* et al., 1983). Furthermore, budburst events of the same vine do not occur each year at the same day nor at the same mean temperature. The previous winter temperature may have a decisive role, as budburst occurs more equally if the winter is cold. A later winter pruning does postpone the budburst and might avoid frost damages (*Robinson*, 1995) but risks to reduce the maturation phase of the grapes later on.

Shoot growth Environmental factors highly influence shoot growth, with light, temperature and water supply equally important. Warm conditions, especially warm nights, are favourable to shoot growth. A cooler but luminous environment is good for shoot elongation but inhibits the formation of inflorescences. Generally, bud break and shoot growth is supposed to start at daily mean temperatures above 10 ℃, but for some varieties shoots already grow at lower temperatures (*Moncur* et al., 1989). Above the threshold temperature, the rate of bud break and shoot growth increases rapidly. The optimal growing temperature is about 25 ℃ - 30 ℃. Temperatures above 30 ℃ are only favourable at high air humidity.

Too low soil moisture inhibits shoot growth more than root growth. If the soil is too wet, roots are not getting enough oxygen and CHLOROSIS might occur. A good supply with nitrogen is favourable for shoot growth, but is also depending on soil moisture.

Not only climate conditions affect growth, but also pruning practices. For example, more, shorter, and thinner shoots are produced when pruning is minimal. Shoot growth can continue until fall, but usually this is not desirable because shoot maturation might be delayed which reduces frost resistance and bud survival, and nutrients are drawn away from the ripening fruit. Various procedures can be applied in order to stop vegetative growth: the vine is exposed to water stress, the shoot tips are trimmed, or devigorating (i.e., growth inhibiting) ROOTSTOCKS are used.

Formation of primordial inflorescences Bud development is highly influenced by environmental conditions. As the compound buds are already fixed in July, climate conditions affect the yield in the current and in the next year. All impacts favourable for photosynthesis enhance bud fertility. High light intensity, long day lengths, high temperatures and sufficient water supply encourage the development of inflorescence primordia (ANLAGEN). The formation of anlagen is favourable at temperatures above 25 ℃ with a temperature optimum between 30 ℃ and 35 ℃. This optimum is similar for all vine varieties, but there are differences in the development of inflorescences at low temperatures. Experiments have shown that Riesling exposed during three months to 20 ℃ developed a good productivity, in contrast to vine varieties of warmer regions which developed scarcely inflorescences (*Buttrose*, 1969). Cool summers provoke smaller and less anlagen. Also shading effects due to too dense plantation, trees, buildings, etc., decrease fertility and thus productivity.

Flowering and fruit setting Approximately two weeks after bud break flowering occurs, but the exact time is highly weather dependant. Usually the first flowers are observed at the uppermost shoots, but looking at flower clusters, blooming starts at the bottom of the cluster. The flowering event for a single cluster lasts only a few days under warm and sunny conditions. Looking at a whole vineyard, flowering is observable during 7 to 10 weeks, because of timing differences. The petals fuse into a unified enclosing structure, the CALYPTRA. Just before flowering the calyptra is separated from the RECEPTACLE and falls off. Discarding the calyptra often involves the rupture of the pollen sacs (ANTHESIS) which may lead to self-fertilisation. The opening of the pollen sacs is temperature dependant. In warm regions, flowering often begins when the mean daily temperature reaches 20 ℃, whereas in cooler climates the increase of day length stimulates flowering. However, below 16 ℃ only a few sacs will burst (*Winkler*, 1965). *Draganov and Draganov* (1975) give for the Pearl of Csaba variety a minimum of 14.6 ℃ and for late ripening varieties temperature thresholds between 17 ℃ and 19 ℃. Temperatures above 19 ℃ accelerate the anthesis, but temperatures higher than 32 ℃ are unfavourable for flowering. Under cold and rainy conditions, blooming may extend over several weeks. This may lead to an asynchronous fertilisation, thus to an undesirable range of fruit maturity at harvest.

The young berries need enough nutritive substances to grow, otherwise they may

fall off, which is called blossom drop or coulure. Some varieties are more sensitive to this phenomenon as other. During flowering, the vine has the highest vegetative growth and the shoot tip attracts the assimilates at most. If the conditions are favourable for excessive growth (high supply of nitrate and water, or fast growing vine stock), the berries do not get enough assimilates. Another reason for the lack of nutritive substances are cool periods or photosynthesis unsuitable weather conditions. Separating the terminal shoot will reduce the risk of blossom drop, but will also initiate an early development of lateral shoots.

Berry development and maturation After fertilisation, berries grow fast due to cell division. At the same time the amount of acidity is increasing to a maximum. A good water supply is necessary during this period, otherwise cell division is inhibited. An intelligent irrigation during July and August, in dry regions or in hot summers, may secure a sufficient yield quantity. Extensive irrigation might let grow berries too much and wine quality may decrease. High temperatures seem not to shorten the time between flowering and the acidity maximum, but rather to extent it (*Becker* et al., 1983). The time between flowering and acidity maximum depends on vine variety and is shorter for early ripening varieties like Rivaner.

Following its maximum, acidity is decreasing and must density is increasing (Figure 2.10). This turning point is the start of maturation process. During the maturation period, berries are primarily growing by enlarging the cells with juice and sugar and no more by cell division.

The acidity maximum is higher and earlier for warm sites and decreases faster than at cooler sites. Sugar concentration increases rapidly and simultaneously the amount of juice concentration is augmented. At high temperatures sugar RESPIRATION: $C_6H_{12}O_6 + 6\ O_2 \rightarrow 6\ CO_2 + 6\ H_2O$ is faster than photosynthesis. Therefore more sunlight hours are needed to generate a sugar surplus, rather than high temperatures (*Robinson*, 1995). The sugar content comes not only from the momentous assimilation of the leaves, but also from wood reserves and from the transformation of MALIC ACID ($C_4H_6O_5$). Thus malic acid is reduced because of direct interaction in the metabolism, dilution in the increasing juice amount, and through respiration: $C_4H_6O_5 + 3\ O_2 \rightarrow 4\ CO_2 + 3\ H_2O$. TARTARIC ACID ($C_6H_6O_6$) is reduced only by dilution, while its absolute mass is not varying much. The reduction of acidity and the augmentation of sugar is favoured during sunny and warm weather conditions during autumn. Berries which are directly exposed to sunlight have higher must density (1-6°Oe) and lower amount of acidity as shadowed grapes (*Koblet* et al., 1977). Light intensity is very important for the colour of red wine varieties, but with ongoing maturation the energy of sunlight becomes more important than the light itself. The reduction of acidity mainly depends on temperature. Below 20 ℃ the reduction is small and mainly sugar is respirated. Between 20 ℃ and 30 ℃ malic acid is metabolised and above 30 ℃ also tartaric acid is reduced, which is not always desired. By early ripening varieties or very hot summers/autumns, the must has low acidity. During cooler autumns, however, the wine has higher acidity. The reduction of acidity does not stop when the leaves begin to fall. Must density

can increase also after sugar accumulation by berry shrinkage and augmentation of the juice concentration (i.e., low water supply). Sufficient water supply during maturation is an important condition for sugar production. Excessive water supply leads to wines with a high and unripe acidity.

Chapter 3

3 Viticulture in the Upper Moselle region

3.1 Historical evolution of the wine region

Findings of chalices, storage items or wine-transporting vessels in the region alone do not allow to conclude that wine growing has been practiced in the region. Romans knew, however, about wine cultivation and their presence has been documented in the Moselle region. The first written source of viticulture is the travel report "Mosella" of Ausonius from around 370 AD, where he describes the landscape of the Moselle region (*Hahn*, 1956). The Moselle region became more important for wine with the progress of monasteries in the Middle Ages (*Institut Viti-Vinicole*, 2005). Vine was planted in all regions of today's Grand Duchy of Luxembourg and its surroundings. The famous cold snap in 1709 destroyed, however, almost all vineyards in Europe and in Luxembourg only those near the Moselle Valley survived.

The Congress of Vienna in 1815 had far reaching consequences for the region. Luxembourg lost the territories east of the rivers Our, Sauer and Moselle and many vineyards went to today's Germany. With the new border line also tariff regulations were introduced and the wine could not be easily sold. In 1842 Luxembourg joined the German Customs Union (Deutscher Zollverein) which simplified the commerce. During summer 1904 the American grape louse destroyed many vineyards (*Massard*, 2007). After the First World War (1st January 1919) Luxembourg had to leave the German Customs Union and was isolated from the German market. Sales problems were increasing and the union with Belgium in 1922 did not ameliorate the situation during this period. At the Luxembourgian Moselle mainly Elbling was cultivated and 90 % was exported as bulk wine to Germany. The regulation of the Treaty of Versailles imposed Germany to import 50000 hl of duty free wine from Luxembourg until 1926.

The viticulture gradually became orientated towards high quality production. A national institute for viticulture (Institut Viti-Vinicole) was founded in Remich in 1925. Five cooperative cellars were created in the period 1921-1930. In order to

highlight the quality of the wine, the label Marque Nationale was introduced on 15th March 1935. During the years 1920 and 1935 the cultivated area was reduced and with consolidation of cooperatives new areas for Pinot wine were created.

In contrast to Luxembourg, the German viticulture and the infrastructure at the Upper Moselle did not develop as fast. After the Congress of Vienna in 1815, Luxembourg established a road system, while in Germany most connections ended in Trier. The construction of the German railway line along the Upper Moselle around 1900 was meant only for military purpose. The vineyards were not well tended (the vines were not planted in rows and were too close to each other), although travelling teachers came to the Moselle region and imparted their knowledge (*Denkschrift*, 1911). The German viticulture was functional, limited to personal needs and did not concentrate on wine quality.

3.2 The cultivated vines in Luxembourg

Despite the huge territory losses after the Congress of Vienna, viticulture was responsible for prosperity in the Luxembourgian villages in the Moselle valley. The size of the viticulture area varied in the past: in 1865 it had an extent of only 875 ha which increased until the beginning of the 20th century to 1547 ha (*Denkschrift*, 1911). Today the area has receded to 1299 ha (*Weinjahr*, 2006). In addition, the regional distribution of vineyards has changed since 1911 (Figure 3.1). Nowadays vineyards are situated closer to the Moselle river and the largest areas are found in the southern part of the Luxembourgian Moselle region.

Under the terms of law only few vine varieties are allowed for wine production in Luxembourg (*Mémorial A*, Nº 73):

- Auxerrois (🍃)
- Chardonnay
- Dakapo
- Elbling (🍃)
- Gamay
- Gewürztraminer (🍃)
- Muscat Ottonel
- Pinot Blanc (🍃)
- Pinot Gris (🍃)
- Pinot Noir
- Pinot Noir précoce
- Riesling (🍃)
- Rivaner (🍃)
- Saint Laurent
- Silvaner

Other vine varieties are cultivated only for scientific purpose. The varieties marked by a leaf (🍃) - all are white wine varieties - are the most important and mainly investigated in this work.

The areal extensions of the cultivated vine varieties are shown in Figure 3.2 for three years, 20 years apart (1966, 1986 and 2006). Rivaner is the dominant vine sort for all periods. It is followed by Elbling in the earlier years. The cultivation of Elbling has decreased over the years and becomes comparable to the other vine varieties, except for Traminer whose cultivation area is very small. The bar "other" is very high in 2006 because of Pinot Noir, which was first cultivated in the early 1990s. This variety will not be considered in the further evaluations.

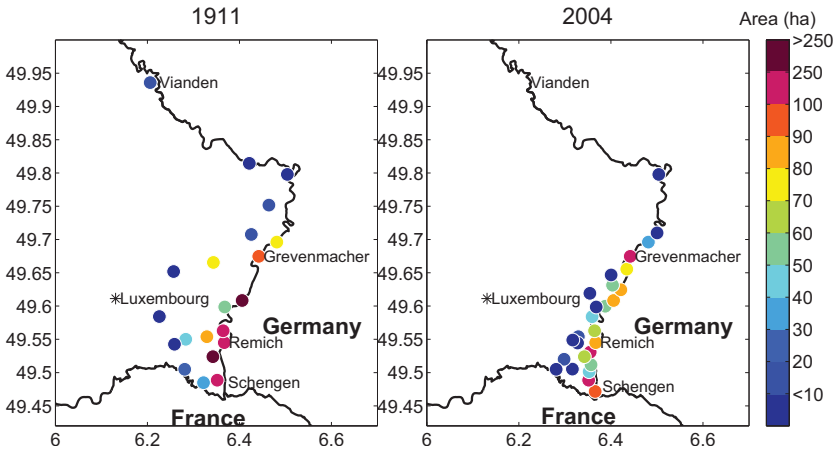

Figure 3.1: Distribution of the vineyards in the years 1911 (left) and 2004 (right).

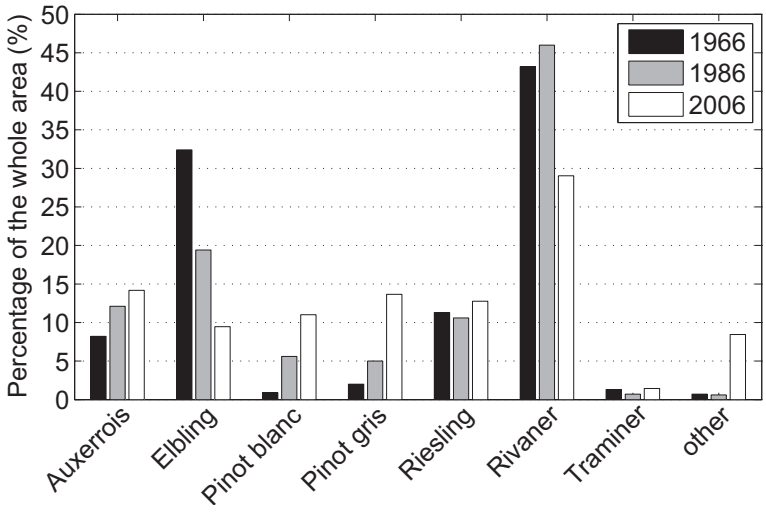

Figure 3.2: The cultivated vine varieties and their areal fractions for three different years. (Data source: *Weinjahr*, 1966-2006)

In the following, the selected vine varieties are presented. The main characteristics given by *Bundessortenamt* (2008) are summarised in Table 3.1.

Auxerrois The Auxerrois variety is a crossbreeding between Pinot and Gouais Blanc and seems to come from France. The flowering date is somewhat later than for Pinot Blanc, Pinot Gris, and Riesling. This variety has a low flowering firmness and is sensitive to spring frosts; therefore the cultivation site should be wind protected. The thin skin makes Auxerrois vulnerable to fungal infections but the grape is loose, thus the overall risk is comparable to other varieties. Must density is intermediate (comparable to Pinot Blanc, Pinot Gris and Riesling), however acidity is lowest compared to other cultivated varieties. The yield is low, which explains e.g. why this variety is not widely spread in Germany (only 0.3 % of the

area of cultivated white wine varieties (*Deutsches Weininstitut*, 2010)). The yield is below 60 hl/ha on average and largely fluctuating from year to year (*Hillebrand* et al., 2003).

Elbling Elbling is a crossbreed between Gouais Blanc, Vitis silvestris and Traminer. It is a very old variety, probably brought to the Moselle region by the Romans, but it could have also been present in this region earlier (*Hillebrand* et al., 2003). Elbling was widely spread over France, Switzerland, Luxembourg and Germany. Nowadays it is mainly found in Lorraine, Luxembourg and the German Moselle region. Flowering is late which protects the vine against late frost periods. The literature is inconsistent concerning blossom drop and ripening time. The *Bundessortenamt* (2008) indicates a low risk for blossom drop and a late ripening time, while *Hillebrand* et al. (2003) and *Robinson* (1995) note a high blossom drop and a very early ripening period. The yield is above 100 hl/ha, often it is around 200 hl/ha. The grapes are very compact, the skin thin, and thus the risk for fungal diseases is very high (e.g., PERONOSPORA, OIDIUM). Must density is lowest compared to other varieties and acidity is intermediate. Elbling is very suitable for the production of sparkling wine blended with other varieties, or nowadays also used genuine.

Pinot Gris or Ruländer Pinot Gris is a mutation of Pinot Noir, and sometimes there are red and white grapes on the same vine. Similar to Pinot Blanc the must density must be above 80 °Oe for quality wines, thus the cultivation site must be favourable. Pinot gris is very frost resistant during winter but less during springtime. It is not too sensitive against fungal diseases, despite the compactness of the grapes. Pinot Gris is also very resistive against BUNCH ROT, therefore it is possible to harvest very late and it is suitable for VENDANGES TARDIVES or VIN DE GLACE. The ripening period is late and the yield is relatively high with 80-120 hl/ha.

Pinot Blanc Pinot Blanc is a mutation of Pinot Gris. Flowering occurs at the same time as Riesling thus intermediate compared to the other varieties. Blossom firmness is high, so the risk of blossom drop is very low. The ripening period has an average length. The grapes are compact; nevertheless Pinot Blanc is resistant against fungal diseases, but sensitive to GRAPE MOTH. For a quality wine, the must density must exceed 80 °Oe; accordingly the site must be favourable and harvest should be late.

Riesling Riesling variety is a cross breeding of Gouais Blanc and an unknown variety. A long ripening period is necessary, thus full maturation is only achieved for warm sites. The vine is mainly cultivated on southwest to southeast exposed sites.The flowering period is similar to Pinot, while the ripening period is the latest of all seven investigated varieties. Riesling is not excessively vulnerable against fungal diseases but bunch rot may occur. Must density is moderate, the high

Table 3.1: Summary of the characteristics of the investigated vine varieties. Classification from *Bundessortenamt* (2008) with 1 low/early to 9 high/late. The blue and red marked values are the lowest and highest values for each characteristic.

	Aux	Elb	PiB	PiG	Rie	Riv	Tra
Budburst date	5	5	5	5	5	5	5
Flowering date	6	6	5	5	5	4	6
Blossom drop	4	3	2	3	3	3	3
Beginning of ripening	5	6	6	6	8	5	7
Grape density	4	7	7	7	6	6	6
Peronospora	4	6	3	3	3	7	3
Oidium	4	7	3	4	4	5	4
Botrytis	5	7	4	5	4	5	3
Must density	6	4	6	6	6	5	7
Acidity	3	6	5	5	7	4	4
Yield	4	7	5	5	5	7	4
Sensitivity to winter frost	5	5	5	4	3	6	3

acidity is a characteristic for Riesling wine and varies depending on the site. The yield is stable from year to year but relatively low (60-110 hl/ha). Riesling has a good lignification and is highly frost resistant. The vine survives frosts down to -20 ℃ to -25 ℃, provided a not too wet soil.

Rivaner The Rivaner, also known by the name Müller Thurgau, is a cross breeding between Riesling and Madelaine Royale; for a long time erroneously a cross between Riesling and Silvaner was supposed. Rivaner is early flowering and ripening, quite sensitive against drought, and has poor lignification. After moderately cold winters some vine plants may not survive. After short, very cold periods, whole vineyards may be destroyed. Rivaner is vulnerable to fungal diseases especially peronospora and has to be harvested before full maturation in case weather conditions are favourable to fungal dispersion. The advantages of Rivaner are high yields of 100-150 hl/ha due to high flowering firmness and very fertile secondary buds. Must density decreases, however, if the yield is very high. Acidity is generally low, and in favourable years it may also become too low.

Traminer The origin of Traminer - a variety for high quality wine - is unknown. Site requirements are very high; wind protection is a prerequisite and the soil must be profound and able to accumulate heat. One of the disadvantages is its sensitivity to chlorosis. Lignification is high and susceptibility to winter or spring frost is low because bud burst and especially flowering occur late. The secondary buds are infertile. Traminer is insensitive to fungal diseases, except when vines are planted too close. Must density is the highest compared to the other varieties while acidity is very low. The yield is very low with about 50 hl/ha.

3.3 Analysis of vine phenology and must quality

3.3.1 Observations

The Institut Viti-Vinicole of Luxembourg in Remich publishes every year the report *Weinjahr*, dealing with climate, vine phenology, wine quality and viticultural problems like diseases and pests. The first obtainable publication is dated to 1966, although there might exist earlier publications (Personal communication, S. Fischer). The last available booklet is from 2006. Unfortunately the booklets of 1971 and 1972 are not available, and for the year 2000 no differentiations regarding the vine varieties have been made, thus these three years have been left out in the study. Thus the phenological data ranges over 38 years. All data have been digitised for further evaluation.

The documented phenological data contain information about bleeding of pruning cuts, bud swelling, bud burst, primordial inflorescence, shoot growth, flowering, berry growth, berry softening and coloration, must density, acidity, quantity, and the harvest time. The most complete data over the years concern bud burst and flowering date as well as harvest time. The other phenological dates are not differentiated according to vine variety and/or are often missing in the reports, and are therefore not suitable for representative statistical evaluations. The calendar dates reported in the booklets have been converted to the scale day of year (DOY) in order to make the dates continuous. The 1st January corresponds to DOY 1 and the 31st December to DOY 365 (or DOY 366 on leap years). A table for transformation is given in the appendix (Table B.1).

Harvest time is very sensitive to viticultural practices and to a lesser extent to climate variability, thus the influence of climate cannot be easily distinguished from the effects of viticultural decisions. Must quantity is nowadays regulated by law due to an overproduction of wine in the EU and will therefore not be investigated.

Information on wine quality and quantity is very extensive. For each vine variety must density and acidity is divided into classes; the quantity for every class is described and sometimes even the revenues for the grapes is documented. The specifications are not always consistent and clear for every year. Therefore, in this work only the annual mean must density and mean acidity for different vine varieties have been examined.

The booklets do not provide any information about the locations of the observations. The data reflect average values for the Luxembourgian wine region and do not allow a more detailed regionalisation, although the highest density of vineyards is in the southern region (Figure 3.1). The observations will contain some uncertainties due to different observing locations and due to different observers.

3.3.2 Variability in the period 1966-2005

In this section the interannual variability and long-term changes of the phenological phases budburst and flowering, as well as must quality (must density and acidity)

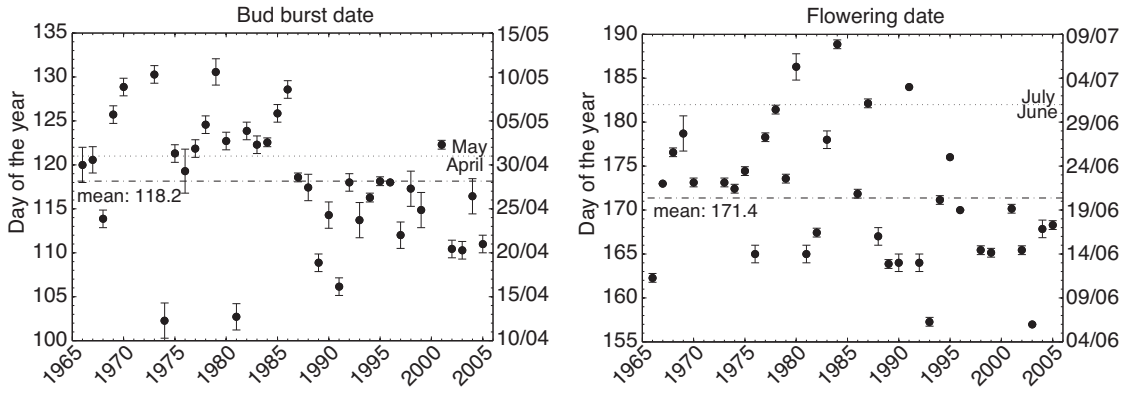

(a) Bud burst date (b) Flowering date

Figure 3.3: Time series of bud burst and flowering dates averaged over all cultivars. The bars show the range between the different varieties.

are presented. The term "quality" used here is not meant to give a full valuation of the must, since many other components determine the quality, which are not considered in this work. Must density is, however, a decisive factor for quality classification of wine in Germany and Austria (*Weingesetz*, 2009).

Phenology dates and must quality are given in the following for each variety separately and as an average of all vine varieties, referred as "ALL".

3.3.2.1 Budburst and flowering dates

Budburst date Budburst begins with the shoots sprouting from the buds (Section 2.3.3). Budburst marks the end of the winter rest and the beginning of the vegetation period. On average over all varieties, budburst occurs at DOY 118.1 (28th April) with a standard deviation of 7.1 days (Table 3.2). The earliest mean bud burst has been observed on DOY 102.3 (12th April) in 1974 and the latest on DOY 130.6 (11th May) in 1979, hence the range is about 4 weeks. Half of the budburst events (i.e. between the first (Q1) and third (Q3) quartile) occur between DOY 113.8 (24th April) and DOY 122.6 (3rd May). The single varieties behave very similar to the mean. Riesling has the latest mean bud burst (DOY 119) and Elbling the earliest (DOY 117.1), thus they differ on average only by two days. Regarding the decadal trends the vine varieties behave similar: budburst date advances between 1.9 and 2.3 days in 10 years. These trends are significant at 95 % level and the trend for the varieties Auxerrois, Pinot Blanc, Pinot Gris and Rivaner are even significant at 99 % level.

The time series of budburst since 1966 are presented in Figure 3.3a. The circles are the values of the mean budburst date ALL and the bars the range between the single varieties. A significant discontinuity of budburst date around 1989 is obvious. Before 1989 the dates were mainly in the beginning of May and afterwards at the end of April. First, a change of observers or observation method has been suspected. Then, an increase of the Moselle temperature was considered, since

Table 3.2: Statistical values for observed bud burst date of different vine varieties. The trend (days/decade) is for all vine variety significant on the 95 % level, some are also significant on the 99 % level and are marked in bold.

[DOY]	Mean	Std	Range	Min	Q1	Q3	Max	Trend
ALL	118.1	7.1	28.3	102.3	113.8	112.6	130.6	-2.1
Auxerrois	118.4	6.9	27.0	103.0	114.0	123.0	130.0	**-2.0**
Elbling	117.1	7.3	30.0	100.0	112.8	122.0	130.0	-1.9
Pinot Blanc	118.2	7.2	28.0	103.0	114.0	123.0	131.0	**-2.3**
Pinot Gris	118.1	7.2	29.0	102.0	113.5	123.0	131.0	**-2.1**
Riesling	119.0	7.0	28.0	104.0	115.0	123.0	132.0	-2.2
Rivaner	118.2	7.1	28.0	102.0	114.0	123.0	130.0	**-2.3**
Traminer	117.6	7.2	30.0	101.0	113.0	123.0	131.0	-2.1

Table 3.3: Statistical values for flowering date of different vine varieties. The trend (days/decade) is for all vine variety significant on the 95 % level.

[DOY]	Mean	Std	Range	Min	Q1	Q3	Max	Trend
ALL	171.3	7.9	31.9	157.0	165.3	176.9	188.9	-2.1
Auxerrois	171.5	7.9	32.0	157.0	166.0	177.3	189.0	-2.0
Elbling	171.1	7.9	32.0	157.0	165.0	177.3	189.0	-2.0
Pinot Blanc	171.4	8.1	32.0	157.0	165.0	177.3	189.0	-2.2
Pinot Gris	171.4	7.9	32.0	157.0	165.0	177.3	189.0	-2.2
Riesling	171.8	7.6	32.0	157.0	165.8	176.3	189.0	-1.9
Rivaner	171.0	7.8	31.0	157.0	165.0	176.3	188.0	-2.0
Traminer	171.2	8.1	32.0	157.0	165.0	176.5	189.0	-2.0

a French nuclear power station went on line about 20 km upstream and also air temperature shows a discontinuity at that time. Unfortunately, this effect could not be analysed, since it was not possible to get the Moselle temperature data from the Service de Radioprotection of Luxembourg (see also Chapter 4.1). But this inhomogeneity does not seem to be a local phenomenon. The same phenomenon has been observed for different plants in Central Europe (*Scheifinger* et al., 2002). The authors have found a close relationship with a change in the Northern Atlantic Oscillation (NAO) but they point out, that this displacement could also have other reasons. Such a regime shift around 1989 is not only observed for plants but also for zooplankton (*Schlüter* et al., 2010): an increasing sea surface temperature has let to earlier "blossom" of zooplankton in the North Sea.

Flowering date Inflorescences are very sensitive to rain or cold temperatures. They can fall off or become infertile if the weather conditions are unfavourable during this period. Hence, the weather during or shortly before blossom plays an important role for the yield in autumn.

The flowering dates of the different vine varieties are very close (on average between the DOY 171 and DOY 172, Table 3.3). The Luxembourgian wine growers use to say, the vine is flowering at National Day which is on 23rd June (DOY 174). In half of the years since 1966 vine flowered between DOY 165 (14th June) and DOY 177 (26th June). The earliest date was in 2003 at 6th June and the latest in 1984 at 8th July. The range of the flowering period is the same as for the budburst dates and amounts to one month. The trends in flowering date are, like for budburst date, between 1.9 and 2.2 days per 10 years. A discontinuity in the flowering time series like the one in the bud burst series is not clearly visible (Figure 3.3b). Perhaps the flowering did not respond to this shift or it is masked by a very late flowering period during the 1980s.

3.3.2.2 Must density and acidity

Must density Must density is a measure for the ripening state of the grapes and is an indicator for the appropriate harvest time. Must contains, besides water, about 90 % sugar, the rest are acids, glycerin, PHENOLS, PECTINS, proteins and minerals. The density of must is higher than water and this difference defines the Oechsle scale (°Oe) for must density: $°Oe = (\rho_{must} - \rho_{water}) \times 1000$ with $\rho_{water} = 1g/cm^3$. Must density is measured using a hydrometer or a refractometer. The latter method is very easy to operate on site in the vineyard; few berries are crushed and the refraction is determined. The higher the refraction, the higher the density is. The degree Oechsle scale is mainly used in Luxembourg, Germany and Switzerland, but there are also other measuring units like KMW, "Klosterneuburger Mostwaage" (Italy, Austria, Hungary, Slovakia), degree Baumé (France and Spain) and Brix (english speaking countries). These units have nonlinear relations, thus usually tables are used for conversions.

Grape sugar content varies depending on species, variety and maturity. When the investigated vine varieties are clustered according to their must density by means of hierarchical cluster analysis using the Euclidean distance (Section A.3) two main groups are formed (Figure 3.4a):

- Group CM1: Auxerrois, Pinot Blanc, Pinot Gris, Riesling and Traminer,
- Group CM2: Elbling and Rivaner.

The differences of must density between varieties are shown in Table 3.4. With a mean must density of 69.4 °Oe, the Group CM1 is characterised by an higher ($\varnothing_{CM1}$ = 72.7 °Oe) and the Group CM2 by a lower ($\varnothing_{CM2}$ = 61.2 °Oe) must density. For all vine varieties the year 1984 produced the lowest must density, while the maximum must density for Group CM1 was reached in 2003 and for Group CM2 in 1997 and 2003 (Figure 3.5). Must density increased significantly since 1966 for both clusters. The trend of Group CM1 (3.9 °Oe or 5.3 % per decade) is stronger than the one of Group CM2 (2.4 °Oe or 3.9 % per decade). The strongest increase of must density shows Riesling with 6 % or 4.3 °Oe per decade.

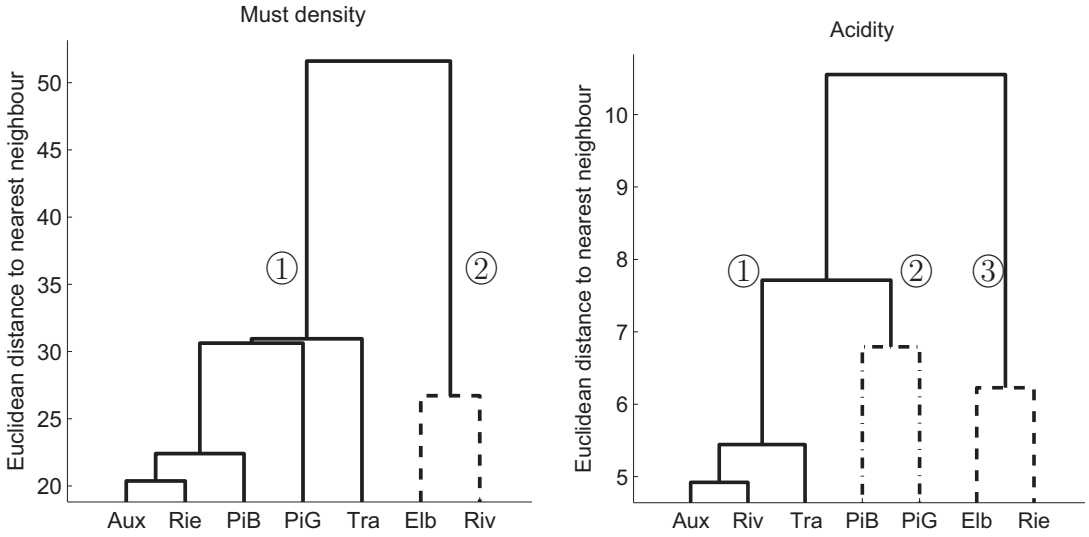

(a) Must density clusters CM1 and CM2 (b) Acidity clusters CA1, CM2, and CA3

Figure 3.4: Dendrogram showing the hierarchical clustering of must density and acidity for different vine varieties. The linkage is done on the base of the shortest distance of must density and acidity, respectively, between the varieties. Clusters are marked by different line types.

Table 3.4: Statistical values for must density of different vine varieties. The trend (°Oe/decade) is for all vine variety significant on the 99 % level and the relative change is given in percent. ALL is the average of all varieties, Group CM1 and Group CM2 are averages of the varieties defined in Figure 3.4a.

[°Oe]	Mean	Std	Range	Min	Q1	Q3	Max	Trend
Cluster CM1	72.7	7.6	32.2	57.4	67.8	76.8	89.6	+**3.9** (5.3 %)
Cluster CM2	61.2	5.8	24.5	50.0	58.5	64.5	74.5	+**2.4** (3.9 %)
Auxerrois	70.6	7.6	31.7	53.3	66.0	75.0	85.0	+**4.0** (5.7 %)
Elbling	59.8	5.9	26.4	48.6	56.0	63.0	75.0	+**2.3** (3.8 %)
Pinot Blanc	70.0	7.1	32.0	54.0	66.0	75.0	86.0	+**3.0** (4.3 %)
Pinot Gris	74.6	7.8	35.0	58.0	69.0	80.7	93.0	+**3.7** (4.9 %)
Riesling	70.5	8.3	33.0	56.0	65.0	75.0	89.0	+**4.3** (6.1 %)
Rivaner	62.6	6.3	29.0	50.0	57.0	66.0	79.0	+**2.2** (3.5 %)
Traminer	78.6	8.5	38.0	61.0	73.0	83.1	99.0	+**4.3** (5.4 %)

Acidity Grapes contain different types of acids which modify the perception of taste and mouthfeel sensations, especially a reduction in perceived sweetness. Acids are involved in the precipitation of pectins and proteins that otherwise could make a finished wine cloudy (*Jackson*, 2008). A low pH has also a beneficial antimicrobial effect. In the following acid types are not differentiated, only total acidity is considered.

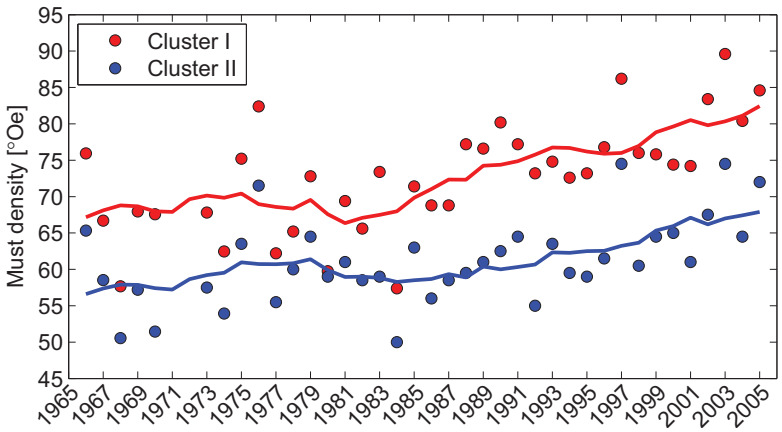

Figure 3.5: Time series of must density of cluster CM1 and cluster CM2 (dots). The line is a moving average of 9 years.

Table 3.5: Statistical values for acidity of different vine varieties. The trend ((g/l)/decade) is for all vine variety significant on the 99 % level and the relative change is given in percent. ALL is the average of all varieties, Group CA1, Group CA2 and Group CA3 are averages of certain varieties defined in Figure 3.4b.

[g/l]	Mean	Std	Range	Min	Q1	Q3	Max	Trend
Cluster CA1	8.4	1.9	7.6	4.8	7.1	9.6	12.5	**-0.87** (10.4 %)
Cluster CA2	10.2	2.1	8.7	5.8	8.7	11.8	14.6	**-0.85** (8.3 %)
Cluster CA3	12.3	2.9	12.3	7.1	10.3	13.9	19.5	**-1.12** (9.1 %)
Auxerrois	8.5	2.1	8.7	4.9	7.1	9.6	13.5	**-0.95** (11.2 %)
Elbling	12.2	2.7	11.1	6.7	10.3	14.1	17.8	**-1.23** (10.1 %)
Pinot Blanc	10.7	2.1	9.2	6.2	9.0	12.2	15.4	**-0.80** (7.5 %)
Pinot Gris	9.7	2.0	8.3	5.5	8.3	11.2	13.8	**-0.91** (9.4 %)
Riesling	12.5	3.2	13.6	7.5	10.5	13.6	21.1	**-1.12** (9.0 %)
Rivaner	8.5	1.4	5.9	5.7	7.4	9.2	11.6	**-0.68** (8.0 %)
Traminer	8.0	2.3	9.7	3.9	6.2	9.4	13.6	**-0.99** (12.4 %)

Similar to must density, the vine varieties are arranged in three groups by their acidity applying cluster analysis (Figure 3.4b):

- Group CA1: Auxerrois, Rivaner and Traminer,
- Group CA2: Pinot Blanc and Pinot Gris,
- Group CA3: Elbling and Riesling.

Group CA1 is characterised by the lowest (8.4 g/l) and Group CA3 by the highest acidity level (12.3 g/l). Group CA2 is an intermediate group, which behaves very similar as the mean acidity of all vine varieties. The year with the lowest acidity was 2003 for all varieties (Figure 3.6). As expected from the results for must density, the

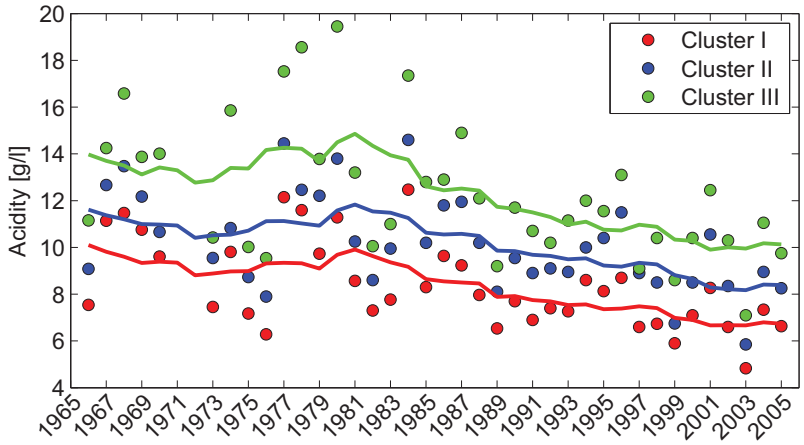

Figure 3.6: Time series of acidity of the cluster CA1, cluster CA2 and cluster CA3 (dots). The line is a moving average of 9 years.

year 1984 brought very acid wines; the year 1980 showed a high acidity, too. From the beginning of the seventies until mid eighties, acidity was very variable from year to year. Afterwards, the year to year variations are lower, accompanied by a significant decreasing trend with 0.9 g/l per decade for Group CA1 and CA2 and 1.1 g/l per decade for Group CA3. Thus, the latter group has the highest acidity but also the highest reduction trend. The highest trend is observed for Riesling (1.1 g/l per decade) but its relative change is only 9 %, i.e., Riesling occupies at mid range compared to other varieties. The highest trend is observed for Traminer where acidity decreased by 12.4 % per decade.

3.3.3 Short summary

In this chapter the seven investigated vine varieties were presented. The main focus was put on the inter-annual variability of budburst and flowering event dates as phenological data, and must density and acidity as must quality measures in the period 1966-2005. Budburst and flowering dates recessed significantly by more than 2 days per decade, equally for all varieties. For must density and acidity the varieties have been split into groups using clustering methods. Nevertheless, the trends follow the same direction and are highly significant. Must density has increased by 2-4 °Oe per decade and must acidity has decreased by 0.7-1.1 g/l per decade depending on vine variety. The highest relative change in acidity is observed for Traminer and Auxerrois, 12.4 % and 11.2 %, respectively. Their relative change in must density is also high (5.5 % - 4.0 %) but the highest is observed for Riesling.

The observed changes in phenology and must quality raise the question about changes in climate as they are closely linked as discussed in Chapter 2, Section 1.1. The characterisation and evaluation of the climate in the Upper Moselle region is presented in the following chapter.

Chapter 4

4 Observed climate of the Upper Moselle region

4.1 Observations

Long climate data sets are essential to analyse climate variability and change. The available phenological data records start in 1966, therefore climate time series are taken for the same period. Long climate records are sparse in the Upper Moselle region and the selection of stations has to be made carefully as the orography is quite structured. Three different institutions operate meteorological stations in the region: the German Meteorological Service (DWD) in Germany, the Administration des services techniques de l'Agriculture (ASTA) and the Institut Viti-Vinicole (IVV) in Luxembourg (see Figure 4.1 for station locations). The measurement periods at eight precipitation and seven temperature stations are shown in Figure 4.2. The stations are listed from north to south. Unfortunately, the precipitation stations Borg, Besch, Nennig, and Grevenmacher do not cover the entire time period while the stations Temmels and Konz are quite distant from the main Luxembourgian wine region. Thus only the stations Remerschen and Remich remain. Since Remerschen offers the longest continuous time series (1954-2007), this station is chosen for the further analysis.

The meteorological data have different time intervals. Precipitation is available at daily resolution. The climate stations report according to different measurement schemes. Most recorded daily maximum, minimum and mean temperature (Grevenmacher, Remich, Nennig, Besch), whereas others have measured at fixed hours (Trier, Nennig) or even hourly (Trier-Petrisberg, Perl). The longest time series are available for Trier-Petrisberg; but this station is too far away from the investigated region. Except for the station in Remich no stations have continuous records. Fortunately, the stations Besch and Nennig are close to each other (< 3 km), which suggests a combined time series. The temperature measured simultaneously by both stations has been averaged. Since the temperature means of the periods before and after the overlapping period are the same and since no inhomogeneity has been detected at the merging points the data is treated as a

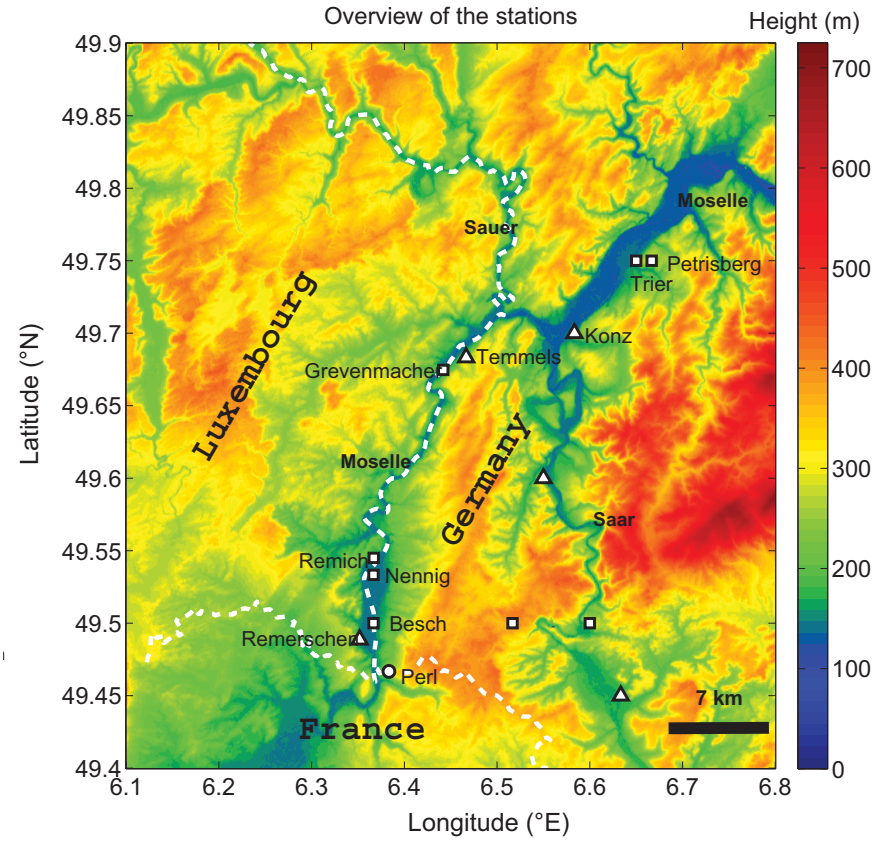

Figure 4.1: Orography of the regions Moselle, Sauer and Saar with location of meteorological stations: △ only preciptitation, ○ only temperature, □ stations measuring several variables.

single time series and will be referred to the time series Besch/Nennig.

Besides temperature and precipitation also sunshine duration is important in this work. This data has been taken from the meteorological station in Trier because the time series are much longer than those of the station in Remich. Both time series are in good agreement in the overlapping periods despite their geographical distance of about 30 km.

Usually, water temperature of big rivers is higher than air temperature in winter and vice versa in summer. It would have been interesting to investigate this influence on the vine phenology for the Moselle region. The Service de Radioprotection in Luxembourg analyses the water of the Moselle for radioactive contamination and monitors the water temperature (*Schmitz*, 2010; *Chambre des Députés*, 2006) since the nuclear power plant in Cattenom in France discharges its cooling water into the Moselle River. Unfortunately the Service de Radioprotection of Luxembourg did not give access to this data.

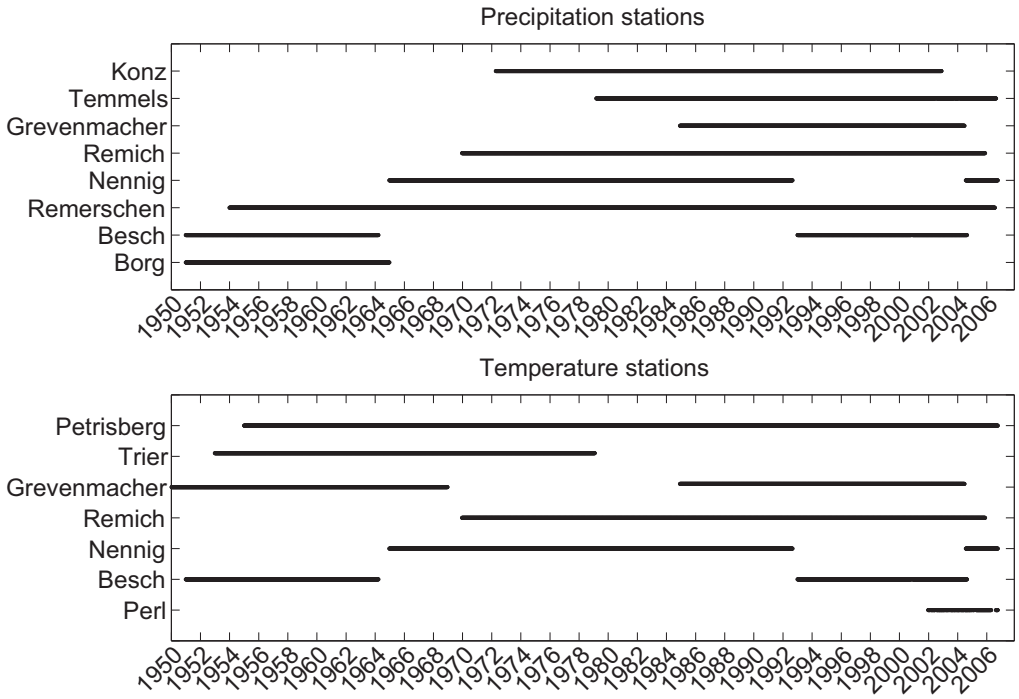

Figure 4.2: Measurement periods for precipitation and temperature.

4.2 Mean climate conditions (1951-2005)

In the analysed period, the observed climate of the Upper Moselle region is characterised by a mean annual temperature of 9.9 ℃, a mean minimum temperature of 5.5 ℃ and a mean maximum temperature of 14.9 ℃ (Table 4.1). On average, there are 165 rainy days (threshold 0.1 mm) per year (45 % of the days per year) at the Upper Moselle with a mean annual precipitation sum of 770 mm. The warmest months are July and August; the coldest ones are January and February with a mean minimum temperature of about -1 ℃. Precipitation is quite homogeneously distributed over the year, except for February, March and April which are characterised by the lowest precipitation amounts (Figure 4.3).

Following the mean thermal and humidity conditions, the climate of the Upper Moselle (represented by the stations Besch/Nennig and Remerschen) corresponds to *Cfb* climate according to climate classification of Wladimir Köppen and Rudolf Geiger (*Köppen*, 1918). This indicates a temperate climate with warm summers and enough precipitation, but without a dry season. The classification result agrees with the results of *Peel* et al. (2007), who classified both France and Western Germany as Cfb. The region of the Hunsrück, a low mountain range east of the Luxembourg-Germany frontier, is classified as Dfb (cold climate with warm summers and no dry season).

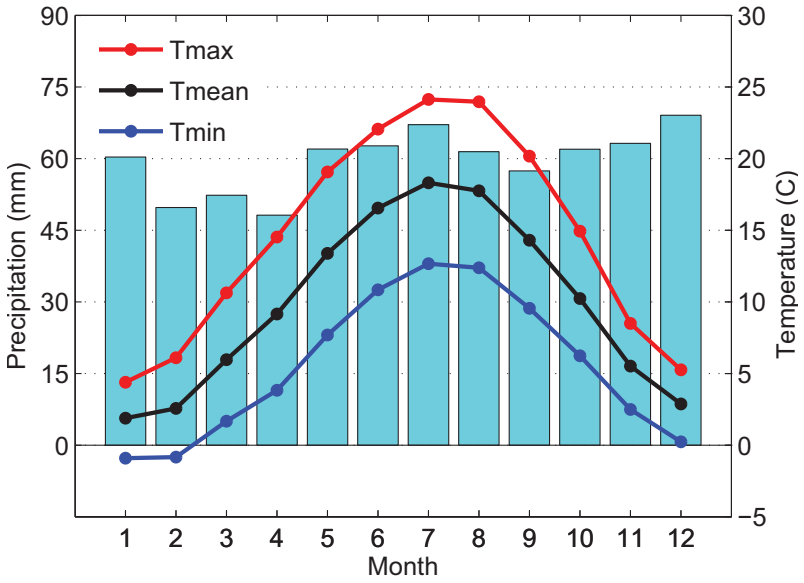

Figure 4.3: Mean annual cycle of precipitation and temperature (1951-2006) at the station Besch/Nennig; precipitation (bars), temperature: minimum (blue), mean (black) and maximum (red).

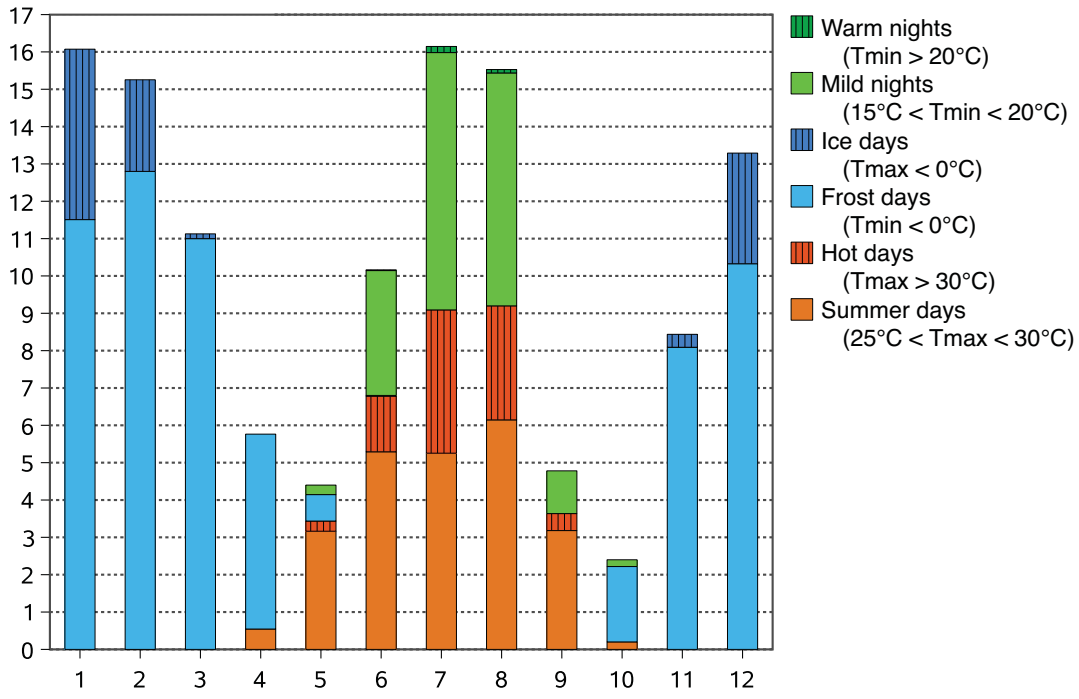

Figure 4.4: Monthly mean number of days above different temperature thresholds in the period 1951-2005. Hot days, ice days and warm nights are special cases of summer days, frost days and mild nights, respectively.

Table 4.1: Statistical characteristics of the annual maximum (Tmax), minimum (Tmin) and mean (Tmean) temperature, precipitation (Prec) and sunshine duration (SD) for the period 1951-2005. Quantities calculated using annual data.

	Tmax [°C]	Tmin [°C]	Tmean [°C]	Prec [mm]	SD [h]
mean value	14.5	5.5	9.9	770	1565
standard deviation	0.9	0.8	0.8	141	171
range	4.1	3.5	3.6	550	844
minimum	13.1	3.9	8.2	483	1298
	(1956)	(1956)	(1956)	(1953)	(1965)
maximum	17.2	7.4	11.8	1033	2143
	(1992)	(2000)	(1992)	(2000)	(2003)
1st quartile	13.8	4.9	9.4	670	1448
3rd quartile	15.1	6.1	10.4	871	1675

Table 4.2: Statistical characteristics of the annual temperature indices (1951-2005).

	Hot days	Summer days	Frost days	Ice days	Mild nights	Warm nights
mean value	9	33	73	11	19	0.3
standard deviation	7	10	18	9	9	0.7
range	31	43	82	45	38	4
minimum	0	15	31	0	5	0
	(1965)	(1965)	(2000)	(1974)	(1974)	(45 years)
maximum	31	58	113	45	43	4
	(2003)	(2003)	(1955)	(1963)	(2003)	(2003)
1st quartile	4	27	61	4	12	0
3rd quartile	13	40	85	14	23	0

The thermal conditions are described in more details by different temperature indices recommended by the Expert Team on Climate Change Detection and Indices (*ETCCDI*, 2010). For every month of the period 1951-2005 the following temperature indices are derived from daily observations: number of frost and ice days, number of summer and hot days as well as number of mild and warm nights (Figure 4.4). During frost days the minimum temperature is below 0 °C. Ice days are the subset of frost days with maximum temperatures below 0 °C. On summer days the maximum temperature is above 25 °C while for its subset hot days the maximum temperature is above 30 °C. Mild nights have a minimum temperature above 15 °C and in its subset warm nights a minimum temperature above 20 °C.

In the following analysis, hot days, ice days or warm nights are not considered as a subgroup of summer days, frost days and mild nights in order to have disjunct groups. Here, e.g., summer days are defined as days with maximum temperature above 25 °C and below 30 °C. Frost days are occurring from October to April,

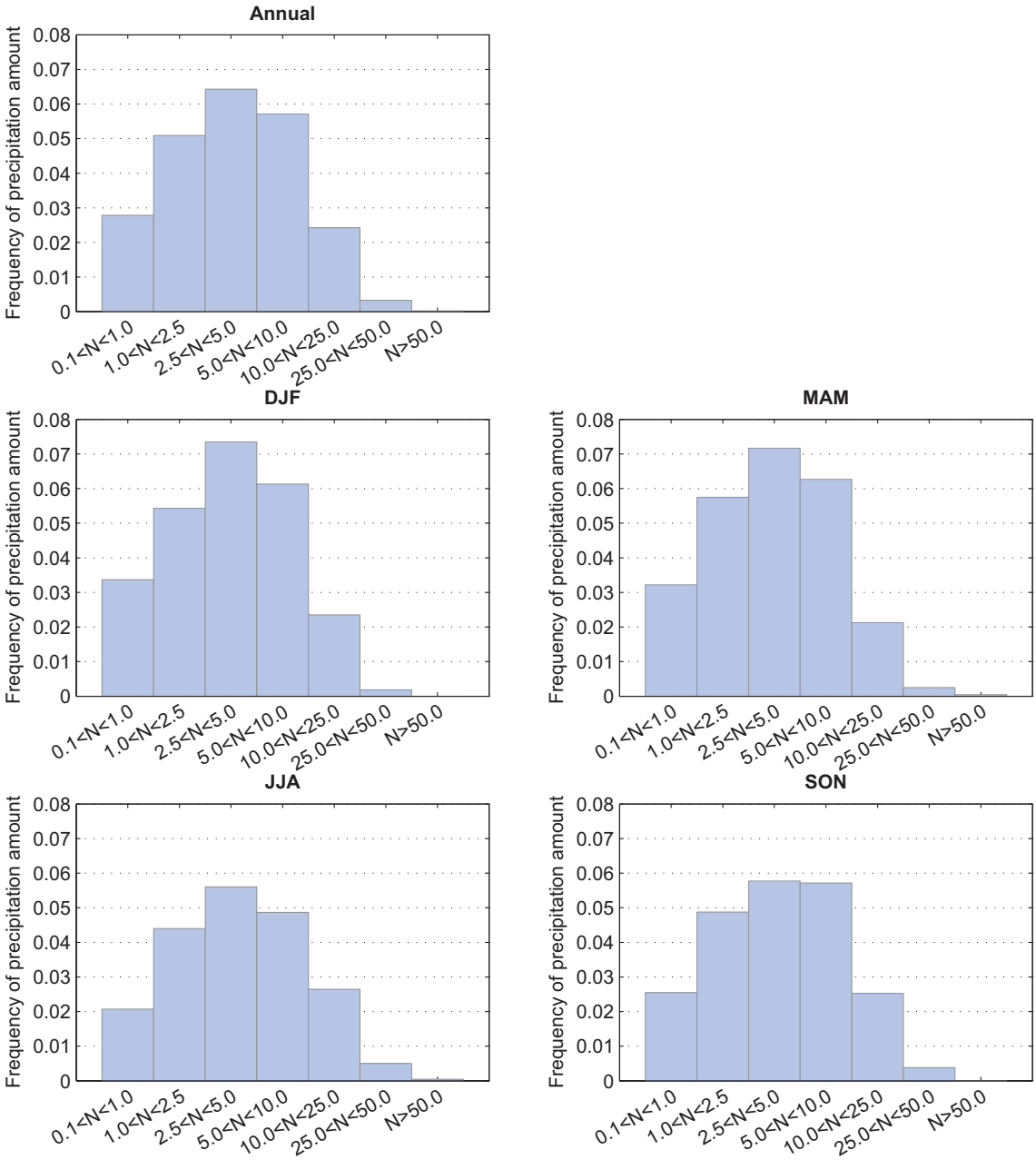

Figure 4.5: Frequency distribution of precipitation amount normalised by the total precipitation weighted with the width of the precipitation classes. (Station: Remerschen (1951-2005))

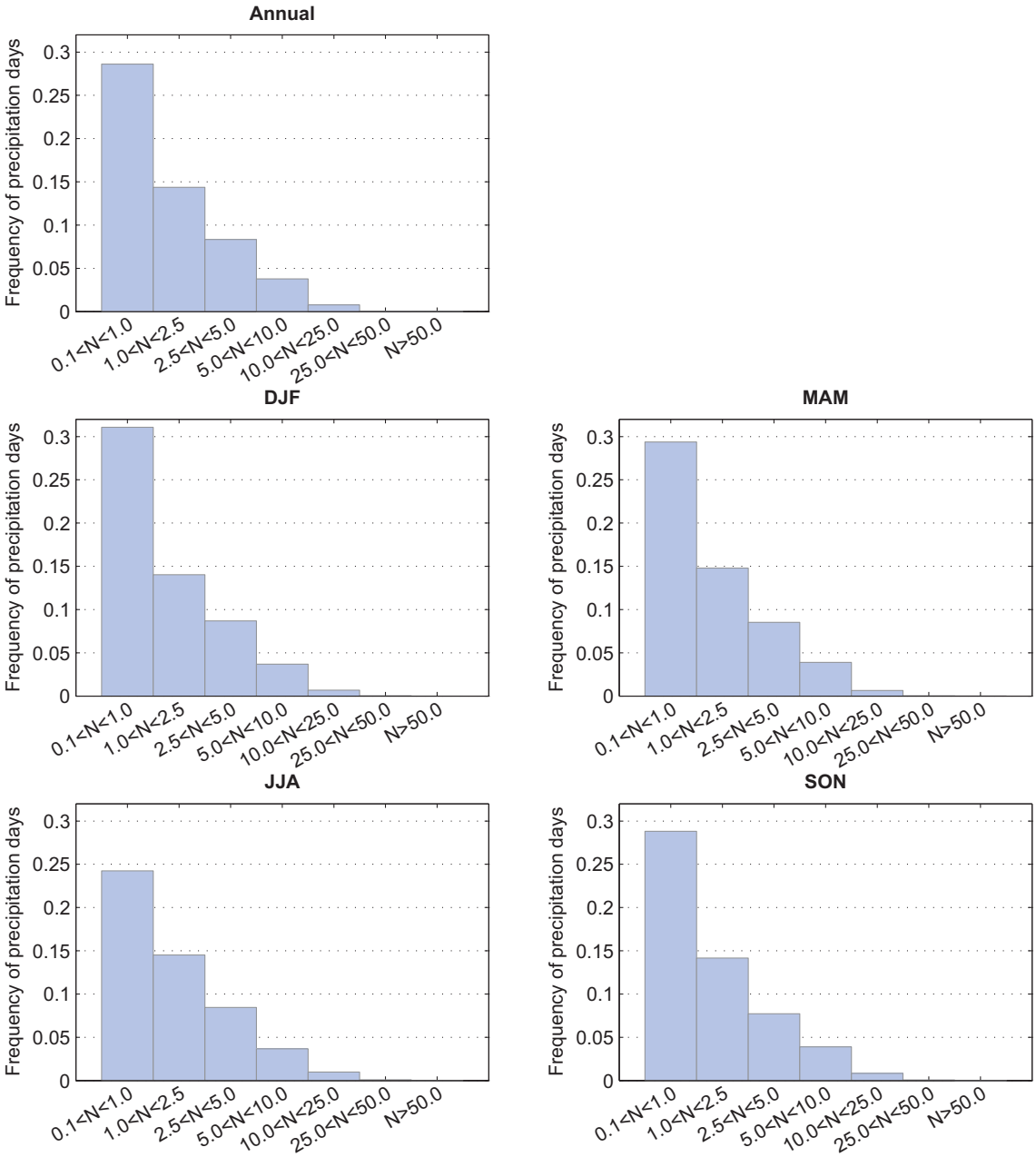

Figure 4.6: Frequency distribution of precipitation days normalised by the sum of rain days weighted with the width of the different precipitation classes. (Station: Remerschen (1951-2005))

exceptionally also in May. The highest amount of ice days happen during January, but also during December and February ice days often occur. Summer days happen on average first in April and last until September, although in some years they can also be found in October. Hot days and mild nights occur mainly between June and August. Warm nights are rather seldom at the Upper Moselle region; only 15 nights where classified as warm since 1951.

Heavy rainfall events are very important for viticulture because they can severely damage vineyards. Therefore, precipitation is divided into intensity classes. The most frequent precipitation class for rainy days is the one with less than 1 mm/day (Figure 4.6). Days with stronger precipitation occur accordingly less frequent. Precipitation events above 25 mm/day are quite rare. Days with more than 50 mm/24h occurred only four times during 1951 and 2005. The distribution of annual precipitation days is comparable for all seasons. Only in summer the first class is less probable when compared to the other seasons. Although the class below 1 mm/day is much more frequent than the other classes, most of the rain comes from the classes between 1 mm/day and 10 mm/day (Figure 4.5). The most representated class of precipitation amount is the one between 2.5-5 mm/day on annual and seasonal scale. In autumn, however, precipitation amounts between 5 and 10 mm/day produces the same amount of rain as the precedent class. Unfortunately, short but heavy rain events cannot be distinguished from long, continuous but light rainfalls.

4.3 Variability and changes of climate in the period 1951-2005

Besides statistical characteristics of mean conditions, the variability and development of the climate on inter- and intra-annual scale is also of high interest. The division into seasons gives more information about the periods in which climate varies most. They also allow better conclusions on plant development than annual means do.

4.3.1 Temperature

The range of the mean annual temperature values is rather narrow with 4.1 ℃ for maximum temperature and about 3.5 ℃ for minimum and mean temperature (Table 4.1). Fifty percent of the maximum temperature data ranges between 13.8 ℃ (1st quartile) and 15.1 ℃ (3rd quartile). The coldest year in the period 1951-2005 is 1956, where minimum, mean and maximum temperature were lowest. The year with highest maximum and mean temperature values is 1992, but the highest minimum temperature has been measured in 2000.

The time series of the annual and seasonal mean temperatures are shown in Figure 4.7. A moving average over 5 years (green line) is applied. The dashed line is a polynomial approximation (4th degree) and shows turning points in the data, as a simple trendline might lead to wrong conclusions. The minimum and

Table 4.3: Annual and seasonal temperature trends in ℃/decade. Significant trends at the 95% level in bold. P1: entire period 1951-2005, P2: period 1951-1979 and P3: 1979-2005.

	Tmax			Tmin			Tmean		
	P 1	P 2	P 3	P 1	P 2	P 3	P 1	P 2	P 3
Annual	**0.20**	-0.25	**0.74**	**0.28**	0.20	0.36	**0.26**	0.12	**0.46**
DJF	0.12	0.08	0.54	0.17	0.47	0.36	0.15	0.34	0.40
MAM	0.09	**-0.07**	**0.90**	**0.31**	0.22	0.36	**0.21**	-0.10	**0.50**
JJA	**0.35**	-0.01	**0.96**	**0.31**	0.05	**0.51**	**0.36**	0.25	**0.59**
SON	-0.01	-0.3	0.35	0.15	0.01	0.13	0.12	-0.04	0.19

mean temperatures monotonically increase by 0.023 ℃ ± 0.015 ℃ and 0.023 ℃ ± 0.013 ℃ per year (99 % significance level) over the whole period, respectively. The maximum temperature reveals no clear tendency. A period of low values fall in the 1970s, while the lowest annual maximum, mean and minimum temperatures were measured in 1956. After a period of slightly decreasing averaged annual daily maximum temperature (by −0.029 ℃/year, non-significant), an increasing trend of +0.066 ℃/year is observed from 1980 onwards, which is significant at the 99 % level.

Although, the year 1992 was the warmest one for the average of annual maximum and the average of mean temperatures, the highest number of hot days, summer days, warm nights and mild days has been registered in 2003 (Table 4.2). The coldest winter was in 1963 with 45 ice days, while the year 1955 had the highest amount of frost days (113 days).

Taking the non monotonic tendency into account, trends were calculated for the entire period (P1: 1951-2005) as well as for the sub-periods 1951-1979 and 1979-2005 (Table 4.3). The least square trend approximation and the test of Mann and Kendall (*Mann*, 1945; *Kendall*, 1970) give a positive trend for all time series, but they are only significant at the 95 % level in spring and summer time. No significant trend in autumn and winter is detectable. The maximum temperature in spring shows a cooling between 1951 and 1979, while a significant increase from 1978 to 2005 is observed. Minimum and mean temperatures rise significantly during the entire spring period. A warming over the periods 1951-2005 and 1978-2005 is highly significant (>95%) in summer.

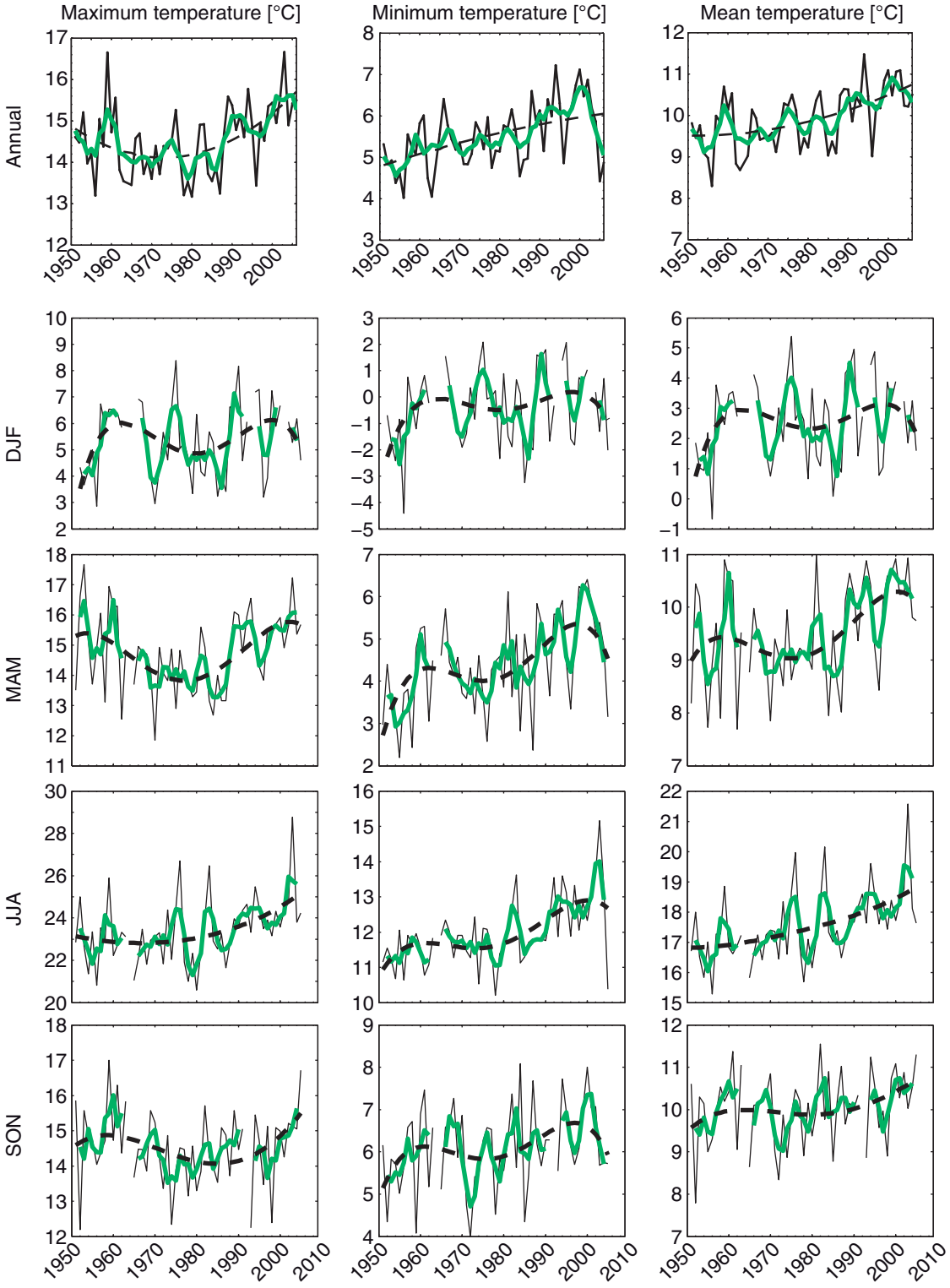

Figure 4.7: Time series of annual and seasonal maximum, minimum, and mean temperature (black line) at the station Besch-Nennig. The green line is a moving average over 5 years and the dashed line a polynomial approximation (4th degree).

4.3.2 Precipitation

Precipitation in the Upper Moselle region fluctuates considerably from year to year (Table 4.1). The year 2000 was the wettest year with the highest total precipitation (1033 mm/year) and 1953 the driest one (483 mm/year). The time series of annual and seasonal precipitation measured at Remerschen are shown in Figure 4.8a and the corresponding statistical characteristics are summarised in Table 4.1. The highest trend is observed in winter, although it is significant only on the 86 % level. Due to decadal/interdecadal variations the long-term changes are more visible in different intensity classes than in the annual and/or seasonal total precipitation time series (Figures 4.8 and Table 4.4).

The first two classes with precipitation lower than 2.5 mm/day are quite constant over the years (Figure 4.9). The other categories up to 50 mm/day have a high variability from year to year. During the whole time period, precipitation of 1 mm/day to 5 mm/day has significantly decreased (Table 4.4). Higher classes have a positive trend at a significance level lower than 95%. Between the years 1951 and 1985, precipitation below 5 mm/day decreased, whereas the precipitation between 10 mm/day and 25 mm/day has become more frequent. The same shift is observed for the period 1961 to 1995, but here precipitation lower than 2.5 mm/day has not changed significantly. During the period 1971-2005 annual precipitation shows no significant shift between the classes.

Table 4.4: Linear trend of precipitation sums for different intensity classes and different periods. Significant trends according Mann-Kendall test are highlighted with colour.

Intensity classes	Period							
	1951-2005		1951-1985		1961-1995		1971-2005	
	Trend	SI*	Trend	SI*	Trend	SI*	Trend	SI*
$N \geq 0.1 < 1.0$	+	62 %	–	98 %	+	63 %	+	86 %
$N \geq 1.0 < 2.5$	–	98 %	–	96 %	–	75 %	–	90 %
$N \geq 2.5 < 5.0$	–	96 %	–	98 %	–	96 %	–	51 %
$N \geq 5.0 < 10$	+	81 %	–	56 %	+	62 %	+	88 %
$N \geq 10 < 25$	+	83 %	+	98 %	+	98 %	–	70 %
$N \geq 25 < 50$	+	85 %	+	83 %	–	81 %	–	51 %

*) Significance level

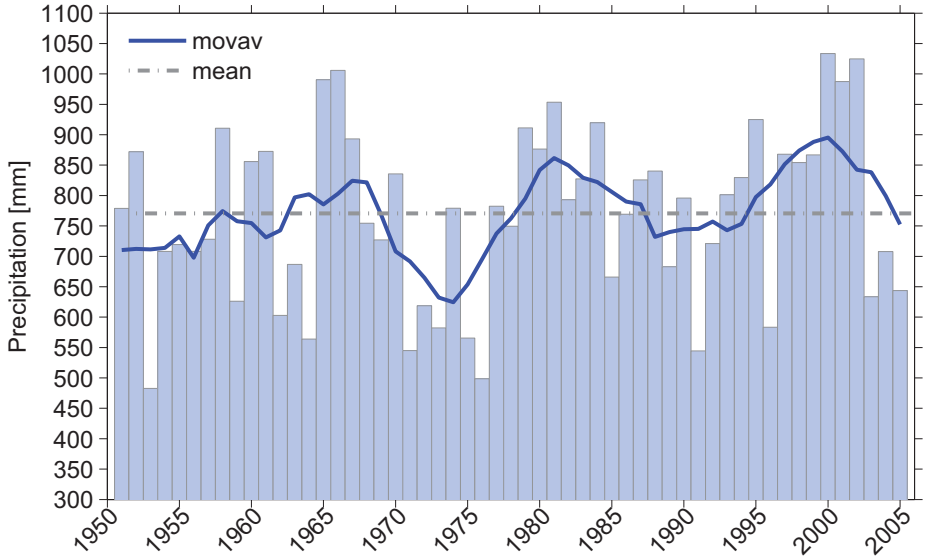

(a) Annual precipitation

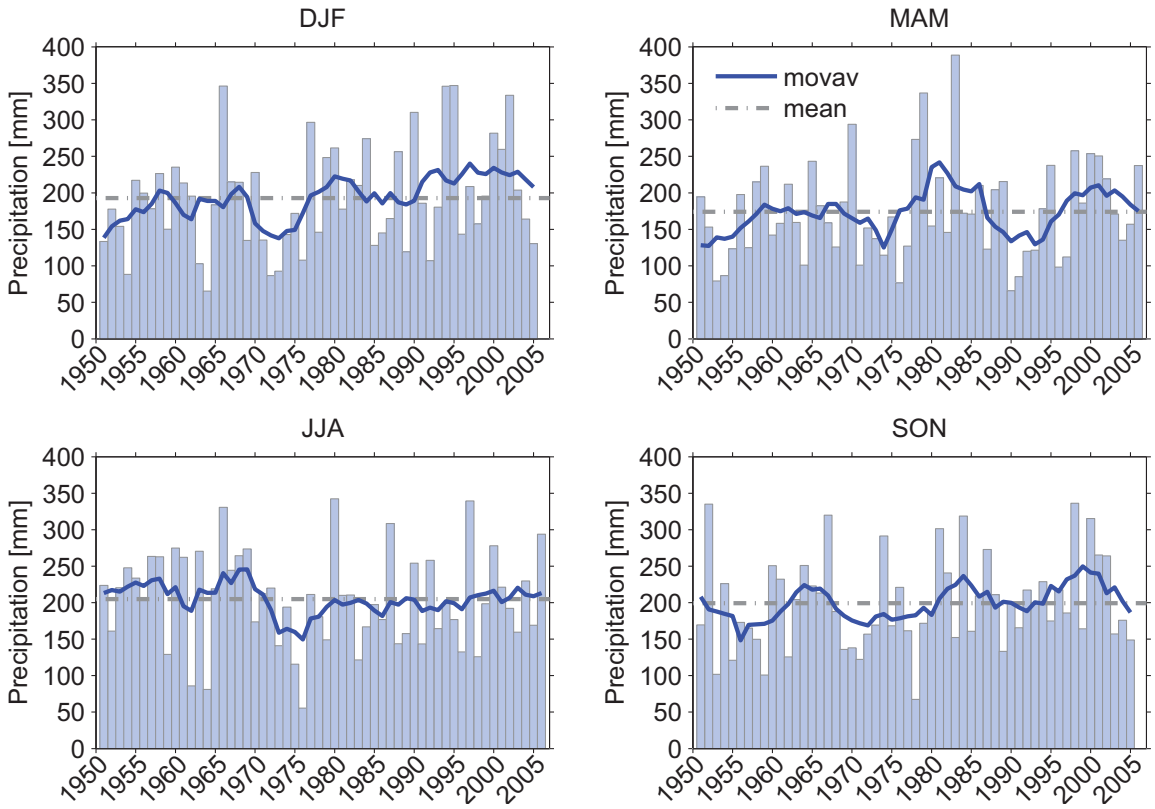

(b) Seasonal precipitation

Figure 4.8: Time series of annual (a) and seasonal (b) precipitation (columns). The blue line is a moving average over 6 years and the dashed line is the mean annual/seasonal precipitation sum. (Station: Remerschen)

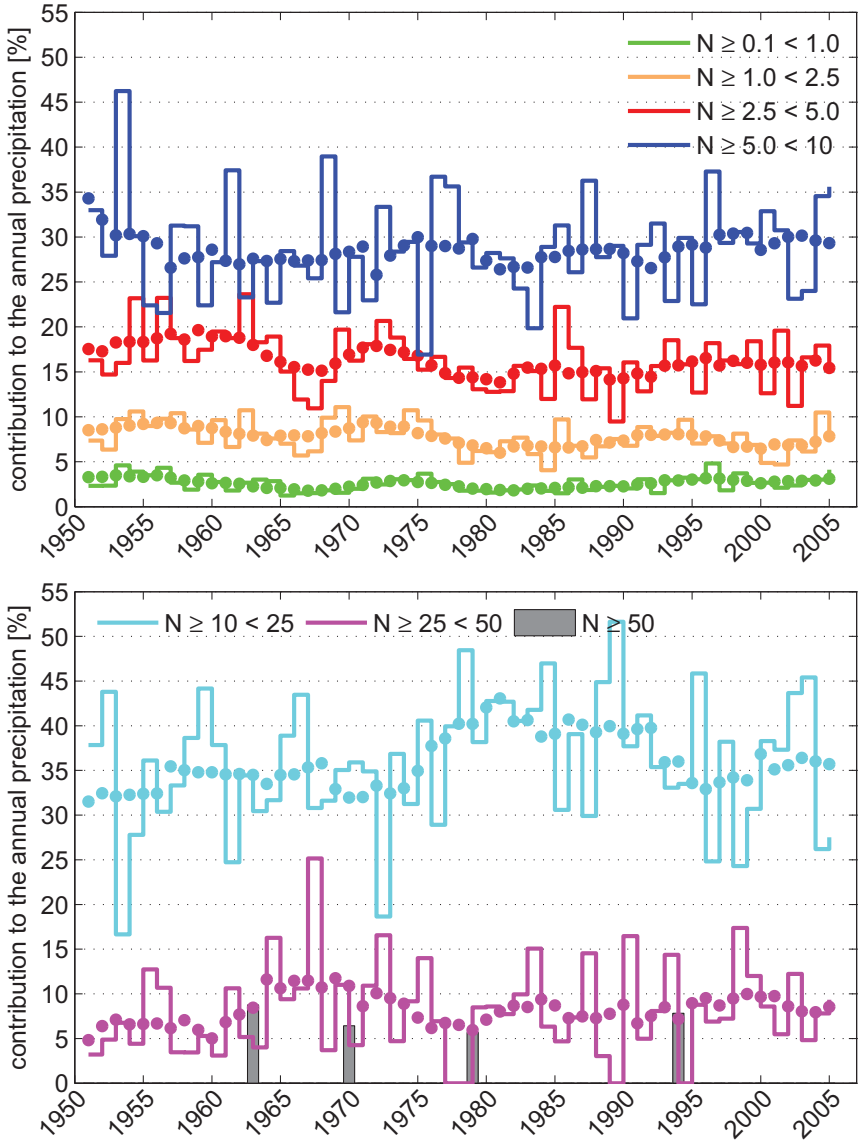

Figure 4.9: Time series of annual precipitation splitted into precipitation classes with moving average. (Station: Remerschen)

4.3.3 Sunshine duration

The course of annual sunshine duration is depicted in Figure 4.10a. The moving average over 6 years shows a local minimum during the sixties and one at the end of the seventies. At the beginning of the seventies sunshine duration has been high and the moving average is above the mean sunshine duration of 1565 h per year. Since 1985 the sunshine duration is higher than average, except for a local minimum between 1998 and 2002. During the year 2003 the highest sunshine duration has been measured since 1950, although it was also exceptionally high during 1959 and 1976.

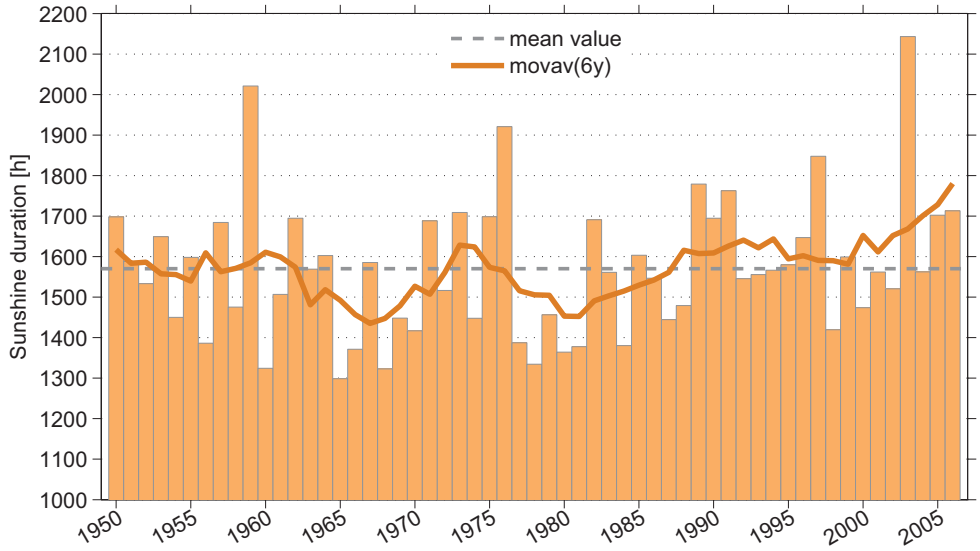

(a) Annual sunshine duration

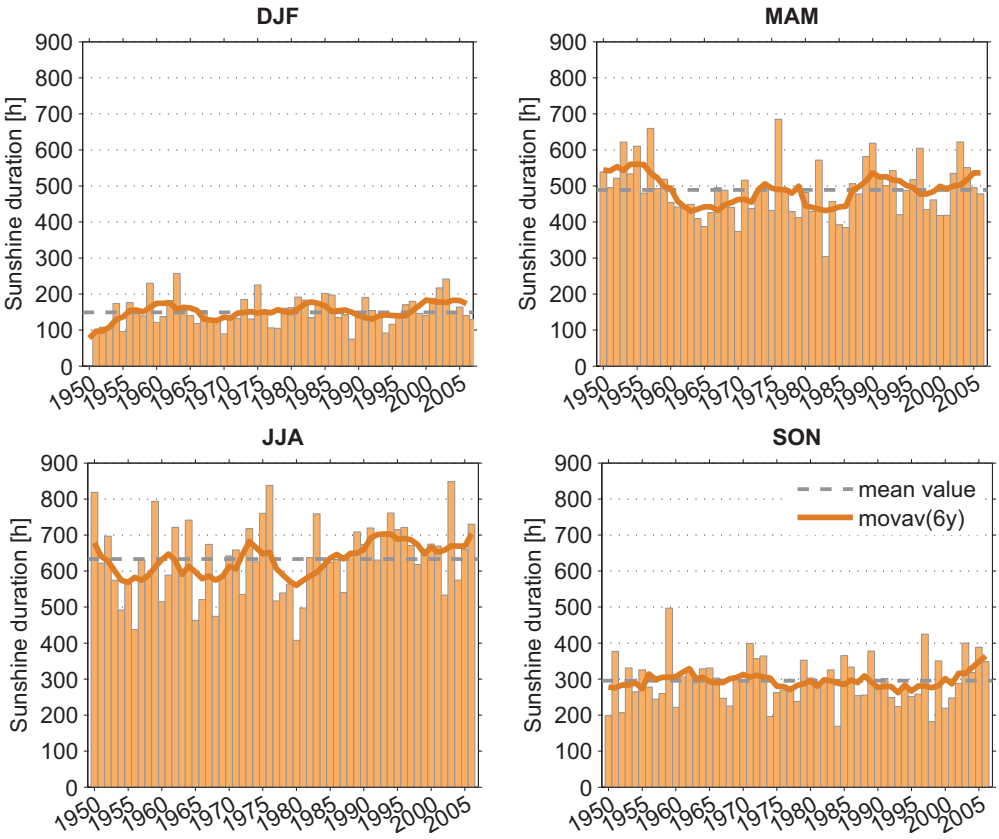

(b) Seasonal sunshine duration

Figure 4.10: Time series of annual and seasonal sunshine duration (1951-2006). The solid line is a moving average over 6 years and the dashed line is the average over the whole period. (Station: Trier-Petrisberg)

Even though annual sunshine duration is highly variable from year to year, an increasing trend of 22 hours per decade is significant on the 90 % level.

The lowest sunshine duration is observed in winter with an average of 150 hours over 3 months (Figure 4.10b). In spring the sun shines on average almost 500 hours and in summer about 630 hours. The sunshine duration in autumn is between spring and winter with 295 hours from September until November.

Sunshine duration has increased significantly (93 % level) by 4.3 hours per decade in winter. A much more important increase is observed during summer. Here, sunshine duration has augmented by 15.5 hours per decade and this trend is significant on the 96 % level. During spring and autumn, however, no significant trend can be detected.

4.3.4 Short summary

Annual mean screen-level temperature has increased significantly since 1951 by 0.26 ℃ per decade. Maximum temperature had a minimum during the seventies, while annual minimum and mean temperature are steadily increasing. This behaviour is less pronounced on the seasonal scale. Significant trends are only observed during spring and summer. These trends are also higher during the period 1979-2005 as for 1951-1979.

Precipitation has not changed significantly during the investigated period. There are high fluctuations on annual and seasonal scale, but on average it is quite equally distributed during the whole year, thus there are no especially dry nor wet intra-annual periods, on average. The division of precipitation into classes shows also no important changes.

Annual sunshine duration has increased by 22 hours per decade since 1951. During winter and summer sunshine duration has significantly increased but during spring and autumn no trend has been detected.

The climate conditions at the Upper Moselle meet the minimum requirements for profitable viticulture according to the criterions from *Stock* et al. (2007), *Huglin and Schneider* (1998) and *Blaich* (2000c) shown in Table 4.5. Sunshine duration and precipitation are sufficiently high. The minimum value of precipitation is below the suggested limit, but water deficit may be compensated by irrigation with water taken from the Moselle. In general, temperature requirements are also fulfilled, although summer temperatures are close to the lower required limit; the Huglin Index actually advises for half of the years against commercial viticulture. On average, however, there is enough heat available for vine-growing especially for Rivaner. The highest Huglin index measured in the region is 2103, which indicates a climate even suitable for Ugni blanc, Grenache and Syrah to become mature. The Huglin index has a highly significant trend of 4.4/year between 1951-2005 and even 15.4/year since 1985.

Table 4.5: Required climate conditions (assembled from *Stock* et al. (2007), *Huglin and Schneider* (1998), *Blaich* (2000c)) and measured mean climate conditions for 1951-2005 in the Upper Moselle region.

	Required	**Measured**
Yearly sunshine duration	>1250 h	1461 h
Days without frost (vegetation period)	>180 d	221 d
Mean temperature:		
Annual	>8°C	9.9°C
Winter (DJF)	around 0°C	2.4°C
Summer (JJA)	around 20°C	17.5°C
April-October	>13°C	14.3°C
July-October	>16°C	15.2°C
or hottest month	>18°C	18.3°C
May-June	>15°C	15.0°C
Tolerable extremes:		
Winter (DJF) temperature	-25°C (-15°C)*	-21°C
Summer (JJA) temperature	around 45°C	40°C
Precipitation during vegetation period:		
Minimum	300 mm	232 mm
Optimum/mean	420 mm	451 mm
Maximum	700 mm	651 mm
Huglin Index:		
Minimum	1500**)	1183
Mean	/	1515
Median	/	1500
Maximum	/	2103

*) depending on duration, and health of the vine plants

**) threshold depends on vine variety, under 1500 no commercial wine cultivation is suggested

Chapter 5

5 Statistical modelling of phenological events and must quality

During the last 40 years budburst and flowering in the Upper Moselle region receded to earlier days, must density has increased, and acidity decreased. Annual mean temperature has increased significantly as well as spring and summer temperatures. Precipitation did not change substantially, but annual sunshine duration shows a significant positive trend. It is known that the growing cycle of grapevine is influenced by the environment, especially climate. The goal of this chapter is to find the important climate signals which are responsible for the trends in phenology and must quality.

In order to find an answer to this issue, the statistical relations between a comprehensive pool of potential predictors and climate variables is analysed in the following. Regression models are developed in order to link phenology and must quality to climate conditions and to estimate phenology and must quality from meteorological parameters.

5.1 Stepwise regression model

A commonly used procedure in the statistical modelling is the stepwise regression, which can be performed using a forward selection method, a backward elimination method or a combination of both (*Wilks*, 2006; *Bortz*, 1993; *Sachs*, 1978). In this study, the combination method is applied.

Regression method Forward selection starts with the predictor, which has maximum correlation with the predictand. In a step-wise fashion further predictors x_i are added from the pool of potential predictors based on maximum positive impact (i.e. increase of explained variance) on the regression. The chosen measure is the regression **sum of squares (SSR)** defined by the difference between the **total**

sum of squares (SST) and the **error sum of squares (SSE)**:

$$\begin{aligned} SSR &= SST - SSE && (5.1)\\ &= \sum_{i=1}^{n}(y_i - \bar{y})^2 - \sum_{i=1}^{n}(y_i - \hat{y}_i)^2 && (5.2)\\ &= \sum_{i=1}^{n}(\hat{y}_i - \bar{y})^2 && (5.3) \end{aligned}$$

where $\hat{y}_i$ estimated predictand for the ith year and $\bar{y}$ mean of n observations y. With $\hat{y}^k$ is the estimated predictand based on k predictors, the corresponding regression sum of squares, SSR^k is given by

$$SSR^k = \sum_{i=1}^{n}(\hat{y}_i^k - \bar{y})^2 \tag{5.4}$$

The model scheme is shown in Figure 5.1, with the forward selection method marked by the green boxes. In the first step SSR^1 is computed for all predictors, and the predictor with the highest SSR^1 is kept. Then a second predictor is added to compute SSR^2; again the predictor leading to the highest SSR^2 is kept, but only if the increase in SSR, i.e. $SSR^2 >> SSR^1$ is significant on 95% level according to the F-test (*Wilks*, 2006). Then, a further predictor is tested in the same way, and the procedure is continued, computing at each step the F parameter via

$$F = \frac{SSR^{k+1} - SSR^k}{\frac{1}{n-(k+1)}SSE^{k+1}} \tag{5.5}$$

where SSR^{k+1} is the SSR for the tested enhanced regression equation with $k+1$ predictors and sample size n, while SSR^k is the SSR of the previous step with k predictors.

The forward selection method would continue until SSR^{k+1} is not significantly greater than SSR^k, meaning that no further contributing predictor can be found. However, an already selected predictor may become insignificant, if a new one is added (*Efroymson*, 1960). This complication is resolved by the backward method (blue boxes in Figure 5.1). Obviously the backward scheme is used if three or more predictors have already been selected by the forward scheme. In the backward scheme, each of the selected predictors is removed once while keeping all the others. This leads to $k-1$ new values of SSR^{k-1}. If the highest SSR^{k-1} is not significantly lower than SSR^k this predictor is removed. The remaining selected predictors are tested again whether one of them becomes insignificant. If, however, $SSR^k \gg SSR^{k-1}$, the omitted predictor is kept and the forward selection method proceeds again.

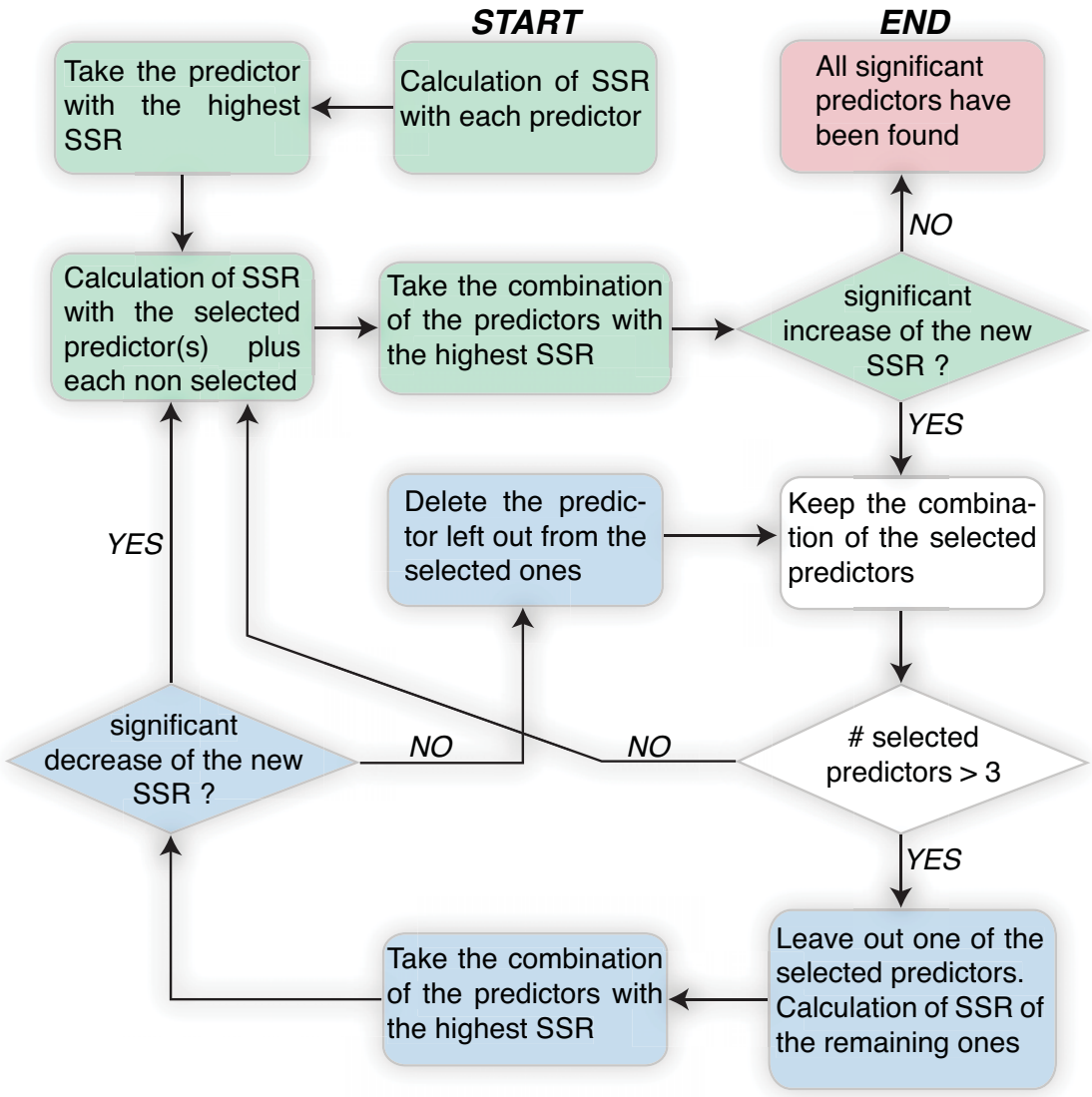

Figure 5.1: Scheme of the stepwise regression model procedure containing the forward selection method (green boxes) and the backward elimination method (blue boxes).

Reduction of the predictor pool For an independent evaluation, the whole data set is usually split into: a training data set based on which the model is developed, and an independent data set, on which the model is tested. In this study, the observational data is too small for separating it into two sufficiently long parts. Instead a bootstrap method is used by repeating the regression model derivation n-times each time omitting one year of the dataset. Only those predictors, which are selected at least once in the n regression models are finally kept in the pool of predictors. The final regression equation is calculated by the forward-backward combination using the reduced pool of predictors.

Cross validation control The interaction of forward and backward regression steps generally prevents model overfitting. Nevertheless controlling the optimum number of predictors is of advantage. In some cases one predictor is very powerful and inhibits the addition of other predictors. In such a case the approximation found would have a high explained variance, but a model with a similar one using more predictors and with a higher biological meaning could also exist.

Cross validation can be used to clarify this aspect (*Wilks*, 2006): Such a situation may exist, when the optimum number of predictors identified by cross validation disagrees considerably with the number of significant predictors found by the regression method. In this study, cross validation often suggested a model with only one predictor, usually a temperature accumulating predictor. Such a model is, however, not very meaningful (*Due* et al., 1993) and e.g., does not explain delay of phenological events. The responsible, i.e. the dominant, predictor is then isolated and a new regression equation is calculated.

In order to obtain the optimum number of predictors (i.e., more than one and less than 10), the cross validation based on the leave-one-out method is used. The number of predictors k is increasing from one to the number of available predictors. Here, the cross validation iteration is stopped at the 10th predictor. For every fixed k the regression model is applied n times using $n-1$ observations, i.e. the ith year is left out. The regression algorithm still contains forward and backward steps, but now it stops when the given number k of predictors is reached.

For every k, $n-1$ equations are obtained and the corresponding dependent variables $\{y_m | m \in [1,n], m \neq i\}$ are called *developmental data*. These equations are applied on the respective omitted ith year and the dependent variables y_i are called *cross validation data*. For every k, the average of the mean squared error of the developmental data (MSE_m) and the cross validation data (MSE_i) is computed. The MSE_i gives an indication of the expected prediction error for other independent data; MSE_m gives the model error (i.e., for dependant data) and is decreasing with increasing k. The optimum number of predictors k_{opt} is where the prediction error is smallest, i.e. $k_{opt} = \min(MSE_i)$. Following *Wilks* (2006) it is not always necessary to strictly limit the number of predictors according the lowest prediction error if the predictors contribute to scientific understanding. However, the prediction error should be low and close to the minimum.

5.2 Results of phenology and must quality estimation

Models for the phenological events budburst and flowering and for must quality (must density and acidity) have been developed. The predictors used are mainly meteorological, but the phenological phases budburst and flowering date are also offered to the regression method as prior phenological phases because they have, from a biological point of view, an important effect on the flowering date and on must quality. For the phenological models the pool of predictors contains about 80

predictors (Tables B.2 and B.3), for must quality models the predictor pool contains about 160 predictors (Table B.4). The meteorological predictors were chosen by systematically dividing the 3 or 4 months before the phenological event into several sub periods of 1-4 weeks. Prior phenological events are taken into account when already a regression equation exists.

5.2.1 Budburst event and flowering dates

Budburst date The budburst model is based on the budburst date averaged over the seven studied vine varieties. The cross validation results are shown in Figure 5.2a. The prediction error is minimal at 3 predictors; an increasing number of predictors would increase the prediction error. Taking three predictors the relative model error is 2.4 % and the relative prediction error 3.2 %. The selected predictors are: degree days in March (DD3), maximum temperature in April (TX4), and number of frost days from January to March (FD1-3). The degree days (DD) are calculated with the single triangle method of *Zalom* et al. (1983):

$$DD = \begin{cases} 0, & \text{if } T_L > T_{max} \ , \\ T_{mean} - T_L, & \text{if } T_L < T_{min} \ , \\ \dfrac{(T_{max} - T_L)^2}{2(T_{max} - T_{min})}, & \text{if } T_{min} < T_L < T_{max} \ , \end{cases} \tag{5.6}$$

with T_L a threshold temperature where the vine begins to grow, T_{max} the maximum temperature, T_{mean} the mean temperature and T_{min} the minimum temperature.

The regression coefficients and the explained variance are presented in Table 5.1. The model is applied to all vine varieties separately with the same predictors but different coefficients. It performs similarly well for the different vine cultivars: the explained variance ranges between 80 % and 84 % depending on variety. The degree days in March contribute most to the explained variance. High values of degree days in March and maximum temperature in April move budburst date backwards. A high amount of frost days from January to March delays bud break. This stands in close agreement with *Pouget* (1964) who concluded: the higher the temperature the faster and earlier the budburst date, provided previous temperatures were not too low. The investigated varieties have similar budburst dates, thus no important differences are expected.

The time series of observed and calculated budburst events are compared in Figure 5.3. The model for budburst event has a correlation of 0.91 with the observations and the root mean squared error is below three days. About 90 % of the residuals are in the range of ± 4.8 days. Beyond this interval a too late budburst date was calculated only for 1991 (7.5 days) and 1974 (5.7 days). During both years, the vegetation period begun very early. In 1974 maximum temperature in April was higher than usual and that year budburst date has been earliest since 1959 (*Weinjahr*, 1974). During April 1991 a strong frost period damaged many vine stocks (*Weinjahr*, 1991).

Table 5.1: Total explained variance (R^2), contribution of the selected predictors to R^2 and regression coefficients of the budburst model for each and averaged (ALL) vine varieties.

	Total R^2	Contribution to R^2			Regression coefficients			
	in [%]	DD3	TX4	FD1-3	const	DD3	TX4	FD1-3
ALL	82.9	64.1	14.0	3.8	142.62	-0.36	-1.69	+0.13
Auxerrois	84.1	66.3	14.2	3.6	142.16	-0.35	-1.62	+0.12
Elbling	80.8	62.8	13.7	4.3	141.27	-0.36	-1.70	+0.14
Pinot blanc	83.2	64.9	15.3	3.0	144.12	-0.36	-1.74	+0.12
Pinot gris	82.2	65.7	12.5	4.0	141.68	-0.36	-1.61	+0.13
Riesling	80.8	63.0	14.6	3.2	144.49	-0.36	-1.73	+0.12
Rivaner	83.3	67.8	12.2	3.3	142.09	-0.38	-1.60	+0.12
Traminer	81.2	59.6	16.4	5.2	143.54	-0.34	-1.89	+0.16

Note: Predictors: **DD3** degree days in March, **TX4** maximum temperature in April, **FD1-3** frost days from January to March

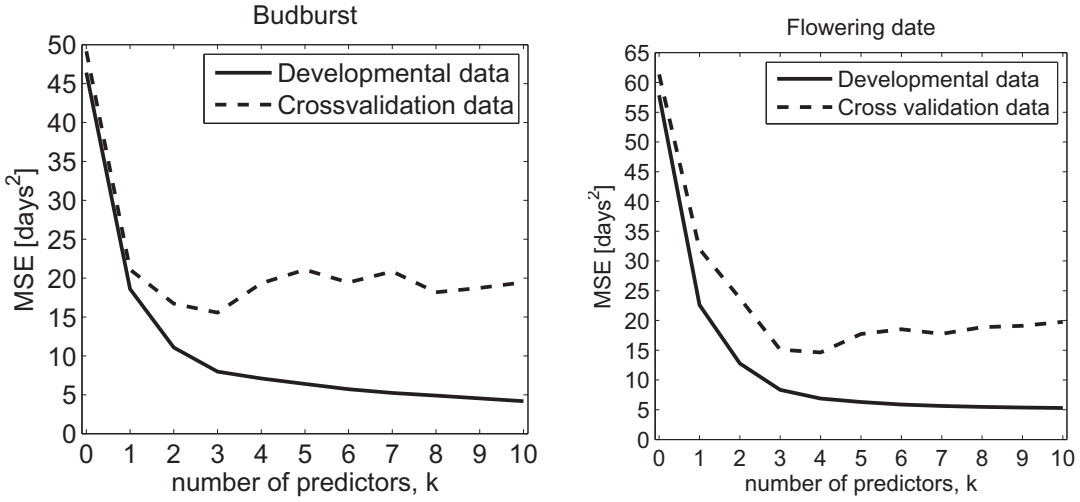

(a) (b)

Figure 5.2: Residual MSE as a function of the number of the regression predictors for budburst date (a) and flowering date (b)

Flowering date Cross validation for the flowering model does not suggest a clear optimal number of predictors; three or four predictors can be chosen with approximately the same uncertainty (Figure 5.2b). The model error is expected to be 2.6 days and the prediction error 3.8 days.

The results of the flowering model are presented in Table 5.2. This model performs slightly better than the budburst model with 87.7 % explained variance for the mean flowering date and between 87 % and 88 % depending on vine variety. The degree days during April and May describe together about 75 % of the variability; the degree days in May is the dominant predictor. Maximum temperature

Table 5.2: Total explained variance (R^2), contribution of the selected predictors to R^2 and regression coefficients of the flowering model for each and averaged (ALL) vine varieties.

	Total R^2	Contribution to R^2				Regression coefficients				
	in [%]	DD5	DD4	TX6	BB	const	DD5	DD4	TX6	BB
ALL	87.7	60.9	16.7	8.0	2.1	207.47	-0.13	-0.08	-1.35	+0.19
Auxerrois	88.3	60.5	16.8	9.4	1.6	211.88	-0.13	-0.08	-1.44	+0.17
Elbling	87.1	61.5	16.2	7.3	2.1	205.96	-0.14	-0.07	-1.29	+0.19
Pinot blanc	86.8	58.5	17.2	8.3	2.8	204.93	-0.13	-0.07	-1.43	+0.22
Pinot gris	88.3	61.2	16.4	8.7	2.0	209.43	-0.13	-0.07	-1.42	+0.18
Riesling	88.5	61.6	17.7	7.0	2.2	205.32	-0.13	-0.08	-1.24	+0.19
Rivaner	87.0	60.0	17.3	7.5	2.2	206.25	-0.13	-0.08	-1.30	+0.18
Traminer	86.3	61.3	15.2	7.9	1.9	208.49	-0.14	-0.07	-1.36	+0.18

Note: Predictors: **DD5** degree days in May, **DD4** degree days in April, **TX6** maximum temperature in June, **BB** budburst date

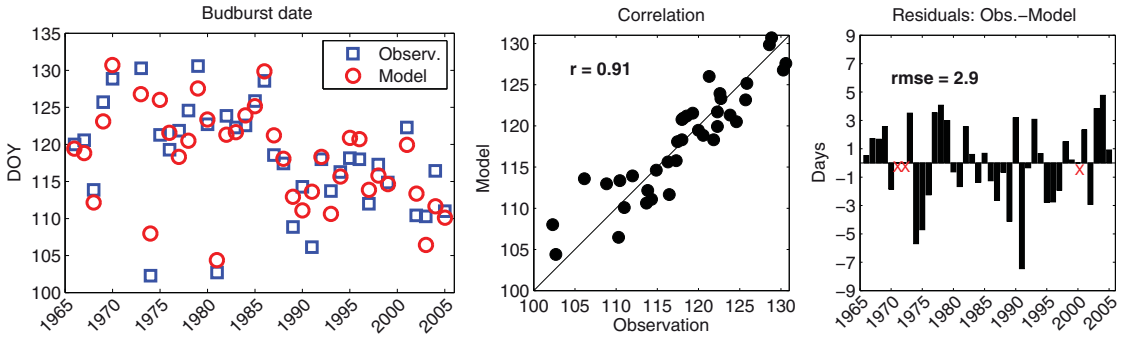

Figure 5.3: Time series of the observed and approximated budburst event date (left), their correlation (centre) and the residuals (right). The red crosses in the residual plot flag the missing data.

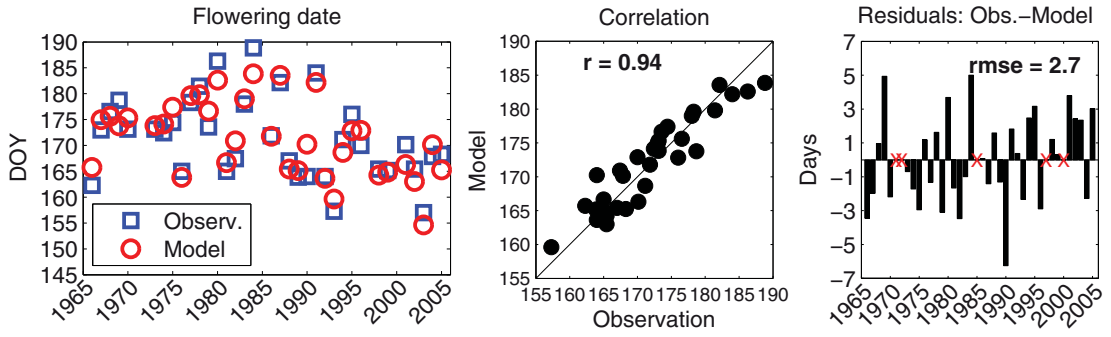

Figure 5.4: Time series of the observed and approximated flowering event date (left), their correlation (centre) and the residuals (right). The red crosses in the residual plot flag the missing data.

in June explains 7 % to 9 % of the observed variance. The last significant predictor is the date of budburst with a contribution of about 2 % to the variance of flowering date. If the estimated budburst is used instead of the observed one, the correlation between the observed and the predicted flowering date is 0.91 and the explained variance is 82.8 %. Again, temperature is the leading factor for the flowering date. Warm periods before flowering move blooming and also fruit setting backward. From a late budburst date it can be concluded that winter and/or spring were rather cold, thus a delay in the initiation of the vegetation cycle is expected. Therefore, a late budburst date means also a later flowering date, but this delay is can be caught up by unusual high temperatures during April to June.

The largest difference between the observed and the calculated flowering date is 6.2 days and happened in 1990 (Figure 5.4). That year is marked by a very early start of the vegetation period; bud swelling was 23 days earlier than on average (*Weinjahr*, 1990). Although late frost damaged the buds and retarded the flowering period, it was still 8 days earlier than usual. In 1969 and 1984 calculated flowering event is 5 days too early. Around 24 June 1969 heavy thunderstorms damaged the vines and the Moselle bursted its banks (*Weinjahr*, 1969). Vegetation period was very late in 1984 because March and April were colder than normal. May and June were also cool and the flowering date was 14 days too late (8 July). This date is the latest date during the period 1966-2005.

Besides the years 1971, 1972 and 2000, where no phenological data was available, the years 1985 and 1997 were left out for the flowering event estimation. These years were marked by extreme meteorological conditions (*Weinjahr*, 1985, 1997). In 1985 flowering event was very late because of a cold winter, especially January and also during a period in June. In June 1997 heavy rainfall occurred before and during flowering; 218.55 mm rain have been observed which is 3.25 times more than the long term average (67.18 mm between 1951-2005).

5.2.2 Must density and acidity

Must density Must density models are developed separately for each cluster, see Section 3.3.2.2. The first group (CM1) contains the varieties Auxerrois, Pinot Blanc, Pinot Gris, Riesling and Traminer. The cultivars Elbling and Rivaner are grouped in cluster M2 as their must density is significantly lower than for the first cluster.

The cross validation results suggest, for cluster CM1, an optimal number of 4 or 5 predictors (Figure 5.5). Taking five predictors the model error would be 3.0 °Oe and the prediction error 5.1 °Oe. The smallest prediction error for cluster CM2 is obtained choosing between 2 to 4 predictors. At four predictors, the prediction error is 5.0 °Oe, where the model error is 3.2 °Oe.

The pool of predictors consists of meteorological parameters and the phenological phases budburst and flowering events. The phenological phases have been taken into account as they mark important growing events, and as shown previously, they can be predicted by meteorological parameters. The significant predictors selected

by the regression method are listed in Table 5.3. Must density of the vine varieties in cluster CM1 are estimated using degree days from April to October, mean daily minimum temperature from 16 to 22 September, budburst date, mean daily maximum temperature from 8 to 22 August and total rainfall in September. High degree days and high maximum temperature are favourable for a high must density. This can be explained by a favourable heat accumulation during the entire vegetation period and especially during the véraison period in August (Section 2.3.3). The other predictors have a decreasing effect on must density when they rise because low night temperatures reduce the metabolism and less aroma is accumulated, but they are beneficial for building up sugar (*Robinson*, 1995; *Jackson*, 2008). A late budburst date is correlated to a shorter ripening time although it is possible to be compensated by ideal conditions in summer and some sugar can be retrieved from the old wood reserves when the vine has a good wood maturation. Rainfall during maturation period increases the water supply and the vine resorbes water and stores it in the berries, which leads to a dilution of the sugar and thus to a lower must density.

The predictors for the first cluster explain 79.7 % of the variance on average, with degree days explaining more than 50 %. Although the range of the total explained variance among the varieties is rather small, the contribution of the single predictors are very different for the individual varieties. The degree days predictor contributes by 60.0 % to the must density variability for Auxerrois, but only 32.0 % to the one of Pinot blanc. The effect of the minimum temperature in September is lowest for Auxerrois compared to the other varieties, and the budburst date is very important for the Traminer variety but not so much for Riesling.

The must density model for the second cluster (Elbling and Rivaner) shows less performance than the first cluster. The explained variance for the cluster mean is 70.5 % and for Rivaner only 59.2 %. An increasing number of hot days before and during the flowering period increases must density. Sunshine duration during the ripening phase favours photosynthesis and has also a favourable warming effect. Late budburst is (see above) not suitable for a high must density. A high number of summer days in August has a decreasing effect on must density because high temperatures postpone the véraison state by extending the time between flowering and acidity maximum, and thus the sugar accumulation period becomes shorter (*Becker* et al., 1983). This effect is more important for the early ripening Rivaner. The application of the cluster model to Rivaner leads to only fair results. But developing a model only for Rivaner did not lead to better results. This could be an indication that important predictors have not been taken into account. These could be another phenological phase like véraison or viticultural practices, which cannot be captured easily by a meteorological based model (e.g. early harvest because of fungal disease risk).

The time series of measured and estimated must density are shown in Figure 5.6. Some years have been left out because of missing data (1971, 1972, 2000). The years 1985 and 1995 are not taken into account because of unusual meteorological conditions at flowering date.

Table 5.3: Total explained variance (R^2), contribution of the selected predictors to R^2 and regression coefficients of the must density model for each and averaged vine varieties in cluster CM1 and CM2.

	Total R^2	Contribution to R^2					Regression coefficients					
	in [%]	DD4-10	$TN9_{16\text{-}22}$	BB	$TX8_{8\text{-}22}$	RR9	const	DD4-10	$TN9_{16\text{-}22}$	BB	$TX8_{8\text{-}22}$	RR9
CM1	79.7	54.0	10.7	7.9	4.3	2.8	61.75	+0.03	-1.04	-0.32	+0.66	-0.05
Auxerrois	77.2	60.0	4.6	6.8	3.2	2.6	52.36	+0.03	-0.69	-0.30	+0.56	-0.04
Pinot blanc	67.9	32.0	14.1	9.2	7.8	4.8	74.62	+0.02	-1.09	-0.32	+0.83	-0.05
Pinot gris	73.0	37.3	15.1	8.8	6.8	5.0	76.81	+0.02	-1.24	-0.36	+0.85	-0.06
Riesling	78.0	63.6	7.9	3.8	2.5	0.2	36.75	+0.04	-1.23	-0.23	+0.59	-0.01
Traminer	78.8	56.2	9.6	8.4	2.0	2.6	68.70	+0.04	-1.14	-0.40	+0.48	-0.05

	Total R^2	Contribution to R^2				Regression coefficients				
	in [%]	HOT5-6	SD8-10	BB	SUMMER8	const	HOT5-6	SD8-10	BB	SUMMER8
CM2	70.5	43.2	19.3	4.4	3.6	63.19	+0.97	+0.04	-0.17	-0.30
Elbling	71.5	47.4	20.2	3.2	0.7	57.74	+1.11	+0.04	-0.15	-0.14
Rivaner	59.2	31.6	14.9	4.9	7.8	68.64	+0.83	+0.04	-0.20	-0.46

Note: Predictors: **DD4-10** degree days from April to October, **$TN9_{16\text{-}22}$** minimum temperature between 16-22 September, **BB** budburst date, **$TX8_{8\text{-}22}$** maximum temperature between 8-22 August, **RR9** precipitation in September, **HOT5-6** hot days in May and June, **SD8-10** sunshine duration between August and October, **SUMMER8** summer days in August.

An interesting question is how well must density can be estimated if the phenological predictors are not available. To answer this question, first, the budburst predictor has been taken out from the predictor pool. The resulting must density model has an explained variance of 88 % but the number of predictors is very large. It has to be noted that in absence of the budburst predictor the flowering date becomes a significant predictor, which strengthen the importance of prior phenological events. Omitting also the flowering date, the regression method selects 4 predictors: degree days from April to October, mean daily minimum temperature from 16 to 22 September, mean daily maximum temperature from 8 to 22 August, and mean daily maximum temperature from 16 to 22 September. In this case the explained variance is reduced to 73 %. Hence, the phenological events, especially the budburst date, are essential for approximating must density. Replacing the observed budburst date by the estimated one and by keeping the initial regression coefficients, the explained variance of the cluster mean is reduced only marginally to a value of 77 %. Doing the same experiment for the must density cluster CM2, omitting first the budburst date, the selected predictors remain the same as in the initial regression equation, except the budburst predictor is replaced by the flowering date. Omitting also the flowering predictor, it is only substituted by the mean daily minimum temperature from 8 to 15 August. In both cases the explained variance is 70 %. When the calculated budburst date is filled in, the explained variability is also 70 %. Consequently, the estimation of must density model for CM2 can also be done without the prior phenological phases maintaining about the

Table 5.4: Total explained variance (R^2), contribution of the selected predictors to R^2 and regression coefficients of the acidity model for each and averaged vine varieties in cluster CA1, CA2 and CA3.

	Total R^2	Contribution to R^2			Regression coefficients			
	in [%]	DD4-10	BLU	SUMMER8-10	const	DD4-10	BLU	SUMMER8-10
CA1	82.1	66.1	9.3	6.7	-3.480	-0.006	+0.126	-0.116
Auxerrois	81.4	69.2	5.6	6.6	1.258	-0.007	+1.111	-0.124
Rivaner	61.8	45.7	11.5	5.6	-2.710	-0.003	+0.095	-0.069
Traminer	82.3	65.2	10.2	6.9	-8.744	-0.007	+0.171	-0.156
CA3	88.2	76.7	6.2	5.3	4.075	-0.011	+0.153	-0.152
Elbling	85.6	76.5	4.5	4.6	8.946	-0.011	+0.124	-0.134
Riesling	86.0	72.8	7.5	5.7	-0.616	-0.011	+0.182	-0.170

	Total R^2	Contribution to R^2				Regression coefficients				
	in [%]	DD4-10	BLU	$TX9_{8\text{-}22}$	SD8	const	DD4-10	BLU	$TX9_{8\text{-}22}$	SD8
CA2	88.5	62.9	11.8	9.7	4.1	5.490	-0.005	+0.114	-0.247	-0.011
Pinot Blanc	88.3	62.4	12.2	10.4	3.3	6.201	-0.006	+0.118	-0.268	-0.011
Pinot Gris	85.8	61.4	10.7	8.6	5.1	5.236	-0.005	+0.108	-0.225	-0.121

Note: Predictors: **DD4-10** degree days from April to October, **BLU** flowering date, **SUMMER8-10** summer days between August and October, **$TX9_{8\text{-}22}$** maximum temperature between 8-22 September, **SD8** sunshine duration in August.

same quality, but in agreement with the results for CM1 the configuration including the budburst event is kept.

Acidity The cluster analysis for acidity characteristics splits the vine varieties into three groups (Figure 3.4b). The first group (CA1) encompasses Auxerrois, Rivaner and Traminer. The lowest prediction error for CA1 is achieved by choosing 2 predictors (1.18 g/l), but the error does increase only marginally by taking 3 predictors (1.22 g/l) while the model error is much lower with 0.87 g/l (Figure 5.7a). The second cluster (Pinot Blanc, Pinot Gris) should be approximated by 2 to 4 predictors regarding the prediction error (Figure 5.7b). Taking the model error into account the best combination consists of 4 predictors because the model error (0.81 g/l) is much lower by a nearly constant prediction error (1.52 g/l). The cross validation results give for the third group an optimal number of 3 predictors (Figure 5.7c). Taking more than 3 predictors the prediction error increases rapidly.

The pool of predictors is the same as for the must density model. The significant predictors for CA1 and CA3 are equal: degree days from April to October, flowering date and number of summer days between August and October. The estimation of acidity for cluster CA2 uses besides the degree days from April to October and the flowering date, the mean daily maximum temperature from 8 to 22 September and the sunshine duration in August. Increasing degree days, sum-

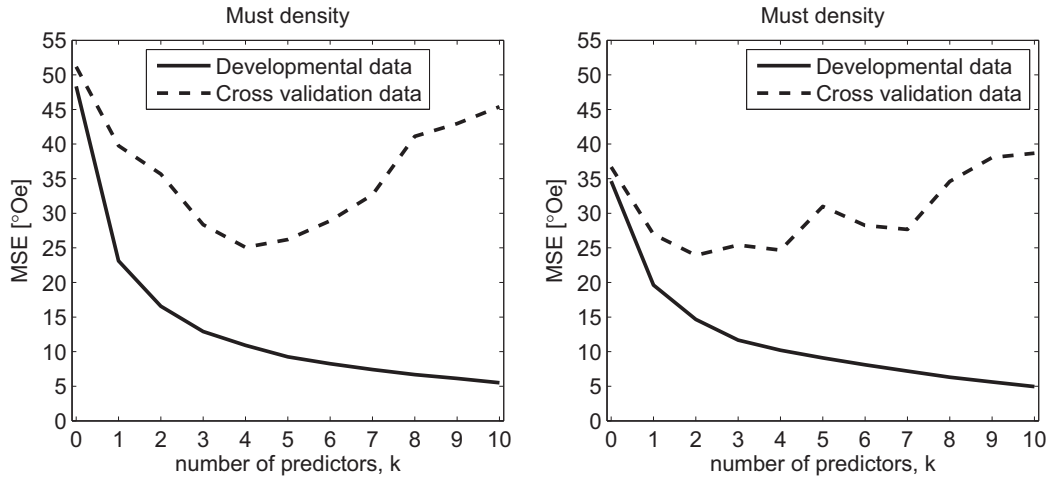

(a) Cluster CM1 (b) Cluster CM2

Figure 5.5: Residual MSE as a function of the number of the regression predictors for must density for the groups CM1 (a) and CM2 (b) defined in Figure 3.4a.

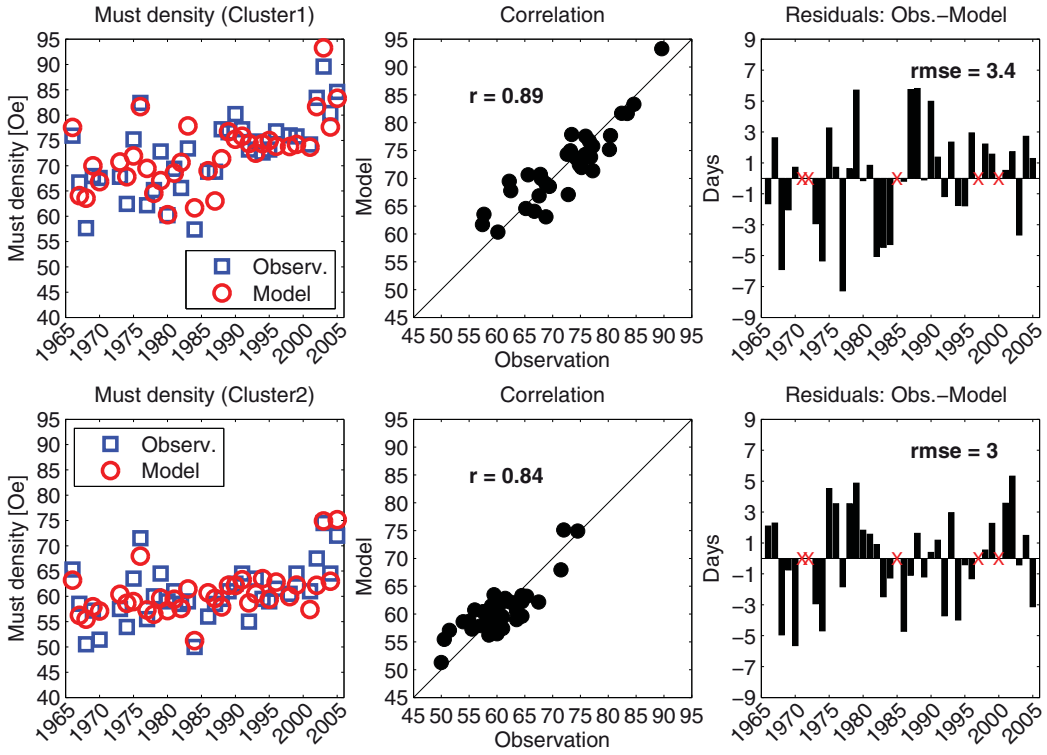

Figure 5.6: Time series of the observed and approximated must density (left), their correlation (centre) and the residuals (right) for the clusters CM1 (top) and CM2 (bottom). The red crosses in the residual plot flag the missing data.

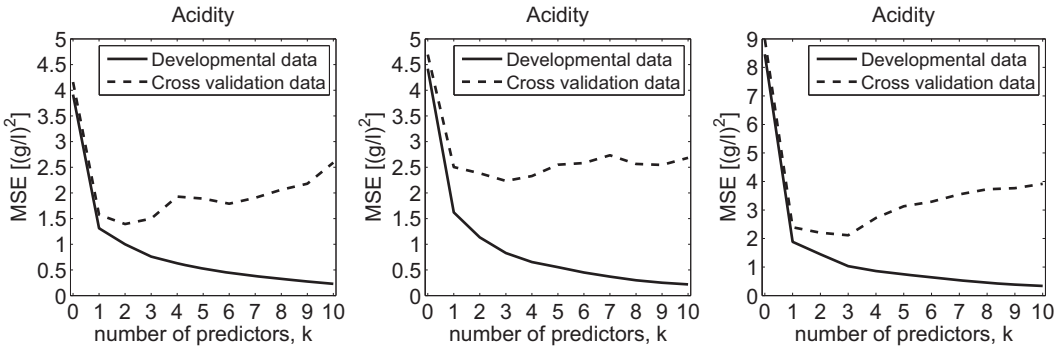

(a) Cluster CA1 (b) Cluster CA2 (c) Cluster CA3

Figure 5.7: Residual MSE as a function of the number of the regression predictors for acidity for the groups CA1 (a), CA2 (b) and CA3 (c) defined in Figure 3.4b.

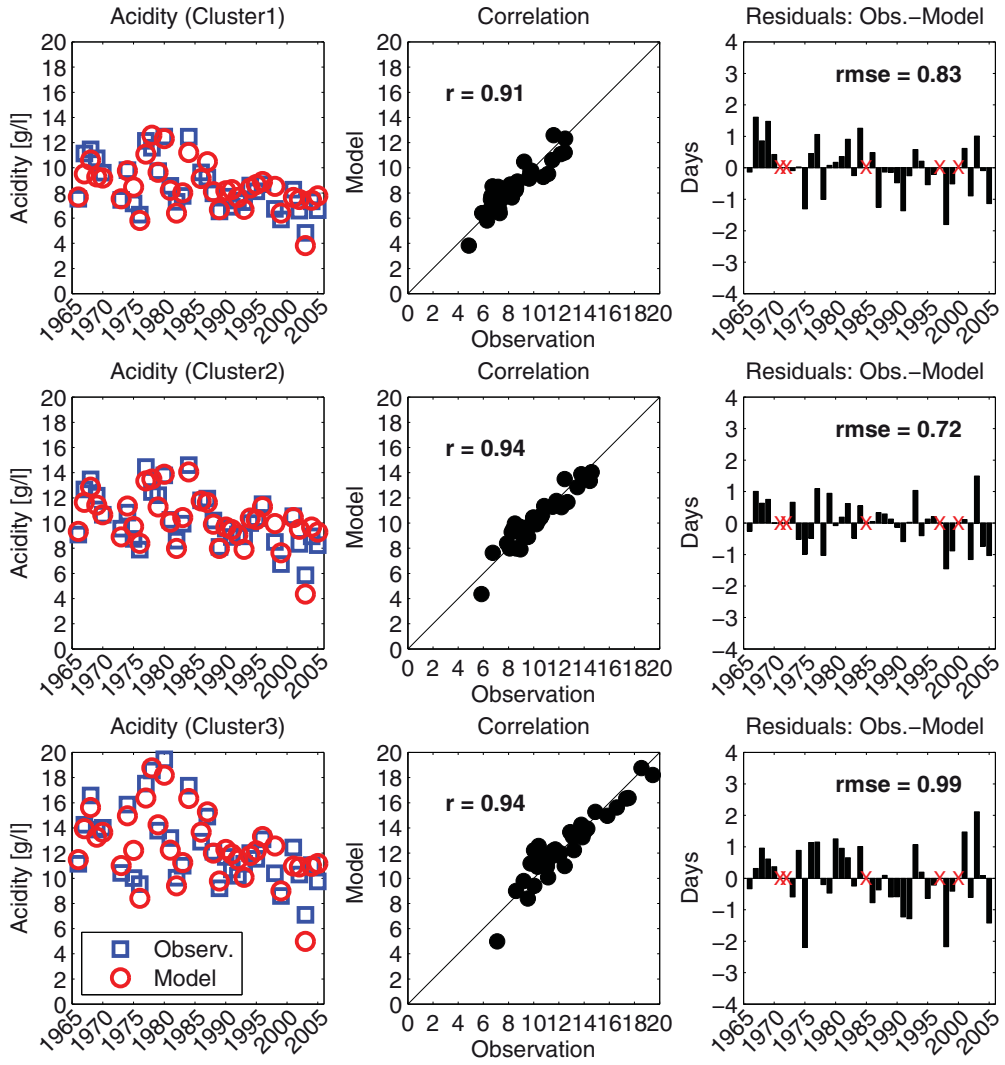

Figure 5.8: Time series of the observed and approximated must density (left), their correlation (centre) and the residuals (right) for the clusters CM1 (top) and CM2 (bottom). The red crosses in the residual plot flag the missing data.

mer days, maximum temperature and sunshine duration have a decreasing effect on acidity. They describe heat accumulation which is favourable for the growth of the vine but also for the degradation of different types of acidity (Section 2.3.3). Besides, sunshine duration is decisively involved in photosynthesis. A late flowering date postpones the maturation period because the berries are developing later and the acidity maximum is delayed. The most important predictor, the degree days from April to October, shows up not only for each acidity cluster but also in the estimation of must density for CM1. Regarding acidity, the flowering date is more relevant than the budburst date. The total explained variance for CA1, CA2 and CA3 ranges between 81.4 % (Auxerrois) and 88.3 % (Pinot Blanc), except Rivaner for which the explained variability reaches only 61.8 %.

The correlation between observed and estimated acidity (Figure 5.8) is high and ranges between 0.91 (CA1) and 0.94 (CA2, CA3). The root mean squared error is highest for CA3 but in relation to the mean acidity, it ranks second by 8.0 %. The model for the second cluster, CA2, has the lowest error with 0.72 g/l or 7.1 %.

Removing flowering date from the pool of predictors, the budburst date comes in. Replacing the observed flowering date by the estimated one, keeping the same regression coefficients, the explained variance drops to 75 % from 82 % and the rmse is 0.96 g/l. The cluster CA2 behaves like CA1; eliminating the flowering date the budburst date enters the list of significant predictors. Excluding also budburst date the explained variance is 86 % with 5 predictors. The acidity model for CA2 calculated with the predicted flowering date has an explained variability of 86 % and a rmse of 0.77 g/l. The third cluster depends less on phenological phases as the other two. Removing the flowering predictor, only two predictors become significant (80 %): degree days April-October and precipitation 1-15 September; budburst date does not enter the regression equation. The introduction of the calculated flowering date reduced the explained variance of CA3 from 88 % to 84 % and the rmse is 1.14 g/l.

Chapter 6

6 Modelled climate of the Upper Moselle region

Numerical models in meteorology are developed in order to investigate atmospheric processes, weather and climate variability, and to predict future climate conditions, starting from an approximation of the atmospheric true state (the initial conditions). The model types can have different spatial and/or temporal scales.

General circulation models (GCM) are global models and their resolution is of the order of hundred kilometres. They capture well the atmospheric circulation and provide the forcing data for regional models. GCM's used for weather prediction in the short (1-3 days) and medium (4-10 days) time range, but have a lack of information on the regional or smaller scale due to their resolution (*McGuffie and Henderson-Sellers*, 2005).

The regional models which are limited area models are nested from the global models which provide also the lateral boundary conditions. These regional models are driven either on a long term scale as climate models (RCM) or on a short term scale for weather predictions (NWP). Their spatial resolution depends on the objectives and ranges between 50 km and 1 km.

6.1 COSMO-CLM and scenario simulations

The climate model used in this work is the COSMO-CLM (abbr. CCLM) which is the climate version of the COSMO model (former LM, "Lokal-Modell"), the operational limited-area weather prediction model developed by the German Meteorological Service (DWD) and COSMO community. The data used in this work are scenario runs, simulations based on emission scenarios computed at "Deutsches Klimarechenzentrum" (DKRZ) by the group "Model and Data" of MPI-M, Hamburg, in close cooperation with Brandenburg University of Technology (BTU Cottbus), Helmholtz-Zentrum Geesthacht Centre for Materials and Coastal Research (former GKSS Geesthacht) and Potsdam Institute for Climate Impact Research (PIK), funded by the Federal Ministry of Education and Research (BMBF). They

have also been used for the assessment reports of the Intergovernmental Panel on Climate Change (IPCC).

COSMO-model and the extension to the climate version The COSMO-model is a non hydrostatic limited area atmospheric prediction model (*Doms and Schättler*, 2002) and is part of the model system of the German Meteorological Service. It has been designed for operational numerical weather prediction, but also for scientific applications on the meso-β and meso-γ scale. It is based on the primitive hydro-thermodynamical equations describing the fully compressible non-hydrostatic flow in a moist atmosphere without any scale approximation.

The model equations are formulated in respect to a rotated geographical coordinate system in order to avoid convergence of the meridians in the model region and to get a more regular grid (Figure 6.1). This rotation is made by tilting the North Pole in such a way that the equator crosses the centre of the model domain. The vertical coordinate is a generalised terrain-following coordinate which follows the orography close to the surface and changes to horizontal in around 11 km height. Model layers are closer in the planet boundary layer as in the upper troposphere. The variables are defined on an Arakawa-C/Lorenz grid (*Mesinger and Arakawa* (1976), Figure 6.2).

The integration in time can be performed by three different integration schemes. The default is based on a Leapfrog integration proposed by *Klemp and Wilhelmson* (1978). Alternatively to the Leapfrog scheme, a two-time level Runge-Kutta scheme, or a three-dimensional semi-implicit integration scheme can be used. The Runge-Kutta scheme is often used for very high resolution modelling.

The CCLM version 2.0, based on the COSMO-LM version 3.1 is used for the scenario runs. Besides technical changes (e.g., restart option, new data file format, changes in soil model computation) some implementations important for climate runs have been included in the COSMO model. In the climate mode the sea surface temperature, vegetation, ozone and CO_2 concentrations cannot be considered as constant anymore. During the year vegetation and land use are changing and thus, also the albedo cannot be considered constant. Leaf area index of plants, depth of the roots, fraction of plant cover have to be varied through the annual cycle.

The runs used in this work are also called consortial simulations (`http://www.clm-community.eu`). They are computed offline, so there is no retroaction of the regional model to the global model. The forcing data used is described in the following section.

6.1.1 Past and future climate scenarios

ECHAM5/MPIOM forcing runs The boundary fields are generated from the IPCC4 AR experiment output of the coupled global climate and ocean model ECHAM5-MPIOM (*Roeckner* et al., 2003). The horizontal resolution of the atmospheric model component ECHAM5 is 1.9°x 1.9°, with 96x192 grid points and

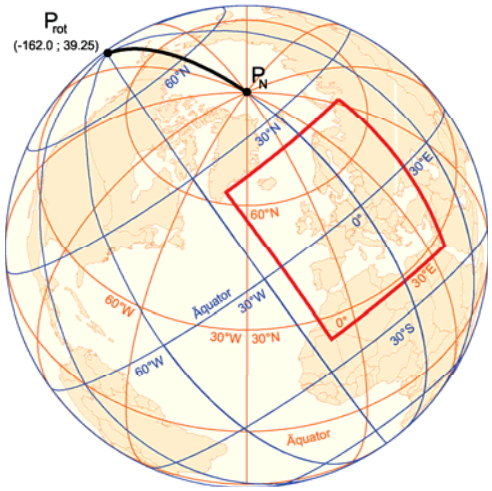

Figure 6.1: Rotated coordinates in the CCLM configuration (blue). The unrotated coordinates with North Pole P_N are shown in orange (From *Böhm* (2007)).

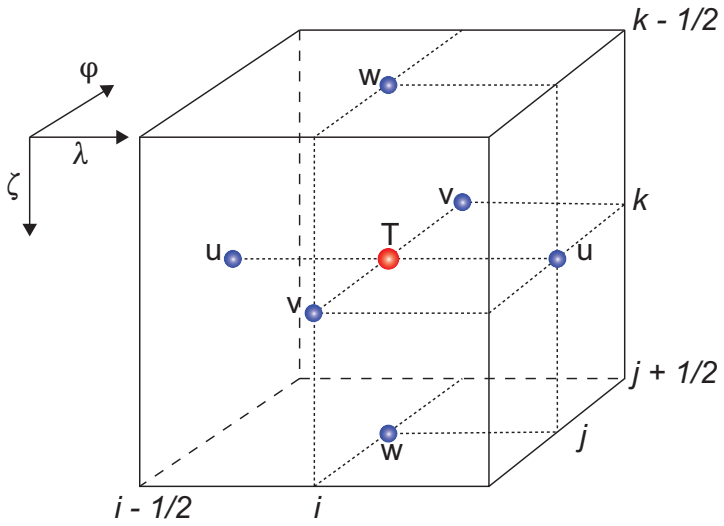

Figure 6.2: Staggered Arakawa-C/Lorenz grid. Temperature, pressure, specific humidity, cloud water content, cloud ice content and turbulent kinetic energy are defined in the centre of the grid box. The velocity components are defined on the box faces (adapted from *Doms and Schättler* (2002)).

31 vertical levels. The horizontal resolution of the ocean component model MPIOM varies regionally between approximately 10 km and 150 km.

The global experiments are started from model states within a 505-year long integration of the coupled global model ECHAM5/MPIOM with pre-industrial conditions (PIcntrl in Table 6.1, where all the forcing data are listed). In PIcntrl the concentrations of well-mixed greenhouse gases reflect the state of 1860 AD. The three simulations of the 20th century (20C3M) differ because fields from different years of PIcntrl are used to initialise the 20C3M simulations. Only anthropogenic forcing, (i.e., changes in CO_2, CH_4, N_2O, F_{11} (effective), F_{12}, ozone and sulphate) have been considered. The 20C3M simulations reach until the year 2000 and are used for initialising the scenario realisations SRES which simulate the future climate evolution until 2100 under assumed anthropogenic forcings. The scenario simulations of SRES correspond to the continuation of the single 20C3M simulations where the main differences between the single SRES scenarios are the different anthropogenic forcings (Figure 6.3).

Future climate scenarios The variation of anthropogenic forcing is made using assumptions (i.e., storylines) about different structures and growth of economy, society and technology. In this section, the storylines described in *Nakicenovic* et al. (2000) are summarised and a short overview is given in Table 6.2.

The A1 storyline, which contains the A1B scenario, assumes a rapid and successful economic development, in which current distinctions between "poor" and "rich" countries eventually dissolve. Global population grows to about nine billion until 2050 and declines to about seven billion until 2100. Energy and mineral resources are abundant in this scenario family because of rapid technical progress. With the rapid increase in income, dietary patterns shift initially toward increased consumption of meat and dairy products, but may decrease subsequently with increasing emphasis on the health of an ageing society. High incomes also translate into high car ownership, urban sprawl, and dense transport networks, nationally as well as internationally. The A1B scenario assumes a balanced mix of technologies and supply sources, with technology improvements and resource assumptions such that no single source of energy is overly dominant.

The central elements of the B1 future are a high level of environmental and social consciousness combined with an approach to a more sustainable development. In the B1 storyline, governments, businesses, media, and public care mor about the environmental and social aspects of development. Technological change plays an important role. Economic development in B1 is balanced, and efforts to achieve equitable income distribution are effective. As in A1, the B1 storyline describes a fast-changing and convergent world, but the priorities differ. Whereas the A1 world invests its gains from increased productivity and know-how primarily in further economic growth, the B1 world invests a large part of its earnings in improved efficiency of resource use, social institutions, and environmental protection. The demographic transition to low mortality and low fertility occurs at the same rate as in A1, but for different reasons. Global population reaches nine billion by

Table 6.1: Extract of IPCC AR4 experiments carried out using the global model ECHAM5/MPIOM. The realisations in bold are those which are used in this work.

	Experiment name	Realisation	Period	Initialisation run	Model year of initialisation run*
Past	PIcntrl	Run 1	2150 - 2655	NA**	NA
	20C3M	**Run 1**	1860 - 2000	PIcntrl	2190
	20C3M	**Run 2**	1860 - 2000	PIcntrl	2215
	20C3M	**Run 3**	1860 - 2000	PIcntrl	2240
Future	SRESA1B	**Run 1**	2001 - 2200	20C3M, run 1	2001
	SRESA1B	**Run 2**	2001 - 2300	20C3M, run 2	2001
	SRESA1B	Run 3	2001 - 2200	20C3M, run 3	2001
	SRESA2	Run 1	2001 - 2100	20C3M, run 1	2001
	SRESA2	Run 2	2001 - 2100	20C3M, run 2	2001
	SRESA2	Run 3	2001 - 2100	20C3M, run 3	2001
	SRESB1	**Run 1**	2001 - 2200	20C3M, run 1	2001
	SRESB1	**Run 2**	2001 - 2200	20C3M, run 2	2001
	SRESB1	Run 3	2001 - 2200	20C3M, run 3	2001

(From: `http://www-pcmdi.llnl.gov/ipcc/time_correspondence_summary.htm`)
*) year in control or 20C3M simulation that corresponds to the first year of this run
**) Not available

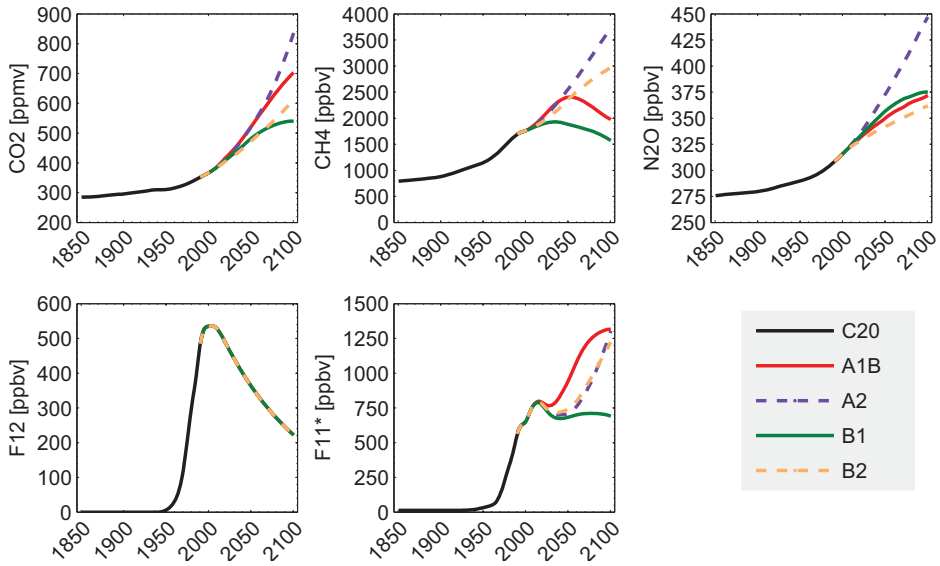

Figure 6.3: Greenhouse gas forcing for different scenarios. The dashed scenarios A2 and B2 not used for the consortial runs of CCLM. (Data from `http://www.cnrm.meteo.fr/ensembles/public/results/results.html`).

Table 6.2: Scenario characteristics from *Nakicenovic* et al. (2000)

Scenario	A2	A1B	B1	B2
Population growth	high	low	low	medium
GDP* growth	medium	very high	high	medium
Energy use	high	very high	low	medium
Land-use changes	medium-high	low	high	medium
Resource availability	low	medium	low	medium
Pace of technological change favouring	slow regional	rapid balanced	medium efficiency, dematerialisation	medium "dynamics as usual"

*) GDP: gross domestic product

2050 and declines to about seven billion by 2100. The B1 storyline foresees a relatively smooth transition to alternative energy systems as conventional oil and gas resources decline.

The A2 scenario is characterised by less focus on economic, social, and cultural interactions between regions. People, ideas, and capital are less mobile so that technology diffuses more slowly than in the other scenarios. Economic growth is uneven and the income gap between now-industrialised and still developing parts of the world remains constant.

In the B2 world, government policies and business strategies at the national and local levels are influenced by environmentally aware citizens. International institutions decline in importance, with a shift toward local and regional decision-making structures and institutions. Human welfare, equality, and environmental protection have high priority, and they are addressed through community-based social solutions in addition to technical solutions. Energy systems differ from region to region, depending on the availability of natural resources. The need to use energy and other resources more efficiently stimulate the development of less carbon-intensive technology in some regions.

6.1.2 Characteristics of the scenario simulations

The storylines (20C, A1B, B1), simulated with the global model ECHAM5/MPIOM, are downscaled using the regional climate model CCLM. The specified region contains Europe and a part of North Africa (Figure 6.4). The horizontal extension is approx. 4500 km to approx. 5000 km. The resolution of 18 km requests a time step of 75 seconds.

The CCLM output is stored as different data streams in the WDCC (World Data Center for Climate, Hamburg) data base. The first data stream D0 (the raw data) and the second stage, D1 (designated for nesting experiments) are not accessible.

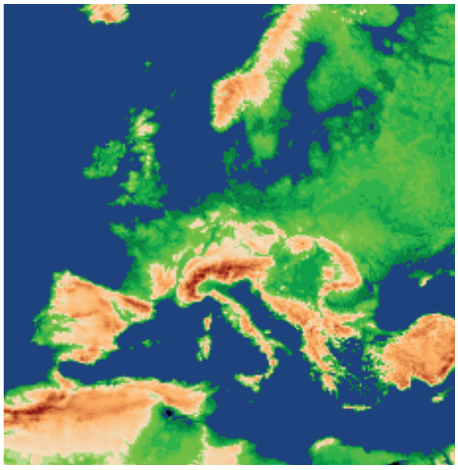

Rotated location of north pole	lon: -162.0°, lat: 39.25°
Extension of longitude (rot.)	-23.73° to 15.87°
Extension of latitude (rot.)	-20.87° to 21.04°
Grid size	0.165°
Number of grid-cells	241 x 255

Figure 6.4: Orography of model domain excluding the relaxation zone and domain characteristics of the CCLM scenario simulations.

Only data stream D2 and D3 are available from WDCC. D2 is obtained by removing the relaxation zone and separating the climatological variables in different files. The coordinates are still rotated with the zero-latitude in the middle of the domain. D3 is the transformation of D2 to the geographical grid. The D2 domain has nearly equal-area grid-cells around the rotated equator, but the transformation to D3 expands the grid-cells. In this study the D2 data stream is used.

The CCLM simulations of the 20th century start in 1955, but the first 5 years are considered as spin up time. Thus, the available data span from 1 January 1960 to 31 December 2000. The period for future scenarios encompasses 1 January 2001 to 31 December 2100. In this work the considered period is restricted to 31 December 2050 because of viticultural interests. For the 20th century there are three simulations, described in the previous section, and for the future period only two. The future scenarios are A1B and B1; scenario A2 has not been computed.

6.1.3 Model domain of the investigated region

The model domain of the investigated region (Figure 4.1) has a spatial resolution of about 18 km, thus topographic details are not captured accordingly by CCLM (Figure 6.5). The grid-cells are clearly visible. The Ardennes and Eifel Region can be identified, but the Hunsrück region southward the Moselle and eastward the Saar is barely visible by the CCLM orography.

In order to make a better approximation of the model output at the station location and to reduce model variability, the data of the four neighbouring grid cells are averaged (Figure 6.5b). The average can be done by giving the same or different weights to the grid values. As the stations are located closer to one grid cell than to other grid cells, higher weights are given to the nearest grid cell value.

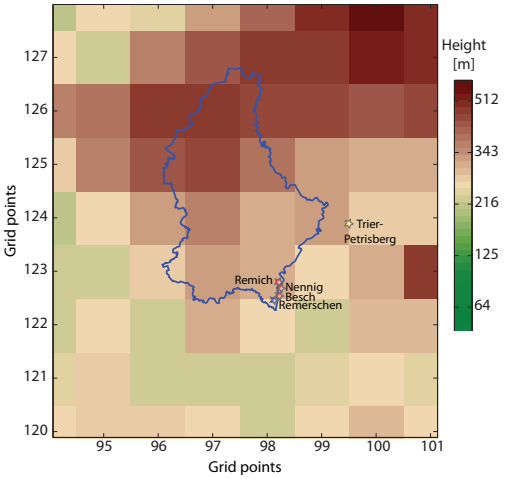

(a) CCLM grid cells with orography in the investigated region

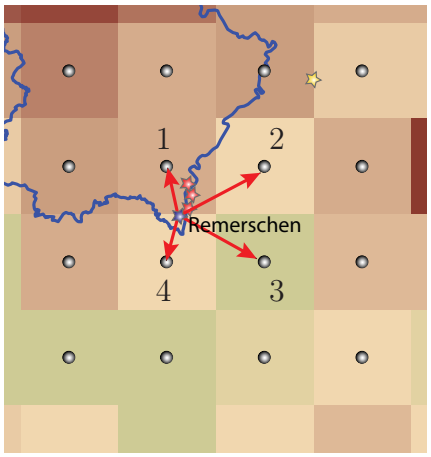

(b) More detailed view on the investigated region

Figure 6.5: Orography defined in CCLM. The observation sites are marked by stars with blue: precipitation (Remerschen), red: temperature (Nennig, Besch, and Remich), yellow: sunshine duration (Trier-Petrisberg). Grey points indicate the location of variables in the CCLM model grid. For illustration, red arrows show the distance between the Remerschen station to the CCLM grid box centre.

Shepard (1968) introduced the simple inverse distance weighting function:

$$w_i(\mathbf{x}) = \frac{1}{d(\mathbf{x}, \mathbf{x}_i)^p} \tag{6.1}$$

with d a given distance from the known point $\mathbf{x}_i$ to the unknown point $\mathbf{x}$, and p the positive real power parameter. The interpolated value of a general quantity u at the location $\mathbf{x}$ is calculated by

$$u(\mathbf{x}) = \sum_{i=1}^{N} \frac{w_i(\mathbf{x}) u_i}{\sum_{j=1}^{N} w_j(\mathbf{x})}, \tag{6.2}$$

with u_i the values at the known positions $\mathbf{x}_i$ and N the total number of known points used for the interpolation. In Figure 6.5b, $\mathbf{x}_i$ are the centres of the grid cells, where the prognostic variables are defined (Figure 6.2). The meteorological station is located at point $\mathbf{x}$ and the distance d is marked by arrows between the station and the grid values. Increasing the power parameter p (in Eq. 6.1) gives higher weights to nearby points. Here, only a small weighting is done with a value of p=1. The positions for the stations Besch and Nennig have been averaged. The station in Trier-Petrisberg which provides the longterm observations of sunshine duration, is located outside of the four grid cells around Remich and Remerschen. It will, however, be handled as located in Remich, because the monthly sunshine duration of both stations are highly correlated (Section 4.1).

6.2 Validation of the past climate simulations (1960-2000)

The quality of the consortial runs for the Upper Moselle region is analysed by comparisons with the observed climate at the combined station Besch/Nennig, using time series, quantile-quantile plots, and frequency distributions. In the following different methods are presented.

6.2.1 Validation methods

Root mean square (RMS) The root mean square is a quadratic mean and defined as

$$x_{rms} = \sqrt{\sum_{i=1}^{n} \frac{x_i^2}{n}} \tag{6.3}$$

Although it is not used often, in this work it is chosen because CCLM has difficulties with high temperature values. In this way higher weight are given to higher values.

Characterisation of probability density functions A probability density function (pdf) is characterised by (*Wilks*, 2006)

- the central value or location parameter (LOC) also called median or the 50th percentile:

$$LOC = q_{0.5} = \begin{cases} x_{([n+1]/2)}, & \text{if } n \text{ is odd} \\ \frac{1}{2}(x_{([n/2])} + x_{([n/2]+1)}), & \text{if } n \text{ is even} \end{cases} \tag{6.4}$$

  with n the length of x.

- the range between the 25th and 75th percentile or scale parameter (SCALE), also called the interquartile range (IQR):

$$SCALE = IQR = q_{0.75} - q_{0.25} \tag{6.5}$$

- the symmetry of the distribution or shape parameter (SHAPE), comparing the distances between the 25th and 75th percentiles to the median:

$$SHAPE = \frac{(q_{0.75} - q_{0.5}) - (q_{0.5} - q_{0.25})}{q_{0.75} - q_{0.25}} \tag{6.6}$$

  A negative/positive value of SHAPE describes a distribution skewed to the left/right side of the median. A symmetric distribution has a SHAPE value of zero.

Quantile-Quantile-Plot (QQ-plot) Quantile-Quantile plots are used to determine whether the sample data, of two time series to be compared, come from the same distribution. For evaluation the percentiles of one time series are plotted against the percentiles of the other time series as a scatter plot. If the two time series belong to the same distribution, i.e., the percentiles are identical, all data points are arranged on the 1:1 line.

Two-sample Kolmogorov-Smirnov test The two-sample Kolmogorov-Smirnov test (*Wilks*, 2006; *Sachs*, 1978) compares two distributions, F_B and F_E, by calculating the maximal difference between the cumulative probability functions (CDF) of these distributions:

$$D = \max_x |F_n(x_1) - F_m(x_2)| \tag{6.7}$$

The two distributions of the length n_1 and n_2 were drawn from the same distribution at a significance level α if

$$D \leqslant D_\alpha = \sqrt{-\frac{1}{2}\frac{n_1 + n_2}{n_1 n_2} \ln \frac{\alpha}{2}} \tag{6.8}$$

The Kolmogorov-Smirnov test is very sensitive to small differences in median, dispersion, skewness, and kurtosis (*Sachs*, 1978). In order to get significant results and because of the small sample size, the Kolmogorov-Smirnov test is bootstrapped N times. Let h be a logical number with h=0 if the distributions are equal and h=1 if they differ. At least 75% of the compared distributions are significantly ($\alpha = 0.05$) different if

$$\begin{aligned} P(D > D_\alpha) \equiv P(h = 1) = \frac{m}{n+m} &\geqslant 0.75, \\ \text{with } n &= \{\text{number of } h | h = 0\}, \\ m &= \{\text{number of } h | h = 1\}, \\ N &= n + m \end{aligned} \tag{6.9}$$

Bootstrap The bootstrap resampling method (*Efron*, 1979) is used to calculate the uncertainty and to test the significance of a parameter. Independent data is resampled with replacement and a test statistic is computed a large number of times. In this work the test statistics are resampled 1000 times. A confidence interval of 95 % for the test statistic is the range between the 2.5th and 97.5th percentile of the distribution of all resampled test statistics.

Other methods of validation are relative entropy (Kullback-Leibler divergence) or skill scores. Unfortunately both methods could not be applied because the datasets in this work are often too small.

6.2.2 Modelled versus observed climate variability (1960-2000)

In this section the capability of the three CCLM runs of the 20th century to reproduce the observed climate variability in the Upper Moselle region is examined. In the first step the modelled annual and seasonal climate parameters (temperature, temperature indices, precipitation and sunshine duration) are compared to the observations for the period 1960-2000. The second step examines the key climate parameters which influence the phenological events and must quality (Section 5.2).

As additional information, an overview of the statistical evaluations of the three CCLM runs of the 20th century is given in Section B.3 and will not be further discussed here.

6.2.2.1 Validation of annual and seasonal data

For each climate parameter the CCLM simulations are evaluated on the annual and on the seasonal time scale by averaging or accumulating the daily values accordingly.

Temperature The three CCLM runs are depicted in Figure 6.6. They have a large variability and correlations between the simulations and the observations on annual scale are very low (mainly below 0.40). The first realisation of CCLM is even anti-correlated to the observation (e.g., -0.25 for maximum temperature). Taking the daily data, however, correlations are much higher (> 0.6) and positive.

According to Table 6.3 and Table 6.4, the root mean square (RMS) of the CCLM for annual maximum and mean temperature is significantly underestimated. Especially during autumn and winter periods, the RMS for temperature is underestimated, thus variability is underestimated. In summer, however, CCLM RMS of maximum temperature is significantly higher than the observations. This large variability is also reflected by the SCALE parameter: the range between the 25th and 75th percentile is significantly larger for CCLM maximum and mean temperature in summer than for the observations.

The QQ-plots (Figure 6.7) reflect again deficiencies of the CCLM simulations. The single runs of daily maximum temperature for the whole period overestimate values above 25 ℃ and slightly underestimate the frequency of the temperature range between 5 ℃ and 20 ℃. CCLM mean temperature shows a similar distribution pattern as maximum temperature but less pronounced. CCLM overestimates minimum temperature below 0 ℃ and above 15 ℃. The temperature range in between agrees very well with the observation. The high frequency of 0 ℃ values in the CCLM data is conspicuous. From the QQ-plots the peak is hard to identify, but in Figure 6.9 it is clearly visible for minimum temperature; maximum and mean temperature have also a too high frequency of 0 ℃ values. This peak has also been reported by *Hollweg* et al. (2008) and a weaker peak exists even in ECHAM5/MPIOM data. Probably this is caused by setting the temperature to

0 ℃ during melting and freezing processes. The classification of temperature using climate indices (definition cf. Section 4.2) is presented in Figure 6.8. Hot days are largely overestimated by CCLM, while summer days are underestimated. The amount of frost days is quite well reproduced by CCLM, but ice days are slightly overestimated. For mild nights a bias towards a lower number is observable.

Table 6.3: RMS and pdf-parameters LOC, SCALE, SHAPE of annual maximum (Tmax), minimum (Tmin) and mean (Tmean) temperature, precipitation (RR) and sunshine duration (SD) for the period 1960-2000. The coloured boxes mark significant differences between CCLM and observational values on a 95 % significance level.

		RMS	LOC	SCALE	SHAPE
Tmax	OBS	14.45	14.41	1.19	-0.20
	CCLM R1	13.51	13.41	1.30	-0.02
	CCLM R2	13.51	13.51	1.48	-0.20
	CCLM R3	13.82	13.82	1.06	-0.05
Tmean	OBS	9.97	9.99	1.13	-0.16
	CCLM R1	9.16	9.10	0.78	0.10
	CCLM R2	9.13	9.11	0.92	-0.02
	CCLM R3	9.42	9.47	0.74	-0.10
Tmin	OBS	5.69	5.64	1.04	-0.10
	CCLM R1	5.71	5.71	0.62	-0.10
	CCLM R2	5.63	5.65	0.70	-0.22
	CCLM R3	6.00	5.98	0.75	-0.25
SD	OBS	1549	1546	239	-0.07
	CCLM R1	1546	1522	227	-0.16
	CCLM R2	1550	1542	230	-0.02
	CCLM R3	1546	1562	252	0.22
RR	OBS	788	796	190	-0.23
	CCLM R1	938	916	179	0.31
	CCLM R2	953	934	129	0.12
	CCLM R3	940	938	130	-0.28

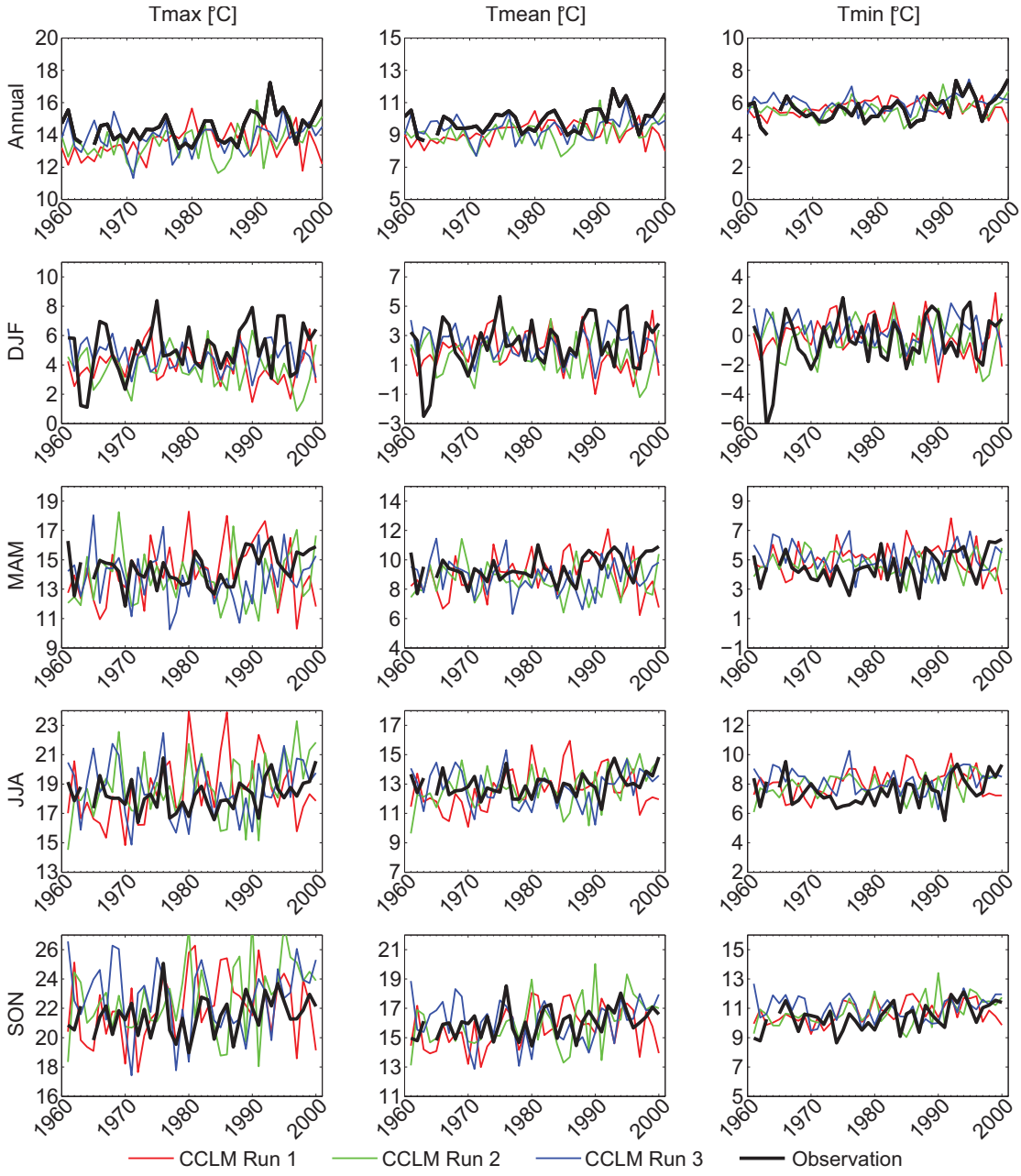

Figure 6.6: Time series of mean annual and mean seasonal maximum, mean and minimum temperature (1960-2000). The three coloured lines show the CCLM runs. The black line presents the measured temperature.

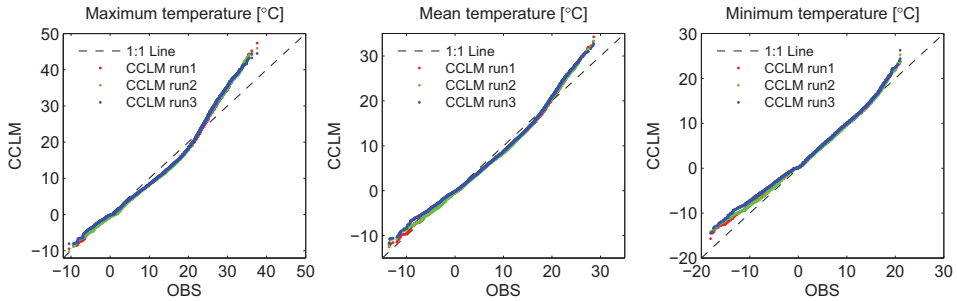

Figure 6.7: Daily temperature QQ-plots for CCLM against observations for the period 1960-2000.

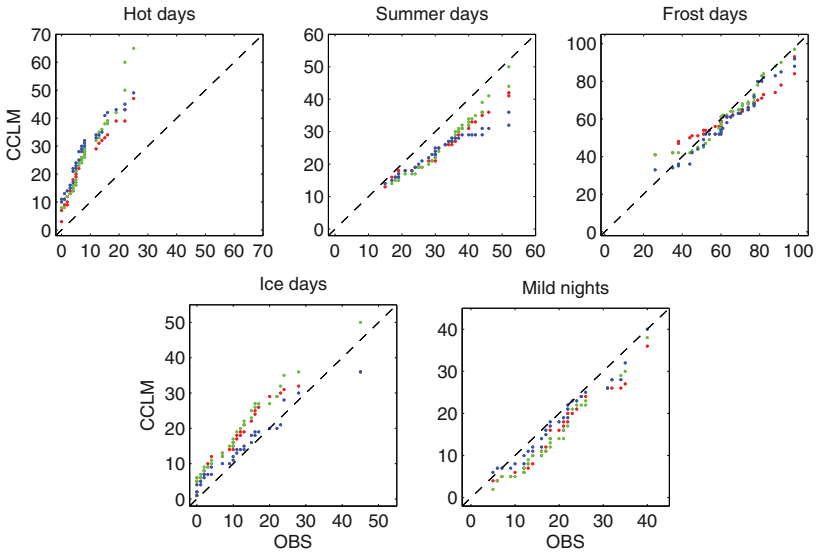

Figure 6.8: QQ-plot of temperature indices (number of days per year exceeding different temperature thresholds) for CCLM against observational data 1960-2000.

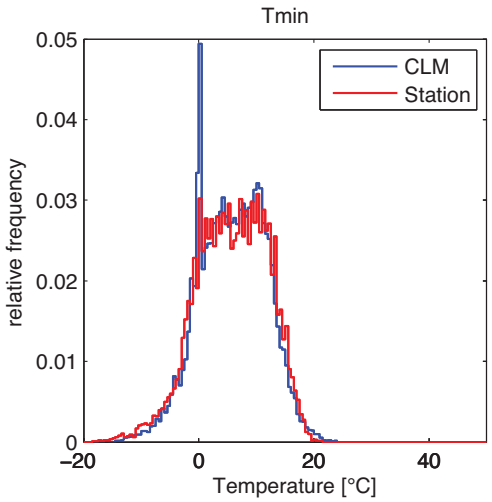

Figure 6.9: Frequency of daily minimum temperature for CCLM (blue) and observations (red) for the period 1960-2000.

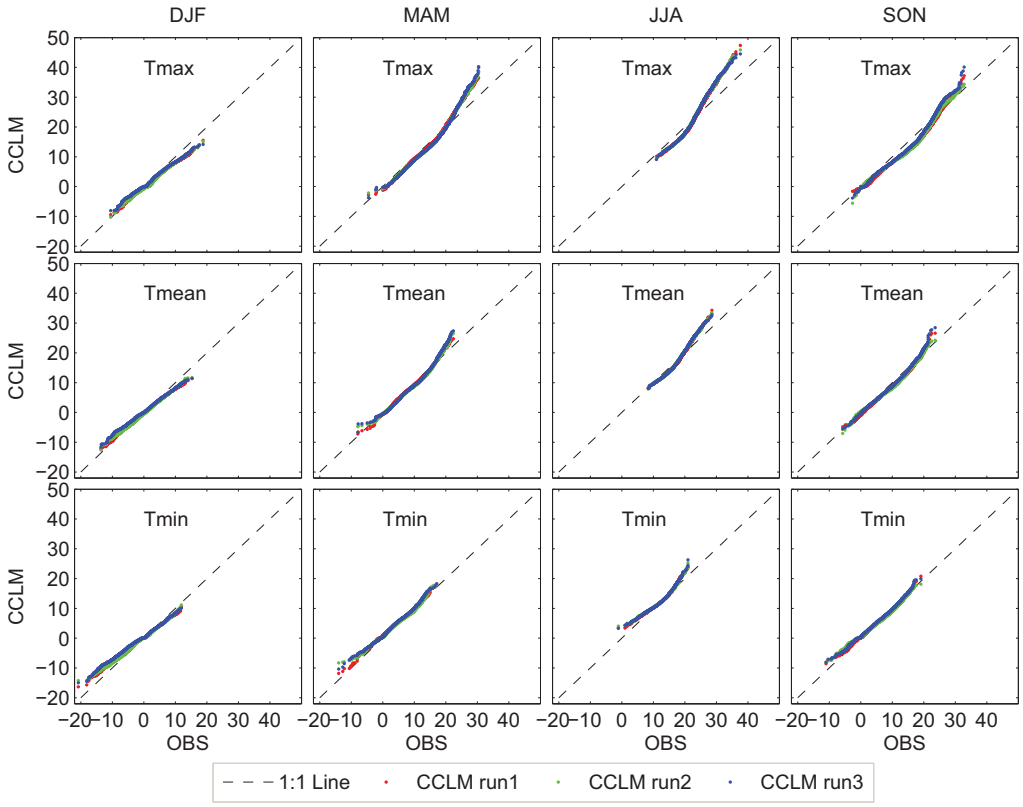

Figure 6.10: QQ-plot of daily maximum, mean, and minimum temperature for winter (DJF), spring (MAM), summer (JJA), and autumn (SON), 1960-2000. CCLM data is plotted against observations.

Precipitation Precipitation modelled by CCLM is too high over the whole period and for all realisations (Figure 6.13 and Table 6.3). The QQ-plot (Figure 6.11) indicates an underestimation of the daily precipitation rates, but high rain rates tend to be overestimated by Run 2 and Run 3. An outlier (>99th percentile) of 184 mm/day on one day in Run 3 has been discarded. The overestimation of total precipitation and the underestimation of rain rates is due to an overestimation of the number of rainy days (days with >0.1 mm/day). From 1951 to 2000 CCLM produces 3260 more rainy days than observed at a threshold of 0.1 mm/day and 1745 more days with a threshold above 1 mm/day.

Daily precipitation simulated by CCLM agrees best with the observations during winter. In spring, rain rates above 15 mm/day are clearly underrepresented. During summer and autumn, however, rain rates above 15 mm/day agree well with the measurements. Only at high rain rates the three CCLM runs have different results.

The difference in annual precipitation between CCLM and observations is mainly due to an overestimation during winter, though one could expect that the overestimation would be located in summer due to overestimated convective events. Nevertheless, the scale and the shape of the precipitation distributions do not differ significantly (Table 6.4).

Table 6.4: RMS and pdf-parameters LOC, SCALE, SHAPE of seasonal temperature, precipitation and sunshine duration for the period 1960-2000. Significant (95 %) differences to the observation are labelled in red/blue for higher/lower values.

		RMS				LOC				SCALE				SHAPE			
		DJF	MAM	JJA	SON	DJF	MAM	JJA	SON	DJF	MAM	JJA	SON	DJF	MAM	JJA	SON
Tmax	OBS	6.79	15.55	23.70	15.71	5.20	14.00	23.00	14.65	5.90	8.40	6.60	8.80	0.02	0.05	0.06	-0.06
	R1	5.40	15.75	24.72	13.68	4.28	13.00	22.47	11.71	5.74	8.49	11.63	7.59	-0.12	0.15	0.14	0.04
	R2	5.43	15.37	25.03	13.76	4.17	12.41	23.10	11.35	6.04	8.40	12.16	7.54	-0.14	0.18	0.09	0.10
	R3	5.70	15.50	25.08	14.55	4.75	12.58	22.92	12.25	5.31	8.34	12.25	8.57	-0.10	0.16	0.14	0.03
Tmean	OBS	5.03	10.55	17.84	11.20	2.70	9.40	17.40	10.50	5.70	6.70	4.75	7.05	0.02	-0.01	0.01	-0.11
	R1	4.11	10.21	17.64	9.96	2.03	8.66	16.23	8.75	4.89	6.13	6.26	6.32	0.01	0.06	0.18	-0.02
	R2	4.14	9.90	17.84	9.97	1.94	8.29	16.55	8.52	4.92	5.85	6.55	6.36	-0.01	0.04	0.13	0.08
	R3	4.14	10.22	17.88	10.55	2.37	8.55	16.48	9.33	4.85	6.22	6.52	6.80	0.00	0.04	0.17	-0.06
Tmin	OBS	4.85	6.39	12.38	7.82	0.00	4.50	12.00	6.50	5.80	6.60	4.30	6.80	-0.03	0.06	0.02	-0.03
	R1	3.88	6.43	12.38	7.35	0.06	5.21	11.70	6.18	4.42	5.66	3.60	6.09	0.08	-0.07	0.10	-0.07
	R2	3.96	6.18	12.44	7.25	0.03	4.88	11.76	5.94	4.44	5.66	3.60	5.95	0.01	-0.08	0.13	-0.02
	R3	3.64	6.67	12.53	7.76	0.14	5.31	11.84	6.57	4.08	5.98	3.74	6.23	0.23	-0.08	0.07	-0.06
SD	OBS	155	477	641	297	143	459	639	292	46	76	137	77	0.52	0.18	0.06	-0.01
	R1	194	475	597	311	176	469	604	298	55	97	164	83	0.02	-0.19	-0.17	-0.08
	R2	198	463	619	297	190	464	576	285	87	141	175	75	-0.02	-0.25	0.23	-0.14
	R3	209	438	607	311	198	427	603	293	71	133	153	92	0.03	0.01	-0.30	0.28
RR	OBS	207	189	211	213	185	163	198	199	99	91	110	68	0.08	0.10	0.06	-0.08
	R1	282	211	215	247	277	210	206	235	90	70	95	55	0.04	-0.18	-0.06	0.27
	R2	288	212	222	254	278	198	197	244	91	43	103	87	0.03	0.19	0.35	0.12
	R3	263	231	216	256	255	226	204	232	59	71	72	102	0.10	-0.09	0.25	0.18

Abbr.: maximum (Tmax), minimum (Tmin), mean (Tmean) temperature, precipitation (Prec) and sunshine duration (SD), observation (OBS), CCLM simulations (R1, R2, R3)

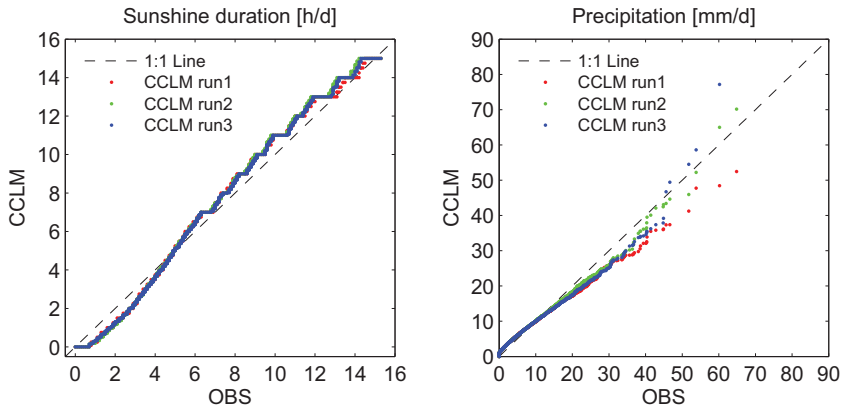

Figure 6.11: QQ-plot of daily sunshine duration and precipitation for CCLM against observational data (1960-2000).

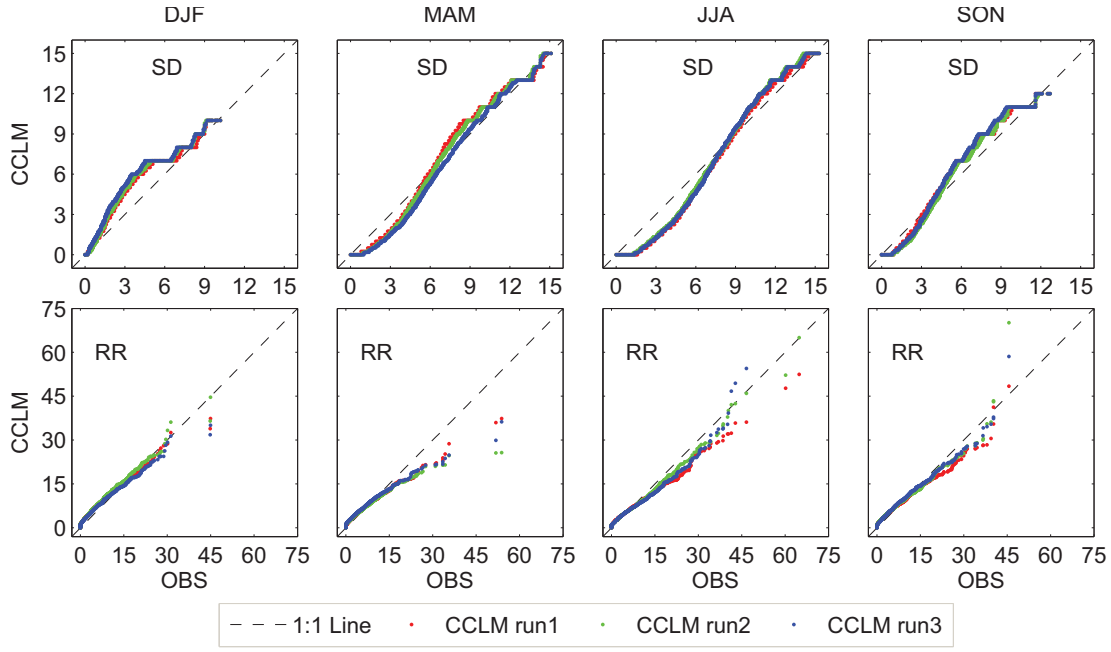

Figure 6.12: QQ-plot of daily sunshine duration and daily precipitation for winter (DJF), spring (MAM), summer (JJA), and autumn (SON), 1960-2000. CCLM data is plotted against observations.

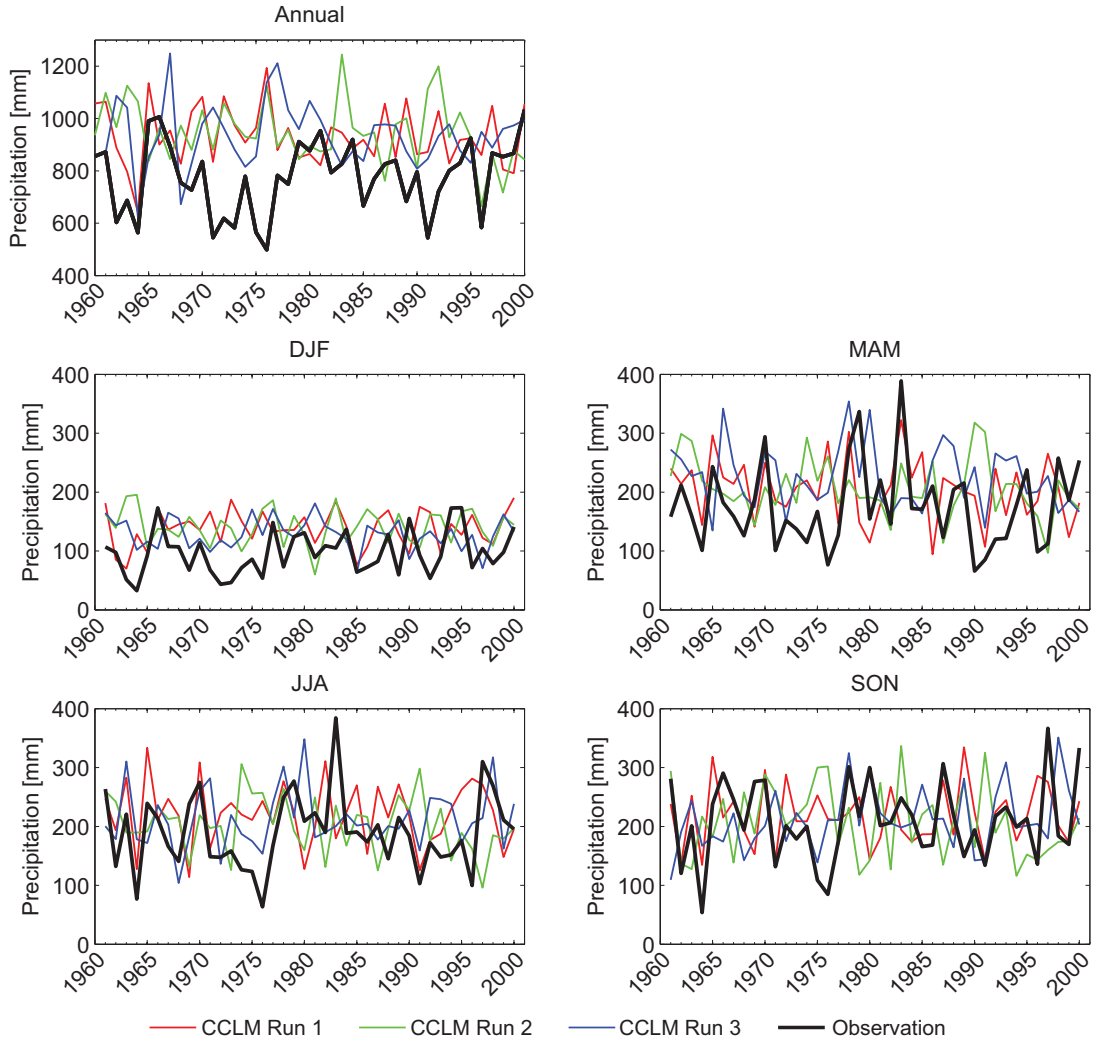

Figure 6.13: Annual and seasonal time series of accumulated hourly precipitation sums (1960-2000). The coloured lines indicate results from the different CCLM runs and the black line represents the observed precipitation.

Sunshine duration Annual sunshine duration shows disagreements between the three CCLM runs (Figure 6.14). The 3rd CCLM realisation shows high variability during the first years. Sunshine duration below 4 hours is underestimated and above 5 hours overestimated (Figure 6.14). The stepwise increase of CCLM sunshine duration is remarkable. The CCLM produces, in this case, after 7 hours of sunshine an abnormal high frequency of sunshine duration values for every full hour. But, also the observation seems to increase the measurement time resolution after 8 hours of sunshine. The reasons for the behaviour of the observations and the model output data have not become clear.

The QQ-plots for seasonal sunshine duration shows also clear jumps like the annual data (Figure 6.12). Sunshine durations below 6 hours are overestimated

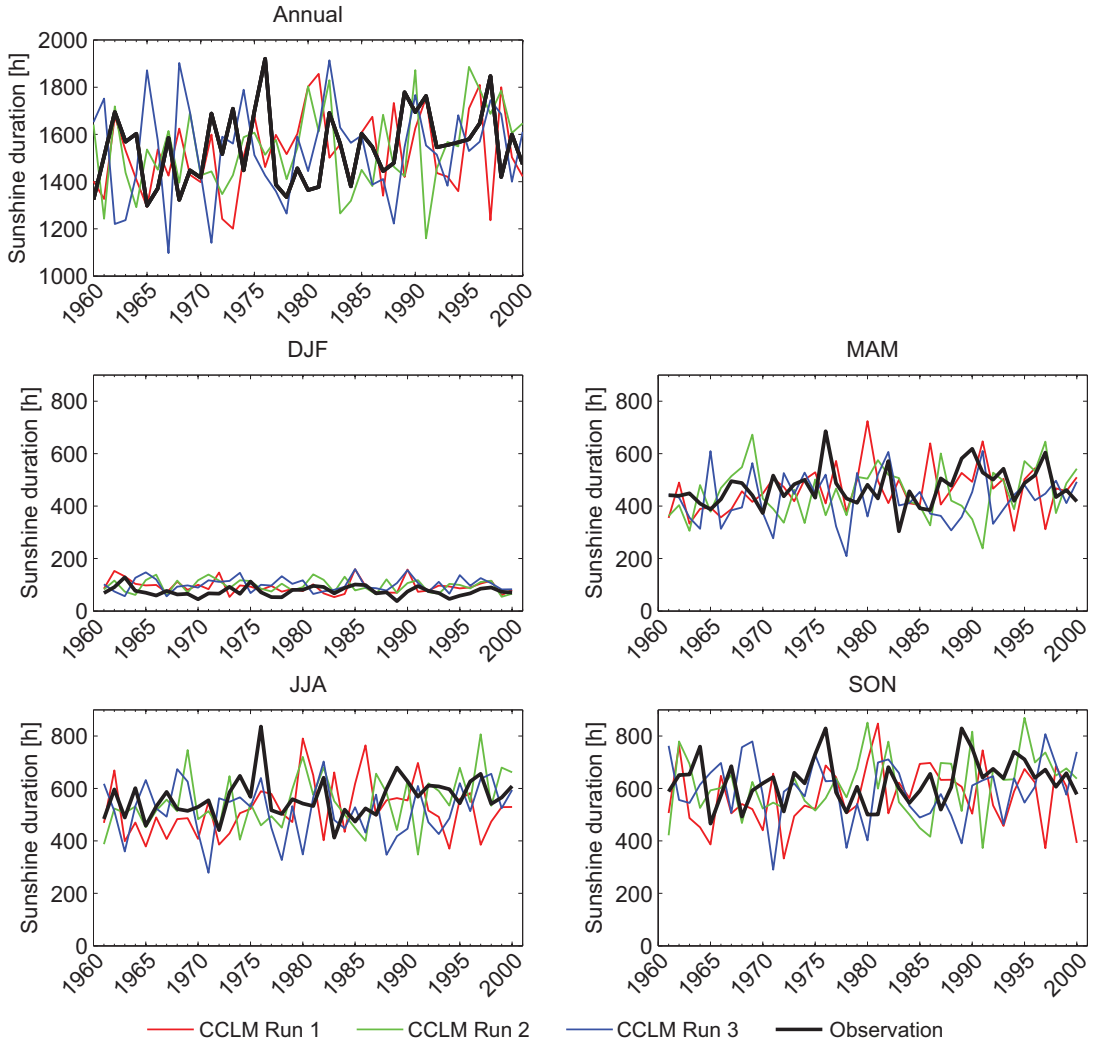

Figure 6.14: Annual and seasonal time series of accumulated hourly sunshine duration sums (1960-2000). The coloured lines indicate results from the different CCLM runs and the black line represents the observed sunshine duration.

during winter. For the rest of the year, this range is underestimated by CCLM and the range above 6 hours is overestimated. Sunshine duration during winter is generally overestimated by CCLM (Table 6.4).

6.2.2.2 Validation of the selected predictors

The observed atmospheric predictors used in the phenological and must quality models are compared to the CCLM model output. The Quantile-Quantile plots of the predictors are shown in Figures 6.15-6.18 and the corresponding distribution parameters in Table 6.5.

Budburst As seen in Section 5.2.1, budburst date is mainly influenced by the degree days in March (DD3), maximum temperature in April (TX4) and number of frost days January-March (FROST1-3). DD3 is underestimated by CCLM; especially for values higher than 20 observed degree days the differences are large (Figure 6.15). At about 20 observed degree days the CCLM produces rapidly an increased number of degree days but the values are still underestimated. Run 3 underestimates the amount of degree days significantly and also the inter-quartile range is smallest. CCLM TX4 agrees quite well with the observations at lower temperatures. Above 17 ℃, however, the maximum temperature is clearly overestimated by CCLM Run 1 and Run 2, whereby the distribution scale of Run 1 is significantly too wide (Table 6.5). Although the pdf parameters of the second realisation are not significantly different from the observation, the Kolmogorov-Smirnov test detects significant differences between the distributions. The number of frost days is well captured by all CCLM runs.

Flowering For flowering estimation following predictors are selected (Section 5.2.1): degree days in May (DD5), degree days in April (DD4) and maximum temperature in June (TX6). DD5 and DD4 are well reproduced by CCLM, although high values of the degree days are overestimated (Figure 6.16). However, significantly too high is only the inter-quartile range (IQR) of the DD4 in Run 1 (Table 6.5). TX6 is underestimated at low values and clearly overestimated at high values. Thus, the IQR of the distributions and their median are overestimated; the scale parameter of Run 2 and Run 3 is larger than in the observations by a factor of two. These considerable deviations are also reflected in the KS-test: the probability that the CCLM distributions for these predictors are different from the observation is above 95 %.

Must density Taking the clusters together, seven distinct predictors are selected for must density estimation: degree days between April and October (DD4-10), minimum temperature between 16th and 22nd September ($TN9_{16-22}$), maximum temperature from 8th to 22nd August ($TX8_{8-22}$), precipitation in September (RR9), number of hot days May-June (HOT5-6), sunshine duration August-October (SD8-10), and number of summer days in August (SUMMER8).

The predictor DD4-10 is generally underestimated by CCLM (Figure 6.17). Run 3 is closest to the observations, for Run 1 and Run 2 the KS-test detects significant deviations from the observations. However, only the median of Run 2 is significantly too low and the inter-quartile range of this run is too high. The modelled $TN9_{16-22}$ agrees well with the observation. No significant differences are detected in the distributions, however, the scale parameter is (insignificantly) very small. $TX8_{8-22}$ is underestimated below 25 ℃ and the median of the distributions is lower than observed. The IQRs, though, are significantly overestimated by Run 1 and Run 3. Total precipitation in September (RR9), around 60 mm, is well reproduced by all CCLM runs. Also the scale parameter of the distributions agrees well with the observations, although it is quite small in Run 2. The modelled predictor

HOT5-6 significantly deviates from the observations for almost all pdf parameters. Actually the probability that the modelled and observed distributions are different is 100 %. The mean values for CCLM are much too high for all runs. The IQR in Run 2 and Run 3 is significantly too wide; in Run 1 IQR is three times higher than the observed range. These large differences occur because the maximum temperature of CCLM is too high in summer and the threshold temperature of 30 °C defining hot days is exceeded too often by CCLM. For the same reason the number of summer days in August (SUMMER8) is significantly underestimated by CCLM. SD8-10 is slightly underestimated by CCLM; only the median of Run 2 is significantly lower than observed. On the other hand, the IQR of the CCLM distributions is marginally higher than measured.

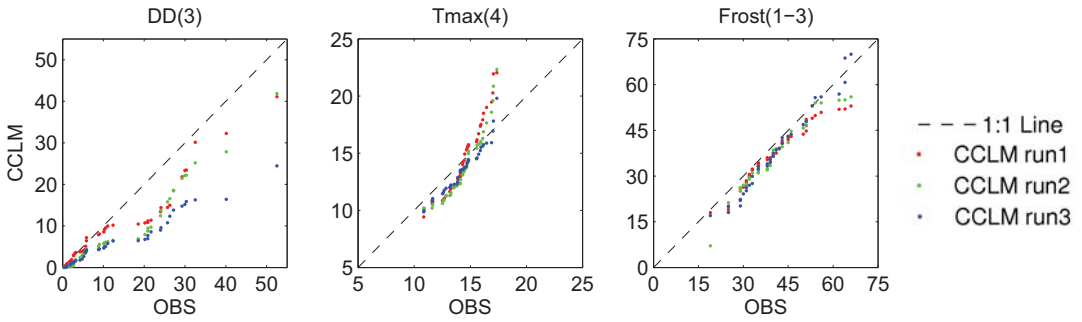

Figure 6.15: QQ-plot of the predictors for the budburst estimation 1960-2000: Degree Days in March (DD3), mean maximum temperature in April (TX4) and frost days from January to March (FROST1-3). CCLM data is plotted against observations.

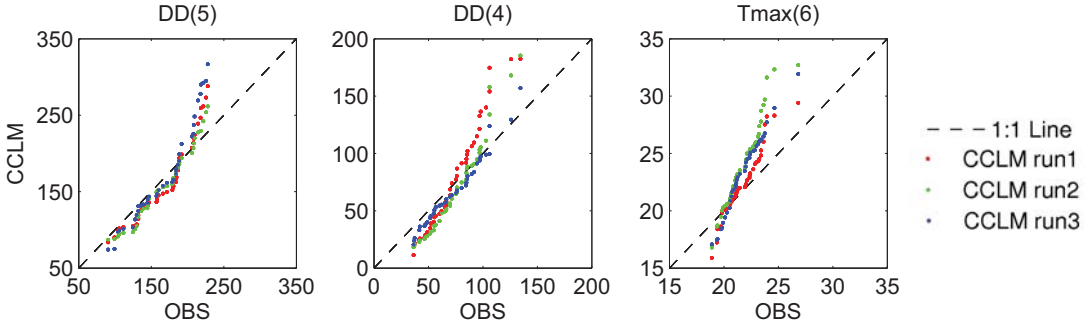

Figure 6.16: QQ-plot of the predictors for the flowering estimation: Degree Days in May (DD5), degree days in April (DD4) and mean maximum temperature in June (TX6). CCLM data is plotted against observations.

Acidity As shown in Section 5.2.2 acidity is essentially determined by the following four climate parameters: degree days between April and October (DD4-10), number of summer days August-October (SUMMER8-10), maximum temperature from 8th to 22nd September ($TX9_{8-22}$) and sunshine duration in August (SD8). The weaknesses of the CCLM to reproduce the observed predictors for the acidity

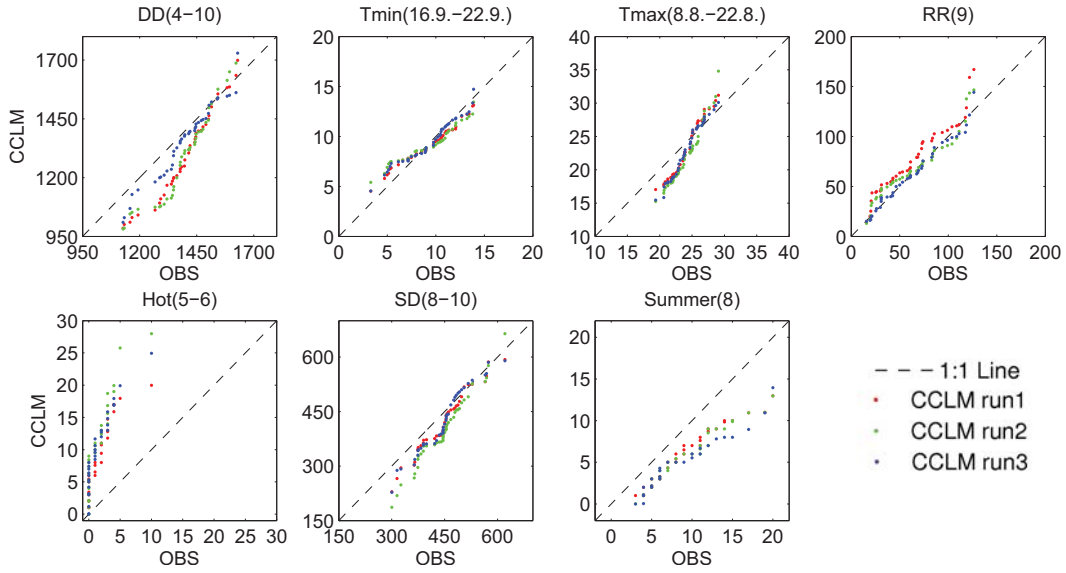

Figure 6.17: QQ-plot of the predictors for the must density parametrisation: Degree Days from April to October (DD4-10), mean minimum temperature between 16-22 September ($TN9_{16-22}$), mean maximum temperature between 8-22 August ($TX8_{8-22}$), precipitation in September (RR9), hot days in May and June (HOT5-6), sunshine duration from August to October (SD8-10) and summer days in August (SUMMER8). CCLM data is plotted against observations.

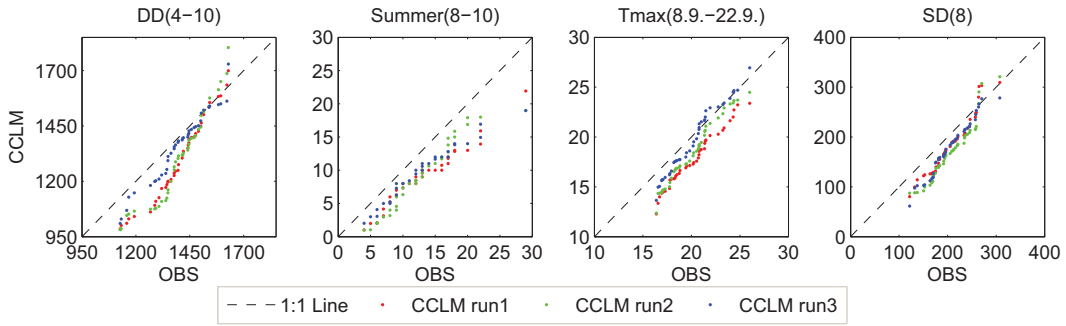

Figure 6.18: QQ-plot of the predictors for the acidity parametrisation: Degree Days from April to October (DD4-10), summer days from August to October (SUMMER8-10), mean maximum temperature between 8-22 September ($TX9_{8-22}$) and sunshine duration in August (SD8). CCLM is plotted against observations.

model are similar to those of must density. The main predictor (DD4-10), the same as for must density, and also the predictor SUMMER8-10 are underestimated because maximum temperature in summer is overestimated by CCLM (Figure 6.18). During September, however, the predictor $TX9_{8-22}$ is slightly underestimated. This difference is only significant for the median of Run 1. SD8 is in all CCLM runs lower than in the observations. These differences are only significant for the median of Run 2.

Table 6.5: RMS and pdf-parameters LOC, SCALE, SHAPE of the predictors used in the parametrisations of budburst, flowering, must density and acidity for the period 1960-2000. The coloured boxes point out differences between CCLM and observational values on a 95 % significance level. The values in bold point out significant differences between observation and CCLM according Equation 6.9.

		RMS	LOC	SCALE	SHAPE	KS-test*
DD3	OBS	18.99	10.15	20.31	0.37	
(Budburst)	CCLM R1	13.94	8.96	10.53	0.00	0.37
	CCLM R2	12.76	5.74	11.37	0.34	0.53
	CCLM R3	8.66	4.89	7.56	0.14	**0.92**
TX4	OBS	14.39	14.32	2.46	0.10	
(Budburst)	CCLM R1	14.84	14.12	4.57	-0.02	0.54
	CCLM R2	14.13	13.18	4.47	0.17	**0.76**
	CCLM R3	13.76	13.59	2.58	-0.14	0.50
Frost1-3	OBS	42.68	39.50	18.50	0.19	
(Budburst)	CCLM R1	38.40	36.00	14.25	0.16	0.19
	CCLM R2	38.87	36.00	17.25	0.19	0.18
	CCLM R3	40.29	36.00	21.00	0.14	0.28
DD5	OBS	171.67	175.36	64.83	-0.25	
(Flowering)	CCLM R1	172.79	150.83	78.77	0.31	0.29
	CCLM R2	168.88	157.52	75.53	0.06	0.21
	CCLM R3	185.52	162.41	86.83	0.28	0.25
DD4	OBS	77.14	70.74	37.37	0.07	
(Flowering)	CCLM R1	91.54	73.43	69.17	0.00	0.54
	CCLM R2	79.63	56.38	58.38	0.15	0.57
	CCLM R3	73.38	63.26	36.60	0.07	0.22
TX6	OBS	21.87	21.69	2.42	0.13	
(Flowering)	CCLM R1	22.64	22.00	3.54	0.27	0.36
	CCLM R2	24.43	23.78	4.83	0.00	**0.97**
	CCLM R3	23.49	23.46	4.77	-0.01	**0.96**
DD4-10	OBS	1402.80	1406.40	254.51	0.00	
(Must density)	CCLM R1	1310.80	1301.70	253.73	-0.05	**0.86**
(Acidity)	CCLM R2	1318.20	1318.20	306.82	-0.35	**0.87**
	CCLM R3	1364.70	1384.90	216.58	-0.41	0.18
TN 16.-22.9	OBS	9.60	9.80	4.00	-0.31	
(Must density)	CCLM R1	9.40	9.40	2.73	-0.16	0.27
	CCLM R2	9.30	9.00	2.69	0.05	0.49
	CCLM R3	9.70	9.20	3.52	0.11	0.16

Table 6.5: (continued)

		RMS	LOC	SCALE	SHAPE	KS-test*
TX 8.-22.8.	OBS	24.30	23.90	3.78	0.08	
(Must density)	CCLM R1	23.60	22.60	8.00	0.17	**0.88**
	CCLM R2	22.90	22.10	5.85	-0.14	**0.95**
	CCLM R3	23.30	22.90	7.71	-0.05	**0.81**
RR9	OBS	70.60	60.50	53.65	-0.10	
(Must density)	CCLM R1	83.30	68.20	50.22	0.28	0.53
	CCLM R2	74.00	65.00	35.64	-0.01	0.22
	CCLM R3	69.40	59.10	47.23	0.11	0.11
Hot5-6	OBS	2.40	1.00	2.00	0.00	
(Must density)	CCLM R1	9.20	6.00	6.00	0.67	**1.00**
	CCLM R2	12.00	10.00	8.25	-0.21	**1.00**
	CCLM R3	10.70	9.00	8.00	0.00	**1.00**
SD8-10	OBS	451.80	448.10	95.30	-0.22	
(Acidity)	CCLM R1	426.60	418.50	99.31	-0.02	0.47
	CCLM R2	408.60	387.10	104.50	0.30	**0.87**
	CCLM R3	431.00	412.80	137.55	0.23	0.64
Summer8	OBS	10.40	9.00	6.00	0.00	
(Acidity)	CCLM R1	7.00	7.00	6.00	-0.33	**0.91**
	CCLM R2	6.60	6.00	3.75	-0.20	**0.95**
	CCLM R3	6.10	5.00	3.25	0.23	**0.99**
Summer8-10	OBS	13.90	12.50	8.00	0.00	
(Acidity)	CCLM R1	9.60	9.00	5.00	-0.20	**0.88**
	CCLM R2	10.40	9.00	8.25	-0.21	0.68
	CCLM R3	10.30	10.00	6.25	-0.36	0.70
TX 8.-22.9.	OBS	20.30	20.2	3.40	-0.26	
(Acidity)	CCLM R1	17.90	17.40	3.82	0.15	**0.97**
	CCLM R2	18.70	18.40	4.54	0.09	0.74
	CCLM R3	19.90	19.50	5.14	0.08	0.49
SD8	OBS	209.70	200.80	65.90	0.15	
(Acidity)	CCLM R1	191.00	175.00	82.25	-0.12	0.69
	CCLM R2	179.10	164.70	80.04	-0.02	**0.92**
	CCLM R3	186.50	180.40	75.61	-0.04	0.65

*Probability $P(D > D_\alpha)$ (Equation 6.9)

The comparisons of the observed predictors with those computed by CCLM showed that some predictors agree well and others are completely deviating from the observation. These differences have a large impact on the results of the phenological and must quality models when they are used in combination with CCLM. These effects and possible calibration methods are discussed in the next section.

6.3 Adjustment of model data to the observations (1960-2000)

The results of the CCLM validation suggest a limited performance to reproduce the observed key climate parameters temperature, precipitation, and sunshine duration (Section 6.2). Especially the frequency distribution of the maximum temperature differs considerably from observations. This influences nearly all "thermal" predictors which are used for the statistical modelling of the phenological events and must quality. Consequently, without post-processing the original CCLM data, the future scenarios cannot be used for an assessment of phenology or must quality changes. Some methods for adjusting data are discussed in the following.

6.3.1 Calibration methods

The most common and easiest adjustment method is the **bias correction**. The time series are corrected by their mean difference; their distribution shape remains untouched. This method is usually chosen when a systematic error (under or overestimation) has occurred in one of both time series, where one data set is defined as reference data.

Especially the tails of a distribution can be corrected by manipulating the data distribution by a **transfer function**, expressed in the form $x' = T(x)$. Basic transformation functions are logarithmic (log and $\log^{-1}$ transformations) and power-law (nth power and nth root transformations) functions (*Gonzalez and Woods*, 2008). The *log* and nth power transformations enlarge the range of low values and compress the range of high values. This method is often used for precipitation to obtain a normal distribution (*Legates*, 1991). The $\log^{-1}$ and nth root transformations have an opposite effect by enlarging the range of higher values. The transformation function should be chosen carefully, because the data range and units of the data play a decisive role. E.g., logarithmised extreme temperature is adjusted unequally when expressed in degree Kelvin or degree Celsius, putting aside the fact that log(0) is not defined. Depending on the data the appropriate function has to be found.

Histogram matching (or histogram equalisation) deforms a distribution in such a way that it corresponds to a reference distribution (*Burger and Burger*, 2006). This technique has its origin in image processing adjusting colour distributions for several images, e.g., taken by different cameras. The cumulative density functions (CDF) of two distributions of length K are considered: the reference P_R (e.g., measurements) and original P_A (model data to be adjusted). For every value a of the original data set a new value a' is found such that

$$a' = P_R^{-1}(P_A(a)) = f_{hs}(a) \tag{6.10}$$

with $f_{hs}(a)$ the transformation function.

For this technique the distribution must be continuous at least within a range so that the cumulative distribution is strictly monotonic increasing. Only in this case

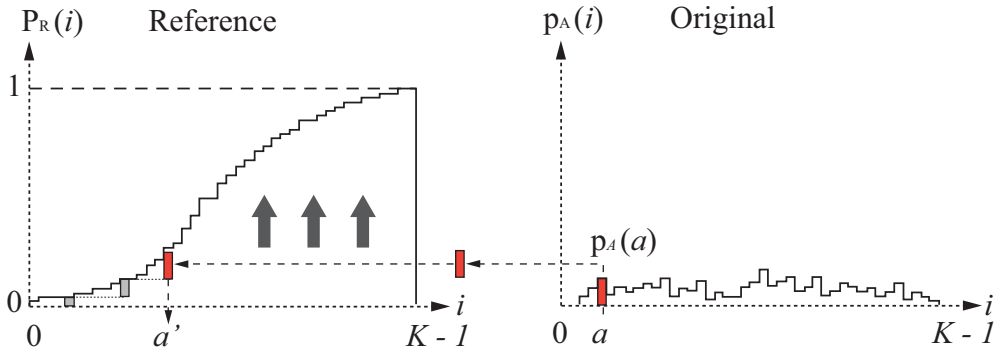

Figure 6.19: Discrete histogram matching method. The reference distribution P_R is "filled" stepwise with the original distribution p_A. The values a are transformed into the values a'.

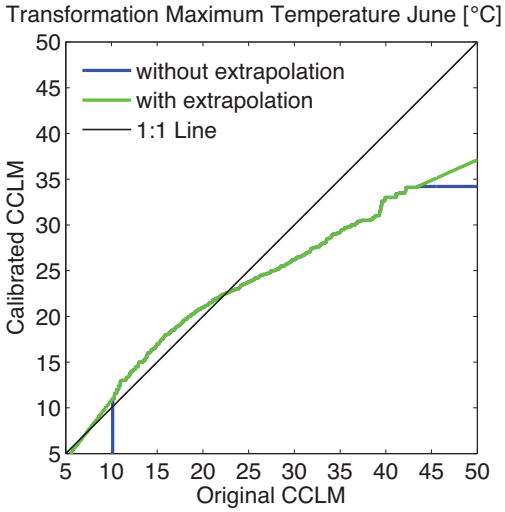

Figure 6.20: Example of transformation: maximum temperature in June with and without extrapolating the edges of the distribution.

there exists the inverse function P_R^{-1}. Real data is mostly not continuous and the CDF only monotonic increasing. In such a case the transformation is not done by inversion but by mapping the cumulative density probability function P_R by the probability function p_A for every value i with $i \in [0, K-1]$ (Figure 6.19). Beginning with $i = 0$ the probability $p_A(i)$ is projected below the cumulative density function P_R. For every value i this projection is continued layer over layer, accumulating the probabilities $p_A(i)$ and building a new cumulative distribution function. The value a' is the new/transformed value for a. The transformation condition can be written as

$$f_{hs}(a) = \min\{i \mid (0 \leq i < K-1) \wedge (P_A(a) \leq P_R(i))\}. \tag{6.11}$$

The distribution functions are normalised, thus all bins of p_A are placed below P_R.

Figure 6.20 stands as example how the transformation of temperature with histogram matching may look like. The high values of June temperature, which are overestimated in the original CCLM data, are transformed to lower values. The original values have been lowered if the green line is below the 1:1 line and they have been increased if the green line is above the 1:1 line. Here, it becomes clear that this transformation is only made in the value range of the reference distribution; values of the original data set which are higher or lower than the reference highest or lowest values are set to the extreme values of the reference (red line end). An extrapolation of the first and last values (e.g., 10°C) of the transformation line (extremes of the green line) can avoid to strictly limit the transformation to the reference data range.

In this work the histogram matching method was chosen because a bias correction was not sufficient and a transfer function not applicable due to the occurrence of negative values for temperature. The adjustments have been applied to daily data and only for temperature, precipitation and sunshine duration. Temperature indices, degree days, or accumulations of precipitation and sunshine duration are adjusted only indirectly. The results of calibrated predictors and corresponding predictands are shown in the next sections.

6.3.2 Adjustments for budburst event

In Section 6.2.2.2 it has been observed that the budburst predictor with the highest explained variance, degree days in March (DD3), calculated with CCLM data highly deviates from the observations. The frost days (FROST1-3), however, agree with the observation. In Figure 6.21 the CCLM predictors used for the budburst date calculation are shown as QQ-plots for all three runs. Figure 6.21a presents the daily data (i.e., the predictor input data) and Figure 6.21b the averaged or accumulated data. DD3 does not fit exactly the observation after the adjustment because only the input temperature data have been adjusted before calculating the degree days; the degree days themselves have not been transformed and its relationship with temperature is not linear. Nevertheless, a good agreement with the observational data is observed for daily data and the predictors. After transformation, the distribution of daily maximum temperature in April (TX4) corresponds to the observation as it is expected after histogram matching. For the mean value, no significant improvements are observed in the QQ-plots: the high values are still overestimated in the CCLM data. FROST1-3 already was in good agreement with the measurements, thus no changes are expected and did not occur.

Figure 6.22 shows the QQ-plot of budburst events with original and modified CCLM data. The budburst date calculated with data of the first realisation is close to the observations and no large differences between original and transformed data is observable. For Run 2 and Run 3, however, the budburst date calculated with the original CCLM data has a clear bias compared to the observations; budburst date calculated with the transformed CCLM data agrees well with the observations.

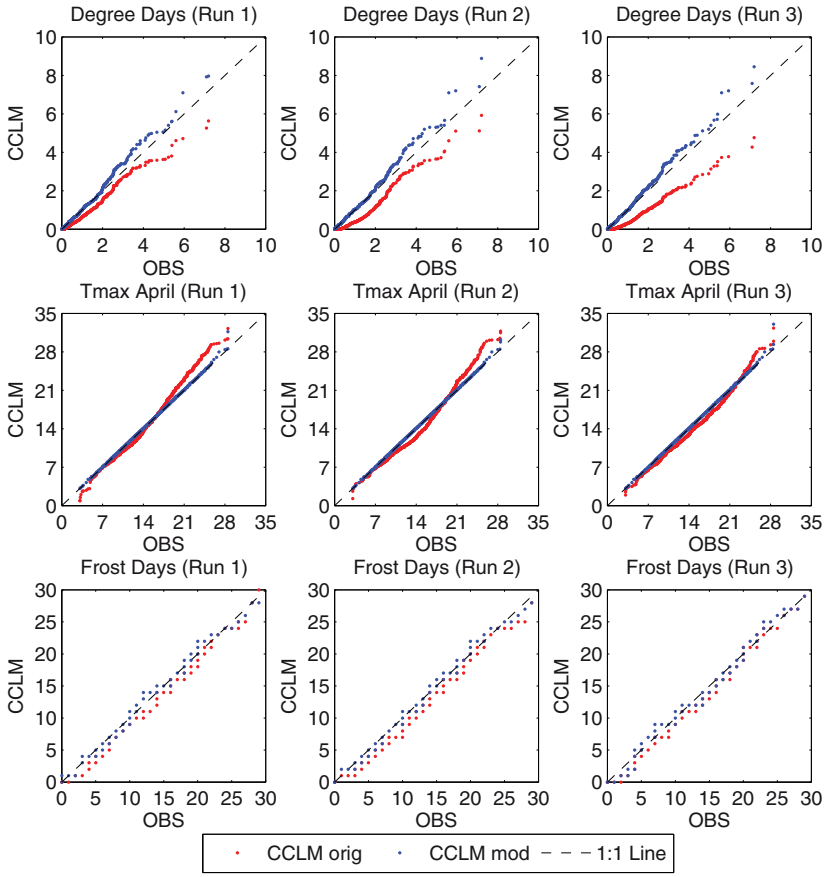

(a) Daily values

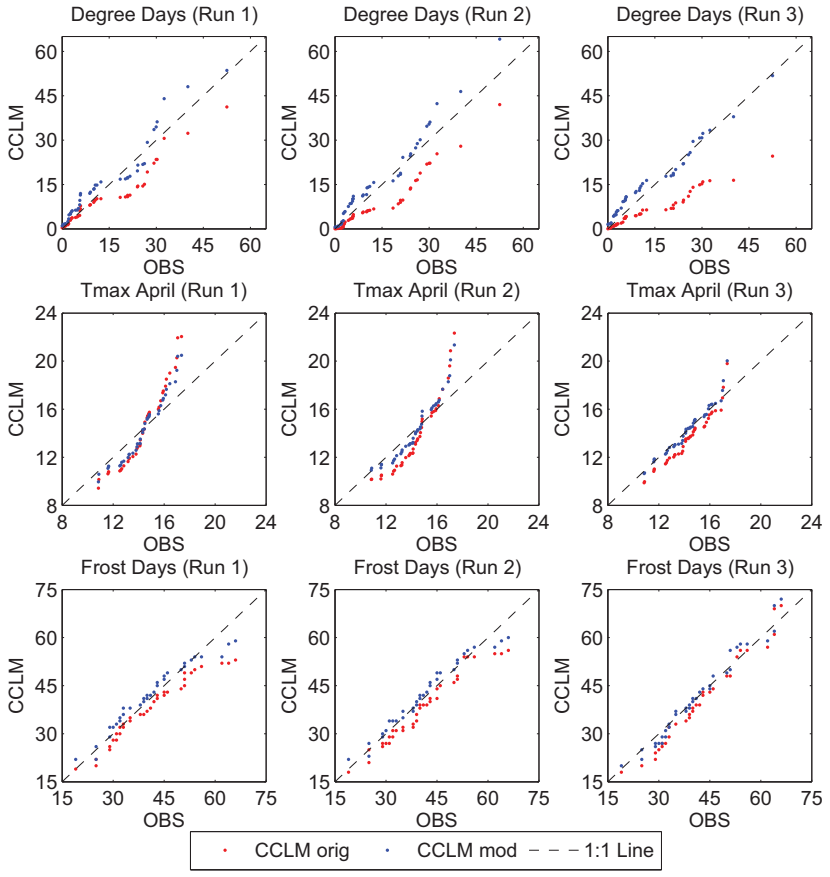

(b) Averaged/accumulated values

Figure 6.21: Daily and averaged/accumulated CCLM data for the predictor periods. The red dots mark the original CCLM and the blue ones the by histogram matching modified data.

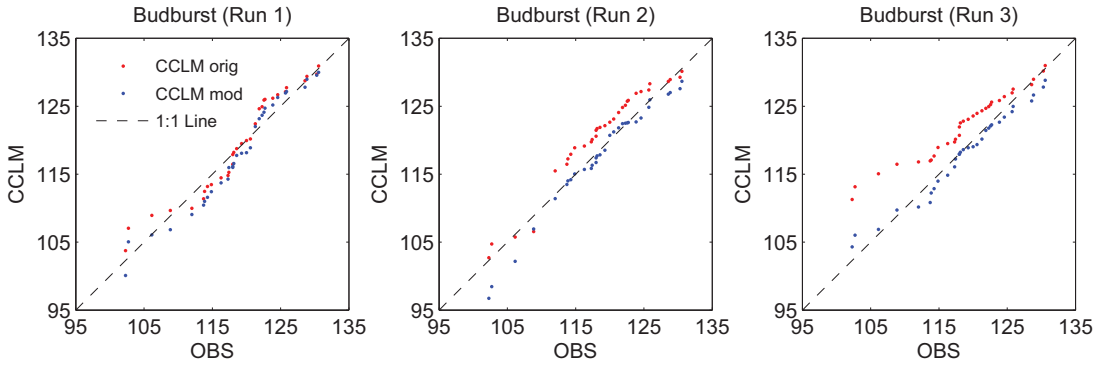

Figure 6.22: Calculation of budburst event (1966-2000) using original CCLM data (red) and adjusted data (blue).

A more objective measure to determine significant differences of distributions, is the KS-test as formulated in Equation 6.9. The probability that CCLM data is different from observational data presents Table 6.6. Transformation of the CCLM data by histogram matching approaches the distribution of DD3 up to 58 % (Run 3) to the observational distribution. Run 1 shows only a small improvement, but it was already closer to the observations than Run 2 and Run 3. The enhancement of TX4 is between 14 % (Run 1) and 51 % (Run 2) and even the predictor FROST1-3 comes closer to the observations by 13 % (Run 2) to 18 % (Run 3). The probability that the budburst date calculated with original CCLM data differs from the observation, amounts up to 82 % (Run 3). Using the transformed CCLM data this probability is reduced to a maximum of 34 % (Run 1). This calibration method is able to correct the budburst date up to 72 % (Run 3) even when only daily data is transformed, i.e., the effect is not lost after several calculations (averages, indices, etc).

Table 6.6: Probabilities [%] of budburst predictors and budburst date calculated by the KS-test (Equation 6.9) that the distribution of original and adjusted CCLM output data differs from the observational data ($P_{\neq}$). The differences between $P_{\neq}$ of original and adjusted CCLM is denoted by Δ.

		DD3		Tmax 4		Frost(1-3)		*Budburst*	
		$P_{\neq}$	Δ	$P_{\neq}$	Δ	$P_{\neq}$	Δ	$P_{\neq}$	Δ
Run 1	original	39	− 3	54	− 14	20	− 14	39	− 5
	adjusted	36		40		6		34	
Run 2	original	53	− 30	77	− 51	19	− 13	64	− 47
	adjusted	23		26		6		17	
Run 3	original	91	− 58	51	− 40	27	− 18	82	− 72
	adjusted	33		11		9		10	

Table 6.7: Probabilities [%] of flowering predictors and flowering date calculated by the KS-test (Equation 6.9) that the distribution of original and adjusted CCLM output data differs from the observational data ($P_{\neq}$). The differences between $P_{\neq}$ of original and adjusted CCLM is denoted by Δ.

		DD5		DD4		Tmax6		*Flowering*	
		$P_{\neq}$	Δ	$P_{\neq}$	Δ	$P_{\neq}$	Δ	$P_{\neq}$	Δ
Run 1	original	31	− 5	53	− 7	36	− 26	15	− 6
	adjusted	26		46		10		9	
Run 2	original	22	− 12	58	− 32	96	− 85	31	− 14
	adjusted	10		26		11		17	
Run 3	original	27	− 7	24	− 11	96	− 78	29	− 14
	adjusted	20		13		18		15	

6.3.3 Adjustments for the flowering event

The estimation of the flowering event is based on the meteorological predictors degree days in May (DD5), degree days in April (DD4) and maximum temperature in June (TX6), besides budburst date (BB). The QQ-plots comparing the CCLM data to the observation are presented in Figure 6.23.

Daily DD5 are clearly overestimated for high values which is successfully corrected by histogram matching (Figure 6.23a). This calibration effect is nearly lost when the degree days are accumulated (Figure 6.23b). The Kolmogorov-Smirnov test indicates a convergence between 5 % (Run 1) and 12 % (Run 2) to the observed values (Table 6.7). The daily DD4 does not diverge much from the observations, but differences become visible in the accumulation. The histogram matching method corrects Run 2 by 32 %. The predictor TX6 has a lower impact on the flowering event than the degree days (Table 5.2), but it shows large deviations from the observations, especially for high values. The probability that the unmodified CCLM data is different from the observation is 96 % for Run 2 and Run 3. Here, the calibration method shows the largest effects: TX6 moves closer between 28 % (Run 1) and even up to 85 % (Run 2) to the observations.

In addition to the above discussed main climate predictors, budburst date calculated from original and adjusted CCLM data is used to compute the corresponding flowering dates. The calibration effects are not very high for the flowering event (Figure 6.24). Early dates are still underestimated after adjustment. The results of the KS-test (Table 6.7) show, however, an improved approximation of 6 % to 14 % to the observations.

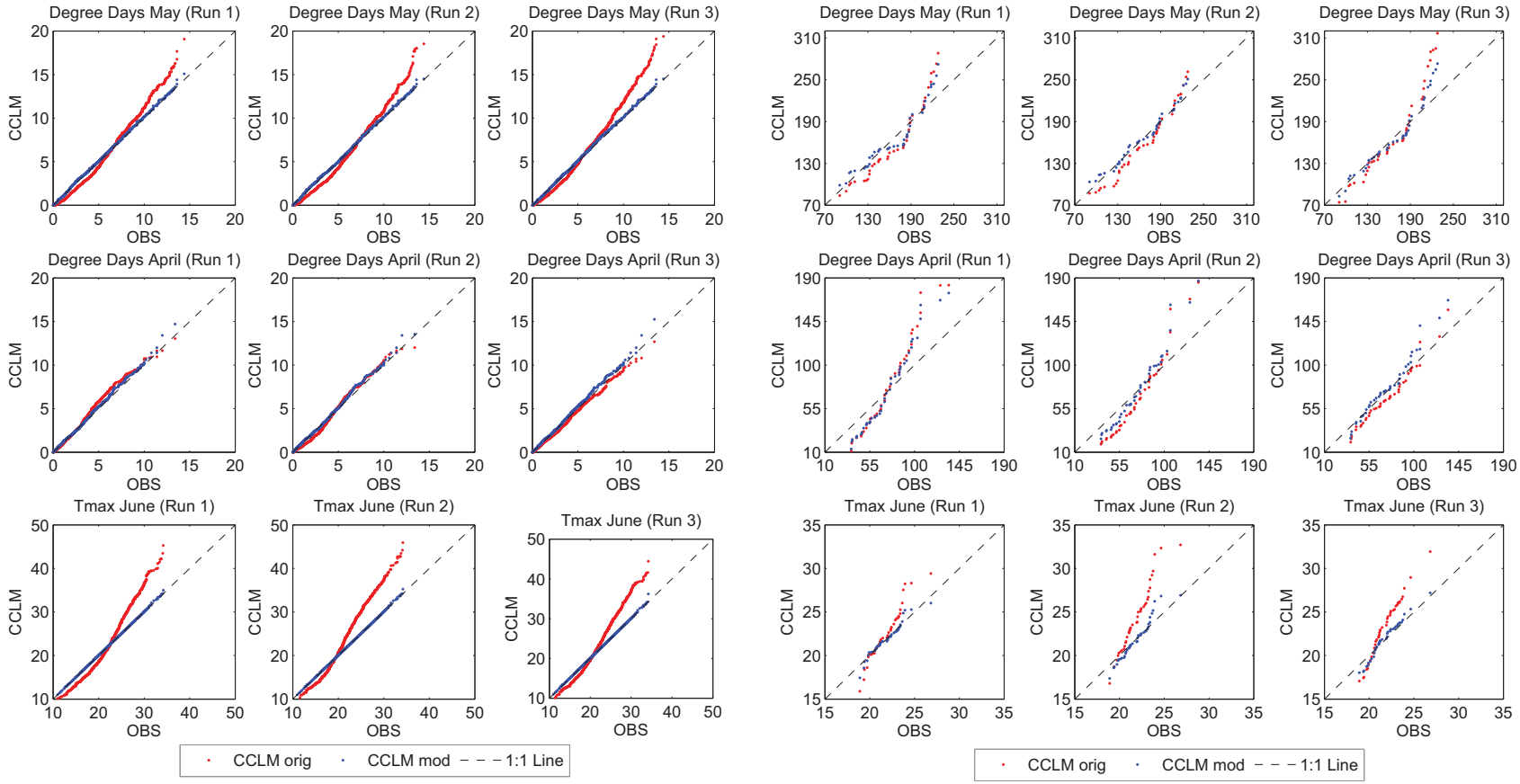

(a) Daily scale

(b) Predictor (annual) scale

Figure 6.23: CCLM data for flowering estimation on daily and predictor scale for the predictor periods. The red dots mark the original CCLM data and the blue ones the modified data.

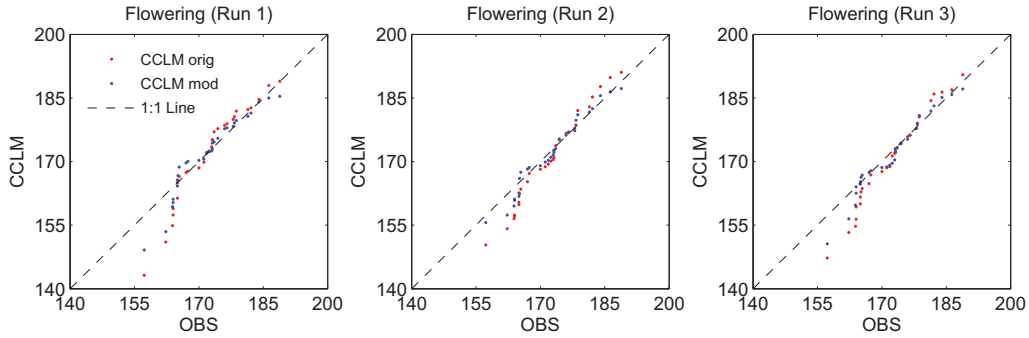

Figure 6.24: Calculation of flowering event using original CCLM data (red) and adjusted data (blue).

6.3.4 Adjustments for the must density

Must density is calculated separately for cluster CM1 (Auxerrois, Pinot Blanc, Pinot Gris, Riesling and Traminer) and cluster CM2 (Elbling and Rivaner).

Cluster CM1 The predictors for the first cluster are shown in Figure 6.25. High values of degree days from April to October (DD4-10) are overestimated for daily data (Figure 6.25a), and underestimated for low values of accumulated DD4-10 (Figure 6.25b). Both deviations are corrected by histogram matching. The calibration method has also a large effect on maximum temperature from 8 to 22 August ($TX8_{8-22}$) but the corrected values have still a small bias compared to the observations. This can be due to the fact that temperature calibration has been made with data of the whole month but this predictor covers only 2 weeks. Modifications of minimum temperature from 16 to 22 September ($TN9_{16-22}$) and precipitation during September (RR9) do not show large changes.

The distributions of DD4-10 and $TX8_{8-22}$ are clearly different from the observations: according to the Kolmogorov-Smirnov test on equal distribution is, in most cases, lower than 20 % (Table 6.9a). The histogram matching method adjusts the modified CCLM predictors DD4-10 and $TX8_{8-22}$ to the observational distribution by around 70 %. The calibration effect for $TN9_{16-22}$ and RR9 is much smaller. The must density itself is corrected by a large amount (Figure 6.27a). After calibration it is by 28 % (Run 3) to 73 % (Run2) closer to the observed must density.

Cluster CM2 Must density of the second cluster is calculated using following predictors: number of hot days between May and June (HOT5-6), sunshine duration from August to October (SD8-10), and the number of summer days in August (SUMMER8). These predictors are poorly reproduced by CCLM; the probability to be different from the observation is even 100 % for HOT5-6 (Table 6.9b and Figure 6.26). Histogram matching reduces this probability nearly completely (compare Figures C.4b and C.4a in Appendix). Daily SD8-10 is underestimated by CCLM for small values, especially below 6 hours, but it can be corrected (Figure 6.26a).

Table 6.8: Probabilities [%] of must density predictors and must density calculated by the KS-test (Equation 6.9) that the distribution of original and adjusted CCLM output data differs from the observational data ($P_{\neq}$). The differences between $P_{\neq}$ of original and adjusted CCLM is denoted by Δ.

		DD (4-10)		TN 16.-22.9.		TX 8.-22.8.		RR(9)		*Must density I*	
		$P_{\neq}$	Δ	$P_{\neq}$	Δ	$P_{\neq}$	Δ	$P_{\neq}$	Δ	$P_{\neq}$	Δ
Run1	original	85	− 63	27	− 13	88	− 72	46	− 32	81	− 60
	adjusted	22		14		16		14		21	
Run2	original	86	− 72	47	− 23	95	− 76	25	− 8	88	− 73
	adjusted	14		24		19		17		15	
Run3	original	16	− 9	15	− 4	82	− 70	16	− 4	49	− 28
	adjusted	7		11		12		12		21	

(a) Must density Cluster CM1

		Hot (5-6)		SD (8-10)		Summer (8)		*Must density II*	
		$P_{\neq}$	Δ	$P_{\neq}$	Δ	$P_{\neq}$	Δ	$P_{\neq}$	Δ
Run1	original	100	− 94	56	− 34	89	− 85	100	− 76
	adjusted	6		22		4		24	
Run2	original	100	− 98	90	− 68	94	− 90	100	− 90
	adjusted	2		22		4		10	
Run3	original	100	− 100	70	− 39	99	− 94	100	− 87
	adjusted	0		31		5		13	

(b) Must density Cluster CM2

The cumulative sunshine duration of this period is closer to the observational distribution after calibration (34 % to 68 %), but for all realisations, sunshine duration is slightly overestimated by calibrated CCLM. SUMMER8 is underestimated by original CCLM because of the overestimation of maximum temperature. After calibration SUMMER8 is less than 5 % different from the observations. Must density of Elbling and Rivaner has been overestimated using original CCLM predictors, especially for high must densities (Figure 6.27b). After calibration these differences are reduced: adjusted distribution of must density has only a probability from 10 % (Run 2) to 24 % (Run 1) to be different from the observations.

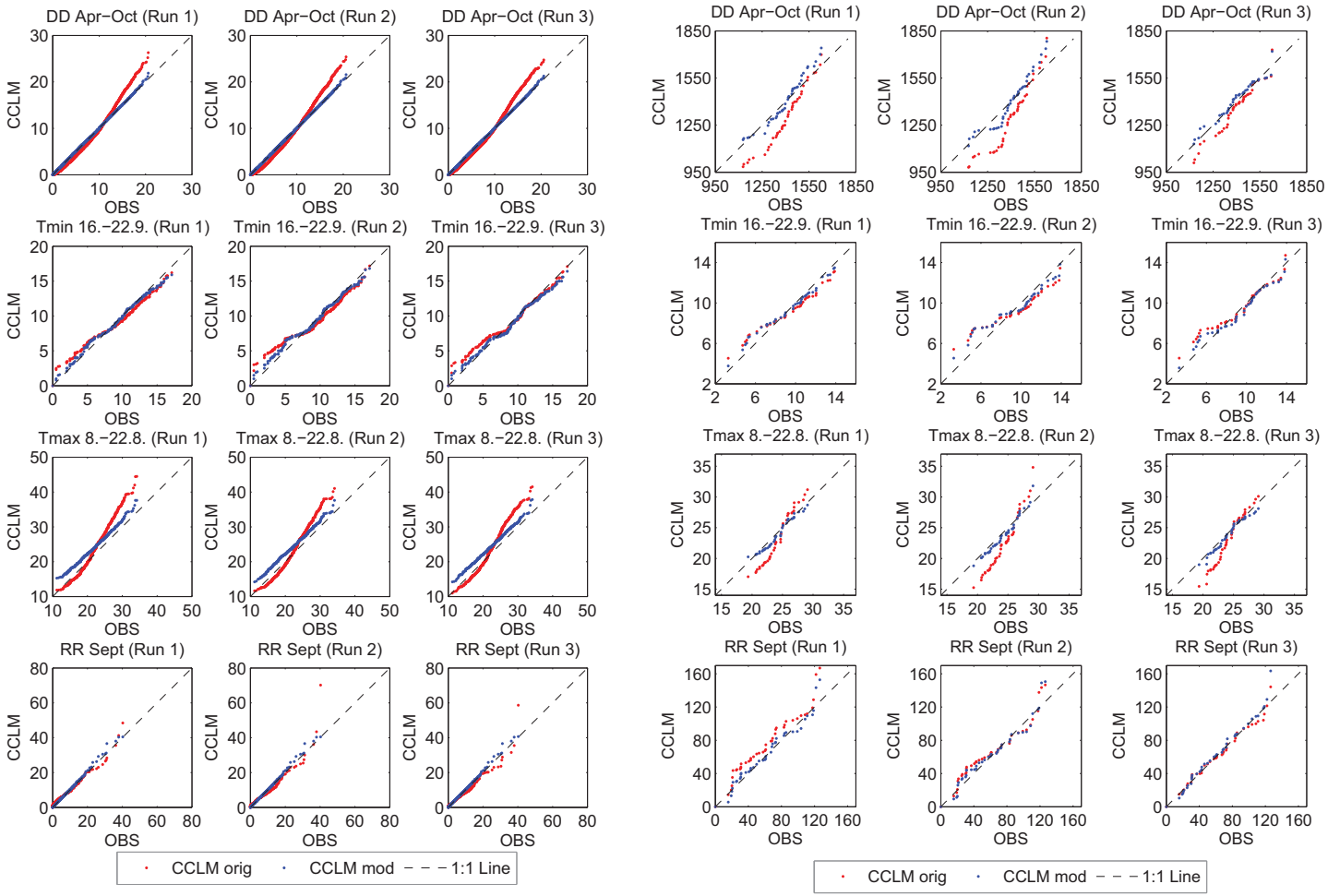

(a) Daily scale

(b) Predictor (annual) scale

Figure 6.25: CCLM data for must density estimation of cluster CM1 on daily and predictor scale for the predictor periods. The red dots mark the original CCLM data and the blue ones the modified data.

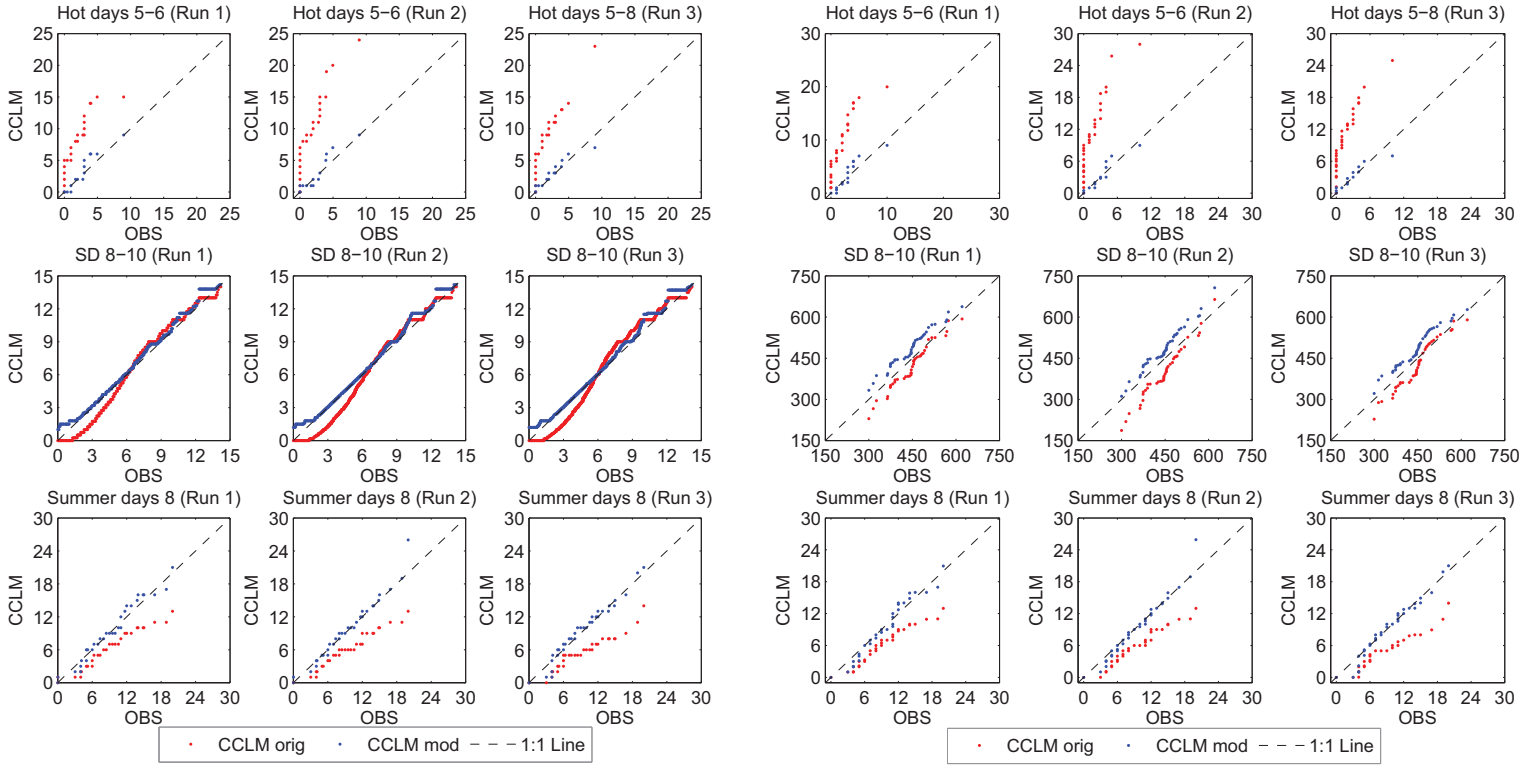

(a) Daily scale

(b) Predictor (annual) scale

Figure 6.26: CCLM data for must density estimation of cluster CM2 on daily and predictor scale for the predictor periods. The red dots mark the original CCLM data and the blue ones the modified data.

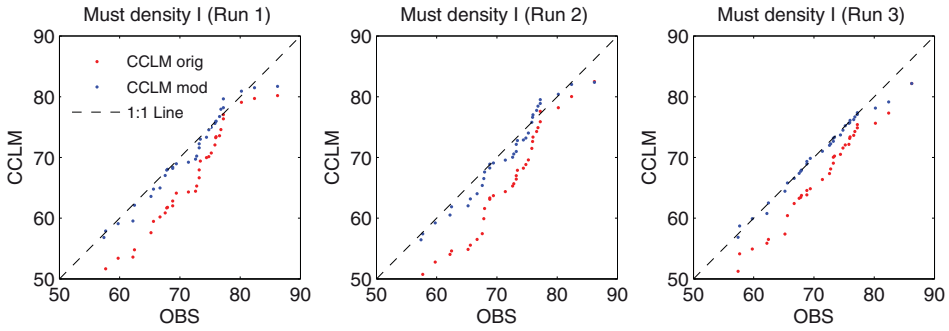

(a) Cluster CM1

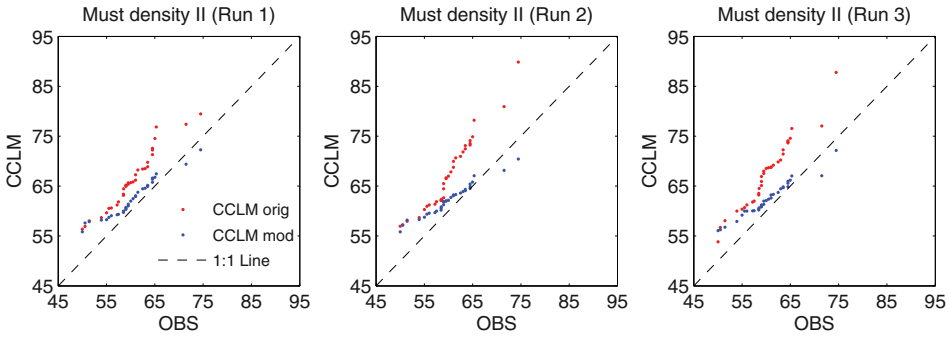

(b) Cluster CM2

Figure 6.27: Calculation of must density of the clusters CM1 and CM2 using original CCLM data (red) and adjusted data (blue).

6.3.5 Adjustments for the acidity

The acidity is estimated for three clusters:

- Cluster CA1: Auxerrois, Rivaner, Traminer
- Cluster CA2: Pinot Blanc, Pinot Gris
- Cluster CA3: Elbling, Riesling

The amount of degree days from April to October (DD4-10) is the dominant predictor for all acidity clusters as it is for must density (cluster CA1). Therefore it will not be discussed in this section again.

Clusters CA1 and CA3 The cluster CA1 and cluster CA3 of acidity have the same predictors, but their weights are different. The number of summer days from August to October (SUMMER8-10) is underestimated by CCLM data (Figure 6.29) because maximum temperature is overestimated during summer. After calibration it has a probability between 5 % (Run 3) and 17 % (Run 2) to be equal to the observational distribution (Table 6.9). Estimated acidity for cluster CA1 and CA3 is calculated too high using original CCLM data. The calibration method reduces this deviation and finally the probability that CCLM and observations are different is below 20 %.

Table 6.9: Probabilities [%] of predictors and acidity of the clusters CA1 and CA3 calculated by the KS-test (Equation 6.9) that the distribution of original and adjusted CCLM output data differs from the observational data ($P_{\neq}$). The differences between $P_{\neq}$ of original and adjusted CCLM is denoted by Δ.

		DD (4-10)		Summer (8-10)		*Acidity I*		*Acidity III*	
		$P_{\neq}$	Δ	$P_{\neq}$	Δ	$P_{\neq}$	Δ	$P_{\neq}$	Δ
Run1	original	85	− 63	88	− 80	69	− 51	70	− 53
	adjusted	22		8		18		17	
Run2	original	86	− 72	67	− 50	49	− 29	51	− 31
	adjusted	14		17		20		20	
Run3	original	16	− 9	70	− 65	21	− 5	24	− 5
	adjusted	7		5		16		16	

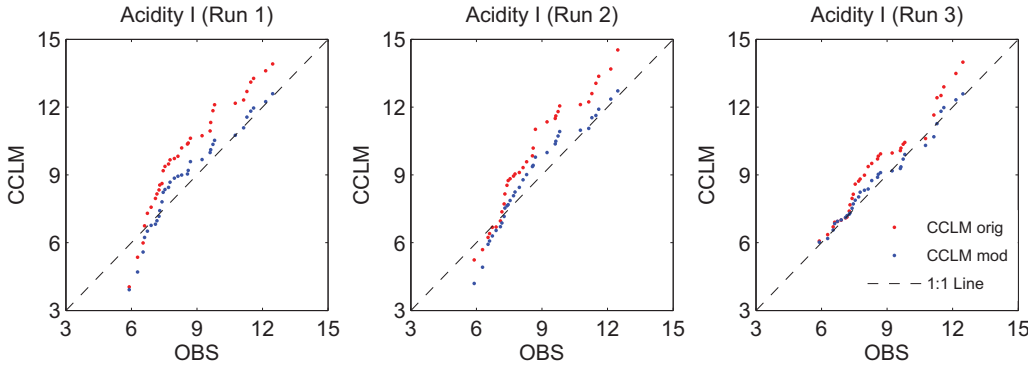

(a) Cluster CA1

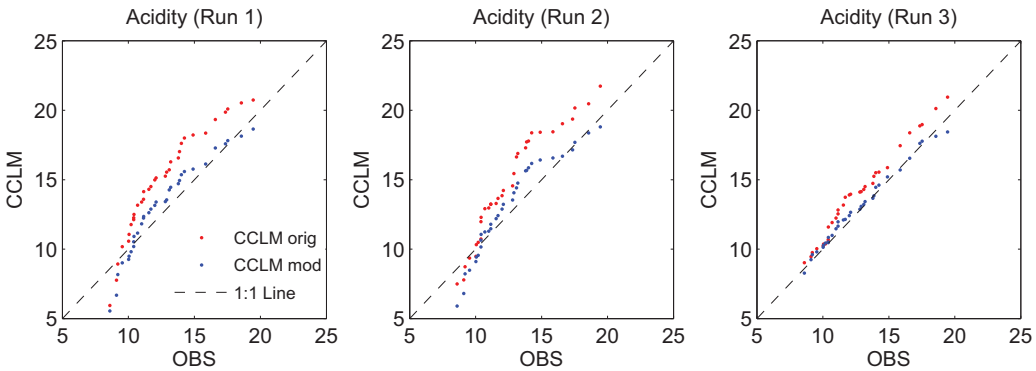

(b) Cluster CA3

Figure 6.28: Calculation of acidity (clusters CA1 and CA3) using original CCLM data (red) and adjusted data (blue).

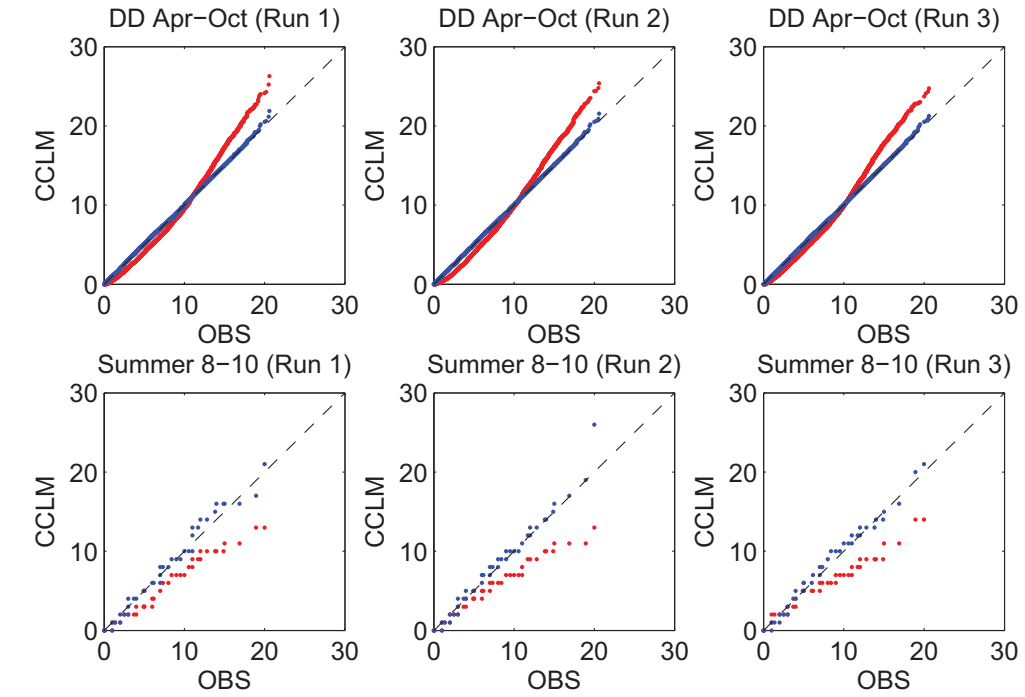

(a) Daily scale

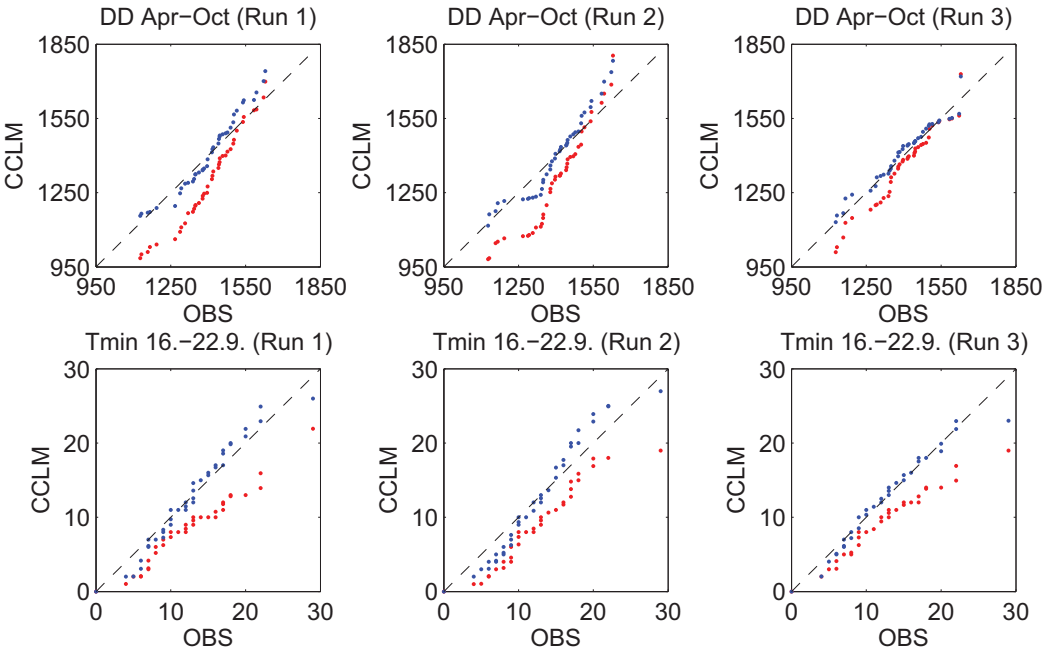

(b) Predictor (annual) scale

Figure 6.29: CCLM data for acidity estimation (cluster CA1 and cluster CA3) on daily and predictor scale for the predictor periods. The red dots mark the original CCLM data and the blue ones the modified data.

Table 6.10: Probabilities [%] of predictors and acidity of cluster CA2 calculated by the KS-test (Equation 6.9) that the distribution of original and adjusted CCLM output data differs from the observational data ($P_{\neq}$). The differences between $P_{\neq}$ of original and adjusted CCLM is denoted by Δ.

		DD (4-10)		TX 8.-22.9.		SD 8		*Acidity II*	
		$P_{\neq}$	Δ	$P_{\neq}$	Δ	$P_{\neq}$	Δ	$P_{\neq}$	Δ
Run1	original	85	− 63	97	− 78	80	− 52	90	− 71
	adjusted	22		19		18		19	
Run2	original	86	− 72	74	− 61	94	− 81	86	− 64
	adjusted	14		13		13		22	
Run3	original	16	− 9	48	− 33	72	− 56	18	− 1
	adjusted	7		15		16		17	

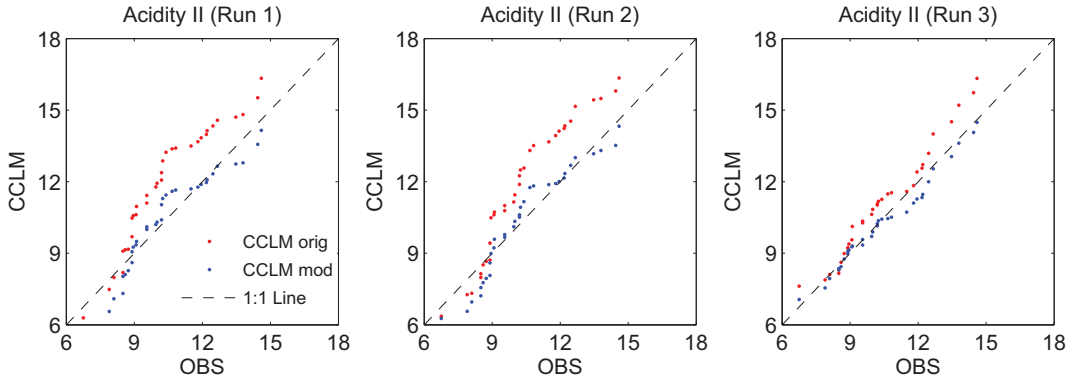

Figure 6.30: Calculation of acidity (cluster CA2) using original CCLM data (red) and adjusted data (blue).

Cluster CA2 Acidity of cluster CA2 is predicted, besides DD4-10, using maximum temperature from 8th to 22nd September ($TX9_8 - 22$) and sunshine duration of August (SD8). Both parameters are underestimated by the original CCLM data (Figure 6.31). The derived acidity is consequently overestimated because both predictors have a decreasing effect on acidity. After calibration of the CCLM data, the acidity is much closer to the observations (Table 6.10): the distributions of observed and estimated acidity are equal with a probability around 80 %.

6.3.6 Short summary

Histogram matching shows good results for the phenological and must quality models even though the time periods chosen for calibration have to be set arbitrarily; here it is set to one month periods. Calibrating the input data corrects also the derived variables like degree days and temperature indices. This effect is maintained for the predictand. The budburst date, must density and acidity could be largely corrected; the effect for the flowering event was less successful. For most realisations, the probability that the distributions of observed and estimated predictands are different is reduced to less than 20 % after the application of histogram matching. Not shown here, this calibration method manages to reduce the variability by a huge amount for some predictors (e.g., degree days in May, maximum temperature in June, degree days between April and October, maximum temperature between 8 and 22 August). The correspondent time series are presented in Appendix C.1.

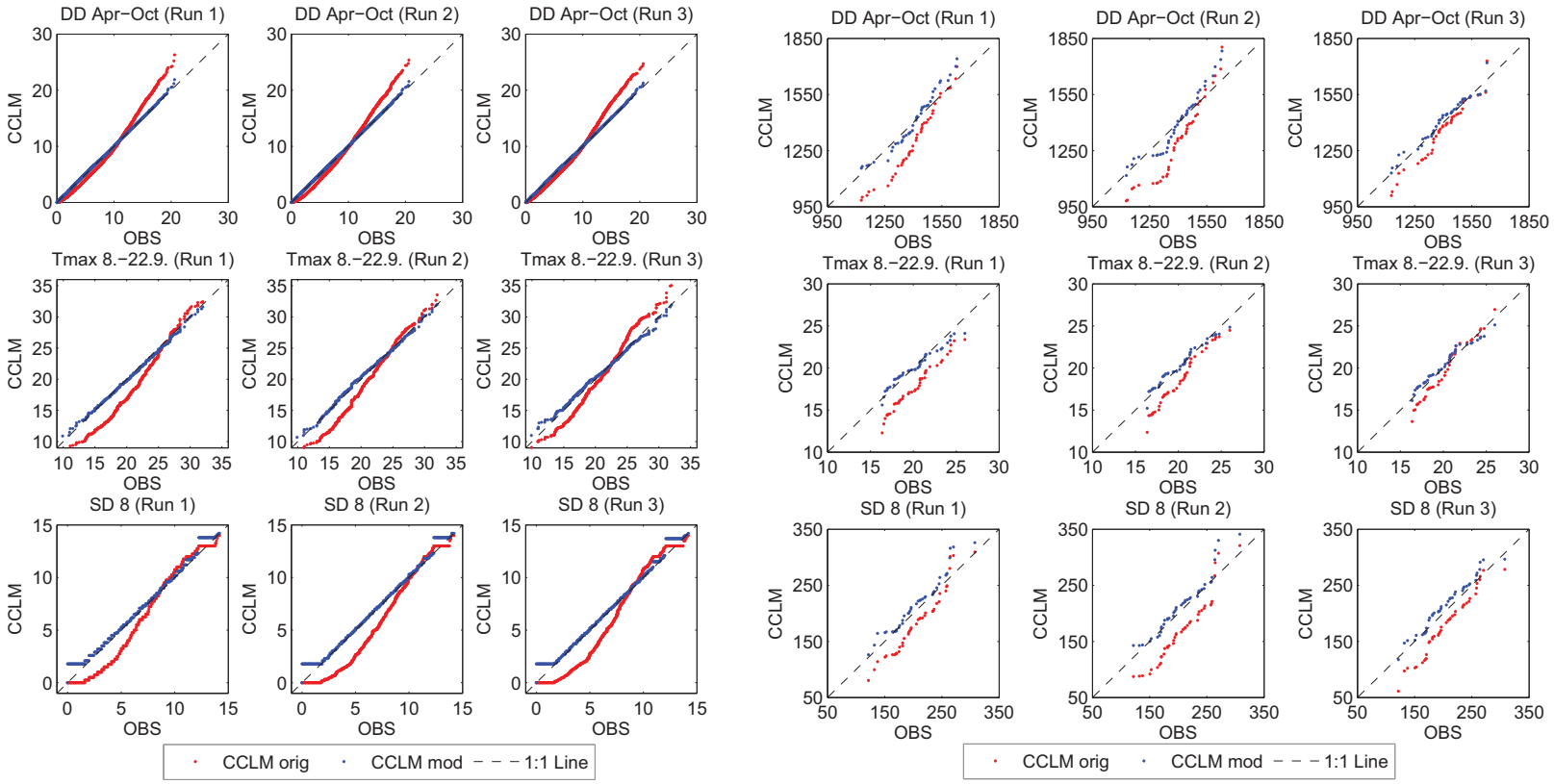

(a) Daily scale

(b) Predictor (annual) scale

Figure 6.31: CCLM data for acidity estimation (cluster CA2) on daily and predictor scale for the predictor periods. The red dots mark the original CCLM data and the blue ones the modified data.

Chapter 7

7 Comparison of past and future climate conditions in CCLM

For the analysis of the future climate projections 2001-2050 only the first two simulations under the scenarios A1B and B1 are available (Table 6.1); as a consequence the third realisation of the past period C20 (1960-2000) will not be compared to the future period. This chapter presents only the changes between original (i.e., without histogram matching calibration) CCLM data during the past period 1960-2000 and the future period 2001-2050. In this chapter, no observational data is taken into account. The analysis of original CCLM output focusses on annual means of key climate parameters and 16 predictors, estimating vine phenology and must quality for past and future periods. The calibration and transformation of predictors will be discussed in Chapter 8.

7.1 Expected climate change in the Upper Moselle region

The statistical evaluation of CCLM data for the scenarios is given in Table 7.1 and the trends are shown in Table 7.2. According to the consortial runs, the annual temperature in the Upper Moselle region increases by about 1 °C during the period 2001-2050 compared to 1960-2000 for all scenarios and runs. The temperature range (difference between maximum and minimum) is only in Run 1 of A1B significantly augmented. The lower and upper extremes of temperature increase substantially depending on scenario and realisation. While the first quartile of the maximum temperature distribution remains almost constant, it is significantly higher for minimum and mean temperature. The third quartile of all temperatures and for both scenarios is significantly higher than C20.

Table 7.1: Statistical evaluation of annual temperature, precipitation and sunshine duration of CCLM data for the periods 1960-2000 (C20) and 2001-2050 for the scenarios A1B and B1. Significant differences (95 % level) between C20 and A1B or B1 are labelled in red/blue for higher/lower values.

		Tmax [°C]		Tmin [°C]		Tmean [°C]		Prec [mm]		SD [h]	
		Run1	Run2	Run1	Run2	Run1	Run2	Run1	Run2	Run1	Run2
mean value	C20	13.48	13.47	5.69	5.60	9.14	9.10	932	945	1537	1540
	A1B	14.47	14.34	6.49	6.58	10.05	10.01	955	988	1553	1489
	B1	14.07	14.50	6.40	6.54	9.81	10.07	1010	955	1467	1542
standard deviation	C20	0.88	1.03	0.47	0.56	0.61	0.73	113	120	169	177
	A1B	1.22	1.07	0.73	0.71	0.92	0.81	119	126	208	193
	B1	0.89	1.07	0.53	0.72	0.64	0.84	109	113	159	160
range	C20	3.86	4.52	1.78	2.76	2.53	3.50	558	580	658	727
	A1B	5.71	4.41	3.17	3.44	4.38	3.50	498	501	773	773
	B1	3.89	5.73	2.07	4.22	2.42	4.88	535	444	694	641
minimum	C20	11.77	11.62	4.71	4.37	7.95	7.65	635	664	1214	1160
	A1B	11.88	12.08	5.26	4.60	8.20	8.02	739	726	1170	1107
	B1	12.03	11.18	5.33	4.03	8.52	7.26	756	724	1162	1214
maximum	C20	15.63	16.15	6.49	7.13	10.49	11.15	1193	1244	1872	1887
	A1B	17.60	16.49	8.43	8.04	12.57	11.52	1237	1227	1943	1880
	B1	15.92	16.91	7.40	8.25	10.94	12.15	1290	1167	1856	1855
1st quartile	C20	12.75	12.63	5.37	5.23	8.75	8.64	854	877	1427	1426
	A1B	13.78	13.60	5.95	6.13	9.36	9.47	879	908	1380	1332
	B1	13.59	13.93	6.02	6.07	9.35	9.40	936	881	1326	1423
3rd quartile	C20	14.05	14.11	5.98	5.93	9.53	9.57	1033	1006	1654	1656
	A1B	15.21	15.00	6.86	7.10	10.60	10.55	1034	1086	1714	1647
	B1	14.66	15.15	6.80	7.01	10.31	10.60	1067	1020	1568	1648

Abbr.: maximum (Tmax), minimum (Tmin), mean (Tmean) temperature, precipitation (Prec), and sunshine duration (SD)

Table 7.2: Evaluation of annual trends (per year) for temperature, precipitation and sunshine duration of CCLM data for different time slices. Trends with a significance level of 99 %/95 %/90 % are labelled in red/orange/yellow respectively.

Period	Scenario	Tmax [°C]		Tmin [°C]		Tmean [°C]		Prec [mm]		SD [h]	
		Run1	Run2	Run1	Run2	Run1	Run2	Run1	Run2	Run1	Run2
1960 - 2050	A1B	0.03	0.02	0.02	0.02	0.02	0.02	0.28	0.68	0.70	-1.10
	B1	0.01	0.02	0.01	0.02	0.01	0.02	1.45	0.13	1.2	0.00
2001 - 2050	A1B	0.04	0.02	0.03	0.03	0.04	0.02	-0.07	1.45	0.90	-4.30
	B1	0.00	0.01	0.01	0.02	0.01	0.02	1.70	1.36	-3.50	-2.40
2001 - 2030	A1B	0.03	-0.04	0.02	0.00	0.02	-0.02	-3.00	6.04	2.80	-12.40
	B1	-0.01	0.00	0.01	0.02	0.00	0.01	2.16	4.62	-5.50	-5.50
2011 - 2040	A1B	0.05	0.04	0.04	0.04	0.04	0.04	-1.86	3.27	-0.10	-3.40
	B1	-0.02	0.02	-0.01	0.01	-0.01	0.02	-0.40	-0.94	-0.20	0.70
2021 - 2050	A1B	0.05	0.06	0.04	0.05	0.05	0.05	4.04	-2.20	-1.20	1.90
	B1	0.01	0.00	0.02	0.01	0.01	0.00	1.10	-0.08	-4.00	-3.60

Abbr.: maximum (Tmax), minimum (Tmin), mean (Tmean) temperature, precipitation (Prec), and sunshine duration (SD)

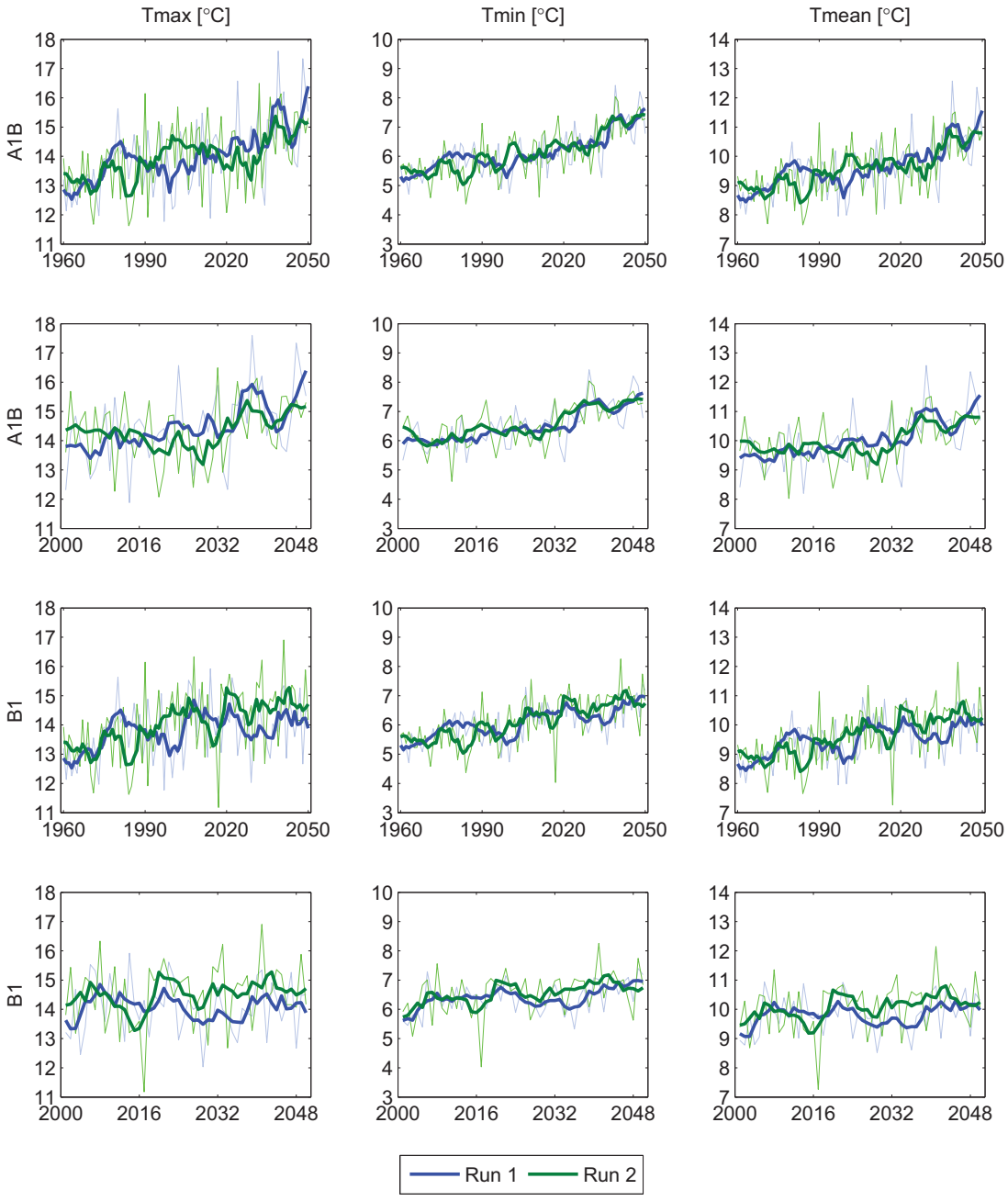

Figure 7.1: Temperature time series (1960-2050 and 2001-2050) of CCLM simulations for the scenarios A1B and B1, each including two runs. The thick lines are a moving average of 5 years. Trends for different time slices are listed in Table 7.2.

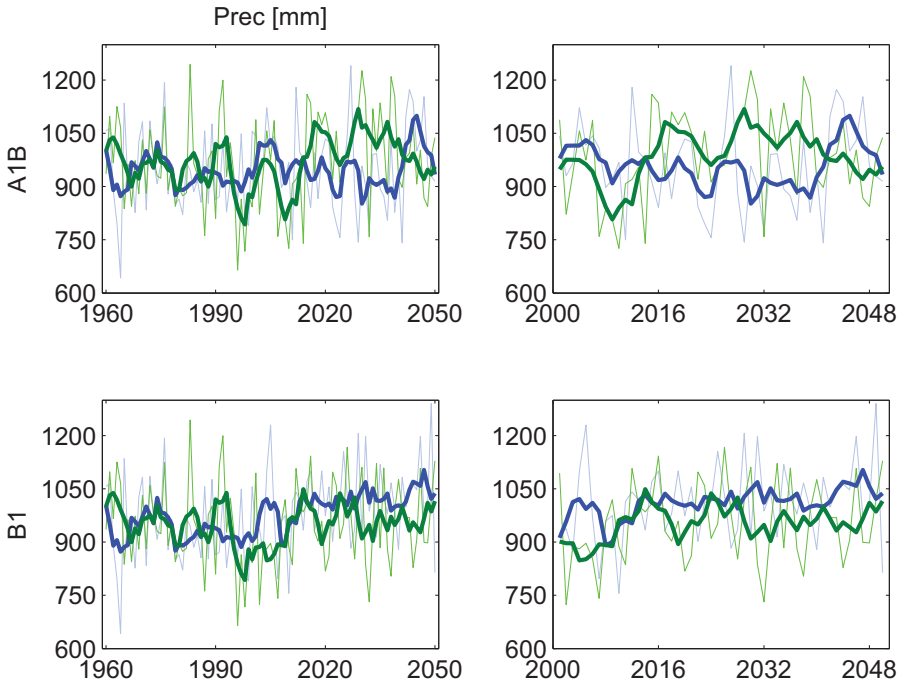

Figure 7.2: Precipitation time series (1960-2050 and 2001-2050) of CCLM simulations for the scenarios A1B and B1, each including two runs. The thick lines are a moving average of 5 years. Trends for different time slices are listed in Table 7.2.

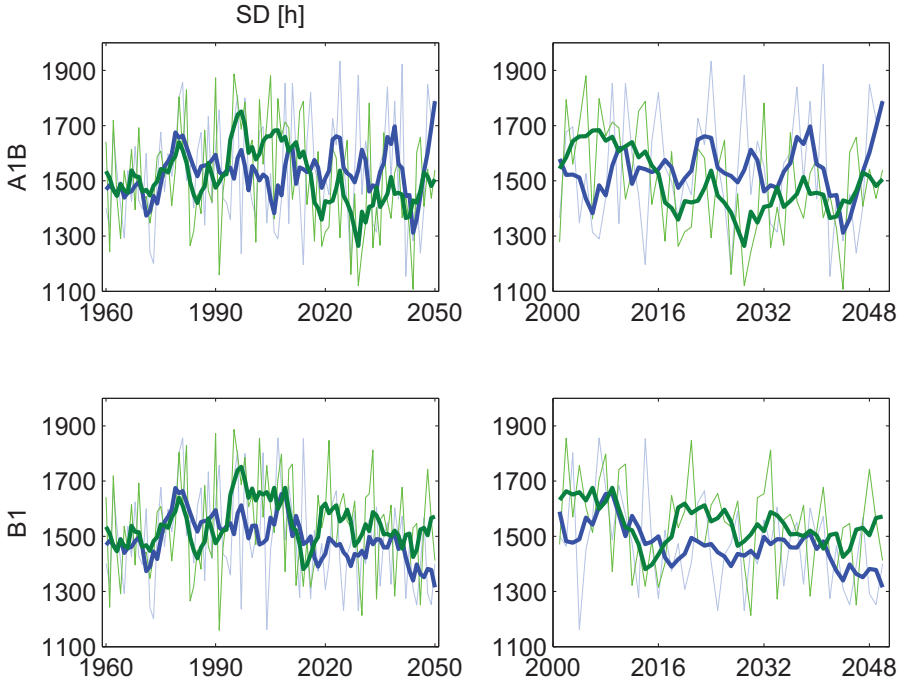

Figure 7.3: Sunshine duration time series (1960-2050 and 2001-2050) of CCLM simulations for the scenarios A1B and B1, each including two realisations. The thick lines are a moving average of 5 years. Trends for different time slices are listed in Table 7.2.

Precipitation and sunshine duration do not change substantially during the future period compared to the past. Only mean, maximum and first quartile values of precipitation in the B1 scenario clearly increase. Sunshine duration remains unchanged except for an extended range in the first realisation of the A1B scenario.

A similar, but less pronounced behaviour is observable in the evaluation of trends (Table 7.2). During the whole period 2001-2050 temperature shows significant upward trends. In the scenario B1, however, only minimum temperature is significantly increasing. During the first 30 years, i.e., 2001-2030, temperature remains nearly constant; even an decreasing trend is observed in Run 2 of A1B. During the period 2011-2040 temperature calculated for scenario A1B is increasing, where it remains unchanged for B1. In the last period 2021-2050 the trends become more important for A1B, but B1 shows no clear increasing trends. The corresponding time series are shown in Figure 7.1. The two runs differ, however: it seems they fluctuate with asynchrony phases. This is clearly visible in the maximum temperature time series and weaker for minimum temperature. The differences become smaller approximately after 2010, thus this phenomenon is a characteristic mainly for the past period 1960-2000.

In accordance with Table 7.1 no significant trends in annual total precipitation are detected for the period 2001-2050 and for most sub-periods; during 2001-2030 Run 2 shows an increase of precipitation at a significance level of 90 %. Sunshine duration, however, has a decreasing trend for some future periods. Over the whole period it decreases at a significance level of 95 % for Run 2 in A1B and Run 1 in B1. A very high decrease is detected for Run 2 of A1B during the period 2001-2030. Afterwards, sunshine duration does not change significantly in all realisations and scenarios. The time series of precipitation and sunshine duration for the period 1960-2050 are presented in Figure 7.2 and Figure 7.3, respectively.

7.2 Expected changes in the selected predictors

The comparison of predictors' behaviour during the future period A1B and B1 to the past period C20 is of high interest because of the impact on phenology and must quality. In a first approach the predictors are analysed by QQ-plots. Figures 7.4 to 7.7 show differences of CCLM data between past (1960-2000) and future (2001-2050) for different scenarios and realisations.

Budburst The predictors for budburst are depicted in Figure 7.4 as QQ-plot comparing the distributions of C20 to A1B and B1 periods. The distributions of degree days in March (DD3) and maximum temperature in April (TX4) remain constant for most of the values. Higher values of future DD3 and TX4 are, however, slightly lower than those for the past period. Future frost days (FROST1-3) become generally less frequent. Only a significant negative trend of DD3 is expected during the period 2001-2030 for the A1B scenario (Table 7.3). TX4 and FROST1-3 have

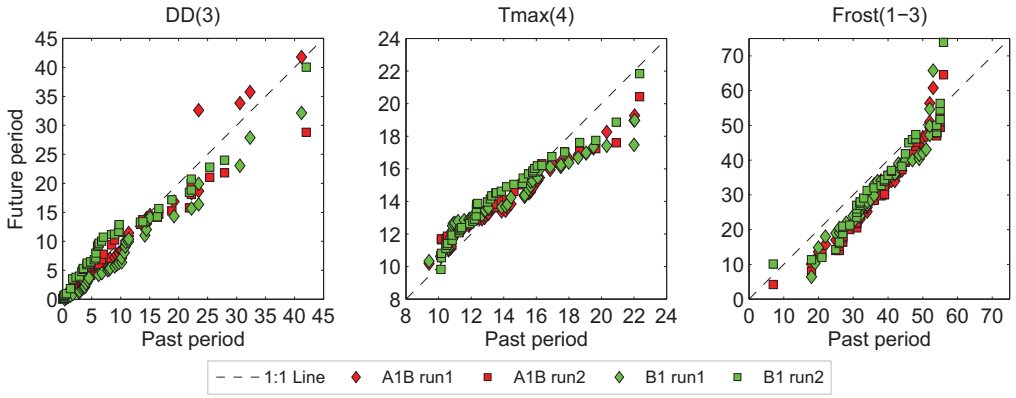

Figure 7.4: QQ-plots of CCLM modelled predictors for budburst estimation during the CCLM past period 1960-2000 against the CCLM future period 2001-2050. The colours distinguish the scenarios and the symbols the runs.

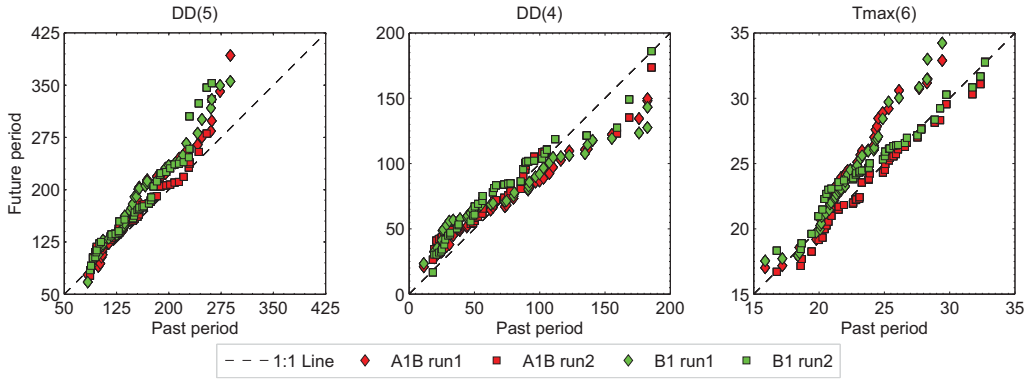

Figure 7.5: QQ-plots of CCLM modelled predictors for flowering estimation during the CCLM past period 1960-2000 against the CCLM future period 2001-2050. The colours distinguish the scenarios and the symbols the runs.

significant trends with opposite directions during the periods 2001-2050 and 2021-2050 for A1B. The B1 scenario shows no reliable trends.

Flowering Degree days in May (DD5) and in April (DD4) remain quite constant comparing future and past periods, but there are high differences for higher values (Figure 7.5). Future high values of DD5 increase while high values for DD4 decrease compared to C20. Maximum temperature in June (TX6) is split for higher values: temperature in Run 1 is increasing during the future period, while the temperature of Run 2 remains similar to the past period. DD5 is, however, not expected to change considerably as suggested by the QQ-plot. In fact, a decreasing DD5 is probable during 2001-2030. DD4 increases significantly during 2001-2050 and 2021-2050 for Run 1 in A1B.

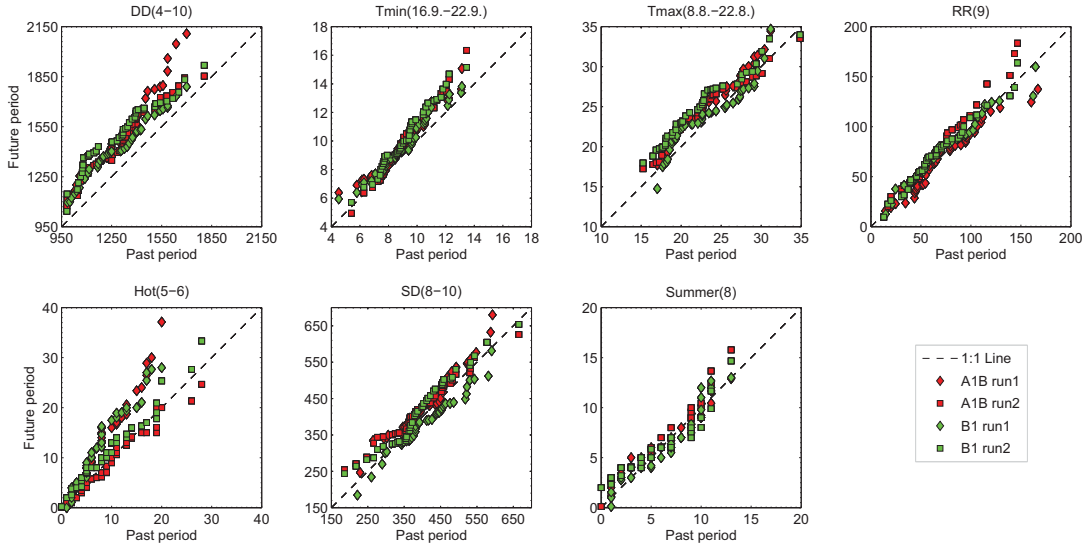

Figure 7.6: QQ-plots comparing predictors for must density parametrisation during the CCLM past period 1960-2000 to the CCLM future period 2001-2050. The colours distinguish the scenarios and the symbols the runs.

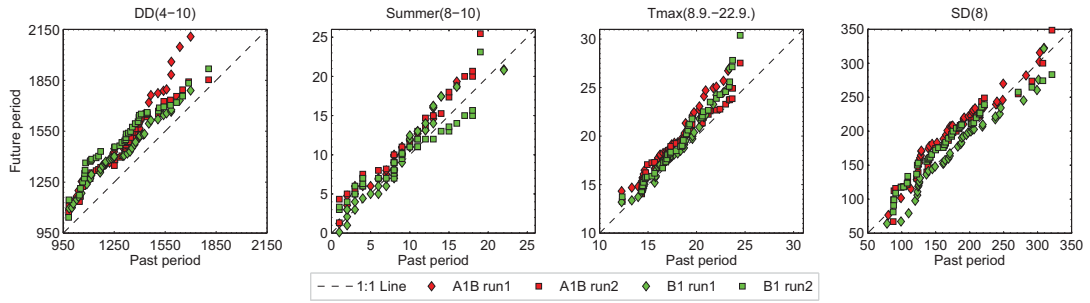

Figure 7.7: QQ-plots comparing predictors for acidity parametrisation during the CCLM past period 1960-2000 to the CCLM future period 2001-2050. The colours distinguish the scenarios and the symbols the runs.

Must density The degree days between April and October (DD4-10), which are important for the parameterisation of must density and acidity, are generally higher in the future than in the past (Figure 7.6). Here, a large significant trend is computed for 2001-2050. The number of hot days during May and June (HOT5-6) show differences between the CCLM realisations greater than between the scenarios A1B and B1. Besides DD4-10 the highest trends are detected for minimum temperature between 16 and 22 September. The leading predictor for the second Cluster, Hot5-6, has no significant trend in A1B.

Acidity The distributions of the acidity predictors remain quite constant for the future period, except DD4-10 (Figure 7.7). The distributions of A1B and B1 scenario do not differ visibly. Focussing on the trends of the predictors, summer days

from August to October (Summer8-10) increase most during 2011-2040. The behaviour of maximum temperature in September ($TX9_{8-22}$) is more complex: in the A1B scenario temperature increases especially during 2011-2040, where in B1 scenario temperature decreases between 2001-2030 and increases during 2021-2050.

The trend evaluation for different time periods shows interesting results (Table 7.3). The CCLM realisations, however, do not have the same trend directions. For example SD8-10 in Run 2 is decreasing significantly (95 % level) but in Run 1 no clear trend is observable; the trend is even reversed. DD4-10 reveal a strong positive trend in Run 1, but only a moderate upward trend in Run 2.

In addition, the QQ-plots suggest that the differences between the CCLM realisations are larger than between the scenarios, thus the CCLM variability is higher than the scenario climate signal in the model. Table 7.4 shows the results from testing the mean of paired differences to be zero and the result of paired Kolmogorov-Smirnov tests. For the period 2001-2050, differences in pairs consisting of different runs within the same scenario, and between different scenarios within the same run are evaluated. The predictors for must quality present differences between scenarios and between runs. The hypothesis that differences between realisations are higher than between scenarios is not corroborated. The KS test also indicates that the distributions of the pairs do not differ significantly, except for sunshine duration in August (SD8), here the distributions between A1B and B1 for Run 1 are significantly different.

To sum up, in view of the trends for different time periods in A1B scenario, budburst and flowering events are expected to change most during the periods 2001-2030 and 2021-2050. The predictors for must density have high significant trends for the whole period but less for the sub-periods, thus here a continuous change in must density is expected for the A1B scenario. The highest trends in the acidity predictors are observed during 2011-2040. Focussing on the B1 scenario, budburst and flowering dates should not change significantly. Must quality, too, is not expected to change significantly during the whole period 2001-2050, but on smaller time frames changes may occur.

Table 7.3: Trends of the predictors for different time periods, scenarios and realisations. Trends at significance levels of 99 %/95 %/90 % are labelled in red/orange/yellow respectively.

Scenario	Period	Realisation	DD(3)	Tmax(4)	Frost(1-3)	DD(5)	DD(4)	Tmax(6)	DD(4-10)	Tmin(16.-22.9.)	Tmax(8.-22.8.)	RR(9)	Hot(5-6)	SD(8-10)	Summer(8)	DD(4-10)	Summer(8-10)	Tmax(8.-22.9.)	SD(8)
			Budburst			Flowering			Must density							Acidity			
A1B	2001	1	0.04	0.06	-0.22	0.80	0.97	0.01	6.98	0.03	0.10	0.04	0.01	0.80	-0.00	6.98	0.03	0.03	0.74
	-2050	2	-0.10	-0.00	-0.53	0.76	0.04	-0.06	1.63	0.06	0.00	-0.45	-0.06	-0.39	0.05	1.63	0.10	0.05	-0.28
	2001	1	-0.79	0.04	-0.01	-0.05	0.49	0.00	5.98	0.01	0.08	-0.49	-0.07	1.41	-0.03	5.98	-0.08	0.04	0.14
	-2030	2	-0.51	-0.04	-0.49	-1.44	-0.52	-0.04	-6.79	0.03	-0.11	-1.36	-0.13	-4.42	-0.05	-6.79	-0.12	-0.02	-2.71
	2011	1	-0.04	0.04	-0.31	-0.61	0.77	-0.05	9.60	0.09	0.21	-0.64	-0.06	4.12	0.01	9.60	0.16	0.09	1.86
	-2040	2	-0.31	-0.02	-0.45	2.12	-0.23	-0.07	5.52	0.04	0.03	0.10	-0.04	1.48	0.07	5.52	0.28	0.14	0.69
	2021	1	0.75	0.11	-0.30	1.38	1.87	-0.01	7.15	0.04	0.13	0.63	0.05	-0.23	0.03	7.15	0.08	-0.01	1.56
	-2050	2	0.40	0.02	-0.59	1.94	0.43	-0.07	6.78	0.08	0.12	-0.24	0.01	2.26	0.14	6.78	0.20	0.09	1.66
B1	2001	1	0.35	-0.01	-0.13	-1.03	-0.16	-0.03	-1.56	0.03	0.02	0.04	-0.09	-0.77	-0.06	-1.56	-0.08	0.02	-0.64
	-2050	2	0.18	0.01	-0.12	-0.46	0.15	0.02	1.49	0.01	-0.01	0.65	0.01	-1.64	-0.02	1.49	-0.05	-0.05	-1.00
	2001	1	0.26	-0.03	-0.23	-0.42	-0.17	-0.02	-4.46	-0.03	0.12	0.63	-0.03	-0.96	-0.01	-4.46	-0.12	-0.13	0.01
	-2030	2	-0.14	0.01	0.12	0.19	0.24	0.07	-0.72	0.02	-0.12	1.83	0.18	-3.87	-0.01	-0.72	-0.13	-0.13	-2.06
	2011	1	0.18	-0.09	0.03	-0.96	-1.29	0.03	-0.37	-0.02	0.02	-0.12	0.02	-1.00	-0.18	-0.37	-0.19	0.04	-2.03
	-2040	2	0.36	-0.01	-0.04	0.87	0.04	0.02	1.27	0.06	0.00	0.66	0.05	-1.09	-0.12	1.27	-0.08	-0.05	-1.75
	2021	1	0.55	0.02	-0.16	-2.11	0.15	-0.08	-0.47	0.11	-0.03	-0.96	-0.27	-0.42	-0.05	-0.47	0.01	0.19	-0.83
	-2050	2	0.31	-0.04	-0.36	-2.20	-0.53	-0.11	-0.40	0.02	0.03	-0.17	-0.33	0.57	-0.03	-0.40	0.01	0.04	-0.38

Table 7.4: Top: Test statistics testing the mean of paired differences to be zero using the t-test. Significant differences at significance levels of 99 %/95 %/90 % are labelled in red/orange/yellow respectively. Bottom: Probability that the distributions are different (KS test, Equation 6.9).

	DD(3)	Tmax(4)	Frost(1-3)	DD(5)	DD(4)	Tmax(6)	DD(4-10)	Tmin(16.-22.9.)	Tmax(8.-22.8.)	RR(9)	Hot(5-6)	SD(8-10)	Summer(8)	DD(4-10))	Summer(8-10)	Tmax(8.-22.9.)	SD(8)
	Budburst			Flowering			Must density							Acidity			
t test																	
A1B(R1)/A1B(R2)	1.60	0.09	0.37	1.07	0.09	0.83	0.82	0.31	1.02	0.95	2.07	1.03	0.60	0.82	1.04	0.18	1.92
B1(R1)/B1(R2)	0.84	0.08	0.42	0.48	0.30	0.98	1.85	1.24	1.27	0.85	0.17	1.61	0.19	1.85	0.24	1.83	1.00
A1B(R1)/B1(R1)	1.04	0.41	0.30	0.46	0.60	0.19	1.40	0.42	1.52	1.21	0.00	3.10	0.54	1.40	0.84	1.67	3.00
A1B(R2)/B1(R2)	1.18	0.41	0.92	0.94	0.24	1.61	1.01	0.47	1.01	0.58	1.85	0.32	1.31	1.01	1.76	0.56	0.13
KS-test																	
A1B(R1)/A1B(R2)	0.34	0.08	0.07	0.31	0.13	0.11	0.12	0.11	0.16	0.17	0.26	0.20	0.04	0.12	0.04	0.11	0.55
B1(R1)/B1(R2)	0.22	0.17	0.15	0.15	0.22	0.54	0.55	0.17	0.34	0.22	0.12	0.51	0.10	0.55	0.05	0.41	0.26
A1B(R1)/B1(R1)	0.06	0.17	0.13	0.08	0.24	0.12	0.27	0.11	0.35	0.34	0.08	0.73	0.19	0.27	0.15	0.39	**0.90**
A1B(R2)/B1(R2)	0.29	0.24	0.12	0.20	0.21	0.64	0.30	0.07	0.09	0.11	0.35	0.23	0.37	0.30	0.14	0.06	0.07

Chapter 8

8 Expected future changes in vine phenology and must quality

In the following, the trends of the predictands based on calibrated CCLM data are analysed by comparing the realisations Run 1 and Run 2 of the scenarios A1B and B1. Between 1960 and 2000 the data of C20 only differ for the two realisations because the scenarios take effect only after 2001. For illustration, the time series of the predictands based on calibrated CCLM are depicted in comparison to the predictands calculated with observational data (reference). Furthermore the average, median, 5th-95th and 25th-75th percentile ranges of the reference are depicted.

The differences between the CCLM simulations and the observations for the past period 1960-2000 require the correction of CCLM output data before changes in the budburst and flowering events, as well as in the must density and acidity, are estimated. For the adjustment, the input parameters for the predictors for the future period, are subjected to the histogram matching obtained for the period 1960-2000 (Section 6.3.1). This procedure assumes similar links between phenology and climate in the past and the future. In the following sections, the future variability of budburst and flowering dates, must density and acidity, is presented.

8.1 Budburst date

Before the late 80's, the moving average (5 years to reduce variability) of the reference is above the average with a clear delay in budburst date during mid 80's (Figure 8.1). The two CCLM realisations do, however, not reproduce this retardation; they vary around the mean within the 25th and 75th percentile of the reference. The two realisations of C20 don't even have the same trend direction: Run 1 shows an advancement of 0.55 days/decade and Run 2 a delay of 0.88 days/decade during the time period 1960 to 2000 (Table 8.1). Both trends are, however, not significant.

This can be due to a high variability from year to year. Even if the time periods of C20 and the reference do not match exactly, the trend magnitude of estimated budburst date is much weaker than the observed budburst date trend (Table 3.2).

The budburst date under the A1B scenario does not have significant trends during 1960 to 2050. Taking the period 2001 until 2050, Run 1 shows a significant advancement in budburst date of 1.20 days per decade at a significance level of 80 %. Around 2015-2035 fewer extremes are detected (Figure 8.1). During 2025 until 2035, budburst date shows a slight delay in both realisations. Afterwards, it becomes rapidly earlier. The decreasing trend calculated between 2020 and 2050 ranges from 2.71-3.83 days per decade for Run 2 and Run 1, respectively, with a significance of 95 %.

The B1 scenario reveals weaker trends than A1B. The year to year variability remains high for the whole time series, but the two realisations are not in agreement. Run 1 remains closer to the mean of the reference, while Run 2 is mostly below the reference average. Run 1 has no significant trend during 1960-2050, but budburst date calculated using Run 2 is decreasing by 0.38 days/decade (95 % significance). After 2020 Run 1 shows a significant (90 %) trend of 2.15 days/decade. Run 2, however, remains constant for the time periods 2001-2050 and 2020-2050.

The single vine varieties behave very similar and the trends are all very close to each other (Table 8.1). During the period 2020-2050 under the A1B scenario, all trends are significant at 95 % level. Traminer shows the largest advancement of budburst date with an amount of 2.90-4.02 days/decade in Run 2 and Run 1, respectively. The lowest advancement is registered for Auxerrois, although it is still very high. Under B1 scenario, budburst date significantly moves backward Run 1 between 2020 and 2050. Here, Rivaner has the highest trend.

8.2 Flowering date

The flowering date marks the beginning of the berry development and should not be too early because of frost damage risks and not too late so that the berries are mature before autumn. The time series calculated by CCLM data are presented in Figure 8.2 and the correspondent trends are in Table 8.2.

The year to year variability is very high, and realisation 2 is closer to the reference. The trends between 1960-2000 show an advancement of the flowering date by 1.54-1.75 days/decade for Run 2 and Run 1, respectively, although the significance level is only 80 %. Until 1992, both realisations are mainly below the reference, afterwards, flowering date of Run 1 delays and of Run 2 advances.

In the period 1960-2050 Run 1 of A1B estimates flowering date significantly earlier by 1.05 days/decade and even 1.94 days/decade during 2001-2050. Run 2 shows only a significant trend for the period 1960-2050. Regarding the period 2020-2050, both realisations reveal a significant advancement of flowering date by 2.56-3.25 days/decade. After 2035 the moving average of both runs is below the reference average of 1960-2000.

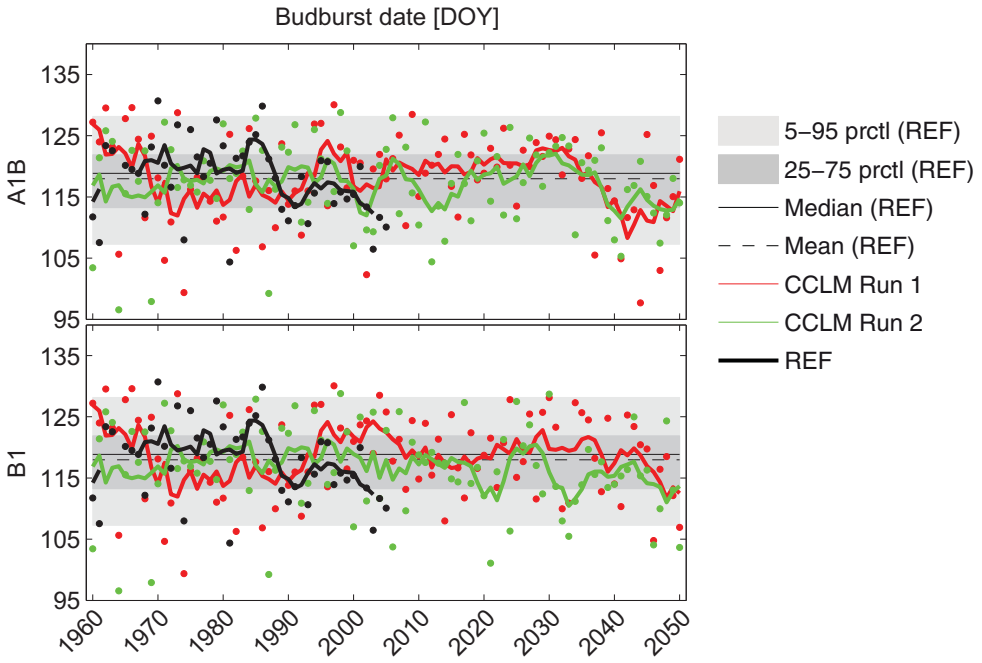

Figure 8.1: Time series of budburst date (dots) with a moving average of 5 years (lines). Budburst date estimated by meteorological observations (REF) is shown in black, budburst date calculated by CCLM output is plotted in red and green for Run 1 and Run 2, respectively.

Table 8.1: Decadic trend (days per decade) in budburst date for different time periods. The colours give information about the significance levels 80 % (grey), 90 % (yellow), 95 % (orange) and 99 % (pink).

			A1B			B1		
Variety	Real.	1960-2000	1960-2050	2001-2050	2020-2050	1960-2050	2001-2050	2020-2050
Mean	Run1	-0.55	-0.24	-1.20	-3.83	-0.08	-1.05	-2.15
	Run2	0.88	-0.13	-0.31	-2.71	-0.38	-0.67	-0.65
Auxerrois	Run1	-0.53	-0.23	-1.14	-3.70	-0.07	-1.03	-2.09
	Run2	0.87	-0.11	-0.27	-2.60	-0.36	-0.90	-0.64
Elbling	Run1	-0.54	-0.26	-1.23	-3.88	-0.09	-1.08	-2.17
	Run2	0.90	-0.15	-0.37	-2.81	-0.39	-0.95	-0.67
Pinot Blanc	Run1	-0.59	-0.23	-1.19	-3.85	-0.07	-1.04	-2.15
	Run2	0.86	-0.10	-0.23	-2.64	-0.37	-0.92	-0.63
Pinot Gris	Run1	-0.49	-0.24	-1.17	-3.82	-0.08	-1.10	-2.17
	Run2	0.94	-0.12	-0.33	-2.76	-0.37	-0.94	-0.69
Riesling	Run1	-0.58	-0.23	-1.19	-3.83	-0.07	-1.04	-2.14
	Run2	0.86	-0.11	-0.25	-2.64	-0.37	-0.92	-0.63
Rivaner	Run1	-0.49	-0.22	-1.15	-3.88	-0.07	-1.13	-2.24
	Run2	0.99	-0.10	-0.26	-2.76	-0.37	-0.96	-0.72
Traminer	Run1	-0.64	-0.29	-1.35	-4.02	-0.11	-1.05	-2.17
	Run2	0.82	-0.20	-0.47	-2.90	-0.42	-0.96	-0.61

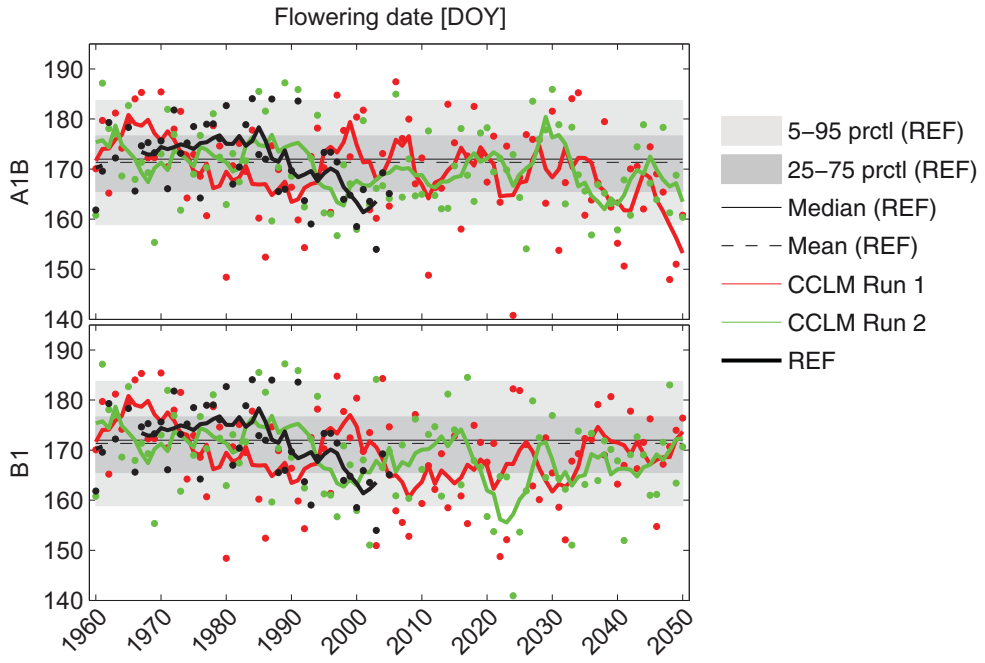

Figure 8.2: Time series of flowering date (dots) with a moving average of 5 years (lines). Flowering date estimated by meteorological observations (REF) is shown in black, flowering date calculated by CCLM output is plotted in red and green for Run 1 and Run 2, respectively.

Table 8.2: Decadal trend (days per decade) in flowering date. The colours give information about the significance levels 80 % (grey), 90 % (yellow), 95 % (orange) and 99 % (pink).

			A1B			B1		
Variety	Real.	1960-2000	1960-2050	2001-2050	2020-2050	1960-2050	2001-2050	2020-2050
Mean	Run1	-1.75	-1.05	-1.94	-3.25	-0.66	1.27	2.22
	Run2	-1.54	-0.61	-0.57	-2.56	-0.93	-0.11	3.63
Auxerrois	Run1	-1.78	-1.06	-1.93	-3.21	-0.67	1.30	2.28
	Run2	-1.61	-0.60	-0.52	-2.45	-0.93	-0.11	3.67
Elbling	Run1	-1.74	-1.05	-1.96	-3.25	-0.66	1.27	2.23
	Run2	-1.50	-0.62	-0.61	-2.63	-0.93	-0.10	3.64
Pinot Blanc	Run1	-1.78	-1.07	-1.96	-3.36	-0.67	1.24	2.16
	Run2	-1.55	-0.60	-0.53	-2.58	-0.94	-0.15	3.62
Pinot Gris	Run1	-1.75	-1.07	-1.93	-3.24	-0.67	1.28	2.26
	Run2	-1.57	-0.61	-0.55	-2.55	-0.94	-0.12	3.67
Riesling	Run1	-1.74	-1.03	-1.94	-3.24	-0.64	1.25	2.16
	Run2	-1.47	-0.61	-0.59	-2.56	-0.91	-0.10	3.56
Rivaner	Run1	-1.74	-1.03	-1.93	-3.25	-0.65	1.24	2.16
	Run2	-1.49	-0.60	-0.57	-2.55	-0.91	-0.12	3.56
Traminer	Run1	-1.74	-1.06	-1.94	-3.20	-0.67	1.30	2.28
	Run2	-1.56	-0.62	-0.60	-2.59	-0.93	-0.10	3.68

Both realisations of the B1 scenario show a general tendency to earlier flowering dates (0.66-0.93 days per decade), and the moving average of 5 years is mostly below the reference average. From 2001 until 2050, Run 1 shows a delay in flowering date by 1.27 days/decade at a significance level of 80 %. This trend becomes even stronger after 2020 but it is not significant. Run 2 calculates a still decreasing trend, although it is not significant. Between 2020-2025 the moving average of Run 2 even falls below the 5th percentile of the observation. After 2020 Run 2 presents a delay of 3.63 days/decade (80 % significance). Thus both scenarios suggest an advancement of flowering date between 1960-2050, but B1 shows a tendency to later flowering dates after 2020, still being below the reference average.

Flowering dates differ, like budburst dates, not much between the investigated vine varieties, thus the trends of the single varieties are very similar. Especially for the A1B scenario all vine varieties show a clear advancement of the flowering date in the period 2020-2050. Estimations done under B1 scenario show a tendency to a flowering delay for all varieties, but it is only significant for some varieties and realisations.

8.3 Must density

In contrast to budburst and flowering dates, must density is very different for vine varieties and is therefore split into two clusters (Section 3.3.2.2). Figure 8.3a shows the time series for cluster CM1 averaged over the varieties Auxerrois, Riesling, Pinot Blanc, Pinot Gris and Traminer, and Figure 8.3b the time series of cluster CM2, averaged over Elbling and Rivaner. Both clusters have very different predictors, thus differences are expected for must density estimation.

For both clusters, must density is very low until 1973 and both CCLM realisations are in agreement with the reference. From 1973 until 1989, the reference must density is still below average and Run 2 follows the reference's behaviour best. Run 1 of cluster CM1, however, shows a large increase in must density after 1971 until 1976: the moving average increases in 6 years by 13 °Oe. After the mid 80s, the reference and estimations from Run 2 of must density increase in good agreement. Trend calculations reveal a significant positive trend in must density of nearly 2 °Oe/decade for cluster CM1 during 1960 to 2000 (Table 8.3). Only Run 2 of cluster CM2 shows a significant increase of must density of 1.03 °Oe/decade.

Taking the A1B scenario for the period 1960-2050 into account, must density increases significantly. Cluster CM1 shows an increase of 0.91-1.37 °Oe/decade for Run 2 and Run 1, respectively. After 2001 this augmentation in must density becomes stronger in Run 1 (2.27 °Oe/decade), while in Run 2 the trend is completely lost. Similar behaviour is observable in cluster CM2. During 1960-2050, the first realisation shows a significant increase of must density of 0.49 °Oe/decade, while during the period 2001-2050 the trend is reduced and becomes insignificant. Average must density of cluster CM1 presents a strong increase after 2030 for A1B scenario and for both clusters much more extremes are expected, especially regard-

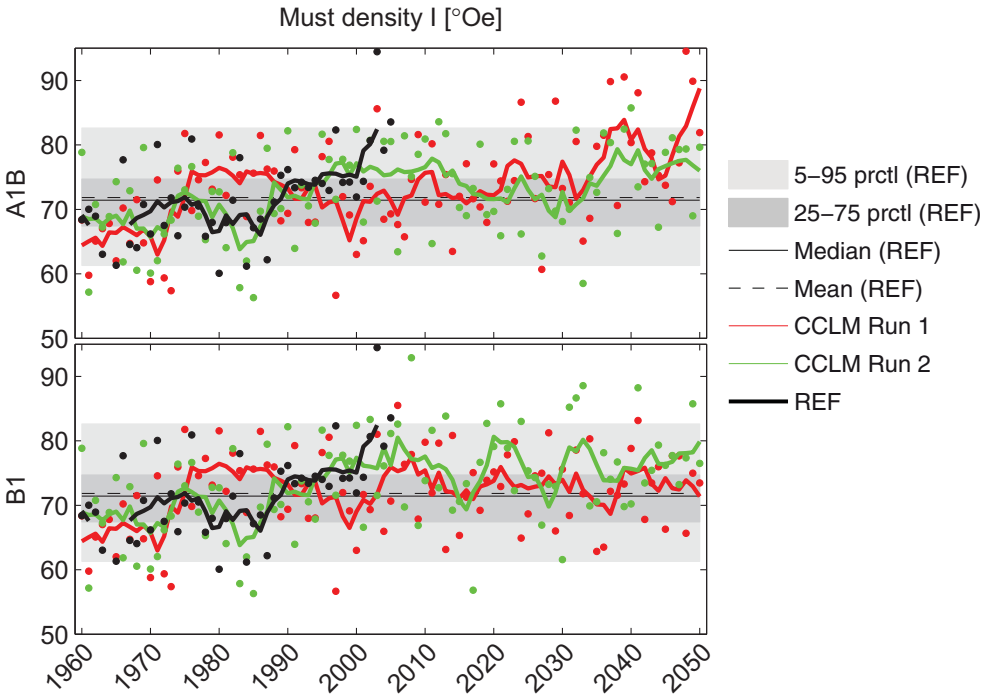

(a) Cluster CM1

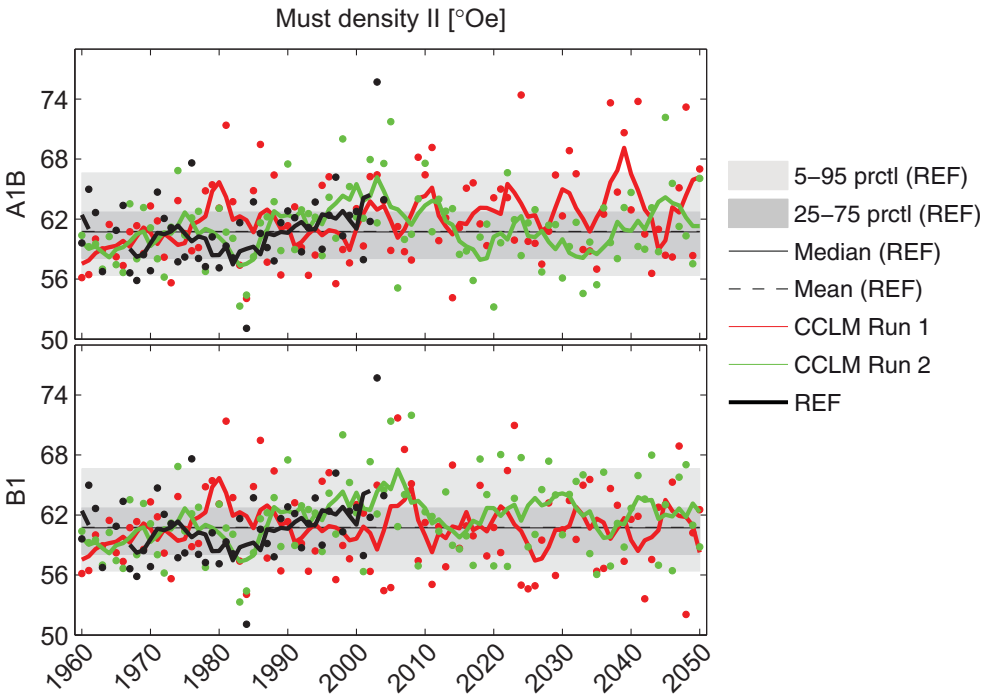

(b) Cluster CM2

Figure 8.3: Time series of must density (dots) with a moving average of 5 years (lines). Must density estimated by meteorological observations (REF) is shown in black, must density calculated by CCLM output is plotted in red and green for Run 1 and Run 2, respectively.

ing Run 1 (Figure 8.3). Must density of cluster CM1 shows a significant increase of 2.58-2.83 °Oe/decade for Run 2 and Run 1, respectively, during 2020-2050. Must density of cluster CM2 has a large variability for Run 2, but no significant changes are expected.

Table 8.3: Decadal trend (°Oe per decade) in must density. The colours give information about the significance levels 80 % (grey), 90% (yellow), 95% (orange) and 99% (pink).

			A1B			B1		
Variety	Real.	1960-2000	1960-2050	2001-2050	2020-2050	1960-2050	2001-2050	2020-2050
Mean[1]	Run1	1.70	1.37	2.27	2.83	0.56	-0.20	-0.23
	Run2	1.98	0.91	0.32	2.58	1.16	0.29	0.16
Mean[2]	Run1	0.52	0.49	0.32	0.09	0.05	-0.06	0.18
	Run2	1.03	0.13	-0.33	1.22	0.32	-0.23	-0.16
Auxerrois[1]	Run1	1.97	1.54	2.48	2.98	0.68	-0.17	0.12
	Run2	2.24	1.08	0.59	3.03	1.32	0.37	0.26
Elbling[2]	Run1	0.69	0.57	0.34	0.14	0.07	-0.25	-0.07
	Run2	1.28	0.20	-0.30	1.43	0.36	-0.31	-0.65
Pinot Blanc[1]	Run1	1.02	0.87	1.58	2.07	0.28	-0.07	-0.30
	Run2	1.22	0.49	0.03	1.70	0.70	0.02	0.16
Pinot Gris[1]	Run1	1.23	1.09	1.91	2.44	0.37	-0.11	-0.32
	Run2	1.57	0.65	0.13	2.11	0.88	0.07	0.19
Riesling[1]	Run1	2.16	1.62	2.54	3.08	0.74	-0.39	-0.59
	Run2	2.30	1.14	0.29	2.74	1.44	0.52	0.00
Rivaner[2]	Run1	0.34	0.40	0.30	0.06	0.02	0.14	0.43
	Run2	0.78	0.06	-0.36	1.01	0.29	-0.15	0.33
Traminer[1]	Run1	2.11	1.72	2.84	3.61	0.74	-0.28	-0.05
	Run2	2.58	1.21	0.57	3.33	1.48	0.46	0.18

[1]) Cluster CM1; [2]) Cluster CM2

The trends of cluster CM1, under the B1 scenario, are still significantly increasing between 1960 and 2050 due to a strong increase of must density before 2000. The positive trends of cluster CM2 are significant only in Run 2. After 2001 the trend sign is partially reversed: must density declines for some realisations and time periods. However, all trends in the periods 2001-2050 and 2020-2050 are not significant for both clusters.

During 1960-2050, Elbling and Rivaner show, especially under the A1B scenario, the lowest trend which is significant only in Run 1. Looking at the sub-period 2001-2050 into account, this significant trend is lost and also the trend direction is different between both runs. For all periods in A1B, Traminer presents always the largest increase of must density (e.g., more than 3 °Oe between 2020 and 2050). Under the B1 scenario, however, no significant changes are observed for any vine variety. The trends are very low and Run 1 shows a reduction of must density, while Run 2 shows an increase of must density. Thus, under B1 scenario no changes in must density are expected.

8.4 Acidity

Similar to must density, acidity depends on vine variety, and is split into three clusters, discussed in Section 3.3.2.2. The time series of the CA1 and CA2 cluster means are presented in Figure 8.4a and Figure 8.4b, respectively. Cluster CA1 and CA3 behave very similar because they estimate acidity by the same predictors, thus they are discussed together.

Until 1970 acidity was relatively high; only few years presented acidity values below the reference mean. After 1975, acidity of Run 1 decreases fast, while acidity of Run 2 increases during 1975-1985 before it decreases again. The negative trends are highly significant (95-99 %) with about 0.68 g/l per decade for Run 1 and about 0.79 g/l per decade for Run 2 for all clusters (Table 8.4).

The A1B scenario shows a significant decrease of acidity through all clusters. During 1960-2050, a decrease of 0.45-0.47 g/l per decade is estimated for Run 1 and a lower but still significant decrease of 0.33-0.37 g/l per decade for Run 2. The trend of Run 2 becomes insignificant in the period 2001-2050, but acidity in Run 1 shows a stronger decrease: 0.65-0.66 g/l per decade. This behaviour might be due to an increase of acidity in Run 2 during 2001-2030, while acidity, and inter-annual variability, calculated by Run 1 decreases constantly. The last period of the time series, 2020-2050, shows a faster decrease of acidity in Run 2 than in Run 1, by more than 1 g/l per decade (Run 2). After 2030, however, both runs reveal only very few acidity values above the reference mean and are mostly located around the 5th percentile of the reference acidity.

Under B1 scenario, which is considered to be moderate, acidity is not decreasing as fast as in A1B. In agreement with A1B, a significant trend towards lower acidity during 1960-2050 is confirmed: 0.21-0.35 g/l per decade depending on the realisation. During 2020-2050, acidity may, however, increase significantly by 0.53 g/l per decade (clusters CA1/CA3, Run 2). On the other hand, acidity remains mostly below the reference mean, independent of the cluster.

In the past period 1960-2000, all vine varieties showed significant decrease in acidity (using both simulations and reference). While Riesling reveals the highest loss of acidity (- 1.13 and - 1.27 g/l per decade, Run 1 and Run 2), Rivaner is the variety with the slowest decrease (-0.44 and -0.40 g/l per decade, Run 1 and Run 2). Under the A1B scenario, this structure is maintained; during 2020-2050 the trend values are increased but Riesling is still the vine variety with the highest and Rivaner with the lowest decrease in acidity. For B1 scenario, no large changes in acidity are expected for the single vine varieties during 2001-2050. After 2020 a significant increase of acidity (only Run 2) is observed for Riesling, Rivaner, and Traminer. Thus, the estimations under A1B and B1 scenarios are opposed for some varieties.

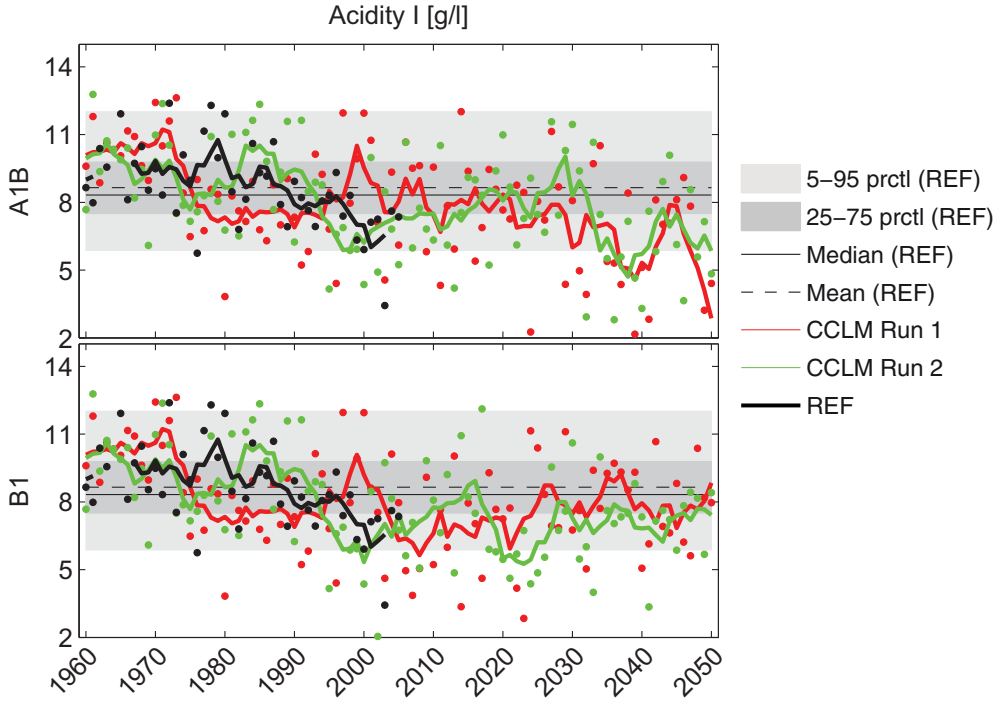

(a) Cluster CA1

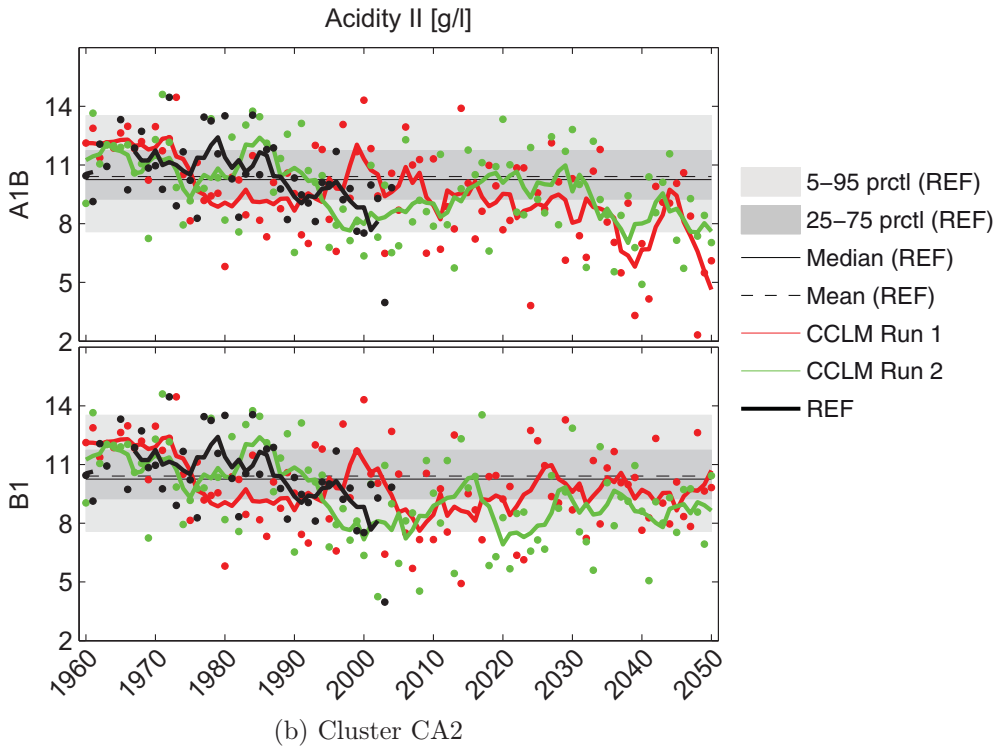

(b) Cluster CA2

Figure 8.4: Time series of acidity (dots) with a moving average of 5 years (lines). Acidity estimated by meteorological observations (REF) is shown in black, acidity calculated by CCLM output is plotted in red and green for Run 1 and Run 2, respectively.

Table 8.4: Decadal trend (g/l per decade) in acidity. The colours give information about the significance levels 80 % (grey), 90 % (yellow), 95 % (orange) and 99 % (pink).

			A1B			B1		
Variety	Real.	1960-2000	1960-2050	2001-2050	2020-2050	1960-2050	2001-2050	2020-2050
Mean[1]	Run1	-0.68	-0.46	-0.65	-0.86	-0.23	0.33	0.20
	Run2	-0.80	-0.36	-0.32	-1.04	-0.35	0.02	0.53
Mean[2]	Run1	-0.66	-0.47	-0.66	-0.79	-0.21	0.24	0.02
	Run2	-0.75	-0.33	-0.26	-1.10	-0.35	0.11	0.30
Mean[3]	Run1	-0.68	-0.45	-0.66	-0.87	-0.23	0.33	0.19
	Run2	-0.79	-0.37	-0.33	-1.05	-0.35	0.02	0.52
Auxerrois[1]	Run1	-0.75	-0.51	-0.72	-0.92	-0.26	0.32	0.18
	Run2	-0.87	-0.41	-0.33	-1.13	-0.39	-0.00	0.54
Elbling[3]	Run1	-1.01	-0.70	-0.99	-1.22	-0.36	0.39	0.19
	Run2	-1.15	-0.56	-0.45	-1.51	-0.56	-0.05	0.59
Pinot Blanc[2]	Run1	-0.70	-0.50	-0.70	-0.84	-0.23	0.22	0.01
	Run2	-0.77	-0.35	-0.26	-1.15	-0.38	0.08	0.35
Pinot Gris[2]	Run1	-0.62	-0.45	-0.63	-0.75	-0.19	0.22	0.06
	Run2	-0.68	-0.31	-0.22	-1.05	-0.33	0.10	0.33
Riesling[3]	Run1	-1.13	-0.76	-1.10	-1.41	-0.39	0.48	0.28
	Run2	-1.27	-0.61	-0.51	-1.71	-0.60	-0.02	0.81
Rivaner[1]	Run1	-0.40	-0.26	-0.39	-0.54	-0.14	0.20	0.17
	Run2	-0.44	-0.21	-0.18	-0.63	-0.20	0.01	0.41
Traminer[1]	Run1	-0.88	-0.59	-0.85	-1.13	-0.30	0.42	0.30
	Run2	-1.00	-0.47	-0.40	-1.37	-0.46	0.01	0.78

[1]) Cluster CA1; [2]) Cluster CA2; [3]) Cluster CA3

8.5 Discussion

The results of the trend analysis of phenology and must quality models calculated with calibrated CCLM data show interesting aspects. Examining e.g., the trends of the scenarios, the evaluations confirm the B1 scenario being moderate. Under A1B (significant) high trends are predicted. Trends calculated under B1 scenario are sometimes contrary to those of A1B (e.g., flowering date, acidity), or the trends of B1 are much lower (e.g., budburst date) with a lower significance level. However, the variability is high for every predictand, scenario and realisation.

Assuming the A1B scenario, i.e., very high energy use and very high GDP growth, the following "extreme" case could be envisioned. During the timeframe 2001-2050, budburst date will advance by approximately 1 day/decade, especially for Traminer. The flowering dates may also become earlier by 2 days/decade independent of vine variety. Generally, an increase of must density and a decrease of acidity can be assumed. The highest increase of must density is estimated for Riesling and Traminer, and the highest loss of acidity is estimated for Riesling.

Elbling and Rivaner could drop also their light acid character leading to a loss of the characteristic taste of the wines produced in the Upper Moselle region.

Under a moderate development, following the B1 scenario, budburst date is likely to become earlier. The behaviour of flowering date is not very clear, because the two simulations have different trend directions and are not highly significant. Must density does not change under B1 scenario; none of the trends are significant. Only during the period 2020-2050 an increase of acidity is expected, especially for Riesling, Rivaner and Traminer. Acidity of Riesling shows the highest increasing trend during 2020-2050 compared to Rivaner and Traminer.

Chapter 9

9 Conclusions and outlook

9.1 Synthesis of the results

Vine phenology is highly influenced by the climate conditions. Besides oenological techniques, an increasing velocity or an earlier initiation of the vegetative cycle affects wine quality, giving more time for the ripening period before temperatures decrease during autumn. A changing climate in a certain region will consequently affect the vegetative cycle, wine quality, and wine styles. Viticultural practises like the configuration of the sites as discussed in Section 2.3 may, however, reduce some risks of meteorological conditions (*Gladstones*, 1992; *Jackson*, 2008; *Vogt and Schruft*, 2000).

During the period 1966 to 2005, vine phenology dates of the investigated vine varieties (Auxerrois, Elbling, Pinot blanc, Pinot gris, Riesling, Rivaner and Traminer) did change at the Upper Moselle. The budburst date occurred on average on 28th April, but until the mid 1980's it mainly occurred in the first two weeks of May. Afterwards, budburst date took place earlier, around the second half of April. This trend of about 2 days per decade is highly significant. The flowering event date also moved backward by about 2 days per decade at a significance level of 95 %, which is comparable to the findings of *Defila* (2003) in Switzerland. The evolvement of the trend is, however, different from the budburst date. At the beginning of the data records, flowering occurred around 23rd June, but after 1975, ten years of relatively late flowering event dates followed. During 4 years (1980, 1984, 1987, 1991) it has been observed even in July. After 1985, the vine stocks bloomed mostly before 20th June.

For both phenological phases, budburst and flowering event, no large differences between the seven white wine varieties exist, and they can be evaluated by their mean. Must quality (must density and acidity), however, behaved different depending on the vine variety. Clusters of varieties were established in order to consider their behaviour in more detail. Must density splits the varieties into two clusters, where the second one contains only Elbling and Rivaner. Both vine varieties have

much lower must densities than the other varieties: 72.7 °Oe for cluster CM1 and 61.2 °Oe for cluster CM2. During the time period 1966 to 2005 must density has significantly (99 % level) increased for all vine varieties. The first cluster gained more sugar content in absolute and relative values than the second cluster: must density of Rivaner increased by 2.2 °Oe/decade which corresponds to an increase of 3.5 % per decade while Riesling is the variety with the fastest increase of 4.3 °Oe/decade which means an increase of 6.1 % per decade.

It is remarkable that the cluster formation of the vine varieties is different for must density and acidity. For acidity, three clusters have been found and the varieties Elbling and Rivaner do not belong to the same group anymore. Rivaner is closer to Auxerrois and Traminer (cluster CA1), and Elbling to Riesling (cluster CA3). Both Pinot varieties, Pinot blanc and Pinot gris, form a separate cluster (cluster CA2). The first cluster is marked with the lowest acidity and the third cluster with the highest; the Pinot group is on an intermediate level. Elbling and Riesling showed a very high acidity level during the time period 1975 until 1985, compared to the other varieties; their range and standard deviation is also much higher than for the other varieties. Their trend between 1966 and 2005 shows the fastest decrease of acidity (1.12 g/l for Riesling, 1.23 g/l for Elbling), but Auxerrois and Traminer lost more relative acidity (11.2 % and 12.4 % respectively).

As phenology and wine quality are closely linked to climate, it is essential to look at the changes in climate during the last decades. First, the annual trends of (maximum, mean and minimum) temperature, precipitation and sunshine duration have been investigated at the Upper Moselle. Temperature has generally increased; maximum temperature increased after a cooler period around 1965-1980. This fact is in accordance with the investigations of *Lüers* (2003). He located the turning point in maximum temperature in the year 1974 analysing temperature during 1945-2000 at the Middle Moselle. Annual precipitation is fluctuating around its mean of 770 mm but has no significant trend during the investigated period. Also *Jones* et al. (2005a) and *Lüers* (2003) did not find any significant trends for precipitation for most of their investigated regions in Europe. The division into precipitation classes shows between 1951 and 1985 a significant (>95 % level) decrease of precipitation amount below 5 mm/day and a corresponding increase for the higher precipitation intensity classes. During the period 1971-2005, the annual precipitation shows no significant shift between the classes. Annual sunshine duration amounts to 1565 hours on average, but since the end of the 1980's it is mainly above average and has an upward trend of 22 hours per decade (significance level 90 %). The highest value of sunshine duration is measured in 2003, but also the years 1959 and 1976 were exceptionally high.

All temperatures show for almost all seasons a local minimum around the mid 1980's. A significant increase in temperature is observed only during spring and summer. The observed warming rate is similar to the region around Geisenheim, but ranks between the rates observed in the Bordeaux and those of the Alsace regions (*Jones* et al., 2005a). Precipitation has also not changed on the seasonal scale. The variability is relatively high but the seasonal means remain constant.

This is not the case for sunshine duration: clear positive trends in winter and summer have been observed. Especially an increase of sunshine duration during summer is important for the grape maturation. Here, an increase of 15.5 hours per decade has been observed during 1951-2005.

In the next step, climate is set into relationship with phenological data in order to assess the responsible climate impacts on vine phenology and must quality. This has been done using a linear multiple regression method containing forward and backward steps, i.e. including and re-excluding predictors. The pool of predictors chosen was very large with 100 to 160 predictors, depending on the predictand. Mainly climate data and climate derived indices have been chosen. Moreover, prior phenological events have been included on condition that a quite reliable regression equation for those predictors exists in order to make a final prediction based only on climate projections. Prior phenological events are very important for getting the vegetative cycle more accurately (Section 2.3.3). Nevertheless, they can only been taken into account if they can be estimated in advance, otherwise estimations for future periods would not be possible. This condition is often a lack in other phenological model studies (e.g., *Hoppmann* (1994) and *Jones and Davis* (2000)). On the contrary, the phenological models presented here can be used without knowing the dates of prior phenological events. Thus the models developed here can also be applied to results of climate models in order to estimate trends and variability of the phenological dates in the future. The budburst predictor used in our flowering model can be replaced by the predicted value, thus also the flowering model depends only on climate data defined on calendar dates.

The phenological models for budburst and flowering event dates have been derived for the average of all vine varieties. Regression coefficients were then searched for the single varieties while keeping the predictors fixed. For must quality the procedure was similar, but here, the cluster means were used instead of the average over all vine varieties. Budburst and flowering events have a strong dependency on temperature, especially on degree days. This predictor, however, does not encounter for chilling periods and delays in development. Therefore, the predictors number of frost days (for budburst) and the budburst date (for flowering) are very important, even if their explained variance is low. The total explained variance of the budburst and flowering models is, nevertheless, quite high: 82.9 % and 87.7 %, respectively. The flowering model has almost the same explained correlation as the model developed e.g. by *Hoppmann* (1994), although predictors are different.

The phenological prediction models for different vine varieties have similar correlations with the observation, thus these models work well for all vine varieties. This is not the case for must density estimation; here the spread between the vine varieties is larger. Temperature is still a leading factor: degree days, maximum temperature and hot days for different time periods increase must density. But there are also restraining factors which lead to a decrease of must density: minimum temperature, precipitation, summer days and budburst date. The total explained variance is smaller than for budburst or flowering estimations. The predictors explain 79.7 % (cluster CM1) to 70.5 % (cluster CM2) of the variance. This might

indicate that some impacts are not included in the predictor pool. Probably the addition of the date of véraison as predictor would lead to better results because it is the initiation of sugar accumulation, but these data were not available. Nevertheless, the must density model presented here performs better in the investigated region than the model of of *Hoppmann and Hüster* (1993) when applied in the Upper Moselle region; the explained variance e.g., for Riesling reaches 78 % instead of 65 %. The estimation of acidity performed better than for must density. The explained variance is between 82.1 % (cluster CA1) and 88.5 % (cluster CA3), but there are large differences between vine varieties. Both models for must quality are worst for Rivaner. Developing a model only for Rivaner did not lead to better results (not shown), thus influences other than climate conditions affect the must quality to a larger extent. In the Upper Moselle region this variety has always been taken as a reference for comparisons between different wine regions or time series, because it matures earlier, in contrast to Riesling which is usually taken as reference variety.

Extreme events like heavy precipitation during or just before the bloom, also have a large impact because the flowers can fall off or become infertile due to the rain (*Jackson*, 2008). However, the data set is too small to find a statistical relationship: during the investigated period only one such event occurred. The introduction of penalty days can be considered to handle extreme events but to this goal a larger dataset is needed. On the other hand, the CCLM model does not seem to be accurate enough to implement this feature with measurable success. Also, early harvest practices to avoid losses due to fungal diseases have a large impact on must quality, but cannot be taken into account in the regression equation. Therefore, harvest date should be estimated in advance, independent from must quality, which is not very promising as must quality normally is the leading factor for harvest date. Estimation of fungal disease risks would be a better approach to include the earlier harvest practices.

In a further step, the proposed models for phenology and must quality are used to estimate changes for future time periods. The climate data of the regional climate model CCLM is taken for the two time periods 1960-2000 and 2001-2050. The comparison of the climate model data output of the first period with the observations has shown large differences, especially for maximum temperature during summer. Especially the hot days could not be reproduced by CCLM and, generally, the variability given by CCLM data is overestimated. Annual precipitation is also overestimated. This corroborates the importance of the evaluation of climate models before they can be used for investigations. The data have been calibrated using the histogram matching method to reduce large errors of the CCLM predictors. On the other hand, this method introduces new errors like extreme values limited to those of the reference data set. This circumstance has been reduced by interpolating the transformation at the extremes. Although only the input data for the predictors have been corrected, the predictands calculated by modified CCLM data are much closer to the observations. For the future period 2001-2050, the transformation information of the past period has been applied under the assump-

tion that the transformation remains constant. Unfortunately, the CCLM output shows large fluctuations from year to year and no significant trend during the past period (unlike the observations) for budburst date. Trends in flowering event dates are only on a 80 % level significant. The different scenarios influence the behaviour of must quality. Must density under A1B (very high energy use, very high growth in GDP) has a high probability to increase, but under B1 (moderate case) must density will not change significantly during 2001-2050. Acidity shows a large decrease for A1B during 2020-2050. Under B1, it remains constant. However, both scenarios show lower acidity in the future time as the currently observed one.

Taking the largest significant trends, the budburst date may be earlier by 1 day per decade during the time frame 2001-2050. Flowering date may be even 2 days per decade earlier independent on vine variety. Must density and acidity trends are quite different depending on vine variety and scenarios. Auxerrois, Riesling, and Traminer show the highest increase of must density combined with a lower decrease in acidity compared to Elbling and Riesling. Because of the large differences between the simulations the trend heights remain uncertain, but the trend directions are mostly consistent for the different runs.

9.2 Outlook

The developed models for phenology and must quality are working well in the investigated region, but they could be improved by searching supplementary predictors for must quality, like the véraison state or other phenological observations between flowering and harvest date. If these observations increase the explained variance of must quality, then regression equations of these new predictors also have to be found in order to remain usable with climate model data. Normally, véraison date is not well documented and a regression equation for véraison would help to close the gap to must density, given this predictor is essential.

The phenological models have only been tested for the Upper Moselle region and it would be interesting to investigate their regional limits. Probably only the regression coefficients have to be adjusted for different regions and not the predictors. However, in areas where, for instance, precipitation is a limiting factor (e.g. Spain, Portugal, South Italy) the phenological models will be different. Nevertheless, the basic algorithm of the models is not complicated and new model equations could be found for those regions and eventually combined with the models derived in this study.

Unfortunately, the regional climate model CCLM did not reproduce the climate at the Upper Moselle accordingly. It should be tested if these differences only occur in this region or on a larger scale, or if a newer version of CCLM gives better results (e.g. including cloud ice content in order to have a better estimation of the 2 m temperature). A further investigation for sunshine duration is meaningful to identify the reason of the discontinuities in the QQ-plots.

In order to get more knowledge about future climate signals other (regional)

climate models should be used to calculate budburst and flowering event dates, as well as must quality. For this reason a multi-model Ensemble Prediction System (EPS) is valuable.

The grapevine yield quantity, yield time and thus the wine quality is often dependent on the health of the grapes. Therefore, it would be interesting to couple the phenological models developed here, with models for fungal diseases already developed and tested. One of these models is called Vitimeteo (*Siegfried* et al., 2004) and is used for predicting Peronospora, it could be applied using the output of CCLM. The danger of Pereonospora or other fungal diseases could be used as a further predictor in the phenological models.

Bibliography

Amerine, M. A. and A. J. Winkler, Composition and quality of musts and wines of california grapes, *Hilgardia*, 15, 493–675, 1944.

Antcliff, A. and P. May, Dormancy and bud burst in sultana vines, *Vitis*, 3, 1–14, 1961.

Ashenfelter, O. and K. Storchmann, Using hedonic models of solar radiation and weather to assess the economic effect of climate change: the case of mosel valley vineyards, *The Review of Economics and Statistics*, 92, 333–349, 2010.

Becker, N., G. Morgenschweis, and G. Luft, Standortfaktoren von zwölf Anlagen der Sorte Ruländer in Südbaden und ihr Einfluss auf vegetatives Wachstum und Entwicklung der Reben, *Die Weinwirtschaft*, Nr. 38, 3–27,75–107, 1983.

Blaich, R., Fruchtphysiologie der Rebe, `https://www.uni-hohenheim.de/lehre370/weinbau/frucht/index.htm`.

Blaich, R., Tierische Schädlinge im mitteleuropäischen Weinbau, `https://www.uni-hohenheim.de/lehre370/weinbau/weinbau/wbm$\_$para.htm`.

Blaich, R., Vorlesung Weinbau I (Produktion). Teil des Moduls H2287., URL: www.uni-hohenheim.de/lehre370/weinbau/index.htm.

Bois, B., Ce que nous apprennent le climat récent et les observations phénologiques sur les effets du changement climatique en Gironde viticole, Acte de la 8ème Journée Technique du CIVB, Bordeaux-Lac, 2007.

Bortz, J., *Statistik. Für Sozialwissenschaftler*, Springer Verlag, 1993.

Bundessortenamt, *Beschreibende Sortenliste Reben*, 2008.

Burger, W. and M. J. Burger, *Digitale Bildverarbeitung. Eine Einführung mit Java und ImageJ*, Springer Verlag, 2006.

Buttrose, M. S., Vegetative growth of grapevine varieties under controlled temperature and light intensity, *Vitis*, 8, 280–285, 1969.

Böhm, U., Konfiguration des CLM, CLM-Workshop und Kontaktforum, Hamburg, 2007.

Caffara, A. and E. Eccel, Increasing the robustness of phenological models for vitis vinifera cv. chardonnay, *International Journal of Biometeorology*, 54, 255–267, 2010.

Caffarra, A. and E. Eccel, Projecting the impacts of climate change on the phenology of grapevine in a mountain area, *Australian Journal of Grape and Wine Research*, 17, 52–61, 2011.

Chambre des Députés, editor, *Compte rendu des séances publiques. Session ordinaire 2006-2007*, number 2, Chambre des Députés, 2006.

Chuine, I., K. Kramer, and H. Hänninen, Plant development models., in *Phenology: An Integrative Environmental Science*, edited by M. D. Schwartz, chapter 4.1, pages 217–235, 2003.

Chuine, I., P. Yiou, N. Viovy, B. Seguin, V. Daux, and E. Le Roy Ladurie, Grape ripening as a past climate indicator., *Nature*, 432, 289–290, 2004.

Corlett, T., Ballade of multiple regression, *Applied Statistics*, 12, 145, 1963.

Currle, O., O. Bauer, W. Hofäcker, F. Schumann, and W. Frisch, *Biologie der Rebe*, Meininger, 1983.

Dalla Marta, A., D. Grifoni, M. Mancini, P. Storchi, G. Zipoli, and S. Orlandini, Analysis of the relationships between climate variability and grapevine phenology in the nobile di montepulciano wine production area, *The Journal of Agricultural Science*, 148, 657–666, 2010.

Defila, C., Klimaerwärmung und Phänologie der Weinrebe, *Schweizerische Zeitschrift für Obst- und Weinbau*, Nr. 20, 9–11, 2003.

Denkschrift, Der Weinbau im Großherzogtum Luxemburg während der Jahre 1904-1911 einschließlich., Distrikts- und Weinbauaufsichtskommissariat in Grevenmacher, 1911.

Deutsches Weininstitut, Deutscher Wein. Statistik, 2010.

Doms, G. and U. Schättler, Part I: Dynamics and Numerics, in *A Description of the Nonhydrostatic Regional Model LM*, Deutscher Wetterdienst, 2002.

Draganov, D. and G. Draganov, Influence des conditions météorologiques sur la floraison et la fécondation de la vigne. I. Influence de la température sur la floraison et la fécondation, *Gradinar. Lozar. Nauka (Sofia)*, 12, 74–83, 1975.

Duchêne, E. and C. Schneider, Grapevine and climatic changes: a glance at the situation in Alsace, *Agronomy for Sustainable Development*, 25, 93–99, 2005.

Due, G., M. Morris, S. Pattison, and B. G. Coombe, Modelling grapevine phenology against weather: considerations based on a large data set, *Agricultural and Forest Meteorology*, 65, 91–106, 1993.

Efron, B., Bootstrap methods: another look at the jackknife, *Annals of Statistics*, 7, 1–26, 1979.

Efroymson, M., Multiple regression analysis, *Mathematical Methods for Digital Computers*, 1960.

ETCCDI, Climate change indices. definitions of the 27 core indices, http://cccma.seos.uvic.ca/ETCCDI/list_27_indices.shtml.

Gladstones, J., *Viticulture and Environment.*, Winetitles, 1992.

Gonzalez, R. C. and R. E. Woods, *Digital Image Processing*, Pearson Education, 2008.

Hahn, H., Die Deutschen Weinbaugebiete, in *Bonner Geographische Abhandlungen*, volume 18, Selbstverlag des Geographischen Instituts der Universität Bonn, 1956.

Hillebrand, W., H. Lott, and F. Pfaff, *Taschenbuch der Rebsorten*, Fraund, 2003.

Hollweg, H.-D., U. Böhm, I. Fast, B. Hennemuth, K. Keuler, E. Keup-Thiel, M. Lautenschlager, S. Legutke, K. Radtke, B. Rockel, M. Schubert, A. Will, M. Woldt, and C. Wunram, Ensemble Simulations over Europe with the Regional Climate Model CLM forced with IPCC AR4 Global Scenarios, Technical report, Max-Planck-Institut für Meteorologie, Gruppe Modelle und Daten, 2008.

Hoppmann, D., Weinqualität Spiegelbild der Jahreswitterung ?, *Das Deutsche Weinmagazin*, 1, 19–22, 1994.

Hoppmann, D. and H. Hüster, Trends in the development in must quality of white riesling as dependent on climatic conditions, *Viticultural and Enological Sciences*, 48, 76–80, 1993.

Hoppmann, D. and H. H. Schmitt, Chancen und Risiken für den Weinbau in Deutschland, *Der Deutsche Weinbau*, 10, 36–39, 2001.

Huglin, P., Recherche sur les bourgeons de la vigne. Initiation florale et développement végétatif, *Annales de l'Amélioration des Plantes*, 11, 113–272, 1958.

Huglin, P., Nouveau mode d'évaluation des possibilités héliothermiques d'un milieu viticole, *C.R. Acad. Agric.*, pages 1117–1126, 1978.

Huglin, P., *Biologie et écologie de la vigne*, Tec & Doc Lavoisier, 1986.

Huglin, P. and C. Schneider, *Biologie et écologie de la vigne.*, Tec & Doc Lavoisier, second edition, 1998.

Institut Viti-Vinicole, *Geschichte*, 2005, Available via URL: http://www.ivv.public.lu/ anbaugebiet/geschichte/, accessed August 2009.

Jackson, R. S., *Wine Science. Principles and Applications*, Elsevier, 2008.

Jones, G. V. and R. E. Davis, Climate Influences on Grapevine Phenology, Grape Composition, and Wine Production and Quality for Bordeaux, France., *American Journal of Enology and Viticulture*, 51, 249–261, 2000.

Jones, G. V., E. Duchêne, D. Tomasi, J. Yuste, H. Braslavaska, H. Schultz, C. Martinez, S. Boso, F. Langellier, C. Perruchot, and G. Guimberteau, Changes in European Winegrape Phenology and Relationships with Climate., in *XIV International GESCO-Viticulture-Congress, Geisenheim, 23.-27. 08.*, volume 1, pages 55–61, 2005a.

Jones, G. V., M. A. White, O. R. Cooper, and K. Storchmann, Climate change and global wine quality, *Climatic Change*, 73, 319–343, 2005b.

Kendall, M. G., *Rank Correlation Methods*, Griffin, London, fourth edition, 1970.

Klemp, J. and R. Wilhelmson, The simulation of three-dimensional convective storm dynamics, *J. Atmos. Sci.*, 35, 1070–1096, 1978.

Koblet, W., Wein aus der Jungsteinzeit, *Schweizerische Zeitschrift für Obst- und Weinbau*, 5, 133, 1997.

Koblet, W., C. Zanier, H. Tanner, P. Vautier, J. Simon, and G. Gnägi, Reifeverlauf von Sonnen- und Schattentrauben, *Schweizerische Zeitschrift für Obst- und Weinbau*, Nr. 113, 558–567, 1977.

Kraus, H., *Die Athmosphäre der Erde*, Springer Verlag, 2001.

Köppen, W., Klassifikation der klimate nach temperatur, niederschlag und jahresablauf, *Petermanns Geographische Mitteilungen*, 64, 193–203, 243–248, 1918.

Legates, D. R., An evaluation of procedures to estimate monthly precipitation probabilities, *Journal of Hydrology*, 122, 129–140, 1991.

Lüers, J., *Agrarklimatologische und phänologische Auswertungen für das Mittlere Moseltal. Auswirkungen des Klimawandels auf die Weinrebe im Moselraum*, Ph.D. thesis, Universität Trier, 2003.

Mann, H. B., Nonparametric tests against trend, *Econometrica*, 13, 245–259, 1945.

Massard, J. A., Vor 100 Jahren: Die Reblaus ist da ! Ein ungebetener Gast aus Amerika bringt den Luxemburger Weinbau in Gefahr, *Lëtzebuerger Journal*, 143, 19–21, 2007.

Maurer, C., E. Koch, C. Hammerl, T. Hammerl, and E. Pokorny, BACCHUS temperature reconstruction for the period 16th to 18th centuries from Viennese and Klosterneuburg grape harvest dates, *Journal of Geophysical Research*, 114, 2009.

McGovern, P. E., *Ancient Wine. The search for the origins of viniculture*, Princeton University Press, 2003.

McGuffie, K. and A. Henderson-Sellers, *A Climate Modelling Primer*, John Wiley & Sons, 2005.

Menzel, A., A 500 year pheno-climatological view on the 2003 heatwave in Europe assessed by grape harvest dates., *Meteorologische Zeitschrift*, 14, 75–77, 2005.

Mesinger, F. and A. Arakawa, *Numerical methods used in atmospheric models*, volume 1, Garb Publications, 1976.

Moncur, M., K. Rattigan, D. Mackenzie, and G. McIntyre, Base temperatures for budbreak and leaf appearance of grapevines, *American Journal of Enology and Viticulture*, 40, 21–26, 1989.

Mémorial A, *Règlement grand-ducal du 6. mai 2004 fixant les variétés de vignes et certaines pratiques culturales et oenologiques*, number 73, Service Central de Législation, 17.05.2004.

Nakicenovic, N., J. Alcamo, G. Davis, B. de Vries, J. Fenhann, S. Gaffin, K. Gregory, A. Grübler, T. Jung, T. Kram, E. Lebre La Rovere, L. Michaelis, S. Mori, T. Morita, W. Pepper, H. Pitcher, L. Price, K. Riahi, A. Roehrl, H. Rogner, A. Sankovski, M. Schlesinger, P. Shukla, S. Smith, R. Swart, S. van Rooijen, N. Victor, and Z. Dadi, *IPCC Special Report on Emissions Scenarios*, Cambridge University Press, 2000.

Negrul, A., Evolution of cultivated forms of grapes, *Comptes Rendus (Doklady) de l'Académie des Sciences de l'URSS*, 18, 585–588, 1938.

Oke, T., City size and the urban heat island, *Atmospheric Environment*, 7, 769 – 779, 1973.

Peel, M. C., B. L. Finlayson, and T. A. McMahon, Updated world map of the Köppen-Geiger climate classification, *Hydrol. Earth Syst Sci.*, 11, 1633–1644, 2007.

Pouget, R., Observations sur la vitesse de débourrement de cépages de Vitis vinifera L. après levée artificielle de la dormance., *Comptes Rendus Hebdomadaires des Seances de l'Academie des Sciences*, 258, 4333–4335, 1964.

Pouget, R., Nouvelle conception du seuil de croissance chez la vigne., *Vitis*, 7, 201–205, 1968.

Pouget, R., Considérations générales sur le rythme végétatif et la dormance des bourgeons de la vigne, *Vitis*, 11, 198–217, 1972.

Pouget, R., Le débourrement des bourgeons de la vigne: méthode de prévision et principes d'établissement d'une échelle de précocité dedébourrement., *Connaissance Vigne Vin*, 22, 105–123, 1988.

Priewe, J., *Wein. Die neue große Schule*, Zabert Sandmann, 2008.

Reuther, G. and A. Reichardt, Temperatureinflüsse auf Blutung und Stoffwechsel bei Vitis vinifera, *Planta*, Nr. 59, 391–410, 1963.

Riou, C., *Le déterminisme climatique de la maturation du raisin: application au zonage de la teneur en sucre dans la Communauté Européenne.*, Centre Commun de Recherche Commision Européenne, 1994.

Robinson, J., *Das Oxford Weinlexikon.*, Hallwag Verlag, 1995.

Roeckner, E., G. Baeuml, L. Bonaventura, R. Brokopf, M. Esch, M. Giorgetta, S. Hagemann, I. Kirchner, L. Kornblueh, E. Manzini, A. Rhodin, U. Schlese, U. Schulzweida, and A. Tompkins, The atmospheric general circulation model echam5 - part 1, Technical report, MPI-Report 349, 2003.

Réaumur, R. A. F., Observations du thermomètre, faites à paris pendant l'année 1735, comparées avec celles qui ont été faites sous la ligne, à l'isles de france, à alger et quelques unes de nos isles de l'amérique, *Memoires de l'Académie des Sciences de Paris*, pages 545–576, 1735.

Sachs, L., *Angewandte Statistik. Statistische Methoden und ihre Anwendung.*, Spinger Verlag, 1978.

Scheifinger, H., A. Menzel, E. Koch, C. Peter, and R. Ahas, Athmospheric mechanisms governing the spatial and temporal variability of phenological phases in Central Europe, *International Journal of Climatology*, 22, 1739–1755, 2002.

Schlüter, M. H., A. Merico, M. Reginatto, M. Boersma, K. H. Wiltshire, and W. Greve, Phenological shifts of three interacting zooplankton groups in relation to climate change, *Global Change Biology*, 2010.

Schmitz, A.-A., Wenig Radioaktivität in der Mosel, *Luxemburger Wort*, Nr. 177, p.12, 2010.

Schultz, H. R., *Deutsches Weinbaujahrbuch 2005*, chapter Veränderungen im Klima und mögliche weinbauliche Konsequenzen, pages 18–25, Eugen Ulmer, 2005.

Schär, C., P. L. Vidale, D. Lüthi, C. Frei, C. Häberli, M. A. Liniger, and C. Appenzeller, The role of increasing temperature variability in european summer heatwaves, *Nature*, 427, 332–336, 2004.

Shepard, D., A two-dimensional interpolation function for irregularly-spaced data, in *Proceedings of the 1968 ACM National Conference*, pages 517–524, 1968.

Siegfried, W., O. Viret, B. Bloesch, G. Bleyer, and H. H. Kassemeyer, «Vitimeteo Plasmopara »- ein neues Prognosemodell für den Falschen Rebenmehltau, *Schweizerische Zeitung für Obst- und Weinbau*, 2004.

Solomon, S., D. Qin, M. Manning, Z. Chen, M. Marquis, K. B. Averyt, M. Tignor, and H. L. Miller, editors, *Climate Change 2007: The Physical Science Basis. Contribution to Working Group I to the Fourth Assessment Report of the Intergovernmental Panal on Climate Change.*, chapter 3 and 11, Cambridge University Press, 2007.

Statec, *Annuaire statistique du Luxembourg 2008.*, STATEC, 2008.

Stock, M., F.-W. Badeck, F.-W. Gerstengarbe, D. Hoppmann, T. Kartschall, H. Österle, P. Werner, and M. Wodinski, Perspektiven der Klimaänderung bis 2050 für den Weinbau in Deutschland (Klima 2050)., PIK-Report 106, Potsdam Institute for Climate Impact Research, 2007.

Stoev, K. and V. Ivantchev, Données nouvelles sur le problème de la translocation descendante et ascendante des produits de la photosynthèse de la vigne, *Vitis*, 16, 253–262, 1977.

Storchmann, K., English weather and Rhine wine quality: an ordered probit model, *Journal of Wine Research*, 16, 105–119, 2005.

Tomasi, D., G. V. Jones, M. Giust, L. Lorenzo Lovat, and F. Federica Gaiotti, Grapevine phenology and climate change: Relationships and trends in the veneto region of italy for 1964–2009, *American Journal of Enology and Viticulture*, 2011.

Tondut, J.-L., F. Laget, and A. Deloire, Climat et viticulture : évolution des températures sur le département de l'herault - un exemple de réchauffement climatique, *Progrès Agricole et Viticole*, 124, 55–61, 2007.

Urhausen, S., S. Brienen, A. Kapala, and C. Simmer, Climatic conditions and their impact on viticulture in the Upper Moselle region, *Climatic change*, 2011a.

Urhausen, S., S. Brienen, A. Kapala, and C. Simmer, Must quality estimation based on climate data in the Upper Moselle region, *Meteorologische Zeitschrift*, 20, 2011b.

Verbrugghe, M., G. Guyot, J. Hanocq, and D. Ripoche, Influence de différents types de sol de la basse Vallée du Rhône sur les températures de surface de raisins et de feuilles de Vitis vinifera, *Revue Française d'Oenologie*, 128, 14–20, 1991.

Villa, P., *Coltivare la vite*, De Vecchi, 2005.

Vogt, E. and G. Schruft, *Weinbau*, Verlag Eugen Ulmer, 2000.

Vučetić, V., Modelling of maize production in croatia: present and future climate, *The Journal of Agricultural Science*, 149, 145–157, 2011.

Weingesetz, Bundesgesetz über den Verkehr mit Wein und Obstwein, in *Bundesgesetzblatt für die Republik Österreich*, 2009.

Weinjahr, Das Weinjahr und seine Ernteergebnisse, Veröffentlichung der staatlichen Weinbaustation in Remich , 1966–2006.

Wilks, D. S., *Statistical methods in the atmospheric sciences.*, Elsevier, 2006.

Winkler, A., Pruning vinifera grapevines, *California Agricultural Extention Service Circular*, 89, 1–68, 1934.

Winkler, A. J., *General viticulture*, University of California Press, 1965.

Zalom, F. G., P. B. Goodell, L. T. Wilson, W. W. Barnett, and W. J. Bentley, Degree-Days: The Calculation and Use of Heat Units in Pest Management, Technical report, University of California, Division of Agriculture and Natural Resources, 1983.

Glossary

acidity Concentration of non volatile organic acids in must or wine

anlagen an embryonic inflorescence

anthesis rupture of the pollen sacs after which the flowers are fully open and functional

bleeding the extrusion of plant sap from pruning cuts in the early spring

blossom drop a diverse collection of environmentally induced disturbances that result in abnormally poor berry development

bunch rot bunch rot is a fruit-rotting disease involving one or more fungal or bacterial species. In cooler climate conditions the fungus botrytis cinerea is the predominant cause of bunch rot

calyptra the apically fused petals of the grape flower

cane woody and older stem of a plant, usually of brown colour

chilling the effect of decreasing temperature

chlorosis the loss of chlorophyll in young plant tissue

compound bud the mature axillary bud that survives the winter; typically it possesses three immature buds in different states of development

correlative inhibition The suppression of the growth of certain plant parts by a compound, such as a food substance or growth substance, produced in another area of the plant

coulure blossom drop

crossing the exchange of genetic material between members of a homologous chromosome pair. In viticulture crossings are usually done between two species (wine producing and non wine producing species) and the result is a hybrid grapes

cytoplasm substance filling the cells

dormancy a period in the vegetative cycle when growth and development are temporarily stopped. The dormancy can be split into organic and forced dormancy

grape moth a small moth which eats the grape flesh

Huglin Index a common used measure for suitability of wine cultivation in a certain climate. It consists in temperature accumulation above a threshold during vegetation period:

$$HI = \sum_{01.04}^{30.09} \frac{(Tmean - 10) + (Tmax - 10)}{2}$$

lignification becoming wood by depositing lignin in the cell walls and the stems are becoming brown

malic acid one of the two major organic acids in grapes and wine ($C_4H_6O_5$)

millerandage blossom drop

must the juice of freshly pressed grapes with the seeds and the before it is fermented into wine

must density a measure for sugar content of must. In some countries it indicates also the potential alcohol of the wine (e.g., France).

oidium a fungal disease affecting vines, caused by a powdery mildew

pectins a series of gel-like galactuonic acid polymers important in holding plant cells together. Out of viniculture they are used as a gelling agent, thickening agent and stabiliser in food

peronospora A genus of destructive downy mildews

phenols a class of chemical compounds with the base compound C_6H_5OH. To this belong natural pigments, the most vegetative tannins and a lot of taste-giving agents

pruning removal or reduction of branches in order to shape the plant or to improve flowering or fruiting

receptacle the end of the flower stalk upon which the floral organs are borne

respiration The oxidative breakdown of food substances within the cells of living organisms, resulting in the liberation of energy for subsequent use in growth, etc

rootstock the lower section of a grafted vine that serves to develop the root system

tartaric acid one of the two major organic acids in grapes and wine ($C_6H_6O_6$)

tendril a twining modified shoot that originates in leaf axils

véraison the beginning of the last growth phase of grapes, when the green colour begins to fade and the pulp starts to soften

vendanges tardives Quality distinction for wines made from grapes which are harvested overripe and they must have a minimum of 105°Oe for Auxerrois, Pinot Blanc, Pinot Gris, Gewürztraminer and 95°Oe for Riesling. The grapes often are affected by nobel rot, benevolent form of a grey fungus, Botrytis cinerea. The term vendanges tardives is comparable to the German classification Auslese, however the term Spätlese in Germany or Austria is reserved for wines having a lower must weight

vin de glace Quality distinction for wine made from grapes harvested and pressed while frozen. They must have a temperature lower than -7°CṪhe vine varieties allowed for ice wine producing are Pinot Blanc, Pinot Gris and Riesling with a minimum of 130°Oe

Winkler Index a technique for classifying the climate of wine growing regions. Depending on the value WI, five climate regions are identified (*Amerine and Winkler*, 1944):

$$WI = \sum_{01.04}^{30.09} \frac{Tmax + Tmin}{2} - 10$$

wood maturation maturation phase of the summer shoots turning from green to brown; i.e., shoots are becoming canes by lignification process. It usually starts in August and ends after harvest. It is very important for frost resistance in winter and the initiation of growth in spring

Appendix A

A Statistical methods

A.1 Mann-Kendall Trend Test

The test of Mann-Kendall tests the significance of trends. Mann, H.B., 1945. Nonparametric tests against trend, Econometrica, 13, 245-259.

A.2 Kolmogorov-Smirnov-Test

There exist two kinds of Kolmogorov-Smirnov tests (*Wilks*, 2006; *Sachs*, 1978): the one-sample and two-sample test. The first one compares the values of the data to a normal distribution. The second one compares the values of one dataset to the values of another dataset. The idea of the test is always the same: the null hypothesis says that they were drawn from the same distribution.

In this work the second type is applied: the two-sample Kolmogorov-Smirnov test compares two distributions, F_B and F_E, by calculating the maximal difference between the cumulative probability functions (CDF) of these distributions:

$$D = \max_x |F_n(x_1) - F_m(x_2)| \tag{A.1}$$

The two distributions of the length n_1 and n_2 were drawn from the same distribution at a significance level α if

$$D \leqslant D_\alpha = \sqrt{-\frac{1}{2}\frac{n_1 + n_2}{n_1 n_2} \ln \frac{\alpha}{2}} \tag{A.2}$$

The Kolmogorov-Smirnov test is very sensitive to small differences in median, dispersion, skewness, and kurtosis (*Sachs*, 1978).

A.3 Cluster Analysis

Having datasets for different variables it is often useful to form groups with similar characteristics. One method is the cluster analysis, where clusters can be formed by hierarchical and non-hierarchical methods; in this work the first method is used. The method is applied to group vine varieties according the properties must density and acidity, respectively.

First, a distance based on a metric is calculated between pairs of objects x_r and x_s of length n (e.g. must quality of the vine varieties at a given time). Here, the Euclidean distance is chosen as metric:

$$dist(x_r, x_s)^2 = (x_r - x_s)(x_r - x_s)^T \tag{A.3}$$

r and s are the different vine varieties or clusters of vine varieies with property x (must density or acidity). The vine varieties and are sorted according their shortest distances, also called nearest neighbour method

$$d(r, s) = \min(dist(x_{ri}, x_{sj})),\ i \in 1 \dots n_r,\ j \in 1 \dots n_s \tag{A.4}$$

Those vine varieties, which are similar, i.e., which have the shortest distance are grouped into clusters, which themselves are grouped according their distance. In the end all vine varieties are in one single cluster. Normally it is not obvious how many clusters are useful, but in this case the clusters were very clear, thus no further analysis of stopping methods has been done.

A.4 T-test for paired differences

In order to test if two samples are significantly different, the t-test is applied to the paired differences (d) of the time series (of length n). The differences are assumed normal distributed.

$$\hat{t} = \frac{\overline{d}}{s_{\overline{d}}} = \frac{(\sum d_i)/n}{\sqrt{\frac{\sum d_i^2 - (\sum d_i)^2/n}{n(n-1)}}} \tag{A.5}$$

B Appendix B
Additional tables

B.1 Day of Year Calendar

Table B.1: Calendar of the Day of Year (DOY). In case of a leap year one day has to be added from March onwards.

	Jan	*Feb*	*Mar*	*Apr*	*May*	*Jun*	*Jul*	*Aug*	*Sep*	*Oct*	*Nov*	*Dec*	
1	001	032	060	091	121	152	182	213	244	274	305	335	***1***
2	002	033	061	092	122	153	183	214	245	275	306	336	***2***
3	003	034	062	093	123	154	184	215	246	276	307	337	***3***
4	004	035	063	094	124	155	185	216	247	277	308	338	***4***
5	005	036	064	095	125	156	186	217	248	278	309	339	***5***
6	006	037	065	096	126	157	187	218	249	279	310	340	***6***
7	007	038	066	097	127	158	188	219	250	280	311	341	***7***
8	008	039	067	098	128	159	189	220	251	281	312	342	***8***
9	009	040	068	099	129	160	190	221	252	282	313	343	***9***
10	010	041	069	100	130	161	191	222	253	283	314	344	***10***
11	011	042	070	101	131	162	192	223	254	284	315	345	***11***
12	012	043	071	102	132	163	193	224	255	285	316	346	***12***
13	013	044	072	103	133	164	194	225	256	286	317	347	***13***
14	014	045	073	104	134	165	195	226	257	287	318	348	***14***
15	015	046	074	105	135	166	196	227	258	288	319	349	***15***
16	016	047	075	106	136	167	197	228	259	289	320	350	***16***
17	017	048	076	107	137	168	198	229	260	290	321	351	***17***
18	018	049	077	108	138	169	199	230	261	291	322	352	***18***
19	019	050	078	109	139	170	200	231	262	292	323	353	***19***
20	020	051	079	110	140	171	201	232	263	293	324	354	***20***
21	021	052	080	111	141	172	202	233	264	294	325	355	***21***
22	022	053	081	112	142	173	203	234	265	295	326	356	***22***
23	023	054	082	113	143	174	204	235	266	296	327	357	***23***
24	024	055	083	114	144	175	205	236	267	297	328	358	***24***
25	025	056	084	115	145	176	206	237	268	298	329	359	***25***
26	026	057	085	116	146	177	207	238	269	299	330	360	***26***
27	027	058	086	117	147	178	208	239	270	300	331	361	***27***
28	028	059	087	118	148	179	209	240	271	301	332	362	***28***
29	029		088	119	149	180	210	241	272	302	333	363	***29***
30	030		089	120	150	181	211	242	273	303	334	364	***30***
31	031		090		151		212	243		304		365	***31***

B.2 Entire list of predictors

Table B.2: Complete list of predictors used for the parameterisation of budburst. The framed ones are the final selected ones.

Mean temperature:	
TM1	in January
TM2	in February
TM3	in March
TM4	in April
$TM3_{1-7}$	1-7 March
$TM3_{8-15}$	8-15 March
$TM3_{16-22}$	16-22 March
$TM3_{23-31}$	23-31 March
$TM3_{1-15}$	1-15 March
$TM3_{8-22}$	8-22 March
$TM3_{16-31}$	16-31 March
$TM3_{1-22}$	1-22 March
$TM3_{8-31}$	8-31 March
$TM4_{1-15}$	1-15 April
$TM4_{16-30}$	16-30 April

Maximum temperature:	
TX1	in January
TX2	in February
TX3	in March
TX4	in April
$TX3_{1-7}$	1-7 March
$TX3_{8-15}$	8-15 March
$TX3_{16-22}$	16-22 March
$TX3_{23-31}$	23-31 March
$TX3_{1-15}$	1-15 March
$TX3_{8-22}$	8-22 March
$TX3_{16-31}$	16-31 March
$TX3_{1-22}$	1-22 March
$TX3_{8-31}$	8-31 March
$TX4_{1-15}$	1-15 April
$TX4_{16-30}$	16-30 April

Minimum temperature:	
TN1	in January
TN2	in February
TN3	in March
TN4	in April
$TN3_{1-7}$	1-7 March
$TN3_{8-15}$	8-15 March
$TN3_{16-22}$	16-22 March
$TN3_{23-31}$	23-31 March
$TN3_{1-15}$	1-15 March
$TN3_{8-22}$	8-22 March
$TN3_{16-31}$	16-31 March
$TN3_{1-22}$	1-22 March
$TN3_{8-31}$	8-31 March
$TN4_{1-15}$	1-15 April
$TN4_{16-30}$	16-30 April

DD4	Degree days in April
DD3	Degree days in March
DD2	Degree days in February

ID1	Ice days in January
ID2	Ice days in February
ID3	Ice days im March
ID1-3	Ice days January - March
FD1	Frost days in January
FD2	Frost days in February
FD3	Frost days in March
FD4	Frost days in April
FD1-4	Frost days January - April
FD1-3	Frost days January - March
WD1-3	Winter days January - March

Precipitation:	
RR1	in January
RR2	in February
RR3	in March
RR4	in April
RR1-3	January - March
RR1-2	January - February
RR2-3	February - March
$RR4_{1-15}$	1-15 April

$VEGT_{T=8}$	sum of minimum temperature above 8°C between January and March
$SVEGT_{T=8}$	days with minimum temperature above 8°C between January and March
$VEGT_{T=9}$	sum of minimum temperature above 9°C between January and March
$SVEGT_{T=9}$	days with minimum temperature above 9°C between January and March
$VEGT_{T=10}$	sum of minimum temperature above 10°C between January and March
$SVEGT_{T=10}$	days with minimum temperature above 10°C between January and March

TEMP_FD1	sum of minimum temperature below 0°C in January
TEMP_FD2	sum of minimum temperature below 0°C in February
TEMP_FD3	sum of minimum temperature below 0°C in March
TEMP_FD4	sum of minimum temperature below 0°C in April
TEMP_FD1-3	sum of minimum temperature below 0°C January-March

SD3	Sunshine duration in March

Table B.3: Complete list of predictors used for the parameterisation of flowering. The framed ones are the final selected ones.

Mean temperature:		Maximum temperature:	
TM3	in March	TX3	in March
TM4	in April	TX4	in April
TM5	in May	TX5	in May
TM6	in June	TX6	in June
$TM5_{1-7}$	1-7 May	$TX5_{1-7}$	1-7 May
$TM5_{8-15}$	8-15 May	$TX5_{8-15}$	8-15 May
$TM5_{16-22}$	16-22 May	$TX5_{16-22}$	16-22 May
$TM5_{23-31}$	23-31 May	$TX5_{23-31}$	23-31 May
$TM5_{1-15}$	1-15 May	$TX5_{1-15}$	1-15 May
$TM5_{8-22}$	8-22 May	$TX5_{8-22}$	8-22 May
$TM5_{16-31}$	16-31 May	$TX5_{16-31}$	16-31 May
$TM5_{1-22}$	1-22 May	$TX5_{1-22}$	1-22 May
$TM5_{8-31}$	8-31 May	$TX5_{8-31}$	8-31 May
$TM6_{1-15}$	1-15 June	$TX6_{1-15}$	1-15 June
$TM6_{16-30}$	16-30 June	$TX6_{16-30}$	16-30 June

Minimum temperature:		Precipitation:	
TN3	in March	RR3	in March
TN4	in April	RR4	in April
TN5	in May	RR5	in May
TN6	in June	$RR5_{16-31}$	16-31 May
$TN5_{1-7}$	1-7 May	RR6	in June
$TN5_{8-15}$	8-15 May	$RR6_{1-15}$	1-15 June
$TN5_{16-22}$	16-22 May	$RR6_{16-30}$	16-30 June
$TN5_{23-31}$	23-31 May	RR3-5	March - May
$TN5_{1-15}$	1-15 May	RR3-4	March - April
$TN5_{8-22}$	8-22 May	RR4-5	April - May
$TN5_{16-31}$	16-31 May		
$TN5_{1-22}$	1-22 May	BB	Bud burst date
$TN5_{8-31}$	8-31 May		
$TN6_{1-15}$	1-15 June		
$TN6_{16-30}$	16-30 June		

$VEGT_{T=8}$	sum of minimum temperature above 8°C between January and May
$SVEGT_{T=8}$	days with minimum temperature above 8°C between January and May
$VEGT_{T=9}$	sum of minimum temperature above 9°C between January and May
$SVEGT_{T=9}$	days with minimum temperature above 9°C between January and May
$VEGT_{T=10}$	sum of minimum temperature above 10°C between January and May
$SVEGT_{T=10}$	days with minimum temperature above 10°C between January and May

DD2	Degree days in February
DD3	Degree days in March
DD4	Degree days in April
DD5	Degree days in May
DD1-6	Degree days January - June

Table B.4: Complete list of predictors used for the parameterisation of must density and acidity. The framed ones are the final selected ones: dashed boxes for must density and solid boxes for acidity.

Mean temperature:	
TM7	July
TM8	August
TM9	September
TM10	October
$TM7_{1-7}$	1-7 July
$TM7_{8-15}$	8-15 July
$TM7_{16-22}$	16-22 July
$TM7_{23-31}$	23-31 July
$TM7_{1-15}$	1-15 July
$TM7_{16-31}$	16-31 July
$TM7_{8-22}$	8-22 July
$TM7_{1-22}$	1-22 July
$TM7_{8-31}$	8-31 July
$TM8_{1-7}$	1-7 August
$TM8_{8-15}$	8-15 August
$TM8_{16-22}$	16-22 August
$TM8_{23-31}$	23-31 August
$TM8_{1-15}$	1-15 August
$TM8_{16-31}$	16-31 August
$TM8_{8-22}$	8-22 August
$TM8_{1-22}$	1-22 August
$TM8_{8-31}$	8-31 August
$TM9_{1-7}$	1-7 September
$TM9_{8-15}$	8-15 September
$TM9_{16-22}$	16-22 September
$TM9_{23-30}$	23-30 September
$TM9_{1-15}$	1-15 September
$TM9_{16-30}$	16-30 September
$TM9_{8-22}$	8-22 September
$TM9_{1-22}$	1-22 September
$TM9_{8-30}$	8-30 September
$TM10_{1-7}$	1-7 October
$TM10_{8-15}$	8-15 October
$TM10_{16-22}$	16-22 October
$TM10_{23-31}$	23-31 October
$TM10_{1-15}$	1-15 October
$TM10_{1-22}$	1-22 October

Maximum temperature:	
TX7	July
TX8	August
TX9	September
TX10	October
$TX7_{1-7}$	1-7 July
$TX7_{8-15}$	8-15 July
$TX7_{16-22}$	16-22 July
$TX7_{23-31}$	23-31 July
$TX7_{1-15}$	1-15 July
$TX7_{16-31}$	16-31 July
$TX7_{8-22}$	8-22 July
$TX7_{1-22}$	1-22 July
$TX7_{8-31}$	8-31 July
$TX8_{1-7}$	1-7 August
$TX8_{8-15}$	8-15 August
$TX8_{16-22}$	16-22 August
$TX8_{23-31}$	23-31 August
$TX8_{1-15}$	1-15 August
$TX8_{16-31}$	16-31 August
$TX8_{8-22}$	8-22 August
$TX8_{1-22}$	1-22 August
$TX8_{8-31}$	8-31 August
$TX9_{1-7}$	1-7 September
$TX9_{8-15}$	8-15 September
$TX9_{16-22}$	16-22 September
$TX9_{23-30}$	23-30 September
$TX9_{1-15}$	1-15 September
$TX9_{16-30}$	16-30 September
$TX9_{8-22}$	8-22 September
$TX9_{1-22}$	1-22 September
$TX9_{8-30}$	8-30 September
$TX10_{1-7}$	1-7 October
$TX10_{8-15}$	8-15 October
$TX10_{16-22}$	16-22 October
$TX10_{23-31}$	23-31 October
$TX10_{1-15}$	1-15 October
$TX10_{1-22}$	1-22 October

Minimum temperature:	
TN7	July
TN8	August
TN9	September
TN10	October
$TN7_{1-7}$	1-7 July
$TN7_{8-15}$	8-15 July
$TN7_{16-22}$	16-22 July
$TN7_{23-31}$	23-31 July
$TN7_{1-15}$	1-15 July
$TN7_{16-31}$	16-31 July
$TN7_{8-22}$	8-22 July
$TN7_{1-22}$	1-22 July
$TN7_{8-31}$	8-31 July

Precipitation:	
RR6	June
RR7	July
RR8	August
RR9	September
RR10	October
$RR9_{1-15}$	1-15 September
$RR9_{16-22}$	16-22 September

Degree Days:	
DD1-12	January-December
DD4-10	April-October
DD7	July
DD8	August

$TN8_{1-7}$	1-7 August	DD9	September
$TN8_{8-15}$	8-15 August	DD10	October
$TN8_{16-22}$	16-22 August		
$TN8_{23-31}$	23-31 August	Sunshine duration:	
$TN8_{1-15}$	1-15 August	SD8	August
$TN8_{16-31}$	16-31 August	SD9	September
$TN8_{8-22}$	8-22 August	SD10	October
$TN8_{1-22}$	1-22 August	SD6-10	June-October
$TN8_{8-31}$	8-31 August	SD8-10	August-October
$TN9_{1-7}$	1-7 September	SD4-10	April-October
$TN9_{8-15}$	8-15 September		
$TN9_{16-22}$	16-22 September	Sum of Average Temperatures:	
$TN9_{23-30}$	23-30 September	SSAT8	accumulation of SAT in August
$TN9_{1-15}$	1-15 September	SSAT9	accumulation of SAT in September
$TN9_{16-30}$	16-30 September	MSAT8	average of SAT in August
$TN9_{8-22}$	8-22 September	MSAT9	average of SAT in September
$TN9_{1-22}$	1-22 September		
$TN9_{8-30}$	8-30 September	Potential Evapotranspiration:	
$TN10_{1-7}$	1-7 October	SPET8	accumulation of PET in August
$TN10_{8-15}$	8-15 October	SPET9	accumulation of PET in September
$TN10_{16-22}$	16-22 October	MPET8	average of PET in August
$TN10_{23-31}$	23-31 October	MPET9	average of PET in September
$TN10_{1-15}$	1-15 October		
$TN10_{1-22}$	1-22 October	BB	Budburst date
		BLU	Flowering date

Summer days:		Hot days:	
SUMMER1-12	January-December	HOT1-12	January-December
SUMMER6	June	HOT6	June
SUMMER7	July	HOT7	July
SUMMER8	August	HOT8	August
SUMMER9	September	HOT9	September
SUMMER6-10	June-October	HOT5-6	May-June
SUMMER8-10	August-October	HOT6-10	June-October
		HOT8-10	August-October

$VEGT9_{T=8}$	days with minimum temperature above 8°C in September
$SVEGT9_{T=8}$	accumulation of minimum temperature above 8°C in September
$VEGT8\text{-}9_{T=8}$	days with minimum temperature above 8°C between August and September
$VEGT7\text{-}9_{T=8}$	days with minimum temperature above 8°C between July and September
$VEGT6\text{-}9_{T=8}$	days with minimum temperature above 8°C between June and September

B.3 Statistical evaluation of the different realisations of CCLM

Table B.5: Statistical characteristics of the CCLM data Run 1 for the annual maximum (Tmax), minimum (Tmin) and mean (Tmean) temperature, precipitation (Prec) and sunshine duration (SD) for the period 1960-2000. The data in parenthesis are the corresponding station data for the same period.

	Tmax [°C]	Tmin [°C]	Tmean [°C]	Prec [mm]	SD [h]
mean value	13.5 (14.4)	5.7 (5.6)	9.1 (9.4)	932 (775)	1537 (1542)
standard deviation	0.9 (0.9)	0.5 (0.8)	0.6 (0.8)	113 (139)	169 (152)
range	3.9 (4.1)	1.8 (3.4)	2.5 (3.2)	558 (535)	658 (622)
minimum	11.8 (13.1)	4.7 (4.0)	7.9 (8.6)	635 (499)	1214 (1299)
	(1997, 1978)	(1963, 1963)	(1997, 1963)	(1964, 1976)	(1973, 1965)
maximum	15.6 (17.2)	6.5 (7.4)	10.5 (11.8)	1193 (1033)	1872 (1921)
	(1980, 1992)	(1987, 2000)	(1980, 1992)	(1976, 2000)	(1981, 1976)
1st quartile	12.7 (13.1)	5.4 (5.1)	8.8 (9.3)	854 (679)	1427 (1419)
3rd quartile	14.0 (14.9)	6.0 (6.1)	9.5 (10.5)	1033 (869)	1654 (1657)

Table B.6: Statistical characteristics of the CCLM data Run 1 for the mean annual climate days for the period 1960-2000. The data in parenthesis are the corresponding station data for the same period.

	Hot days	Summer days	Frost days	Ice days	Mild nights
mean value	23.2 (8.1)	25.4 (31.9)	60.8 (64.5)	16.3 (10.8)	14.4 (18.9)
standard dev.	10.4 (6.3)	7.3 (10.4)	11.4 (16.7)	8.8 (9.1)	8.0 (8.0)
range	44 (25)	30 (52)	60 (72)	35 (45)	33 (35)
minimum	3 (0)	12 (0)	33 (26)	1 (0)	3 (5)
	(1972, 1965)	(1970, 1965)	(1972, 2000)	(1983, 3 years)	(1990, 1974)
maximum	47 (25)	42 (52)	93 (98)	36 (45)	36 (40)
	(1985, 1976)	(1988, 1982)	(1963, 1963)	(1961, 1963)	(1975, 1994)
1st quartile	14.7 (4.0)	19.0 (25.7)	54.0 (53.0)	9.7 (3.5)	7 (13.0)
3rd quartile	29.5 (12.3)	31.0 (38.5)	68.0 (75.5)	22.0 (15.0)	20 (22.5)

Table B.7: Statistical characteristics of the CCLM data Run 2 for the annual maximum (Tmax), minimum (Tmin) and mean (Tmean) temperature, precipitation (Prec) and sunshine duration (SD) for the period 1960-2000. The data in parenthesis are the corresponding station data for the same period.

	Tmax [°C]	Tmin [°C]	Tmean [°C]	Prec [mm]	SD [h]
mean value	13.5 (14.4)	5.6 (5.6)	9.1 (9.4)	945 (775)	1540 (1542)
standard deviation	1.0 (0.9)	0.6 (0.8)	0.7 (0.8)	120 (139)	177 (152)
range	4.5 (4.1)	2.7 (3.4)	3.5 (3.2)	580 (535)	727 (622)
minimum	11.6 (13.1)	4.4 (4.0)	7.7 (8.6)	664 (499)	1160 (1299)
	(1984, 1978)	(1984, 1963)	(1984, 1963)	(1996, 1976)	(1991, 1965)
maximum	16.2 (17.2)	7.1 (7.4)	11.1 (11.8)	1244 (1033)	1887 (1921)
	(1990, 1992)	(1990, 2000)	(1990, 1992)	(1984, 2000)	(1995, 1976)
1st quartile	12.6 (13.1)	5.2 (5.1)	8.6 (9.3)	877 (679)	1426 (1419)
3rd quartile	14.1 (14.9)	5.9 (6.1)	9.6 (10.5)	1006 (869)	1656 (1657)

Table B.8: Statistical characteristics of the CCLM data Run 2 for the mean annual climate days for the period 1960-2000. The data in parenthesis are the corresponding station data for the same period.

	Hot days	Summer days	Frost days	Ice days	Mild nights
mean value	25.0 (8.1)	26.1 (31.9)	61.8 (64.5)	17.4 (10.8)	14.1 (18.9)
standard dev.	13.5 (6.3)	8.9 (10.4)	15.8 (16.7)	10.3 (9.1)	8.4 (8.0)
range	57 (25)	40 (52)	63 (72)	49 (45)	36 (35)
minimum	8 (0)	10 (0)	34 (26)	1 (0)	2 (5)
	(1961, 1965)	(1985, 1965)	(1976, 2000)	(1990, 3 years)	(1961, 1974)
maximum	65 (25)	50 (52)	97 (98)	50 (45)	38 (40)
	(1990, 1976)	(2000, 1982)	(1996, 1963)	(1996, 1963)	(1990, 1994)
1st quartile	14.0 (4.0)	19.0 (25.7)	46.7 (53.0)	9.0 (3.5)	7.7 (13.0)
3rd quartile	32.3 (12.3)	32.0 (38.5)	69.0 (75.5)	23.5 (15.0)	21 (22.5)

Table B.9: Statistical characteristics of the CCLM data Run 3 for the annual maximum (Tmax), minimum (Tmin) and mean (Tmean) temperature, precipitation (Prec) and sunshine duration (SD) for the period 1960-2000. The data in parenthesis are the corresponding station data for the same period.

	Tmax [°C]	Tmin [°C]	Tmean [°C]	Prec [mm]	SD [h]
mean value	13.8 (14.4)	5.9 (5.6)	9.4 (9.4)	932 (775)	1533 (1542)
standard deviation	0.9 (0.9)	0.5 (0.8)	0.6 (0.8)	122 (139)	199 (152)
range	4.4 (4.1)	2.6 (3.4)	3.4 (3.2)	624 (535)	817 (622)
minimum	11.3 (13.1)	4.8 (4.0)	7.7 (8.6)	625 (499)	1097 (1299)
	(1971, 1978)	(1971, 1963)	(1971, 1963)	(1964, 1976)	(1967, 1965)
maximum	15.7 (17.2)	7.4 (7.4)	11.1 (11.8)	1248 (1033)	1914 (1921)
	(1994, 1992)	(1994, 2000)	(1994, 1992)	(1967, 2000)	(1982, 1976)
1st quartile	13.3 (13.1)	5.5 (5.1)	9.1 (9.3)	854 (679)	1408 (1419)
3rd quartile	14.3 (14.9)	6.3 (6.1)	9.8 (10.5)	984 (869)	1660 (1657)

Table B.10: Statistical characteristics of the CCLM data Run 3 for the mean annual climate days for the period 1960-2000. The data in parenthesis are the corresponding station data for the same period.

	Hot days	Summer days	Frost days	Ice days	Mild nights
mean value	26.0 (8.1)	24.6 (31.9)	58.9 (64.5)	12.6 (10.8)	16.9 (18.9)
standard dev.	10.5 (6.3)	5.5 (10.4)	16.0 (16.7)	7.6 (9.1)	7.8 (8.0)
range	39 (25)	23 (52)	63 (72)	35 (45)	34 (35)
minimum	10 (0)	13 (0)	29 (26)	1 (0)	6 (5)
	(1985, 1965)	(1963, 1965)	(1978, 2000)	(1976, 3 years)	(1962, 1974)
maximum	49 (25)	36 (52)	92 (98)	36 (45)	40 (40)
	(1994, 1976)	(1962, 1982)	(1985, 1963)	(1977, 1963)	(1994, 1994)
1st quartile	17.0 (4.0)	20.7 (25.7)	51.3 (53.0)	7.0 (3.5)	10.7 (13.0)
3rd quartile	34.0 (12.3)	29.0 (38.5)	66.2 (75.5)	16.5 (15.0)	22.3 (22.5)

Appendix C

C Additional figures

C.1 Original and adjusted time series (1960-2050) of the predictors

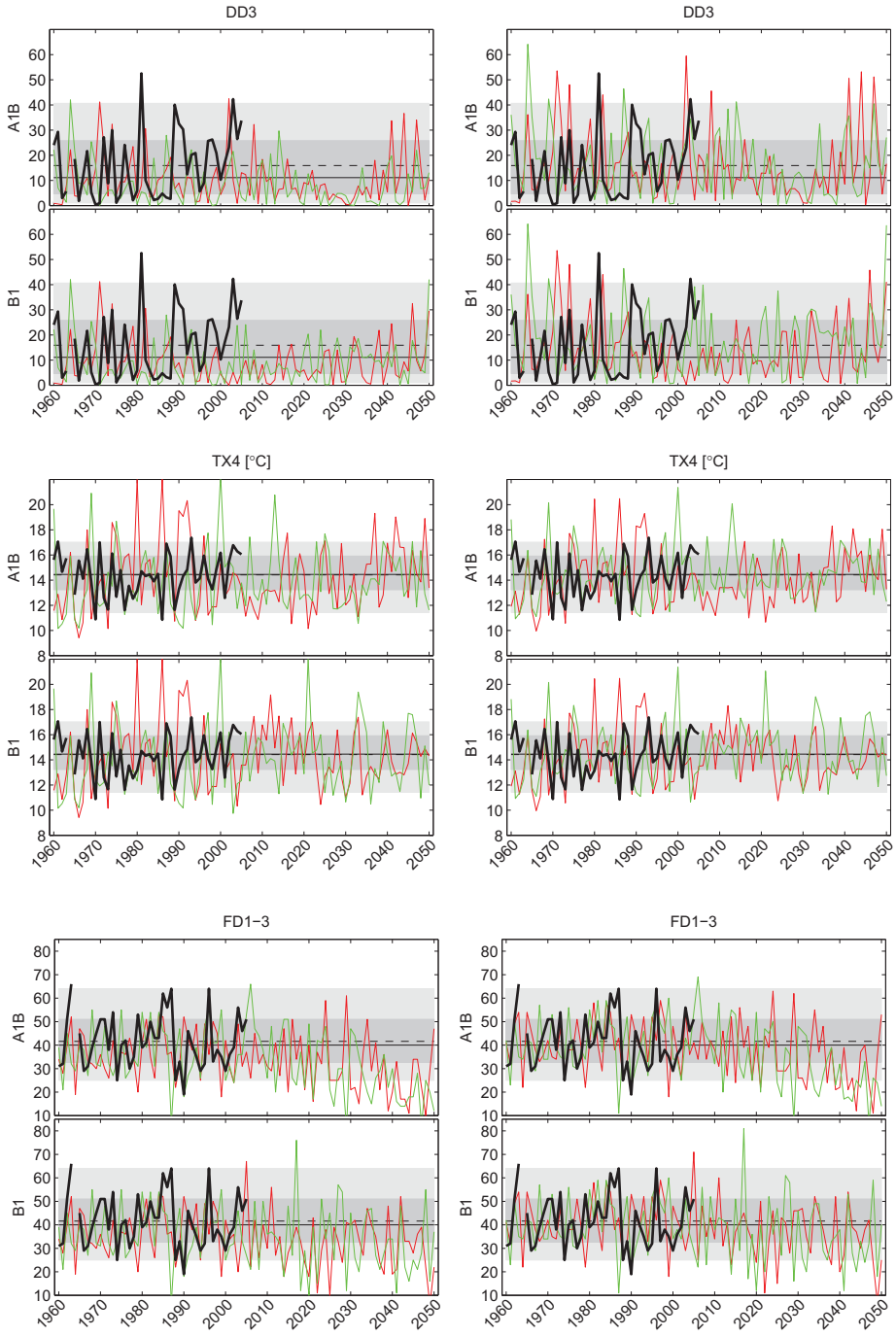

(a) Original CCLM (b) Calibrated CCLM

Figure C.1: Time series of original and calibrated CCLM predictors used for budburst estimation.

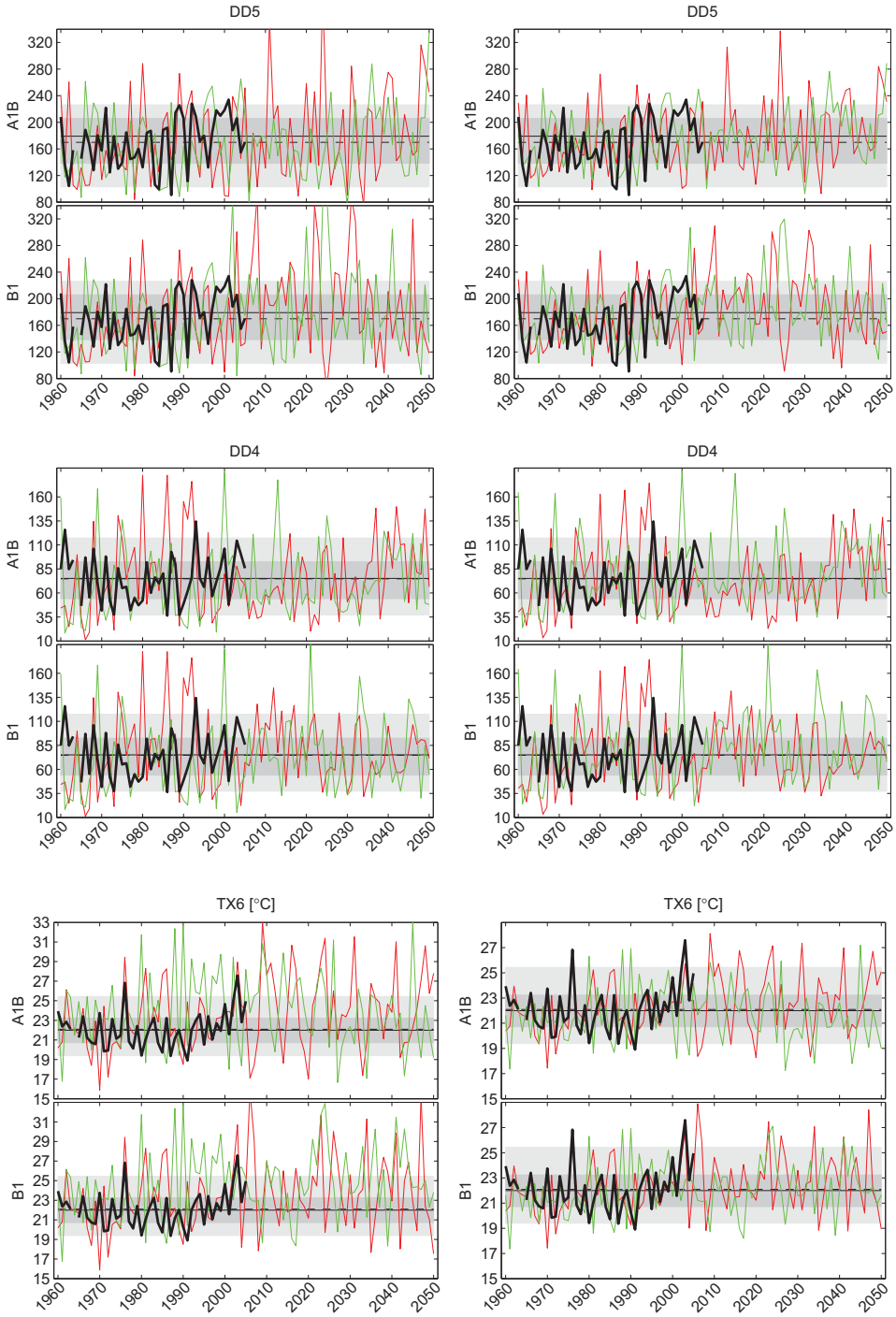

(a) Original CCLM (b) Calibrated CCLM

Figure C.2: Time series of original and calibrated CCLM predictors used for flowering estimation.

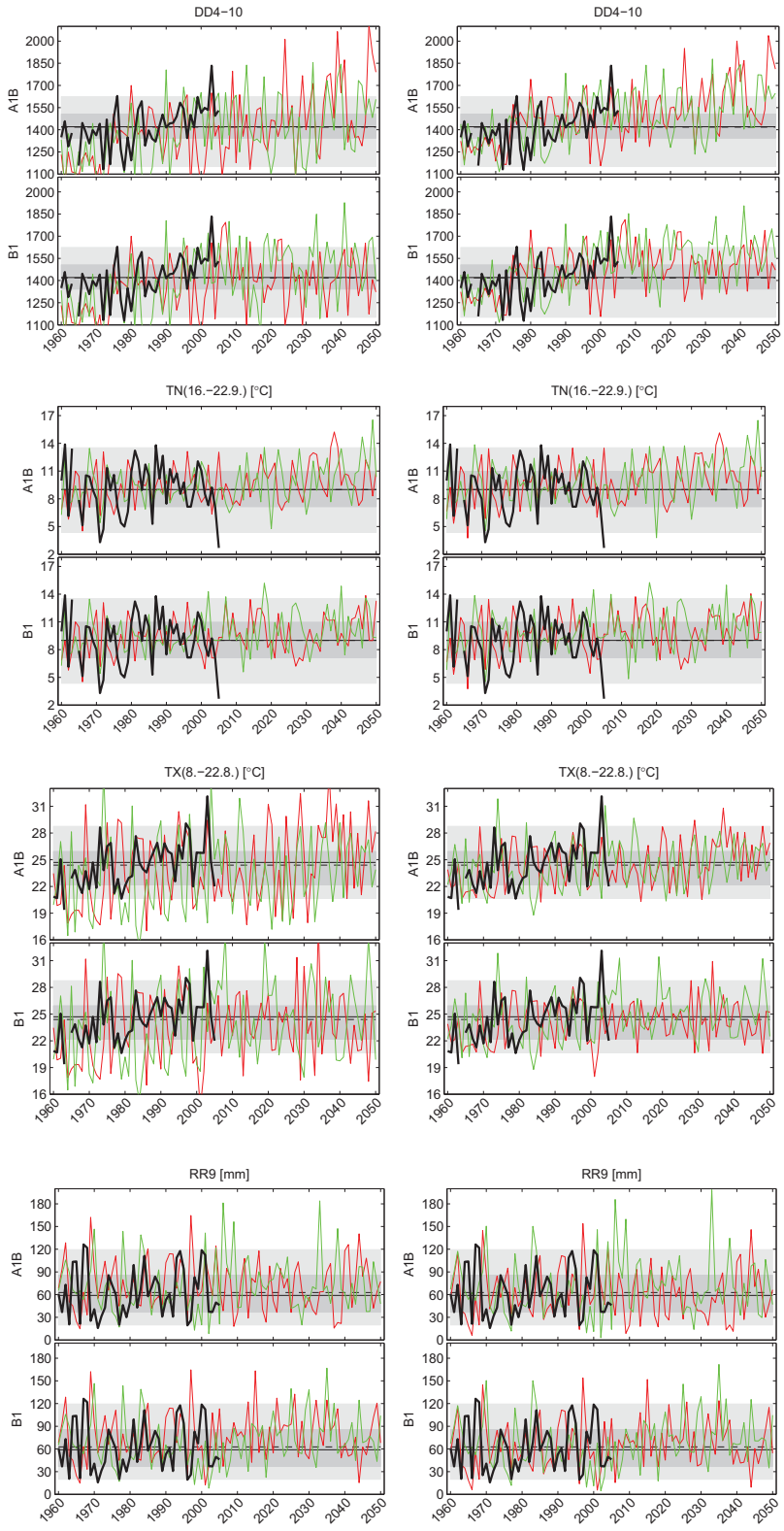

(a) Original CCLM (b) Calibrated CCLM

Figure C.3: Time series of original and calibrated CCLM predictors used for must density (cluster I) estimation.

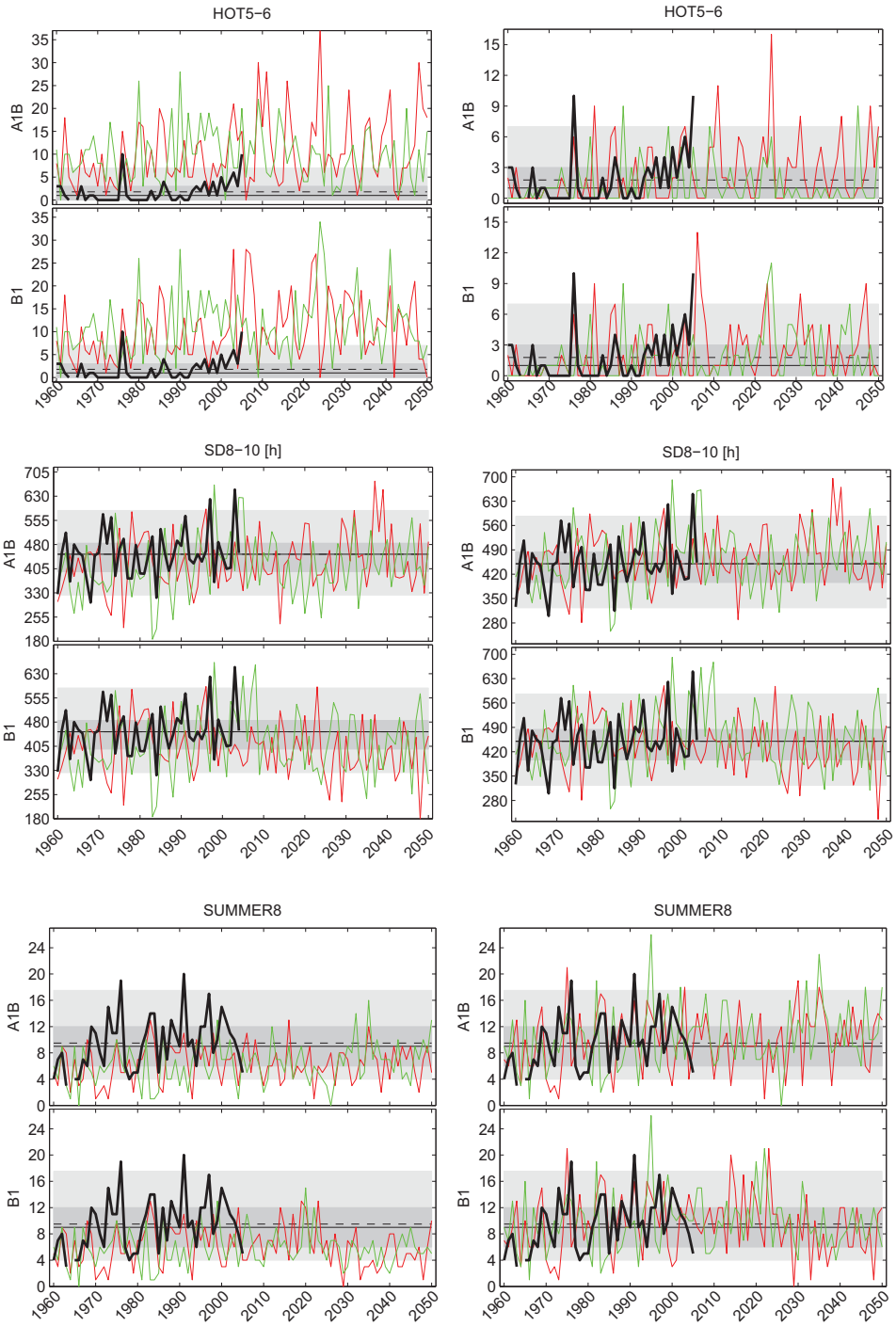

(a) Original CCLM (b) Calibrated CCLM

Figure C.4: Time series of original and calibrated CCLM predictors used for must density (cluster II) estimation.

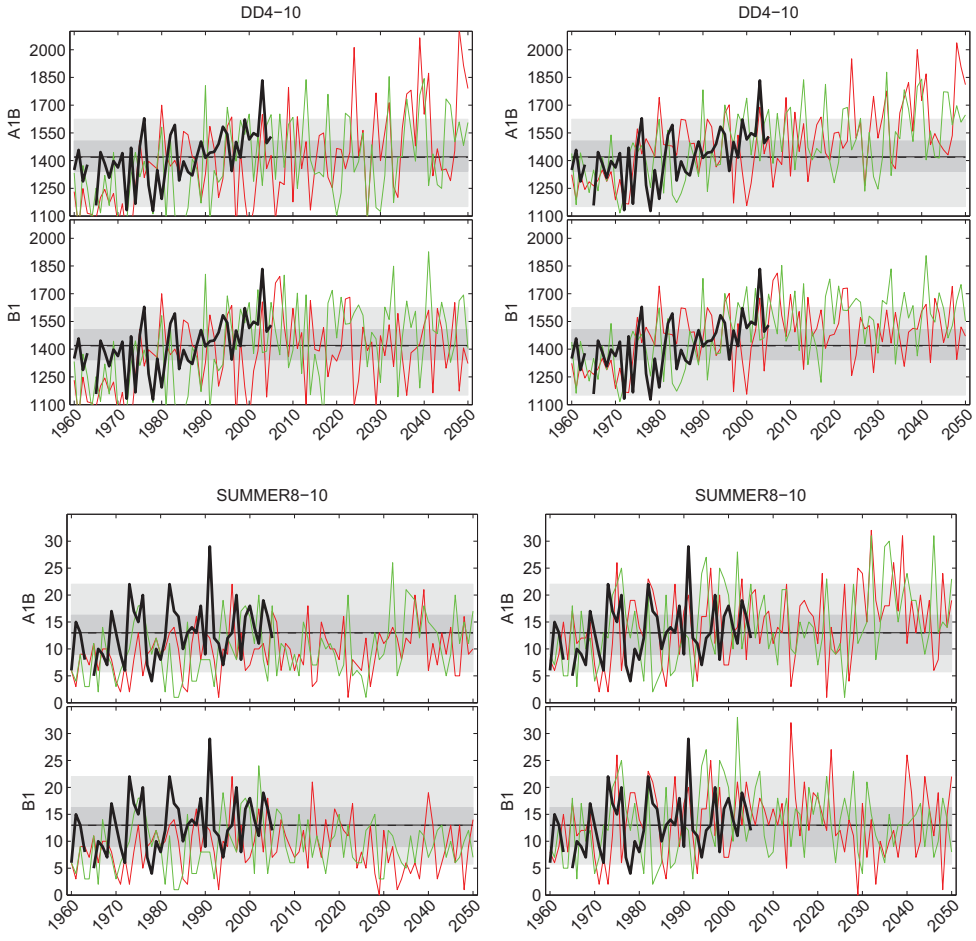

(a) Original CCLM (b) Calibrated CCLM

Figure C.5: Time series of original and calibrated CCLM predictors used for acidity (cluster I/III) estimation.

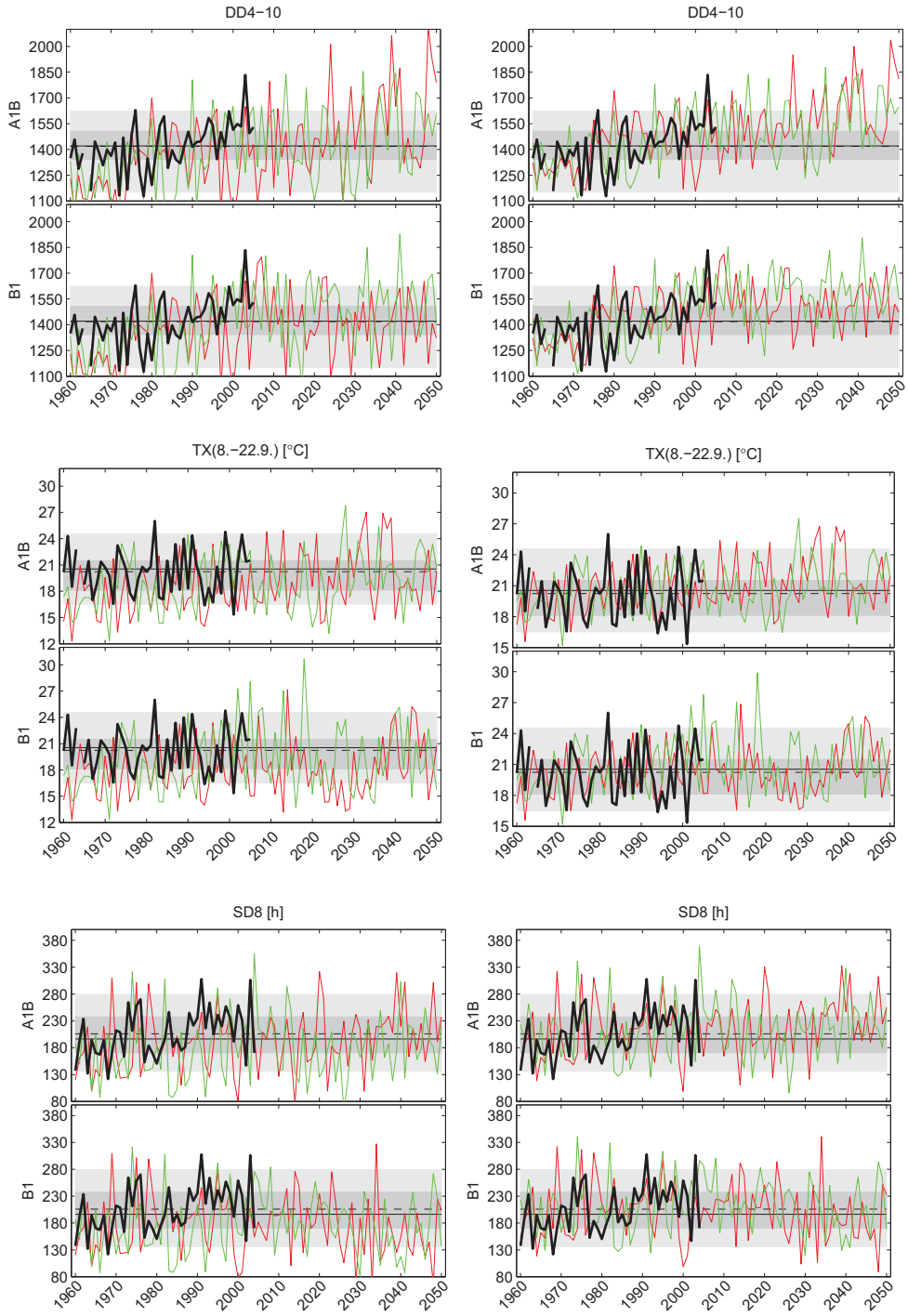

(a) Original CCLM (b) Calibrated CCLM

Figure C.6: Time series of original and calibrated CCLM predictors used for acidity (cluster II) estimation.